ANALYSIS OF EPH RECEPTOR SIGNALING DURING OOCYTE MEIOTIC MATURATION IN *CAENORHABDITIS ELEGANS*

By

Hua Cheng

Dissertation

Submitted to the Faculty of the

Graduate school of Vanderbilt University

in partial fulfillment of the requirements

for the degree of

DOCTOR OF PHILOSOPHY

in

Cell and Developmental Biology

December, 2008

Nashville, Tennessee

Approved :

David Miller

David Greenstein

Ethan Lee

Jin Chen

Chang Chung

To my beloved husband Hanjian Liu

ACKNOWLEDGMENTS

I want to start with expressing my deep and sincere gratitude to my mentor David Greenstein. I joined his lab with barely any experimental research experience and very poor English communication skill. David helped me to be a scientist with his expertise, guidance, and patience. With his enthusiasm and inspiration for science, he always makes so much fun to think and talk about science. David also gave me the confidence and support to work on my dissertation; he never stopped encouraging me and always challenges me to improve my scientific thinking and writing skill. David inspires me not just with his passion for science but also his amazing personality. The way he cares about people and his rule of "students always come first" have been and will continue to be an inspiration to me. From David, I learned to believe in my future and myself.

I would also like to gratefully acknowledge my committee members: David Miller, Ethan Lee, Jin Chen, and Chang Chung. Their guidance and help have been invaluable in my graduate career. I greatly appreciate all your work and your careful and critical thinking about my project.

I would like to thank all the people who provided help for my dissertation work. I am grateful to my collaborator J. Amaranath Govindan for doing the genome wide RNAi screen and analysis of G protein signaling pathway and his great interest and helpful comments in my research work. I also want to thank Amaranath for being a great colleague and friend. I want to thank John Yochem, Barth Grant, Margaret Titus, Sean Conner, and Ethan Lee for their helpful suggestion and generosity to share their reagents

and resources during my graduate study. I want to thank John Yochem, J. Amaranath Govindan, Leslie Bell for their helpful comments for this thesis.

A journey is easier when you travel together. I want to thank several lab members, past and present: Caroline Spike, Todd Starich, Mary Kosinski, and Ikuko Yamamoto who helped me with experimental trouble-shooting and shared fun at work.

I want to thanks my friends Leilei Gong, Xin Hong, Mengnan Tian, Guijin Zheng, Becky Liu, Yi-Ru Zhao, Jie Gu for all the emotional support, entertainment, and caring that they provided. I want to thank them for their lasting friendships and for always being there for me when I need help.

Finally, I want to thank my husband Hanjian Liu. I count myself as a lucky person to have Hanjian in my life. Hanjian is always the strength and asset for me. Without Hanjian's understanding and support, it would have been impossible for me to finish this work. I also want to thank my brother ZhaoBin Cheng, and sister ZhaoXia Cheng for being my best friends and for their continuous support and for taking care of my parents when I was away for pursuing my dreams. I want to thanks my parents YanLan Pu and WangJin Cheng for their love and support. They have always supported and encouraged me to do my best in all matters of life. To all the people I love I dedicate this thesis.

TABLE OF CONTENTS

Page

ACKNOWLEDGMENTS……iii

LIST OF TABLES……...vii

LIST OF FIGURES……viii

LIST OF ABBREVIATIONS……..xii

Chapter

I. INTRODUCTION……..1

The regulation of meiotic maturation…..……2
Meiosis……..……...5
Oocyte meiotic maturation……..……..23
C.elegans as a model organism for studies of oocyte meiotic maturation ……..……38
Eph receptor signaling……...49
G protein signaling……..……...69
Receptor trafficking and signaling……...74
Receptor trafficking regulates signaling……..……..74
Endocytosis and intracellular trafficking……..……..83
Clathrin-dependent endocytosis and its signaling……..……83
Caveolae-mediated endocytosis……..……95
Vesicle Transport and Trafficking……..…98

II. IDENTIFICATION OF NEGATIVE REGULATORS OF OOCYTE MEIOTIC MATURATION.....107

Introduction.....107
Materials and methods.....110
Results.....113
Discussion.....150

III. REGULATED TRAFFICKING OF THE MSP/EPH RECEPTOR DURING OOCYTE MEIOTIC MATURATION IN *CAENORHABDITIS ELEGANS*

Introduction.....154
Materials and methods.....159
Results.....169
Discussion.....206

IV. GENERAL DISCUSSION AND FUTURE DIRECTIONS.....212

REFERENCES.....226

LIST OF TABLES

Table Page

1. Localization and function of Rab proteins.……...105
2. Negative regulators of meiotic maturation identified in genome-wide RNAi screen……..……...119
3. Class II negative regulators identified in the genome-wide RNAi screen……..……....122
4. Parsing the function of negative regulators to the germline or soma……..……131
5. Effect of *vab-1* and *ceh-1* mutations on meiotic maturationrates following RNAi of class I genes in the absence of sperm……..136
6. Genetic analysis of G-protein signaling……142
7. *gsa-1* is necessary and sufficient to promote oocyte meiotic maturation. ……..…149
8. Summary of VAB-1::GFP localization experiments……196

LIST OF FIGURES

Figure Page

1. The cell divisions of meiosis…….....3
2. Pathways of double-strand break (DSB) and DSB repair……..…9
3. Synaptonemal complex structure…….……11
4. Cohesin complex and meiosis…….….17
5. Kinetochore structure…….21
6. Oocyte meiotic maturation and egg activation……...25
7. Development of the mammalian ovarian follicle……..….27
8. Activation of Maturation promoting factor……...…31
9. Mammalian oocyte meiotic arrest and resumption…….33
10. Image of a *C. elegans* hermaphrodite……..…41
11. The Structure of Adult Hermaphrodite Gonad……..……..…43
12. A sperm-sensing control mechanism regulates oocyte meiotic maturation and MAPK activation…….…….47
13. A schematic diagram of ephrin and Eph structure…….…….53
14. ephrin-Eph interaction……...57
15. Bidirectional signaling of Eph receptor…….….61

16. Two models of how attraction turns to repulsion……..65

17. G protein signaling……..…….…71

18. Endocytic trafficking regulates TGFβ signaling…….....77

19. Intracellular trafficking regulates Hedgehog signaling……..……..79

20. Intracellular trafficking regulates Notch signaling……....81

21. Clathrin-dependent endocytosis processes…….……...85

22. Clathrin and AP2……..…….…87

23. Endocytic trafficking……..……....99

24. Vesicle fusion……..…….……103

25. A genome-wide RNAi screen for negative regulators of oocyte meiotic maturation…….……....115

26. RNAi of several negative regulators causes MSP-independent MAPK activation in oocyte……..…….....117

27. Genetic and Biochemical analysis of the VAB-1 Eph/MSP receptor pathway…….…….……125

28. Gαo/i and Gαs signaling antagonistically regulate oocyte MAPK activation…….……....129

29. Expression of GOA-1 in the soma is sufficient to inhibit MAPK activation in oocytes…….……..…..133

30. A model for the parallel control of meiotic maturation in *C. elegans* by antagonistic G protein signaling from the soma and an oocyte MSP/Eph receptor pathway..…… …….. 143

31. *vav-1,pqn-19, pkc-1,* and *dab-1* negatively regulate oocyte MAPK activation in parallel to *ceh-18*…….. 145

32. Oocyte MAPK activation in *goa-1(n1134)* hermaphrodites and females is dependent on OMA-1/OMA-2 function……...147

33. A model for the control of meiotic maturation in *C. elegans* by an oocyte MSP/Eph receptor pathway and antagonistic G-protein signaling from the soma……...157

34. MSP/Sperm alters the localization of the VAB-1 MSP/Eph receptor……..……..……..……..……171

35. MSP signaling affects the accumulation of VAB-1::GFP in recycling endosomes……..……...175

36. DAB-1 and RAN-1 affect VAB-1::GFP trafficking in the absence of MSP/sperm……193

37. DAB-1 and RAN-1 bind to the VAB-1 intracellular domain……197

38. A model for VAB-1 trafficking and signaling in the control of meiotic maturation……207

39. VAB-1::GFP localization to early endosomes is MSP/sperm-independent……..…..177

40. Localization of VAB-1::GFP in hermaphrodites is regulated by *rab-11.1* and *rme-1*……..……181

41. *vps-28* and *vps-37* promote VAB-1::GFP degradation in the embryo……..……..……..……..……...183

42. Spermatozoa localize to the spermatheca and release MSP in *rme-1(b1045)* mutants……..187

43. Localization of VAB-1::GFP is ephrin independent……...191

44. Specificity of anti-Ran antibodies……...……..…201

45. GSA-1, INX-22 and OMA-1/2 affect VAB-1::GFP localization……..…203

46. VAB-1::GFP vesicle purification……..…217

LIST OF ABBREVIATIONS

SC synaptonemal complex

DSB double strand break

MPF M-phase promoting factor / maturation promoting factor

ACY adenylyl cyclase

Cdk1 cyclin dependent kinase 1

RINGO rapid inducer of G2/M progression in oocytes

cAMP cyclic adenosine monophosphate

DAG diacylglycerol

IP3 inositol triphosphate

LH luteinizing hormone

MAPK mitogen activated protein kinase

PKA/PKC protein kinase A/ protein kinase C

MSP major sperm protein

APC/C anaphase promoting complex/Cyclosome

CSF cytostatic factor

M I meiosis I

M II meiosis II

CamKII camodulin depedent kinase II

FGF fibroblast growth factors

EGF Epidermal growth factor

TGFβ Transforming growth factor β

Ptc patched

Smo Smothen

Hh Hedgehog

Ub Ubiquitin

GEF guanine nucleatid exchange factor

GAP GTPase activating protein

CHAPTER I

INTRODUCTION

This dissertation focuses on intracellular and intercellular signaling during meiosis. Meiosis is a conserved biological process that all sexually reproductive animals use to generate haploid gametes (sperm or oocyte) from a diploid individual. Defects in meiosis might produce aneuploid gametes, which are the leading genetic causes of human infertility, pregnancy losses, and congenital birth defects. Since the mechanisms that regulate meiosis are extraordinarily conserved among species, studies in model organism like *Caenorhabditis elegans* can provide insights into meiotic errors in humans. My dissertation work suggests that the trafficking of an integral membrane protein within the oocyte regulates this protein function during meiosis. This work provides new insights into the control mechanisms that regulate meiotic progression, with potential information concerning this receptor signaling in vertebrate systems. To introduce this study and help you understand my experiments, I shall present a brief overview of meiosis, with particular emphasis on the meiotic stages that I have been studying and the mechanisms that control this biological process. I will also introduce some background on the protein that I have been studying and the intracellular trafficking that regulates the function of this receptor within the oocyte.

The Regulation of Meiotic Maturation

In sexually reproducing organisms, a diploid germ cell (2n) uses meiosis to generate haploid gametes (1n), which reunite to form a diploid organism (2n) by fertilization. In meiosis, a germ cell (2n) first replicates its DNA, which is then followed by two rounds of cell divisions without an intervening S-phase. In the first meiotic division, which is termed the reductive division, homologous chromosomes segregate from each other. The daughters therefore have a haploid number of chromosomes but a diploid amount of DNA. At meiosis II, which is called the equational division, and which does not involve DNA replication, the daughter cells undergo a mitosis-like division, which separates sister chromatids (Fig. 1). To ensure the faithful segregation of homologous chromosomes, three meiosis-specific steps are carried out at meiotic division I: 1). homolog pairing and the formation of synaptonemal complex; 2). meiotic recombination that locks the homologous chromosomes together; and 3). separation of homologous chromosomes to opposite poles of the meiotic spindle at the end of meiosis I (Fig. 1) (reviewed by Champion and Hawley 2002). These well regulated steps help ensure that all the gametes inherit exactly one copy of each homologous chromosome pair. Problems that arise during meiosis may result in missegregation of the chromosomes, which can lead to infertility, miscarriage, or birth defects such as Down syndrome (trisomy 21; reviewed by Hassold and Hunt 2001; Wolstenholme and Angell 2000; Sanderson et al., 2008). Thus, understanding the underlying mechanisms of meiosis is very important for identification of new therapies to cure human infertility, and avoiding pregnancy losses and congenital birth defects.

Figure 1. The cell divisions of meiosis

One pair of homologous chromosomes is shown in each cell. At premeiotic phase, each chromosome duplicate to produce two sister chromatids, which are held together by cohesin. At meiotic prophase each chromosome pairs with its homologous chromosome to generate a bivalent structure that contains four chromatids. Genetic recombination occurs between paired homologous chromosomes. At meiotic metaphase I, paired homologous chromosomes align at the metaphase plate, and the meiotic spindle forms. At meiotic anaphase I, homologous chromosomes separate from each other and move towards the spindle poles, while the sister chromatids are still held together by cohesin at the centromere. Cytokinesis occurs and one cell divides into two cells with the haploid chromosomes number and diploid amount of DNA. Completion of first meiosis, followed by second meiosis, which is mitosis-like division soon after. In meiosis II, the cohesin at the centromeres is dissolved, causing the two sister chromatids to separate from each other. Adapted from Molecular Biology of the Cell, Garland Publishing, NY, 1994.

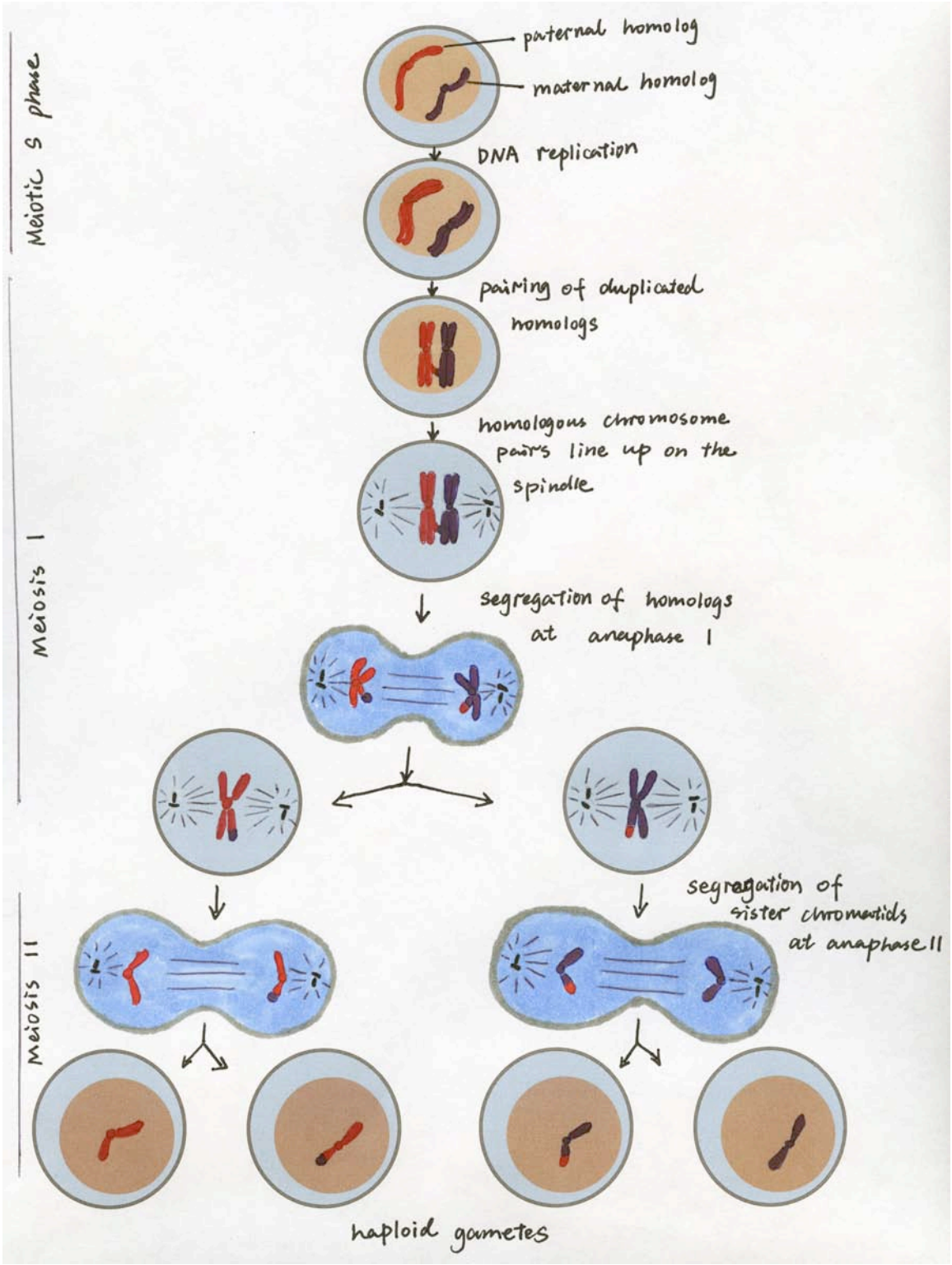
Meiotic S phase
Meiosis I
Meiosis II
paternal homolog
maternal homolog
DNA replication
pairing of duplicated homologs
homologous chromosome pairs line up on the spindle
segregation of homologs at anaphase I
segregation of sister chromatids at anaphase II
haploid gametes

Meiosis

Meiosis I starts with prophase I, in which duplicated homologous chromosomes pair with each other, followed by formation of a specialized structure, called the synaptonemal complex, and genetic recombination between homologs. The next phase of meiosis I is meiotic metaphase I, in which the homologous chromosomes align along an equatorial plane that bisects the spindle, a structure formed with microtubule fibers during cell division. Anaphase I is the stage that follows metaphase I, in which homologous chromosomes separate from each other to form two haploid sets. The last phase of meiotic division I is telophase, in which homologs arrive at the spindle poles. At the end of telophase, a new nuclear membrane surrounds each haploid set and cytokinesis, the pinching of the cell membrane, occurs to complete the creation of two daughter cells. Thus meiosis I generates two daughter cells that each have half the number of chromosomes but each chromosome consists of a pair of chromatids (Fig. 1). Because my dissertation work is focusing on the process that occurs during meosis I, it is very necessary for me to explain what happens in meiosis I: How do homologous chromosome pair? What holds them together at metaphase I to ensure the faithful segregation of homologs? How do homologs separate from each other at the end of meiosis?

Matching duplicated homologous chromosomes is the first step of meiosis I. The homologous chromosomes recognize each other and align along their lengths forming transient interactions. How the homologous chromosomes identify each other is not so clear, and the underlying mechanisms vary between organisms (reviewed by Gerton and Hawley 2005). Several mechanisms have been suggested to contribute to homolog

recognition, including specialized pairing centers and telomere clustering (reviewed by Gerton and Hawley 2005). Studies from *C. elegans* and *Drosophila* suggest that homolog-recognition regions play important roles (McKim and Hayashi-Hagihara 1998; McKim et al., 1993). Several specific homologous recognition regions have been identified at the end of each chromosome in *C. elegans* (Dernburg et al., 1998). Only chromosomes bearing homologous recognition regions are capable of homologous pairing and recombination (McKim et al., 1988, and 1993). In organisms with a heterogametic sex (eg. XY), pairing of sex chromosomes, which occurs between non-homologous chromosomes, is regulated by rDNA regions and a pseudoautosomal region of the sex chromosomes (McKee and Karpen, 1990; McKee et al., 1992). In *Drosophila*, mitotic cells exhibit high levels of homologous alignment, and the gametocytes have already undergone homologous chromosome alignment before meiosis begins (Metz 1926). In *S. pombe*, centromere association plays an important role during homolog pairing: the centromeres of homologous chromosomes pair with each other and mediate bipolar attachment to the spindle pole at meiosis I (Ding et al., 2004). The same study, as well as other investigations, also suggests that telomeres cluster at the periphery of the nuclear envelope, and bring the homologs together to facilitate alignment (Ding et al., 2004; Chikashige et al., 1994, 1997; Cooper et al., 1998; Nimmo et al 1998). Disruption of telomere clustering results in decreased homolog recombination. This obeservation indicates that telomere clustering facilitates homologous alignment, which is important for recombination (Cooper et al., 1998; Nimmo et al 1998). Studies from a number of organisms, including *Drosophila* and humans suggest that different chromosomes occupy particular domains within the nucleus, and chromosome territories are involved in

maintaining homolog alignment and pairing. In humans and *Drosophila* spermatogonia, homologous chromosomes are separated into regions, and these chromosome territories promote the maintenance of chromosome pairing (Vazquez et al., 2002; Scherthan et al., 1996). This early pairing brings the homologous chromosome close to each other and aligns them roughly along their lengths.

Double strand breaks (DSBs), which initiate meiotic recombination (see below), play a very important role in promoting homologous alignment and pairing in some species, such as yeast, mice and human, but double strand breaks are dispensable for synapsis and synaptonemal complex formation in other species, including *C. elegans* and *Drosophila* (reviewed by Page and Hawley 2003). Meiotic recombination is initiated by double strand breaks, introduced by Spo11, a topoisomerase type II-like protein. Depletion of Spo11 in yeast or mice results in reduced synapsis between homologous chromosomes but does not affect pairing and synaptonemal complex formation in *C. elegans* and *Drosophila* (Giroux et al., 1989; Romanienko et al., 2000, Dernburg et al., 1998; McKim and Hayashi-Hagihara 1998). Spo11 introduces a DSB probably by using its catalytic site tyrosine to nucleophilically attack the phophodiester backbone of the DNA. After breaking the double strand of DNA, Spo11 remains covalently bound to the 5' end of each single strand DNA overhangs (Fig. 2). Resection of the 5' end of the DSB requires a conserved DNA repair protein complex Rad50-Xrs-Mre11. The resection of the duplex ends exposes the 3' single stranded tail, which will search for and interact with its homologous DNA. Homologous DNA searching is facilitated by Rad51 and Dmc1, which bind to the 3' DNA tail (Fig. 2). The interaction of the 3' single stranded tail with its homologous DNA allows homologous pairing to occur (Fig. 2). As several DSBs and

homology-searching occur along the chromosome, the chromosome axes become stably aligned (Tesse et al., 2003). Depletion of Rad51, a DSB repair protein, results in reduced recombination in *S. cerevisiae,* and ablation of Dmc1, a DSB repair protein, eliminates synapsis of homologous chromosomes (Cohen et al., 2002; Dresser et al., 1997).

After establishment of transient, rough pairing between the homologous chromosomes, synapsis occurs to stabilize the intimate association of the homologs along their lengths. Synapsis involves the assembly of the synaptonemal complex, which is a meiosis-specific proteinaceous structure that links the cores of paired homologous chromosomes (Fig. 3). During synapsis, homologous chromosomes are aligned along their lengths and are attached in the synaptonemal complex, which is a tripartite structure consisting of two lateral elements and a central element (Fig. 3). The lateral elements are derived from the axial elements of the homologous chromosomes, and the lateral elements are connected to transverse filaments. The structural constituents of lateral elements include synaptonemal complex protein 2 (SCP2) and SCP3 in mice, both of which are putative DNA binding proteins. SCP2 and SCP3 are essential for lateral element formation, since inactivation of *scp3* in mice results in elimination of lateral elements and causes homolog pairing abnormalities (Yuan et al., 2000; 2002). Red1p, Hop1p and Mek1p have been suggested to be the lateral element proteins in *S. cerevisiae* (Hollingsworth et al 1990; Smith and Roeder 1997). *red1p* mutants do not form lateral elements, whereas *hop1p* mutants display abnormal lateral elements (Loidl et al 1994; Rockmill and Roeder 1990); homolog pairing is reduced in both *red1p* and *hop1p* mutants. The transverse filaments contain SCP1 in mammals and Zip1p in yeast.

Figure 2. Pathways of double-strand break (DSB) and DSB repair

A DSB is initiated by Spo11. After DSB break, Spo11 binds to 5' end of the ssDNA strand overhangs. The resection of 5' end of the DSB requires a conserved DNA repair protein complex-Rad50-Xrs-Mre11. Dmc1 and Rad51, two RecA homolog, binds to the 3' end of ssDNA and perform homolog searching. The Dmc1-Mei5-Sae3 together with Mnd1-Hop2 complexes mediates stable invasion of 3'-single stranded DNA to the homologous chromosome, resulting in a D-loop structure formation. Once the 3' end tail recognizes its homolog, 3' end tail annealing to the homologous DNA and starts to DNA repair using the homologous DNA as a template. DNA repair synthesis results in the extending the 3' end DNA strand tail and filling in the single strand gaps. This results in formation of holliday junctions. Modified from Gerton and Hawley 2005.

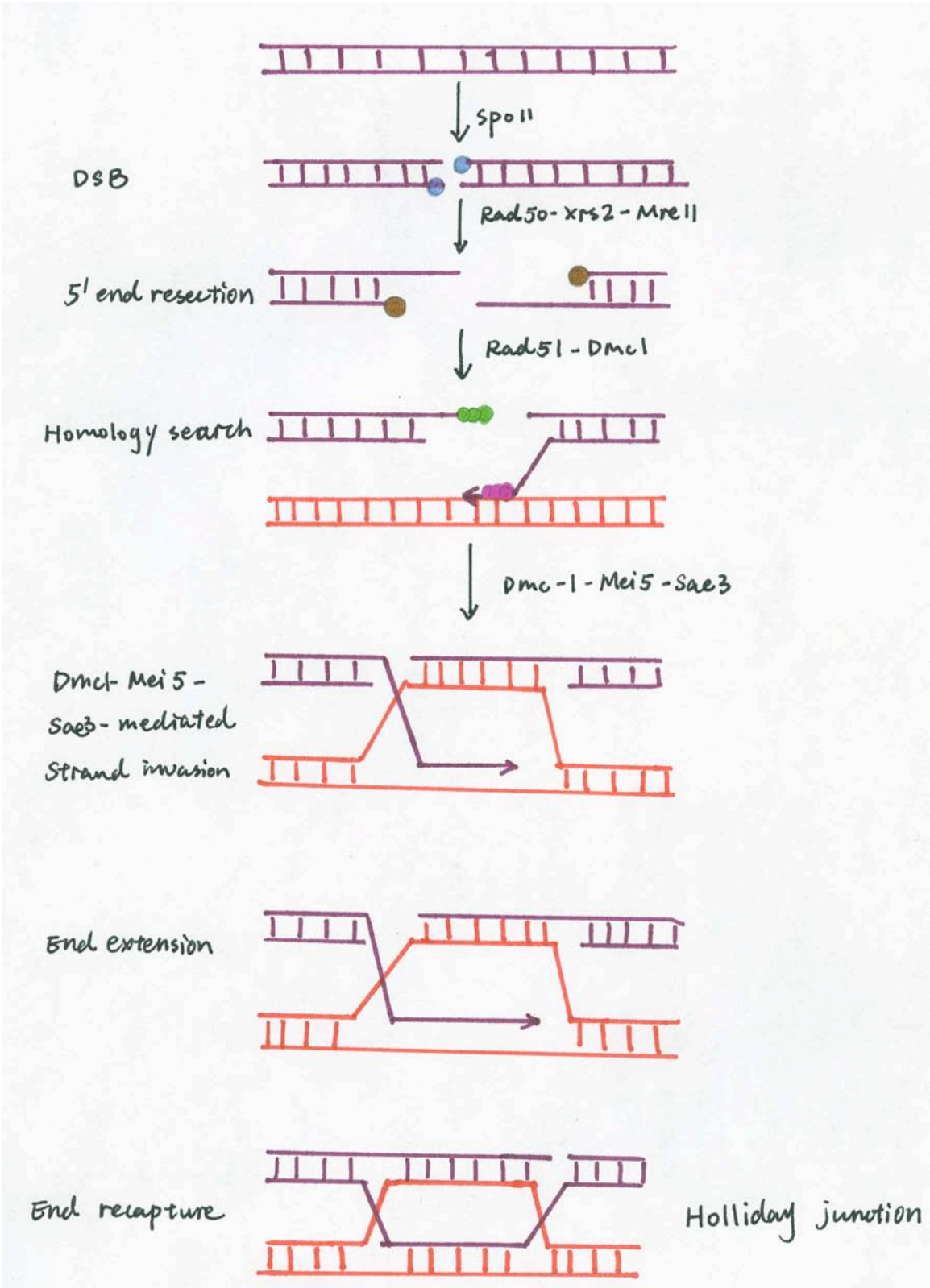
Spo11
DSB
Rad50-Xrs2-Mre11
5' end resection
Rad51-Dmc1
Homology search
Dmc-1-Mei5-Sae3
Dmc1-Mei5-
Sae3-mediated
Strand invasion
End extension
End recapture
Holliday junction

Figure 3. Synaptonemal complex structure

A. Synaptonemal complex (SC) of *C. elegans* visualized by TEM. SC comprised of a central region and a pair of lateral elements. Scale bar equals 500 nm. Reprinted from Colaiacovo, 2006.
B. Schematic graph of synaptonemal complex. SC composed of the lateral elements (red) that anchor the chromatin loops and a central element (blue), transverse filaments (black lines). Modified from Molecular Biology of the Cell, Garland Publishing, NY, 1994.
C. Molecules within a synaptonemal complex. Transverse filament (TF) protein molecules structure is shown to the left. TF proteins interact with axial element (or lateral element) of one chromosome and another TF element that are attached to the homologous chromosome. Genetic recombination occurs between homologs. Modified from Heyting, 2005.

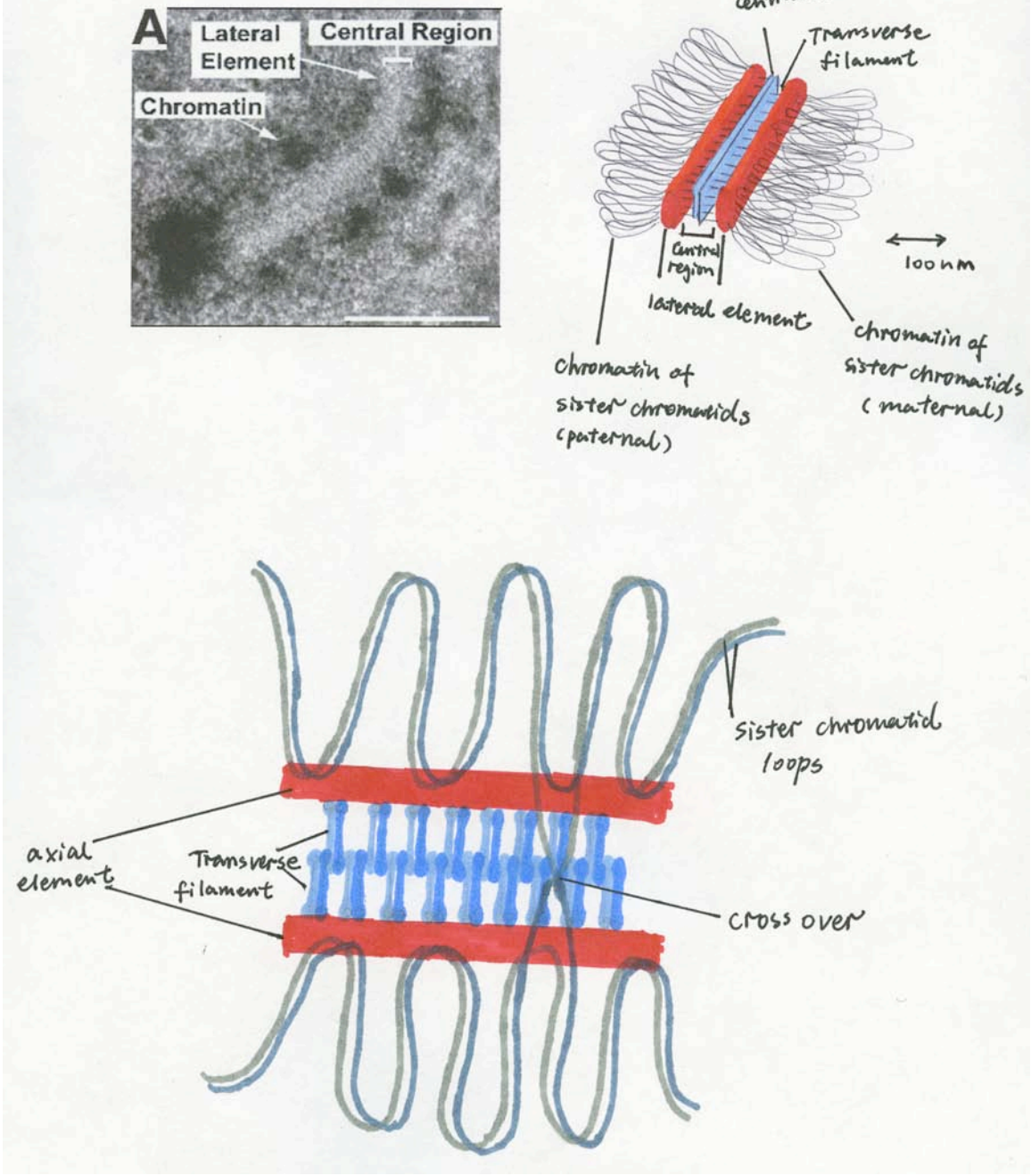
A
Lateral Element
Central Region
Chromatin
central element
Transverse filament
Central region
100 nm
lateral element
chromatin of sister chromatids (maternal)
Chromatin of sister chromatids (paternal)
sister chromatid loops
axial element
Transverse filament
cross over

Although SCP1 and Zip1p do not share sequence similarity, the transverse filaments they form have structural similarities. These transverse filament proteins form dimers through their coiled coil regions, and interact with lateral elements through their C termini, and interact with opposing dimers through their N-termini (Dong and Roeder 2000). The localization of SCP1 is independent SCP3, since in SCP3 mutant mice, SCP1 still localizes to the short fragmented fibers between homologous chromosomes (Yuan et al 2000). Transverse filaments play important roles for crossover maturation; and disruption of Zip1 in yeast or *c(3)G* in *Drosophila* blocks crossover events (Borner et al., 2004).

Beside its important role in homologous chromosome pairing, DSBs also induce genetic recombination. Once the appropriate homolog is identified, genetic recombination occurs. DSBs have been shown to initiate cross overs in yeast, *Drosophila*, *C. elegans* and mammals (Lichten and Goldman 1995; Keeney et al., 1997; McKim and Hayashi-Hagihara 1998; Dernburg et al., 1998; Romanienko and Camerini-Ostero 1999). Artificially inducing DSBs by γ ray radiation can produce meiotic cross overs, bypassing the requirement for Spo11 (Dernburg et al., 1998). Crossing over is facilitated by many proteins that function in the DSB repair pathway, including Dmc1, Rad51, Mei5, Sae3, Mnd1, and Hop2 (Fig. 2). Rad51 is a homolog of eukaryotic RecA that catalyzes homology search and DNA strand exchange, and Rab51 participates in homologous recombination and DSB repair both in mitosis and meiosis. Yeast lacking Rad51 exhibit reduced meiotic recombination compared to the wild type (Cohen et al., 2002). Dmc1, a homologue of *E. coli* RecA, is a meiosis specific DNA strand exchange protein, and Dmc1 forms a complex with Mei5 and Sae3 (Dresser et al., 1997; Hayase et al., 2004). The Dmc1-Mei5-Sae3 complex, together with a Mnd1-Hop2 complex,

mediates stable invasion of 3' single stranded DNA into the homologous chromosome, resulting in the formation of displacement-loop structure at the homologous duplex (Fig. 2). After invading the homologous chromosome, the 3' DNA strand acts as a primer to initiate DNA repair synthesis using the displacement loop of the homologue as a template, which results in extending the 3' DNA strand tail and filling in the single strand gaps. This results in formation of a Holliday junction, in which strands are exchanged between the interacting duplexes (Fig. 2). Two Holliday junctions form a double Holliday junction (reviewed by Cromie and Smith 2007). Deletion of Dmc1, Mei5, Sae3, Mnd1, or Hop2 in yeast or mice leads to a reduction of homologous synapsis and recombination to similar extents (Rabitsch et al., 2001; Leu et al., 1998; Petukhova et al., 2003; Zierhut et al., 2004). In principle, recombination might occur between homologues or between sister chromatids, or even between ectopic locations that share some homology. To ensure that DNA-exchange only happens between homologs, meiotic cells need a specific mechanism to regulate this recombination. Dmc1, Red1, Hop1, and Mek1 have been reported to regulate this interhomologue recombination in *S. cerevisiae*, and depleting any of these proteins decreases the number of DSBs and increases the incidence of intersister chromatid recombination, resulting in meiotic missegregation defects (Schwacha and Kleckner 1997; Bishop et al., 1999; Wan et al., 2004; Niu et al., 2005). Besides its involvement in DSB initiation and repair pathways, the synaptonemal complex has been suggested to be required for meiotic cross overs in *Drosophila* and yeast. Depletion of the synaptonemal complex protein *c(3)G*, a transverse filament component, abolishes synaptonemal complex formation and meiotic recombination (reviewed by Rasmussen and Holm, 1984; Smith and King 1968).

Meiotic recombination does not occur at a uniform rate along the homologous chromosomes. On the contrary, DSBs concentrate at particular sites called hotspots, where cross overs take place. Genome-wide studies in *S. cerevisiae* using Spo11-based chromatin immunoprecipitation suggest that DSB hotspots tend to occur in the promoter regions and are suppressed at the centromeric and telomeric domains (Wu and Lichten 1994). The total number of crossovers is low, but even small chromosomes receive at least one crossover. This is because too many cross-overs would result in chromosome instability and failure to segregate properly (Koehler et al., 1996). Once an obligate crossover per chromosome occurs, a gradient of suppression around each crossover decreases the possibility of additional crossovers at nearby regions, which is a phenomenon called crossover interference. This crossover interference ensures that genetic crossovers are spread out throughout the chromosome. The synaptonemal complex has been reported to mediate this crossover interference (Sym and Roeder 1994).

The crossover event produces a connective structure, visualized microscopically as a chiasma, between the two homologues (Fig. 3). The chiasma structure holds the oriented homologous chromosomes on the meiotic spindle during metaphase I. As I mentioned previously, the faithful segregation of homologous chromosomes requires homologous chromosome pairing and formation of chiasmata to lock the paired homologs together. During prometaphase, chromosomes are organized relative to the developing spindle; chiasmata lock the bivalents and orient the two homologous centromeres such that they face opposite spindle poles (McKim and Hawley 1995). The oppositely oriented centromeres then attach to the closest meiotic spindle.

Cohesin plays a critical role in chromosome segregation at meiosis. As mentioned above, cohesion is required for the lateral elements of the synaptonemal complex. Meiosis cohesion proteins comprise Rec8, Stag3, Smc1β, SA3. It has been proposed that the cohesin complexes form a ring structure that associates with sister chromatids (Fig. 4). To ensure proper chromosome segregation in both meiotic divisions, sister chromatid cohesion needs to be released at two distinct steps (Buonomo et al., 2000). First, cohesin needs to be released at the chromosome arms, but must remain attached at the chiasma and centromeres at metaphase I. At the onset of anaphase I, the cohesin protein Rec8 between chiasmata are cleaved by separase, but the cohesin between centromeres is still preserved, which holds sister chromatids together as they move towards the spindle pole (Fig. 4). Centromeric cohesion at meiosis I is protected by the centromeric protein shugoshin (Shugoshin means "guardian spirit" in Japanese; Ishiguro and Watanabe 2007). At anaphase II, cohesin between sister centromeres is dissolved by separase, which causes separation of sister chromatids (Fig. 4). Thus, Rec8 along the chromosome arm region and the centromeres is cleaved in a stepwise manner in two successive stages of meiosis. The release of cohesin at the centromeres at meiosis I results in premature separation of sister chromatids and missegregation of homologs, which causes non-disjuntion (Bickel et al.,2002).

To ensure the faithful segregation of homologous chromosome during meiosis I, a bipolar meiotic spindle needs to form. The microtubule arrays of the bipolar spindle attach to the kinetochores of the homologous chromosomes. In the oocytes of humans, nematodes, and many insects, meiotic spindles form in the absence of centrosomes and centrioles, which are the microtubule organization centers in mitotic cells.

Figure 4. Cohesin complex at meiosis

Cohesin complex is localized along the sister chromotids at meiotic prophase. At metaphase I, the cohesin along the sister chromatid arms are resolved, but the arm cohesin distal to chiasmata is still intact for holding the homologs together. At anaphase I, separase gets activated and cleaves the arm cohesin distal to the chasmata. The cohesin complex at the centromere region is protected by Sgo, therefore centromere cohesin is preserved to hold the sister chromatids together at the end of meiosis I. At anaphase II, the separases gets activated again and dissolves the cohesin at the centromeres, which leads to the separation of sister chromatids. Adapted from Amon lab homepage.
http://web.mit.edu/amonlab/research.htm

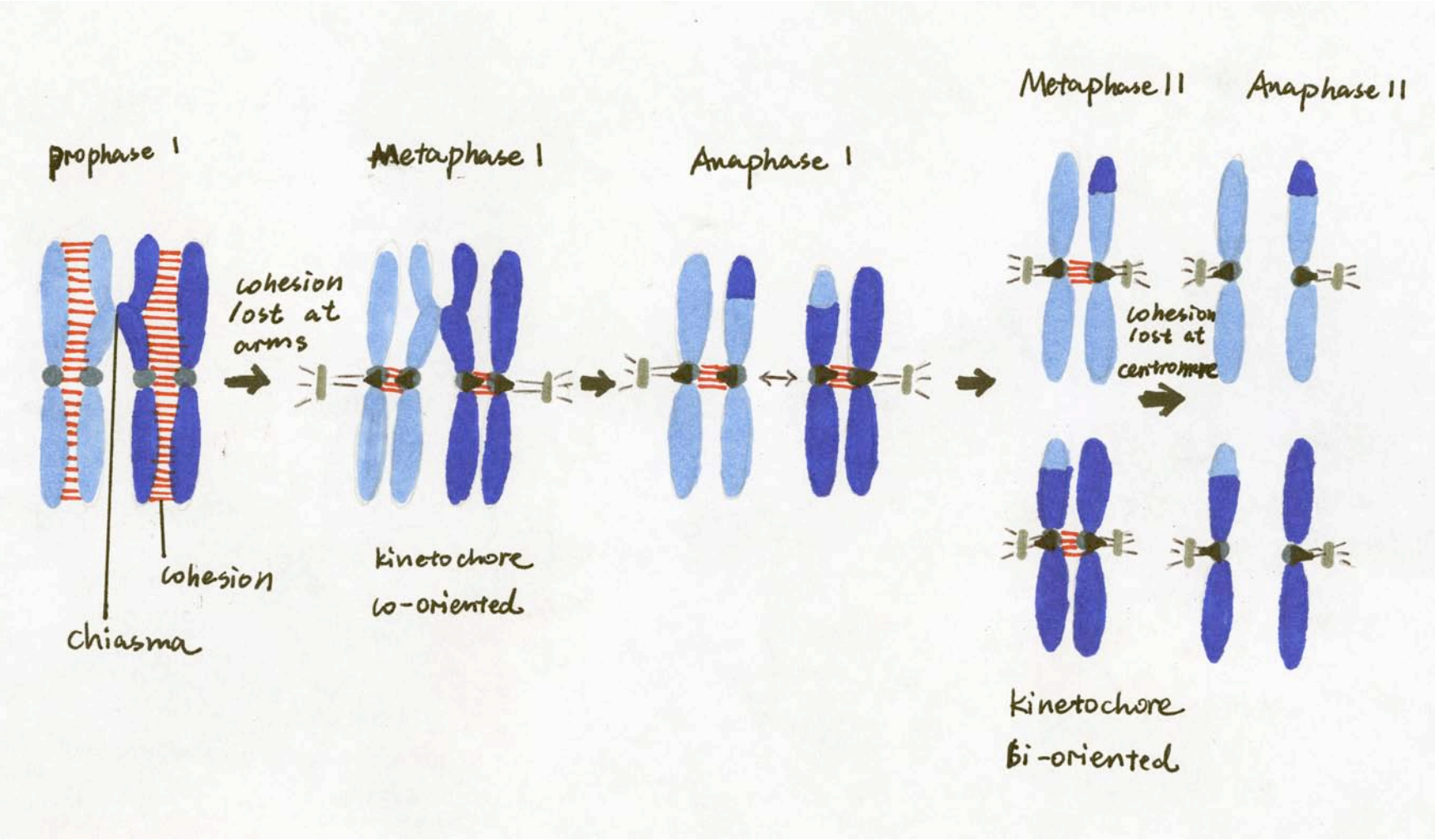
Prophase I
Metaphase I
Anaphase I
Metaphase II
Anaphase II
cohesion lost at arms
cohesion
Chiasma
kinetochore co-oriented
cohesion lost at centromere
kinetochore Bi-oriented

Acentriolar spindle formation starts with a mass of microtubules attaching to the chromosomes; and chromosomes functions as the microtubule nucleation center to form the bipolar spindle (McKim and Hawley 1995). This hypothesis is supported the observation that one chromosome is sufficient to form a bipolar spindle in *Drosophila* and other organisms (Theurkauf and Hawley 1992; and Waters and Salmon 1995). DNA coated beads can nucleate acentriolar spindle in Xenopus egg extract (Hecld et al.,). At the assembly of the meiotic spindle, a tight link between kinetochores and microtubules needs to be established. The microtubule motor protein dynein plays an important role in meiotic spindle formation, and disruption of microtubule components leads to meiotic arrest due to the activation of spindle assembly checkpoint (described beblow) (Brunet and Maro 2005). Kinetochore structures are critical for correct chromosome segregation. The kinetochore is a trilaminar structure that localizes at the centromeres of each sister chromatid and interacts with the plus ends of the spindle microtubules (Fig. 5). The trilaminar structure of kinetochores consists of an inner layer containing conserved centromere proteins (CENPs), an outer layer containing microtubule interacting proteins, such as CENP-E, and spindle assembly checkpoint proteins. Kinetochores capture microtubules to form kinetochore fibers, and align and biorient homologous chromosomes at the spindle equator under spindle tension. Chiasmata hold the homologous chromosomes together and resist the pulling force of the spindle microtubules toward the poles until anaphase begins. Once the chromosomes are under full tension of spindle fibers, the spindle assembly checkpoint is released and anaphase starts. Alterations of kinetochore-microtubule tension will trigger the spindle assembly checkpoint and result in delayed anaphase entry (Kapoor et al., 2000). The poleward

movement of chromosomes is mediated by kinetochore proteins including dynein, CENP-E, and MCAK. CENP-E regulates chromosome alignment, and dynein promotes the movements of the chromosome towards the spindle pole (Wood et al., 1997). MCAK promotes disassembly of kinetochore-fibers, which are the microtubules that attach to the kinetochore, to power chromosome poleward movement. The spindle assembly checkpoint mechanism proteins such as Mad1, Mad2, BubR1, Bub1, Bub3, and Mps1 are known to be recruited to the kinetochore before the onset of metaphase. The spindle assembly checkpoint proteins monitor the attachment and tension of microtubules to the kinetochore, therefore, ensuring accurate chromosome segregation by delaying anaphase until all the chromosomes are correctly aligned on the metaphase plate. Specifically, the spindle assembly checkpoint prevents anaphase by inhibiting the anaphase-promoting complex/cyclosome (APC/C), whose activity is required for onset of anaphase. The APC/C is a multisubunit E3 ubiquitin ligase that triggers degradation of multiple substrates. APC/C catalyzes the assembly of polyubiquitin chains on substrate proteins, which targets them for degradation by the 26S proteasome. Upon release from the spindle assembly checkpoint, the APC/C targets proteins such as cyclin B and securin for degradation. The degradation of securin causes activation of separase, which cleaves cohesion proteins Rec8 at the chiasma (reviewed by Peters 2006)(Fig. 4). Cohesin cleavage releases the homologous chromosomes, and chromosomes undergo poleward movement by the tension of the spindle fiber.

My dissertation work focuses on a stage of meiotic prophase I during oogenesis, termed meiotic maturation, which defines the transition from prophase to metaphase I.

Figure 5. Kinetochore structure

Kinetochore localizes at the centromeres of each sister chromatid and interacts with the plus ends of spindle microtubules. Adapted from http://www.colorado.edu/MCDB/MCDB1150/ohd/kinetochoreattach.jpg

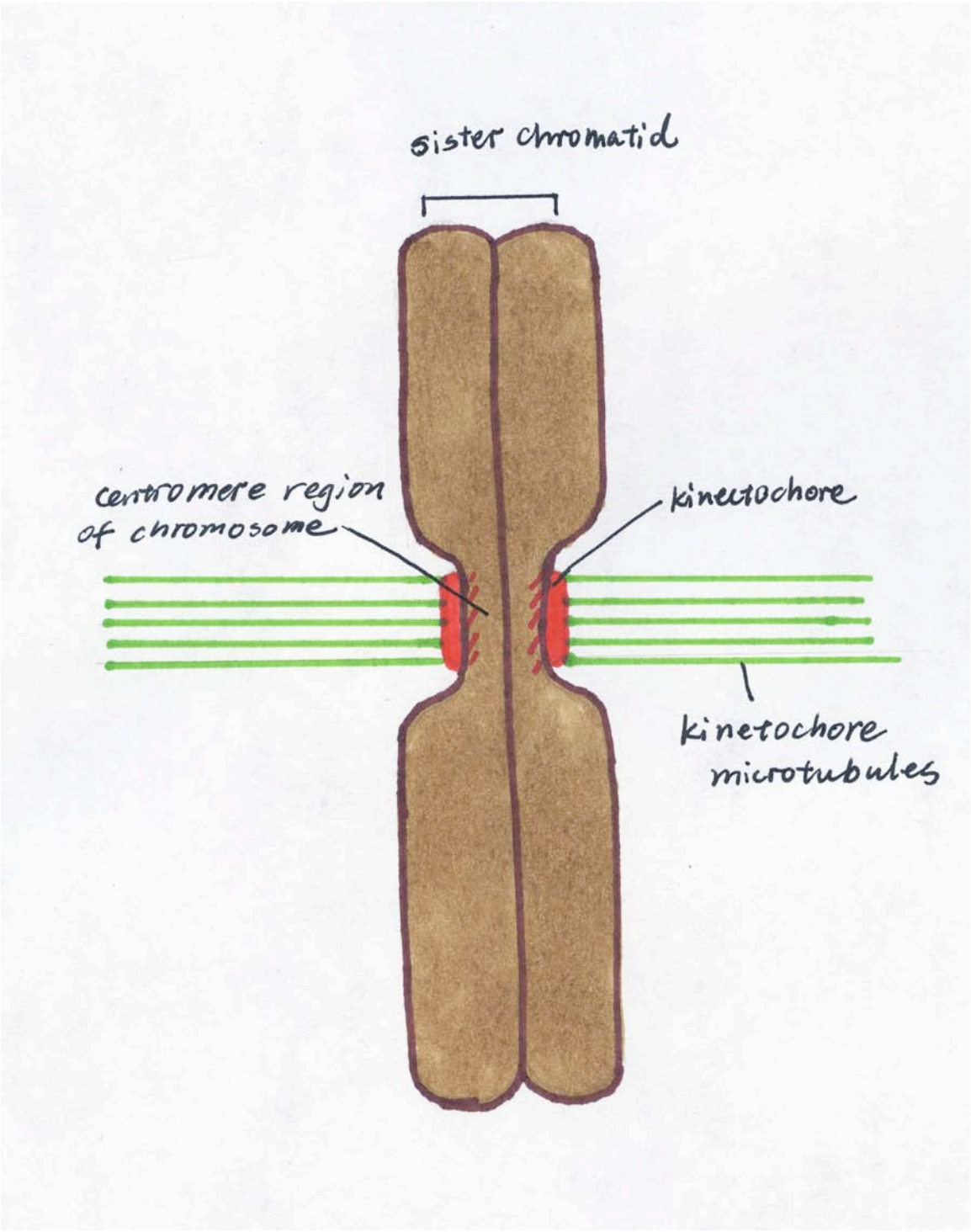
sister chromatid
centromere region of chromosome
kinetochore
kinetochore microtubules

In most female animals, oocytes arrest at meiotic prophase I for a prolonged time and resume meiosis in response to hormonal signaling. I have used *C. elegans* as a model organism to study this conserved biological process. To help you understand what mechanisms regulate this meiotic arrest, and what mechanisms release this meiotic arrest, I will explain meiotic arrest and meiotic maturation and the underlying mechanisms by comparing the known molecular pathways in several mammalian and non-mammalian systems.

Oocyte meiotic maturation

In most female animals, oocytes arrest at meiotic prophase I for a prolonged time and resume meiosis in response to hormonal signaling. The process by which oocytes transit from prophase I to metaphase I is called oocyte meiotic maturation. Meiotic maturation is accompanied by nuclear envelope breakdown, meiotic spindle formation, and cytoskeletal changes. Oocyte meiotic maturation must be temporally coordinated with oocyte growth and ovulation in order to prepare the oocytes for fertilization and subsequent embryogenesis. Therefore, intercellular and intracelluar signals need to function together to regulate oogenesis. After completion of the first meiotic division, oocytes get released from the ovary through ovulation. In mammals, including humans, mature oocytes arrest again at metaphase II until fertilization (Fig. 6). Although the time length of oocyte meiotic arrest varies among species, the underlying mechanisms that regulate oocyte meiotic arrest and meiotic maturation are strikingly conserved (reviewed by Masui 2001). In this section, I will explain the mechanisms that regulate meiotic I

arrest (primary arrest) and meiotic II arrest (secondary arrest) and the mechanisms that regulate the release of these two meiotic arrests. My dissertation has been focused on the primary oocyte meiotic arrest in *C. elegans*, which is the only meiotic arrest in *C. elegans*.(see Fig. 6 for detail) Mammalian oocytes grow in a follicle consisting of somatic granulosa cells and the oocyte (Fig. 7). Granulosa cells are compartmentalized into outer mural granulosa cells and inner cumulus cells by a cavity, the antrum that is filled with protein and hormones that have been secreted by follicle cells and the oocyte. The granulosa cells surrounding the oocyte inhibit meiotic maturation. Indeed an oocyte can spontaneously resume meiosis after removal from an antral follicle (Pincus and Enzmann 1934). Oocytes arrested at meiotic prophase I resume their meiosis and proceed to meiosis II in response to LH stimulation, which acts at the level of the mural granulosa cells. The mechanisms that tightly regulate oocyte meiotic arrest have been very well elucidated. Maturation-promoting factor (MPF) is the key protein complex that regulates meiotic maturation (see below for details). Upon activation of MPF, the nuclear envelope breaks down, meiotic spindle assembles, and homologous chromosomes separate to opposite spindle poles.

It was reported in 1967 that progesterone can induce complete meiotic maturation of *Xenopus* oocytes that had been isolated from follicles (Masui 1967). Further studies were conducted by injecting progesterone into denuded oocytes, and it was found that the externally applied but not injected progesterone was capable of inducing meiotic maturation (Masui and Markert 1971; Ecker and Smith 1971). Furthermore, Masui showed that transferring cytoplasm from maturing oocytes or early embryos into immature oocytes induces maturation of the recipient oocytes (Masui and Market 1971).

Figure 6. Oocyte Meiotic Maturation and Egg Activation

The oocytes of most animal species arrest in meiotic prophase I. In response to a hormonal stimulus, oocytes begin meiotic maturation: the nuclear envelope breaks down (GVBD), as the oocyte enters M-phase from prophase. The point of fertilization is species-specific. (I). Fertilization occurs after maturation but prior to completion of meiosis I, such as *C. elegans*. (II), fertilization occurs at metaphase or anaphase I, such as *Drosophila*. (III), fertilization occurs at metaphase II, such as mouse. (IV) fertilization occurs after completing meiosis such as sea urchins. Reprinted from Greenstein, 2005.

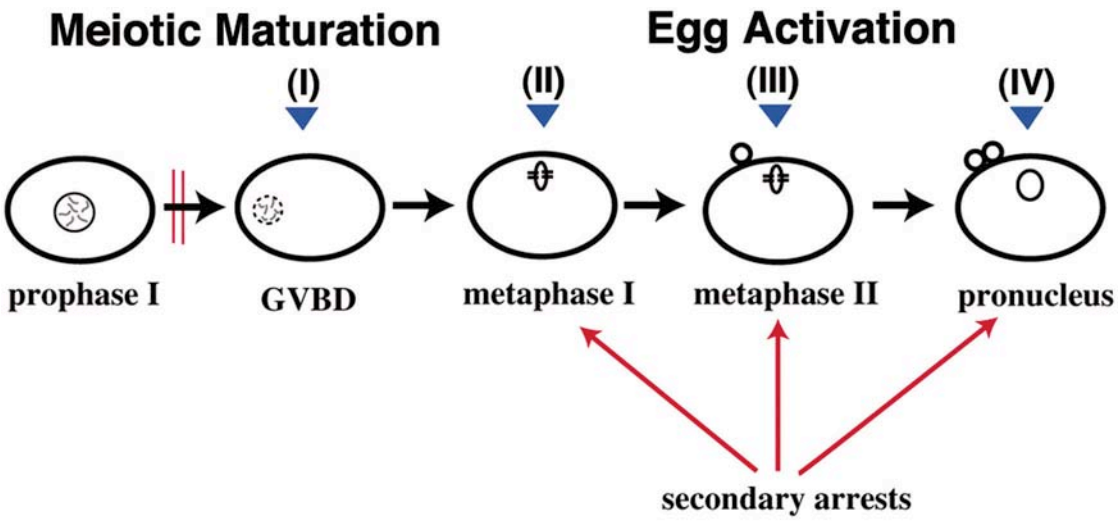

▼ = point of fertilization (depends on species)

‖ = primary arrest (often released by hormonal stimulus)

Figure 7. Development of the mammalian ovarian follicle

The follicle consists of somatic cells (green) surrounding an oocyte (red). The primordial follicle consists of an oocyte arrested in meiotic prophase I and a few follicle cells surround it. While the follicle grows, oocyte size increases, cortical granule and zona pellucida start to appear. The surrounding granulosal cells proliferate, and an antrum forms. In response to the FSH signal, follicle grows further in size and one becomes the dominant antral follicle. A surge of LH stimulates the oocyte to resume meiosis, as well as ovulation of the mature oocyte. Adapted from Molecular Biology of the Cell, Garland Publishing, NY, 1994.

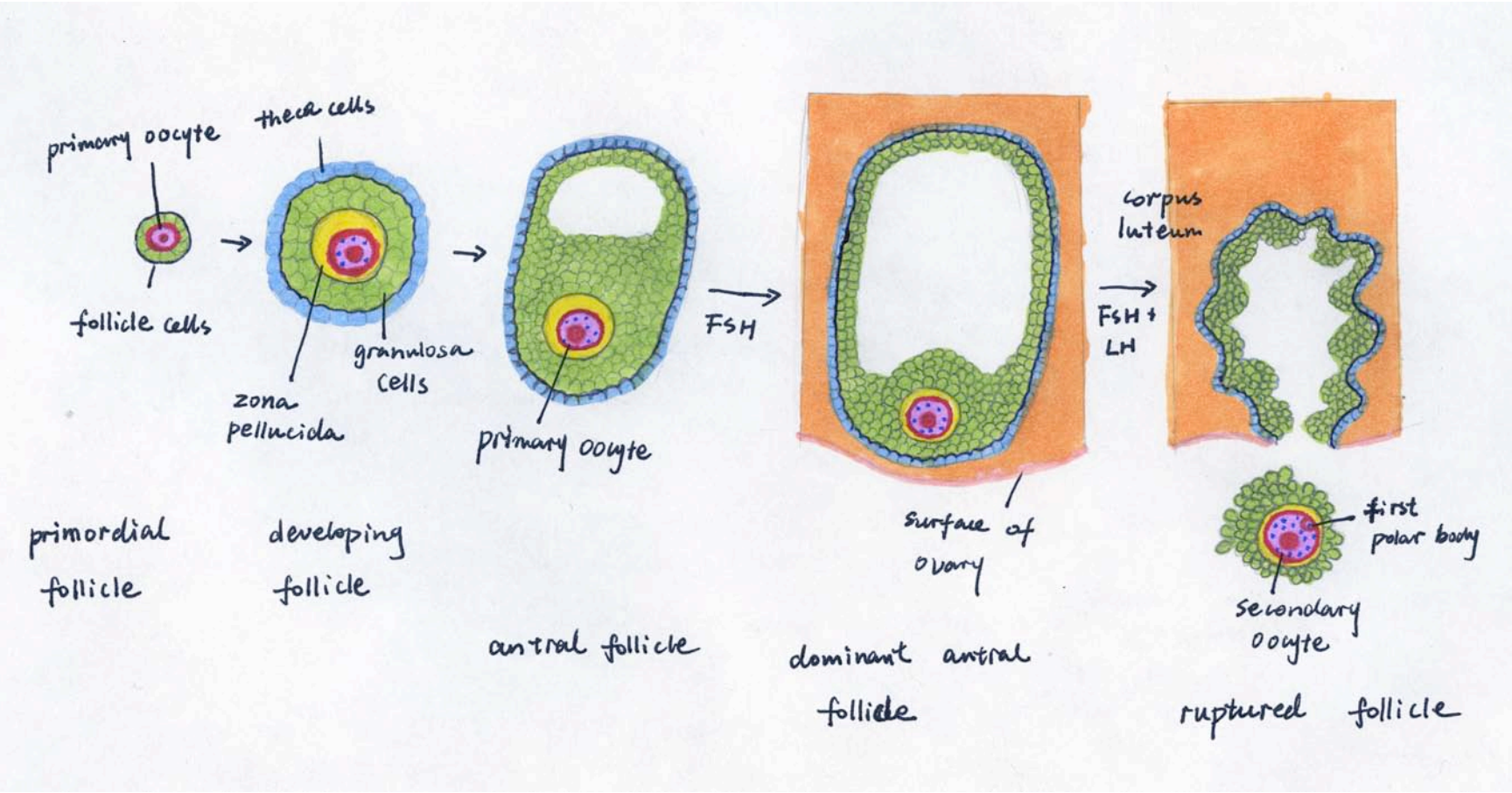
primary oocyte
follicle cells
theca cells
granulosa cells
zona pellucida
primary oocyte
FSH
surface of ovary
corpus luteum
FSH + LH
first polar body
secondary oocyte
primordial follicle
developing follicle
antral follicle
dominant antral follicle
ruptured follicle

The MPF complex is present in the oocyte cytoplasm in an inactive form, pre-MPF, which is activated by progesterone stimulation. MPF activity is regulated by phosphorylation and dephosphorylation of Cdc2 at threonine14 (T14), tyrosine15 (Y15), and threonine 161 (T161) sites. Phosphorylation of Cdc2 at T161 is controlled by cyclin-dependent activating kinase (CAK). Wee1/Myt1 inhibits Cdc2 activity by phosphorylating Cdc2 at T14/Y15. The inhibition of Cdc2 by phosphorylation at T14/Y15 can be removed by a phosphatase Cdc25 (Mueller et al., 1995; Fig. 8). Cyclin and cyclin dependent kinase are evolutionarily conserved and play critical roles in the regulation of mitotic and meiotic cell cycle. (Nurse, 1990).

In mouse oocytes, meiotic arrest depends on a high level of cyclic AMP within the oocyte, and the oocyte resume meiosis in response to LH, whose target is the somatic cells that surround the oocyte and not the oocyte itself (Conti et al., 2002, Richards et al., 2002). In mammals, it was thought for a long time that cAMP is produced in follicle cells and diffuses through gap junctions to the oocyte (Anderson and Albertini 1976; Bornslaeger and Schultz, 1985). Recently, new data suggest that cAMP is produced by the oocyte, through the G protein coupled receptor GPR3 activated G_s protein (Mehlmann et al., 2002). This new hypothesis is supported by the evidence that the denuded mouse oocytes are prevented from spontaneous maturation when they are injected with cAMP analogs (Cho et al., 1974). Furthermore, blocking Gαs function with antibodies or with a dominant-negative $G\alpha_s$ construct can maintain denuded oocytes in meiotic arrest (Mehlmann et al., 2002; Kalinowski et al., 2004), and *Gpr3* mutant mice exhibit spontaneous oocyte maturation within the follicle independent of LH stimulation (Mehlmann et al., 2004). In *Xenopus* oocytes, the activity of adenylyl cyclase is

maintained by Gα and Gβγ subunits of G_s protein as well (Maller and Krebs 1977; Gallo et al., 1995). The signaling pathway downstream of cAMP is incompletely understood. High cAMP levels within the oocyte causes inactivation of Cdc2 by phosphorylation at T14/Y15 (Duckworth et al., 2002). Protein kinase A acts downstream of cAMP and plays an important role in inhibiting pre-MPF activation: blocking protein kinase A activity is sufficient to induce oocyte maturation. Protein kinase A regulates the activities of phosphatase Cdc25 and the Wee1/Myt1 kinase, the two regulators of the cyclin B-Cdc2 complex (Han and Conti, 2006) (Fig. 9). Wee1/Myt1 is a dual-specific kinase that associates with the membrane. Wee1/Myt1 kinase inhibits MPF activity by phosphorylating Cdc2 at T14/Y15 sites, whereas phosphatase Cdc25 activates MPF by removing the inhibitory phosphorylation of T14/Y15 sites of Cdc2 (Han and Conti, 2006; Gould and Nurse 1989) (Fig. 9). Inactivating Myt1 can trigger meiotic maturation in the absence of progesterone in *Xenopus* oocyte (Nakajo et al., 2000).

Progesterone stimulation causes a decrease in adenylyl cyclase activity and cyclic AMP levels in *Xenopus* oocytes, and these decreases are both necessary and sufficient for MPF activation (reviewed by Sadler and Maller 1985; Maller and Krebs 1977; Huchon et al., 1981) (Fig. 9). In the *Xenopus* oocytes, meiotic maturation requires new protein synthesis, as the protein synthesis inhibitors can block progesterone induced MPF activity and oocyte maturation (Wasserman and Masui 1975). Translation of Mos protein has been well documented as being important for initiating oocyte maturation, and injection of Mos protein into immature *Xenopus* oocytes is sufficient to induce oocyte maturation (Sagata et al., 1988, 1989A and 1989B). During meiotic arrest, *mos* mRNA is masked and is unable to be translated.

Figure 8. Activation of maturation promoting factor

MPF consists of two subunits cyclin B and cyclin dependent kinase CDK1. Wee1 phosphorylates CDK1 at T14 and Y15 which inhibits MPF activity. CAK phosphorylates T161 of CDK1, and this phosphorylation is very important for MPF activity. T14/Y15/T161 phosphorylated CDK1 bound cyclin B forms the preMPF complex. preMPF is activated by Cdc25 which dephosphorylates T14/Y15 of CDK1. Adapted from Molecular Cell Biology, Freeman and Company, fourth Edition, 2000.

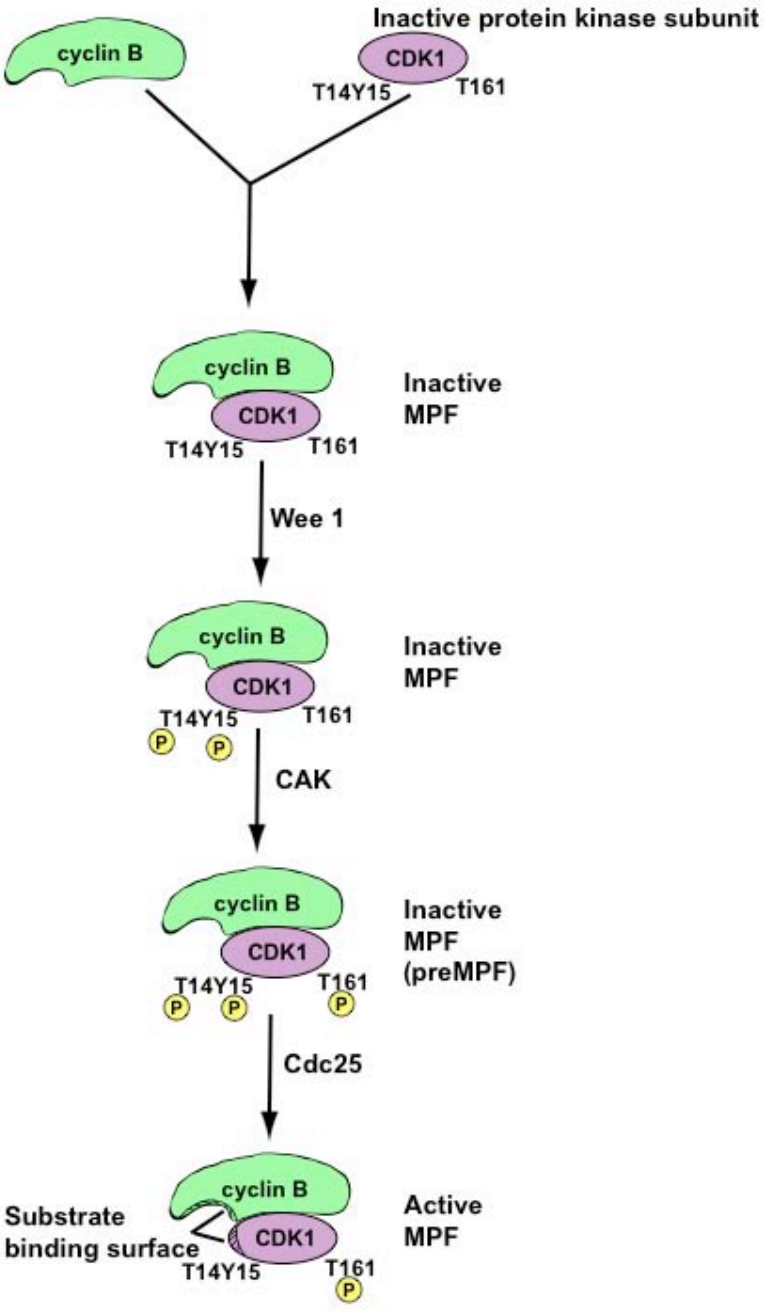
Inactive protein kinase subunit
cyclin B
CDK1
T14Y15
T161
cyclin B
CDK1
T14Y15
T161
Inactive
MPF
Wee 1
cyclin B
CDK1
T14Y15
T161
P
P
Inactive
MPF
CAK
cyclin B
CDK1
T14Y15
T161
P
P
P
Inactive
MPF
(preMPF)
Cdc25
cyclin B
CDK1
Substrate
binding surface
T14Y15
T161
P
Active
MPF

Figure 9. Mammalian oocyte meiotic arrest and resumption

GPR3 activates G_s, which stimulates adenylyl cyclase to cause an elevation of cAMP. cAMP activates protein kinase A, which leads to phosphorylation and inactivation of Cdc25. Because Cdc25 is an activator of CDK1/cyclin B, inactivation of Cdc25 results in inactivation of the MPF complex. PKA also stimulates the activity of the WEE1/MYT1 kinase that phosphorylates and inactivates MPF. This signal network maintains oocyte arrest in meiotic prophase (left). In response to LH signaling, cAMP levels decline, and PKA is inactivated. Because the inhibitory inputs have been removed, Cdc25 dephosphorylate CDK1, which leads to activation of MPF. MPF promotes meiotic resumption (right). Modified from Mehlmann, 2005.

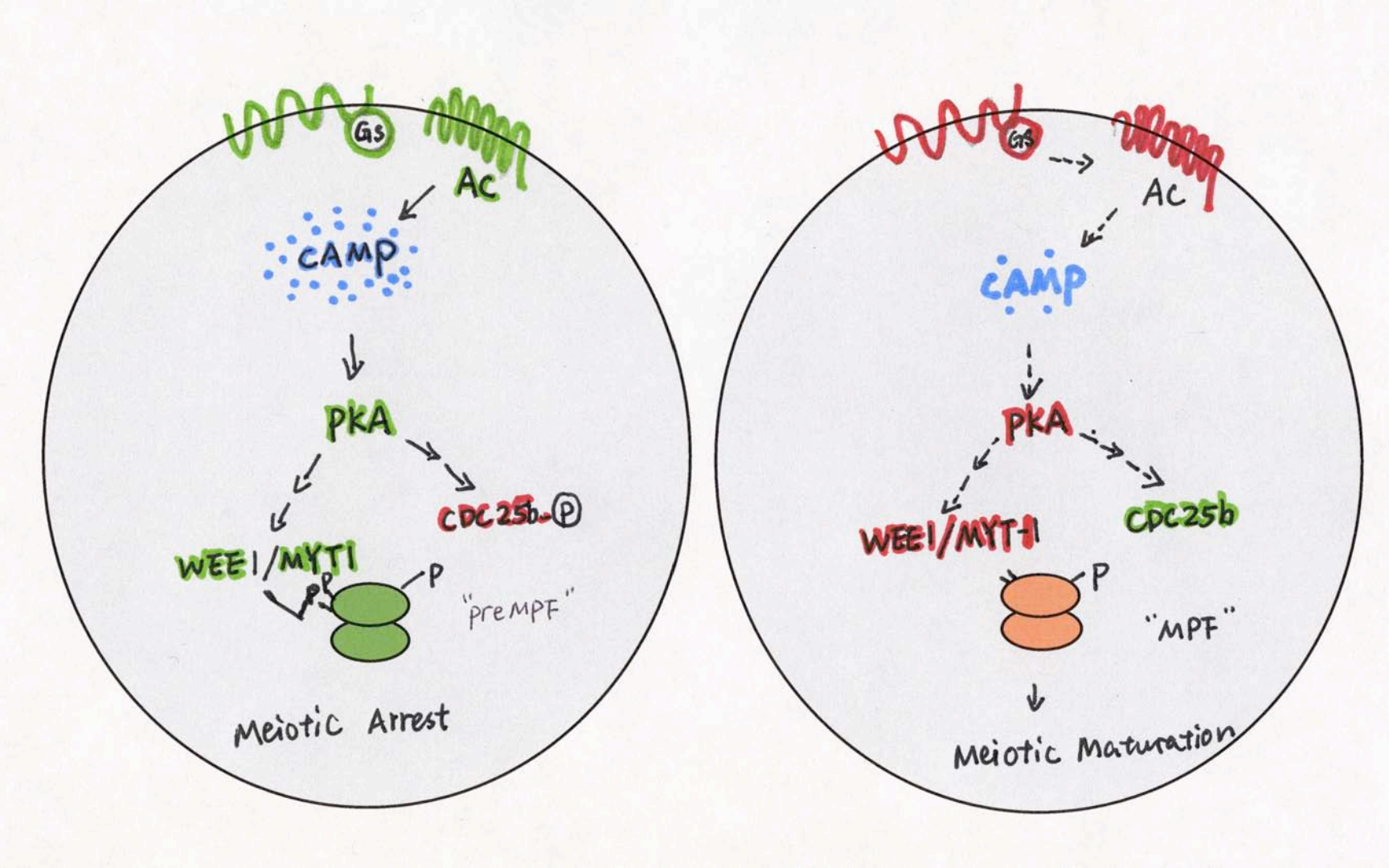
Gs
Ac
cAMP
PKA
CDC25b-P
WEE1/MYT1
P
"preMPF"
Meiotic Arrest
Gs
Ac
cAMP
PKA
WEE1/MYT1
CDC25b
P
"MPF"
Meiotic Maturation

Progesterone stimulation decreases PKA activity and along with Aurora-A-dependent phosphorylation of CPEB, causes activation of the protein synthesis machinery. *mos* mRNA is posttranscriptionally modified by cytoplasmic polyadenylation, and this modification of *mos* mRNA results in its translation. Similar to *Xenopus* meiotic arrested rat oocytes express *mos*-mRNA but have no detectable levels of the Mos protein in the oocyte. Although injection of mos can induce maturation of Xenopus oocytes, the story is not necessarily simple, because *mos* mutant mice still undergo meiotic maturation with subsequent subtle abnormalities such as diffused spindle and loosely condensed chromosomes(Araki et al., 1996). The *mos* null mutant phenotype suggests that mos/MAPK is not necessary for meiotic maturation in mouse. High levels of cAMP inhibit *mos* mRNA polyadenylation to negatively regulate Mos protein expression (Josefsberg et al., 2004). Expression of Mos activates the MEK-MAPK-p90Rsk cascade, which results in direct phosphorylation and inactivation of Myt1 (reviewed by Palmer and Nebreda 2000). p90Rsk associates with and phosphorylates Myt1, which decrease Myt1 inhibition of Cdc2. Plx1, a polo like kinase, is activated in response to progesterone and in turn phosphorylates and actives Cdc25 (Qian et al., 2001). Overexpressing a constitutively active Plx1 can induce Cdc25 activation and subsequent MPF activation (Qian et al., 2001). Interestingly, Cdc25 is also phosphorylated by Cdc2, and this primary phosphorylation is a prerequisite for Cdc25 phosphorylation and activation by Plx1. This suggests that there is a positive feedback loop leading to activation of MPF upon phosphorylation of Cdc25 and Wee1/Myt1 proteins by Cdc2 kinase and Plx1(Abrieu et al., 1998). Activation of Cdc25 and inactivation of Myt1 converge on the activation of cyclin B-Cdc2. Ringo/Speedy, a regulator of Cdc2, has also been reported as a newly

synthesized protein in response to progesterone stimulation; and Ringo/Speedy may regulate Cdc2 activity by phosphorylation (Karaiskou et al 2001, Ingvar et al., 1999).

After undergoing meiotic division I following release from meiotic prophase, most vertebrate oocytes arrest again in meiotic metaphase II. This secondary meiotic arrest is characterized by the presence of a metaphase spindle and high Cdk1 activity. The second meiotic arrest is mediated by cytostatic factor (CSF), and this second meiotic arrest is therefore termed the CSF arrest (reviewed by Tunquist and Maller 2003). CSF activity was first described by Masui as well: injection of cytoplasm from a secondary arrested (MII arrest) oocytes into blastomeres of a two-cell staged embryo arrests these cells in metaphase (Masui and Markert 1971). Mos protein has been document as a component of CSF, because depletion of Mos protein from cytoplasm prepared from second arrested oocytes is incapable of arresting blastomere in mitosis (Sagata et al., 1989). In addition, injecting *mos* mRNA into embryonic blastomeres can arrest them in metaphase, which mimics CSF activity (Sagata et al., 1989). CSF activity emerges after progesterone stimulation and is present in metaphase II arrest oocytes, and declines upon fertilization (Tunquist and Maller 2003). CSF blocks meiotic metaphase by preventing degradation of cyclin. Multiple lines of evidence suggest that CSF inhibits anaphase-promoting complex/cyclosome (APC/C) (Lorca et al., 1998; Tunquist and Maller 2003). First, the Mos/MAPK/p90Rsk pathway activates the spindle assembly checkpoint protein Bub1, which blocks APC/C activity (Schwab et al., 2001). Second, CSF activity in CSF-arrested oocytes is unaffected when the structure of the spindle is disrupted chemically (e.g. nocodazole; Tunquist and Maller 2003). Third, blocking Mad2, a spindle assembly checkpoint protein, prevents release from CSF arrest upon calcium stimulation (Peter et

al., 2001). Lastly, Cdc20/Fzy, a component of APC/C, is required for exit from CSF arrest (Lorca et al., 1998). Although the Mos/MAPK/p90Rsk pathway plays an important role in establishing the secondary arrest, this pathway is dispensable for maintaining MII arrest (Tunquist et al., 2002). The maintenance of MII arrest is mediated by Emi1, which prevents APC/C activity by binding to Cdc20. Depletion of Emi1 is sufficient for release from MII arrest (Reimann and Jackson 2002). Emi appears to be a key component of CSF. First, introducing Emi into two-cell blastomeres blocks mitosis, which resembles CSF activity. Second, Emi1 is necessary and sufficient for MII arrest in *Xenopus* oocytes. Finally, depleting Emi from CSF extracts destroy the ability to induce blastomere arrest after injection into two-cell embryos (Reimann et al., 2001; Reimann and Jackson 2002). However, Ohsumi et al disagree that Emi is a component of CSF. They can not detect Emi in CSF-arrested oocytes, and exogenous Emi1 is unstable when added to maturing oocytes and CSF extracts (Ohsumi et al., 2004). Thus whether Emi is a component of CSF is controversial.

The meiotic arrest at metaphase II is released upon fertilization. The released oocyte proceeds from metaphase to anaphase, followed by protrusion of second polar body. Sperm binding to the egg causes calcium (Ca^{2+}) influx, which actives calcuim-binding protein, calmodulin. The importance of the Ca^{2+} influx has been strengthened by the observation that oocyte can be release from second meiotic arrest by injecting Ca^{2+} directly to the oocyte (Lohka and Maller 1985, Lorca et al., 1991). Activated calmodulin then activates calmodulin- dependent kinase II (CaMKII), which causes degradation of cyclin B. Activated calmodulin also activates a calcium dependent protease, calpian that degrades Mos (Lorca et al., 1991). The degradation of cohesin, which results in the

separation of sister chromatids, is dependent on the level of calcium. Egg activation can also cause cyclin B degradation, which results in loss of MPF activity and exit from metaphase II. The addition of constitutive active CaMKII to CSF extract is sufficient to induce degradation of cyclin B to inactive of MPF, and to destroy the ability of CSF extract to arrest two-cell embryo blastomeres (Lorca et al., 1993). CaMKII also directly activates APC/C by either phosphorylating the APC/C component protein cdc20 or by regulating the binding of Emi1 to cdc20 (Tunquist and Maller 2003).

C.elegans as a model organism for studies of oocyte meiotic maturation and maturation.

Meiotic errors can generate aneuploid embryos upon fertilization. In humans, most aneuploidies lead to miscarriage, although a few of them can survive to term. Aneuploid humans suffer from severe developmental, physiological, and mental disturbances (Pont et al., 2006). For example, Down syndrome is due to 21 trisomy, which occurs in one out of 800 babies. Patients who have Down syndrome suffer from mental and physical developmental retardation. In humans, maternal age is the most significant risk factor for aneuploidy, and a majority of meiotic errors arise from defects in meiosis I (reviewed by Hassold and Hunt 2001). Although meiotic maturation plays such an important role in human fertility and pregnancy, it is very difficult to study meiotic maturation in humans, because the human oocytes and follicles are relatively inaccessible for practical and ethical reasons. However, the maternal age of the mice is also associated with increased frequency of meiotic errors (reviewed by Hassold and Hunt 2001). The mouse has been considered as a strong model for studying the

underlying mechanism of meiotic errors. However, it is also relatively difficult to study oocyte meiosis in mice. Besides the expense in culturing oocyte, the development process of mouse oocyte cannot be observed continuously in the intact animals, and the genetic approaches are time consuming and expensive as well.

The nematode *C. elegans* has been considered a model for studies of meiotic maturation to complement studies in vertebrates (reviewed by Hubbard and Greenstein 2000). *C. elegans* hermaphrodites have a female reproductive tract but produce sperm and self-fertilized. *C. elegans* is amenable to genetic manipulation to manage the presence and absence of sperm and oocytes by using mutant strains (Hodgkin et al., 1998; Schedl and Kimble 1988; Schedl et al., 1989; Ellis and Schedl 2007). *C. elegans* has five pairs of autosomes and one pair of sex chromosome. The sex of *C. elegans* is determined by the ratio of sex chromosomes to autosomes. If the sex chromosome pair is XX, then *C. elegans* will be a hermaphrodite. A XO combination in the sex chromosome pair will produce a male. The XO combination in male is the spontaneous loss of X chromosome. A male can cross with hermphrodites (Meneely and Herman, 1979). The short reproductive life cycle and the linear progression of meiosis within the gonad make the adult worm a particularly attractive model to study meiotic maturation (reviewed by Hubbard and Greenstein, 2000). Full-grown oocytes mature and are ovulated and fertilized in a single file and assembly-line-like fashion (McCarter et al., 1999) (Fig. 10). Lastly, the transparency of *C. elgans* makes it possible to visualize meiotic maturation progression in living animals, and indeed the meiotic progression has been documented in detail by video recordings (McCarter et al., 1999; Rose et al., 1997). The ultrastructure of the *C. elegans* oocyte has been described in details as well (Hall et al., 1999).

The *C. elegans* reproductive tract consists of two U-shaped gonad of arms, each of which are followed by a spermatheca, where sperm are stored, and joined by a common uterus, where embryos develop (Fig. 10). The distal region of a gonad arm is a syncytium with common cytoplasm (rachis) and germ cell nuclei (germ cells), separated by incomplete membranes. In the adult hermaphrodite, germline nuclei proliferate by mitotic division in the distal region (Fig. 11). As the germline nuclei migrate away from the distal region, they enter meiotic prophase I, and the initial pairing of the chromosomes takes place here, which is called the transition zone (Dernburg et al 1998; Fig. 11). As the germ cells migrate away from distal, they proceed through leptotene, zygotene and enter pachytene before reaching the loop region of the gonad, where apoptotic cell death occurs. Apoptosis occurs in approximally 50% of the pachytene-stage female meiotic germ cells. These apoptotic germ cells function like nurse cells to provide proteins and mRNA to the surviving oocytes (Gumienny et al., 1999). When the germ cells transit through the loop region (where the gonad bends ventrally) they enter diakinesis, and become fully enclosed by plasma membranes (Fig. 10). Therefore, oocytes develop, mature and form a queue in the adult proximal gonad arm. Oocyte growth is mediated by the cytoplasmic flow from the distal gonad to developing oocytes near the bend region (Wolke et al., 2007). mRNA, mitochondria, and other protein are synthesized in the gonad distal region and flow promixally into developing oocytes. This cytoplasmic flow is regulated by the actomyosin network (Wolke et al., 2007). Yolk granules also contribute to the size of the oocyte. York protein is synthesized by the intestine, and is secreted into the pseudocoelom (Kimble and Sharrock, 1983).

Figure 10. *C. elegans* hermaphrodite

The reproductive system of a *C. elegans* hermaphrodite consists of two U shaped gonad arms (each followed by a spermatheca) which are connected by a common uterus. 5 pairs of somatic sheath cells surround each germ line. Germ cells proliferate mitotically at the distal gonad arm, and enter meiosis more proximally. Oocytes cellularize in the proximal gonad arm. The most proximal oocyte matures and ovulates into the spermtheca where fertilization occurs. Fertilized oocytes enter the uterus where embryonic cell division begins. Reprinted from Miller et al., 2001.

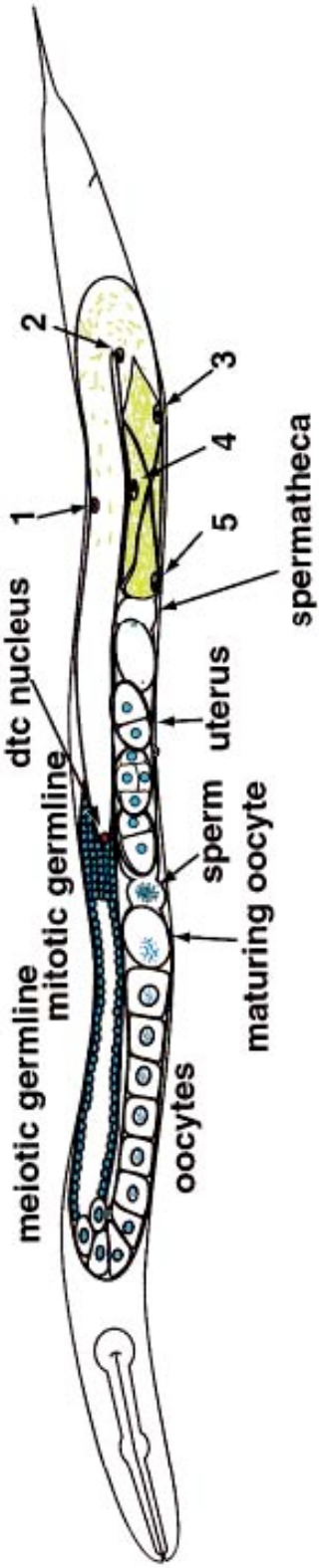
1
2
3
4
5
spermatheca
uterus
sperm
maturing oocyte
dtc nucleus
mitotic germline
meiotic germline
oocytes

Figure 11. The structure of adult hermaphrodite gonad

A. Dissected gonad from a wild-type adult hermaphrodite showing oogenic meiotic progression. B. Immunofluorescent micrograph of the somatic gonadal sheath cells. Nuclei is in blue and myofilaments is in red and green.
C. Gap junction (gj) between oocyte and proximal sheath cell. All the graphs are reprinted from Greenstein, 2005.

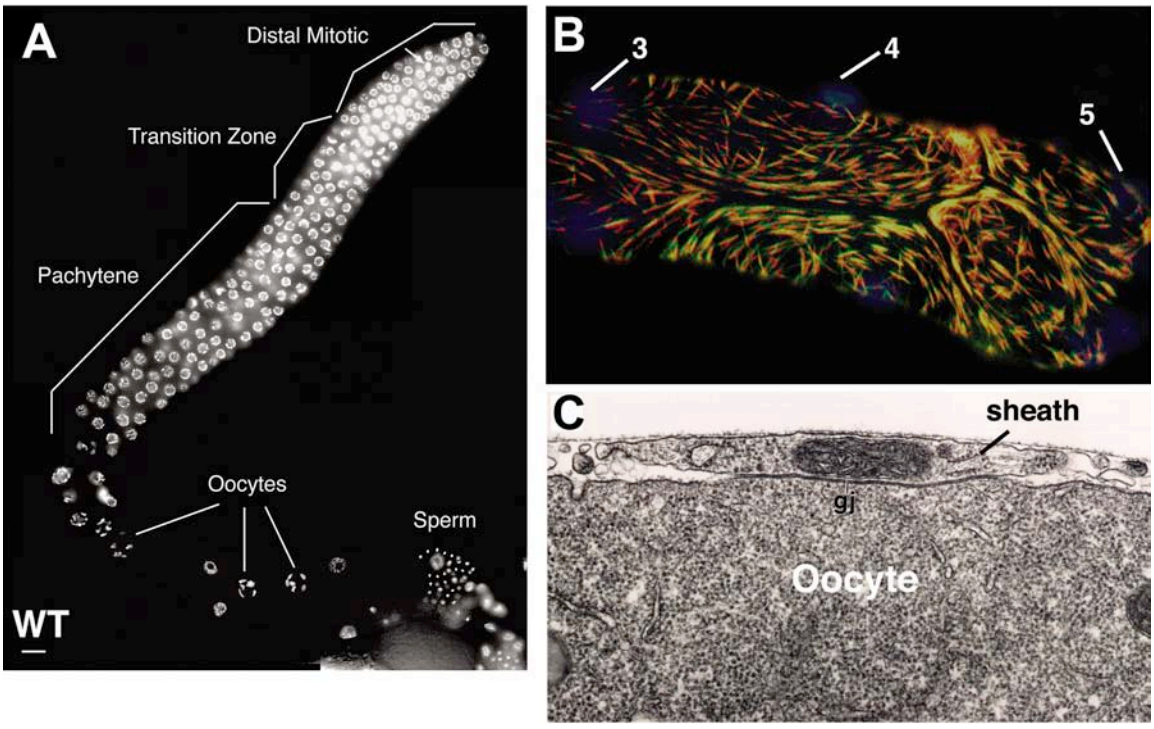
A
Distal Mitotic
Transition Zone
Pachytene
Oocytes
Sperm
WT
B
3
4
5
C
sheath
gj
Oocyte

The yolk proteins pass through a basal lamina and sheath cell pores, and internalize into oocyte and store in membrane bound organelles (Hall et al., 1999). Internalization of york protein into oocyte is mediated by york receptor RME-2 (recepter mediated endocytosis) (Grant and Hirsh 1999). These cellularized oocytes form a queue in the proximal region of a gonadal arm and arrest at diakinesis awaiting for a signal from sperm to trigger meiotic maturation (McCater et al., 1999). The most proximal oocyte matures, ovulates into the spermatheca, and undergoes fertilization there. Afterwards, the second most proximal oocyte occupies the most proximal position and undergoes meiotic maturation 23 minutes later. Therefore, meiotic maturation occurs in an assembly-line fashion in the proximal gonad arm (McCarter et al., 1999).

C. elegans hermaphrodites first produce sperm then they switch to oogenesis after reaching adulthood. In hermaphrodites, sperm are limiting for self fertility; a hermaphrodite produces ~300 sperm and about 300 progeny. In adult hermaphrodites, the most proximal oocyte matures and ovulates every 23 minutes in each gonad arm in the presence of sperm. In contrast, oocytes undergo meiotic arrest when sperm are consumed in older adult hermaphrodites or in certain mutants such as *fem-1,2,3* or *fog-1,2,3* which are females due to disruptions in germline sex determination mechanisms (McCarter et al., 1999). This meiotic arrest can last for many hours but is released by mating with sperm that are introduced into the reproductive tract (McCarter et al., 1999). Since sperm are stored in spermatheca, which is separated from the proximal goand arm, sperm must release a signal to trigger oocyte meiotic maturation at a distance. This sperm signal was identified in our lab (Miller et al., 2001). Miller et al., (2001) injected sperm conditioned medium into the *fog-2* female uterus, and found that this sperm conditioned medium is

sufficient to promote oocyte meiotic maturation and ovulation. Further, they purified the activity of sperm conditioned medium and identified major sperm protein (MSP) as the signal that sperm release to trigger oocyte meiotic maturation. Multiple lines of evidence suggest that MSP is the signal that sperm use to promote oocyte meiotic maturation. First, MSP biochemically purified from sperm conditioned medium or from sperm extracts can signal oocyte meiotic maturation after introducition into the female uterus. Second, recombinant MSP purified from bacteria is sufficient to induce oocyte meiotic maturation in female *C. elegans* as well as in females of another species, *C. remanei*. Third, antibody raised against MSP can reduce the oocyte meiotic maturation rate. Lastly, MSP injection can increase the activation of MAPK in the proximal gonad, which is an important event during oocyte meiotic maturation (Miller et al., 2001). Soon after, Miller et al., (2003) found that an integral membrane protein, VAB-1/Eph is the oocyte receptor for MSP. This hypothesis is supported by numerous lines of evidence. First, vab-1 null mutation greatly reduce the binding of fluorescently labeled MSP to dissected hermaphrodite gonad. This binding is both saturable and competable. (Reinke et al., 2000). Second, expression of VAB-1 in COS-7 cells is sufficient to confer MSP binding activity. Third, VAB-1 negatively regulates oocyte meiotic maturation in the absence of sperm, and this inhibition can be released by MSP. Finally, I found that purified MSP can interact with the VAB-1 ectodomain *in vitro*. Kosinski et al., (2005) later discovered that sperm release MSP by a vesicle budding mechanism to signal oocyte meiotic maturation from a distance (Kosinski et al 2005). VAB-1 functions in parallel with CEH-18, a POU-homeoprotein, to negatively regulate oocyte meiotic maturation and MAPK activation in the absence of sperm (Fig. 12).

Figure 12. A sperm-sensing control mechanism regulates oocyte meiotic maturation and MAPK activation.

Sperm release MSP, which binds to VAB-1 and other receptor(s) on oocytes and sheath cells. MSP promotes oocyte M-phase entry (maturation), MAPK activation, and ovulation by antagonizing ephrin/Eph receptor (EFN-2/VAB-1) and sheath cell-dependent (CEH-18) inhibitory inputs. Reprinted from Miller et al., 2003.

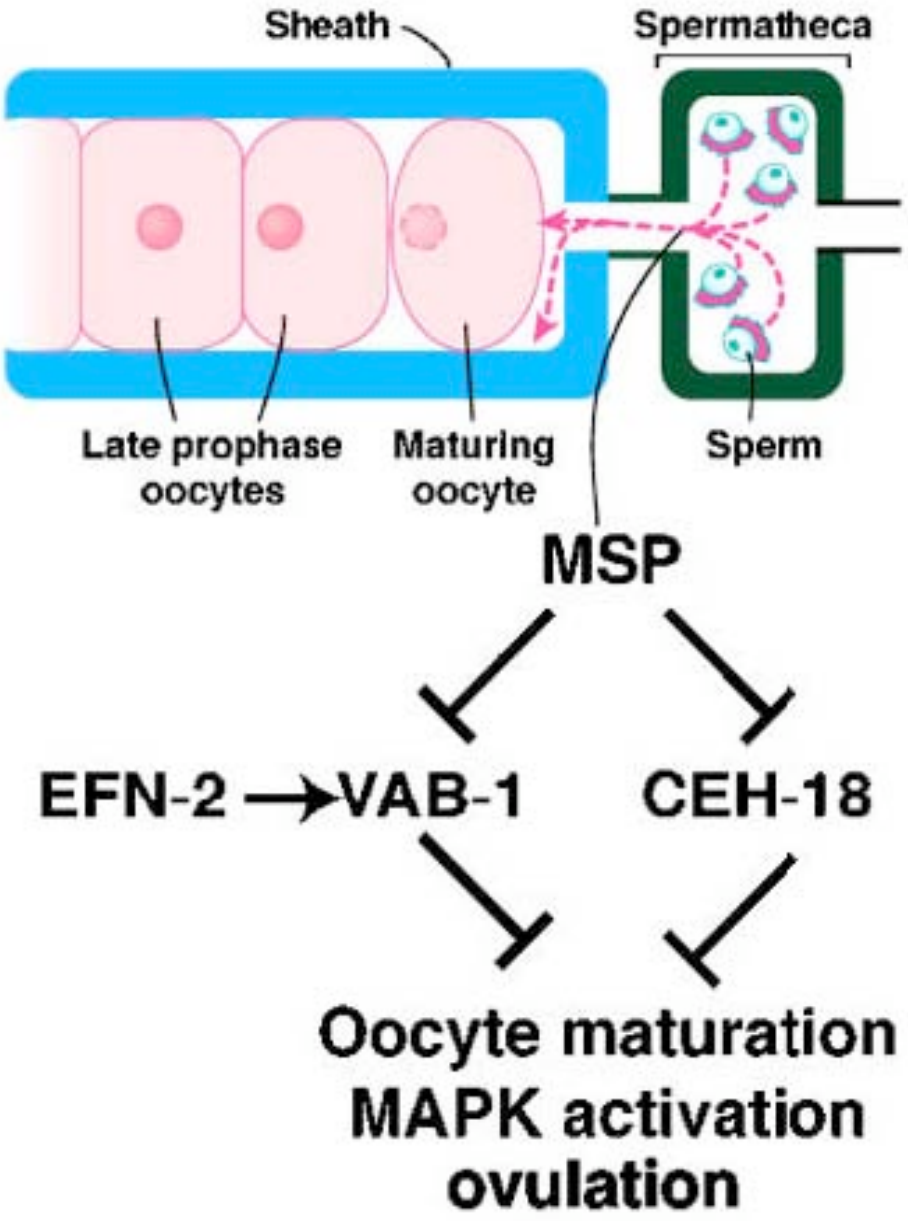
Sheath
Spermatheca
Late prophase oocytes
Maturing oocyte
Sperm
MSP
EFN-2
VAB-1
CEH-18
Oocyte maturation
MAPK activation
ovulation

MSP antagonizes this inhibition to promote oocyte meiotic maturation (Fig. 12). This working model is based on several lines of evidence. First, both *vab-1(0);fog-2* and *ceh-18(0);fog-2* females display an increased rate of oocyte meiotic maturation comparing to *fog-2* females. Second, *vab-1(0);ceh-18(0);fog-2* females exhibit an synergistic effect comparing to *vab-1(0);fog-2* or *ceh-18(0);fog-2* and oocyte meiotic maturation rate of *vab-1(0);ceh-18(0);fog-2* is independent of sperm. However, it was unclear at the time how VAB-1 inhibits oocyte meiotic maturation and how MSP antagonizes this inhibition. I was interested in answering these two questions, and that is what I focused on during my thesis research. By collaborating with J. Amaranath Govindan, we identified five genes that function in a common pathway with VAB-1 to negatively regulate oocyte meiotic maturation. These five genes are disabled protein (DAB-1), a STAM homolog (PQN-19), protein kinase C (PKC-1), a vav family GEF (VAV-1), and a small GTPase (RAN-1). I also recognized that the intracellular trafficking of VAB-1 is a key feature in the inhibition of oocyte meiotic maturation when MSP is absent. Further I showed that regulation of VAB-1 trafficking by MSP is part of the mechanism by which MSP results in a high rate of meiotic maturation. Since my dissertation work involves an investigation of Eph receptor signaling and trafficking, I will give an overview about Eph receptors in the next section.

Eph Receptor Signaling

Eph receptors comprise the largest superfamily of receptor tyrosine kinases (RTKs). Most RTKs are monomers, and their domain structure includes an extracellular ligand-

binding domain, a transmembrane domain, and an intracellular tyrosine kinase domain (reviewed by Schlessinger, 2000). Epidermal growth factor receptor was the first receptor tyrosine kinase to be identified, and the general importance of tyrosine kinases in intracellular communication was recognized soon after (reviewed by Carpenter and Cohen 1990). Stanley Cohen and Rita Levi-Montalcini shared the Nobel Prize in Physiology or Medicine in 1986 for their discovery of growth factors. Ligand binding to the EGF receptors results in oligomerization of the receptor, with subsequent autophosphorylation of the receptor tyrosine kinase domain (reviewed by Carpenter and Cohen 1990). The activated tyrosine kinase then induces formation of signaling complex, which further activates signal transduction cascades. The major signaling pathways regulated by RTKs are the Ras-p42/44 mitogen-activated protein kinase (MAPK) pathway and the phosphoinositide-3 kinase (PI3-kinase) pathway. RTKs are involved in cell growth or survival by functioning directly on gene transcription or indirectly through production of second messengers (reviewed by Schlessinger, 2000). In *C. elegans*, activation of the EGF receptor tyrosine kinase LET-23 activates the LET-60 Ras/MAPK pathway, leading to the induction of development of the hermaphrodite vulva, which is an organ required for egg laying.

The first Eph receptor was identified as a receptor tyrosine kinase in a hepatoma cell line in 1987 as part of the human genome project (Hirai et al., 1987). This divergent receptor was pulled out in a screen for a *v-fps* homologous sequence from an erytheropoietin-producing hepatocellular (Eph) carcinoma cell line (Hirai et al., 1987). In the past twenty years, many Eph receptors have been identified in a variety of species mainly from vertebrates, but also in simple organisms such as sponges, *C. elegans*, and

Drosophila (Drescher, 2002). Eph receptors constitute the largest class within the receptor tyrosine kinase superfamily.

A major question for the field was whether Eph receptors have ligands. The identification of Eph receptor ligands were conducted through an expression cloning strategy. Three ligands that bound to the Eph receptor extracellular domain were recovered from a cDNA library, and were name "ephrins" (Davis et al., 1994). To date, sixteen vertebrate Eph receptors and nine ephrins have been identified, and human are known to have fourteen Eph receptors and eight ephrins. The genes that encode Eph receptors and their ligands are present throughout the animal kingdom (Boyd and Lackmann 2001). Although numerous Eph receptors and ephrin ligands exist in higher species, both the structure and function of Eph receptors and their ligands are extraordinarily conserved (Boyd and Lackmann 2001). Ephrin ligands are divided into two groups based on their structure: EphrinAs (A1–A6) are membrane proteins that utilize a glycosyl phosphatidyl inositol (GPI) group as a membrane anchor. By contrast, ephrinBs (B1-B3) are transmembrane proteins that have a short cytoplasmic tail (Kalo and Pasquale 1999) (Fig. 13). Eph receptors are also grouped into two subclasses based on their sequence similarity and their ligand binding affinity: most type A (A1-A10) Eph receptors bind to ephrinAs, and type B (B1-B6) Eph receptors bind to ephrinBs, with a few exceptions (e.g., EphA4 binds both types of ephrins, and EphB2 binds to ephrinA5) (Himanen and Nikolov 2003A and 2003B, Himanen et al., 2004) (Fig. 13). In humans, there are nine EphA receptors that bind to five ephrinA ligands and five EphB receptors that bind to three ephrinB ligands.

The *C. elegans* genome encodes four ephrins (EFN-1 to -4) and one Eph receptor (VAB-1) (George et al., 1998, Wang et al., 1999, Chin-Sang et al., 1999, Chin-Sang et al., 2002). Because *C. elegans* only has one single Eph receptor, this organism is a very attractive model for studying Eph receptor signaling, which provides a useful complement for studies in vertebrate systems (George et al., 1998). The first mutant alleles of *vab-1* were isolated by Sydney Brenner based on their variable abnormal morphology including a notched head, which results from a morphological defect near the tip of the head, defective mail tail morphogenesis, and variable embryonic and larval lethality (Brenner, 1974). *vab-1* was positionally cloned by George et al., (2000), and found to encode an Eph receptor tyrosine kinase. The VAB-1 sequence is equally similar to EphA and EphB receptors and thus may be a common ancestor of the two vertebrate subclasses. The *vab-1* mutant embryonic phenotype was characterized as well: *vab-1* shows developmental defects, and mutants arrest at a variety of stages. Importantly, arrested *vab-1* null mutant embryos displayed severe defects in cell movements during ventral epidermal enclosure (George et al., 2000). Further investigation showed that VAB-1 is expressed in neuroblasts for regulation of epidermal morphogenesis. These results suggest that VAB-1 is required for epidermal morphogenesis during embryonic development. Around the same time, a mammalian ephrin-B1 ligand sequence was used to search for homology in the *C. elegans* genome database, which led to the identification of four ephrins in *C. elegans: efn-1, efn-2, efn-3,* and *efn-4* (Wang et al., 1999). The four ephrins in *C. elegans* are predicted to be GPI modified, and therefore belong to the ephrinA subclass. *efn-1, enf-2, enf-3* single null mutants display epidermal morphogenesis phenotypes similar to *vab-1* null mutants but with lower penetrance.

Figure 13. ephrin and Eph structure

The Eph receptor extracellular region consists of ephrin binding domain (globular domain), cysteine rich-region, followed by FN-III repeats. The Eph receptor intracellular portion consists of a juxtamembrane domain, follow by a kinase domain, a SAM domain and a PDZ binding motif. EphrinA is a GPI anchored protein, whereas ephrinB is a transmembrane protein possessing a small cytoplasmic tail with PDZ binding motif at its C-terminal. Both the extracellular domain of ephrinA and ephrinB possesses a receptor binding domain. Reprinted from Kullander and Klein, 2002.

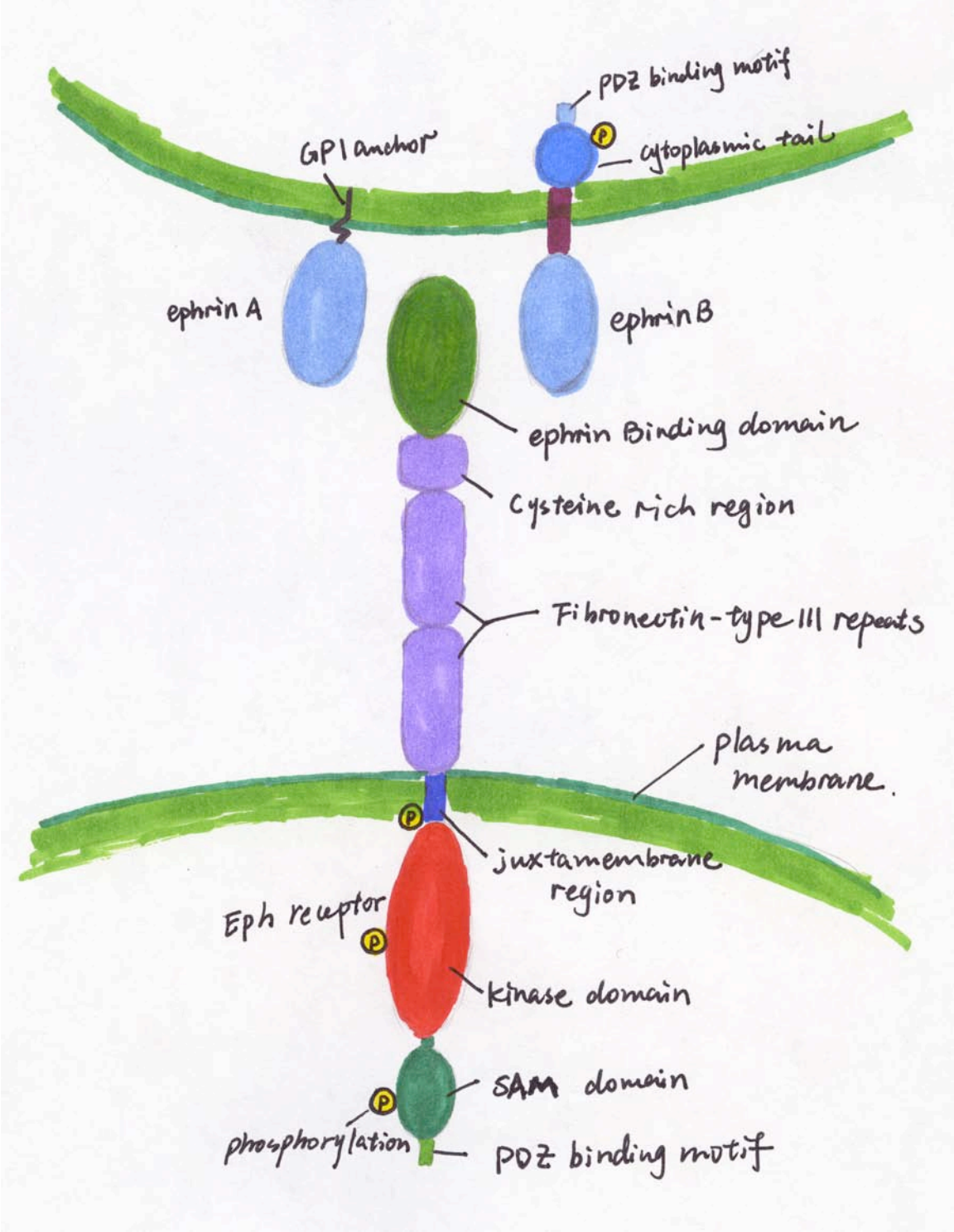
PDZ binding motif
GPI anchor
cytoplasmic tail
ephrin A
ephrin B
ephrin Binding domain
Cysteine rich region
Fibronectin-type III repeats
plasma membrane
juxtamembrane region
Eph receptor
kinase domain
SAM domain
phosphorylation
PDZ binding motif

efn-1;efn-2;efn-3 triple mutants display enhanced embryonic lethality compared to the single *efn* mutants. *efn-1;efn-2;efn-3* triple mutants also display reduced autophosphorylation of VAB-1. EFN-1, EFN-2, EFN-3, and EFN-4 bind to VAB-1 *in vitro*. These data suggest that EFN-1, 2, and 3 function redundantly to serve as ligands for VAB-1 (Wang et al., 1999, Chin-Sang et al., 1999, Chin-Sang et al., 2002). *efn-4* mutants also display a defect in embryonic morphogenesis. Somewhat surprisingly, *efn-4* null mutations show synergistic interactions with *vab-1* null mutations, suggesting that these two genes function in separate pathways. Because VAB-1 is the only member of Eph receptor family in *C. elegans*, this observation raises the possibility that EFN-4 has another receptor, which is not closely related in sequence to the canonical Eph receptors. Interestingly, *efn-4* does not display synergistic interactions with a mutation in the *mab-20* gene, which encodes a semaphorin. This result is consistent with the possibility that EFN-4 and MAB-20 might function in a common pathway during *C. elegans* embryogenesis (Chin-Sang et al., 2002).

Eph receptors are single transmembrane proteins that have an intracellular catalytic domain and an extracellular ligand binding domain (Fig. 13). The extracellular domain of Eph receptors also contains a cysteine-rich region and two fibronectin type-III repeats (Lackmann et al., 1998). The ephrin binding domain is a highly conserved Ig-like motif and is necessary and sufficient for ligand recognition and binding (Labrador et al., 1997; Himanen et al., 1998). The cysteine-rich region facilitates the low affinity binding of ephrins, and the two fibronectin type-III repeats are involved in receptor dimerization (Smith et al., 2004). The intracellular portion of Eph receptors contains a juxtamembrane domain, a kinase domain, a sterile-α-motif (SAM) domain, and a PSD95/Dlg/ZO1

(PDZ)-binding motif (reviewed by Pasquale, 2005). The juxtamembrane domain regulates the phosphorylation of the kinase domains, and the PDZ-binding motif is important for interacting with PDZ domain proteins (Holland et al., 1997; reviewed by Pasquale 2005) (Fig. 13). The ephrinB ligand structure includes an extracellular Eph-binding domain, a linker region, a transmembrane segment, a cytoplasmic region, and a PDZ binding motif (Toth et al., 2001; Nikolov et al., 2005) (Fig. 13). EphrinAs have a similar extracellular domains but are attached to the cell via a glycosylphosphatidylinositol, a lipid anchor (Nikolov et al., 2007) (Fig. 13).

Crystal structures of EphB2, ephrinB2, ephrin-Eph dimer and tetramers reveal that ephrinB2 inserts its loop into a hydrophobic channel on the EphB2 receptor surface (Chrencik et al., 2006; Himanen et al., 2002). In solution, the extracellular domains of Eph and ephrin form high affinity heterodimers, which pair to form a tetrameric ring-like assembly with two distinct interfaces (Pasquale, 2004) (Fig. 14). The larger interface is responsible for high-affinity dimerization of the ligand-receptor complex, whereas the smaller interface is responsible for assembling the heterodimer of the ephrin-Eph complex into a circular tetramer (Himanen et al., 2001, 2002, Chrencik et al., 2006, Smith et al., 2004). Ligand-induced clustering of Eph receptors is essential for kinase-dependent and kinase-independent Eph signaling (reviewed by Egea and Klein 2007). Receptor preclustering is required for soluble ephrin proteins to induce robust Eph phosphorylation and signaling in the nervous system (Davis et al., 1994) (Fig. 14). However, the regulation of Eph–ephrin clustering under physiological conditions is not understood.

Figure 14. ephrin-Eph interaction

A. Ephrin interacts with Eph. One ephrin binds (pink head) to one Eph receptor (blue head), then these dimer interact with another pair of dimers to form a tetramer which leads to ligand-receptor clustering. Interaction of ephrin and Eph receptor causes autophosphorylation (phospho group shows in yellow) of the Eph receptor juxtamembrane (black loop of Eph receptor), which leads to conformation change of juxtamembrane domain. The conformational changes of the juxtamembrane domain removes the inhibition of this domain, which results in kinase (green) catalytic activity. Eph binding to ephrin also results in phosphorylation of the cytoplasmic tail of ephrin.
B. Schematic graph of ephrin-Eph tetramer. Eph binds to ephrin through high affinity dimerization interface, then one dimmer interacts with another pair of dimer through low affinity tetramerization interface. Ephrin-Eph tetramers can interact with each other at the oligomerization interface. Both graphs are modified from Himanen et al., 2007.

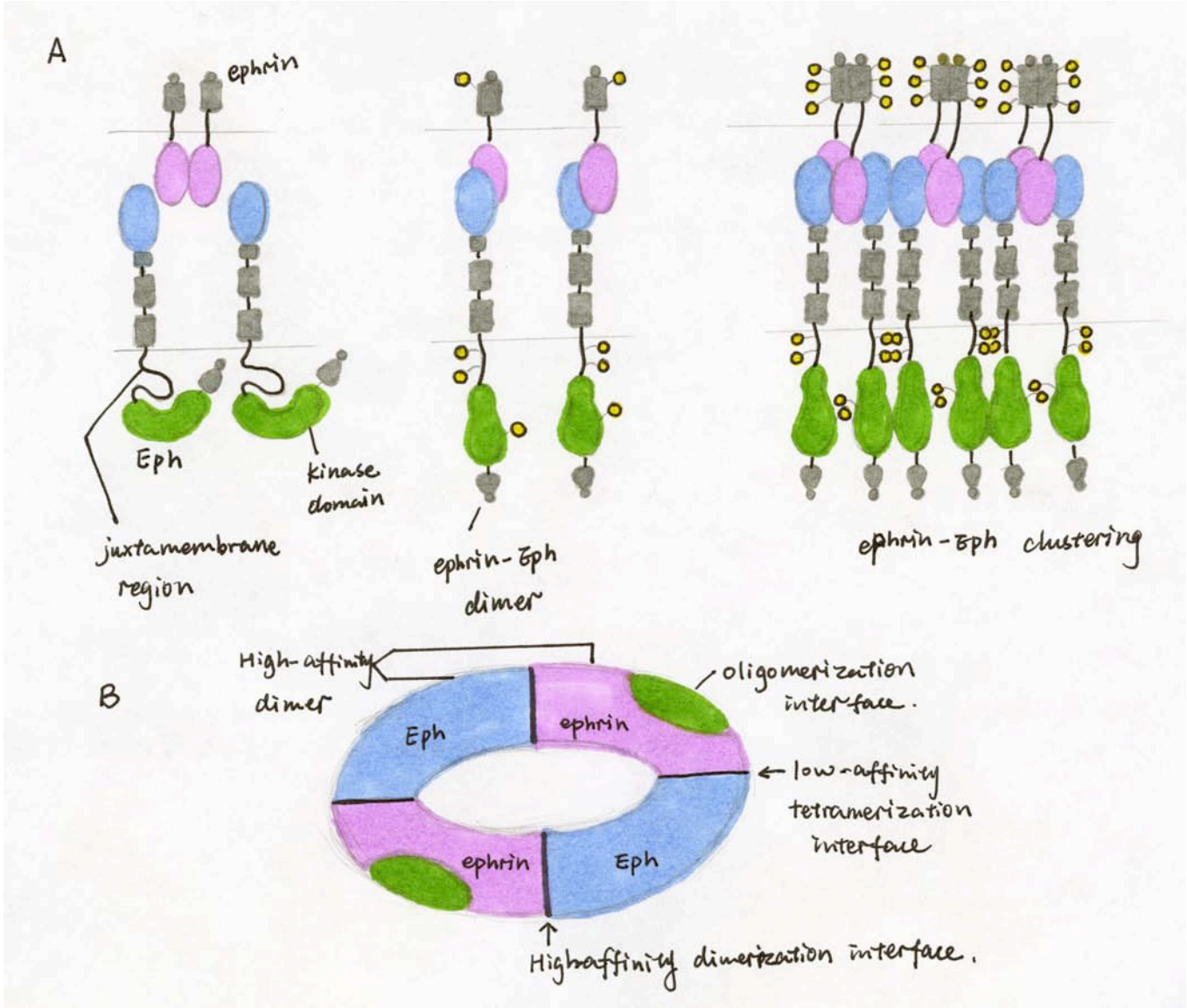
A
ephrin
Eph
kinase domain
juxtamembrane region
ephrin-Eph dimer
ephrin-Eph clustering
B
High-affinity dimer
oligomerization interface.
Eph
ephrin
low-affinity tetramerization interface
ephrin
Eph
High affinity dimerization interface.

Since both Eph receptors and ephrin ligands are membrane proteins, in most cases, Eph receptors on one cell interact with ephrin ligands on another cell (*trans* interaction) (Egea and Klein 2007). The interaction of Eph receptor and ephrins can also occur in the same cell (*cis* interaction) (Yin et al., 2004).

Ephrin binding to Eph receptors leads to activation of the Eph receptor kinase. There are two hypotheses for how this activation occurs. In one hypothesis, ephrin binding locks the receptors together in an orientation that favors phosphorylation of kinases in *trans* (Huse and Kuriyan 2002). The activation of Eph receptor kinase activity involves the phosphorylation of the kinase domain activation loop. The unphosphorylated form of the kinase loop blocks the kinase active site, and phosphorylation removes this inhibition. The active kinase then phosphorylates other molecules and initiates downstream signaling cascades (Murai and Pasquale 2002). The second hypothesis, which derives from crystal structure of intracellular region of EphB2, proposes that the juxtamembrane region regulates the kinase activity (Binns et al., 2000; Wybenga-Groot et al., 2001). In the absence of ephrinB2 ligands, the EphB2 receptor tyrosine kinase activity is regulated by the juxatamembrane domain. The unphosphorylated juxatamembrane domain forms a well-ordered helical structure that interacts intimately with the N-terminal lobe of the kinase domain and results in inactivation of the kinase domain. Phosphorylation of the juxtamembrane domain causes a conformational change that releases the structural constraints that distort the kinase active site (Wybenga-Groot et al., 2001). Upon phosphorylation, the solvent-exposed juxtamembrane domain also leads to interaction of Eph receptor with its downstream signaling proteins.

An interesting characteristic feature of Eph receptors and ephrin ligands is that they are capable of bidirectional signaling. (Zhao et al., 2006; Egea and Klein, 2007; Aoto and Chen, 2007; Pasquale, 2008). Upon ephrin binding, Eph receptors are activated and send a forward signal to the receptor-expressing cell. At the same time a reverse signal is also induced in the ephrin ligand-expressing cell (reviewed by Pasquale 2005; Egea and Klein 2007) (Fig. 15). The forward signaling is carried out by Eph receptors and modulates the actin cytoskeleton through activation of guanine nucleotide exchange factors (GEFs), which regulate axon guidance in the development of the nervous system (Noren and Pasquale, 2004). Forward Eph receptor signaling depends on tyrosine kinase activity. Disruption of the Eph receptor kinase domain impairs forward signaling, but reverse signaling is unaffected (reviewed by Davy and Soriano 2005; Egea and Klein 2007). Reverse signaling requires Src family kinase (SFK), which can activate ephrinB by phosphorylation. The transient tyrosine phosphorylation of ephrinB by SFK creates binding sites for SH2 domain-containing scaffolding proteins like Grb4, which controls actin dynamics and cell migration (Cowan and Henkemeyer, 2001). Reverse signaling through the cytoplasmic domain of ephrinB2 is required for axon pathfinding (Cowan *et al*, 2004). Although ephrinA ligands lack an intracellular domain that could recruit scaffolding molecules, they employ associated transmembrane proteins to modulate cell adhesion. (Davy and Soriano, 2005). EphrinAs can also interact with EphAs in *cis*, which prevents *trans* interaction and silences EphA forward signaling (Carvalho et al., 2006; Yin et al., 2004).

Figure 15. Bidirectional signaling of Eph receptors

Both ephrin A-Eph A and ephrin B-Eph B activate bidirectional signaling. *Trans*-interaction of Eph receptor and ephrins induces forward signaling at the receptor expressing cells and reverse signaling at the ligand expressing cells. The interaction of ephrin and Eph receptor can happen in *cis*, where this interaction can inhibit the signal. Reprited from Arvanitis and Davy, 2008.

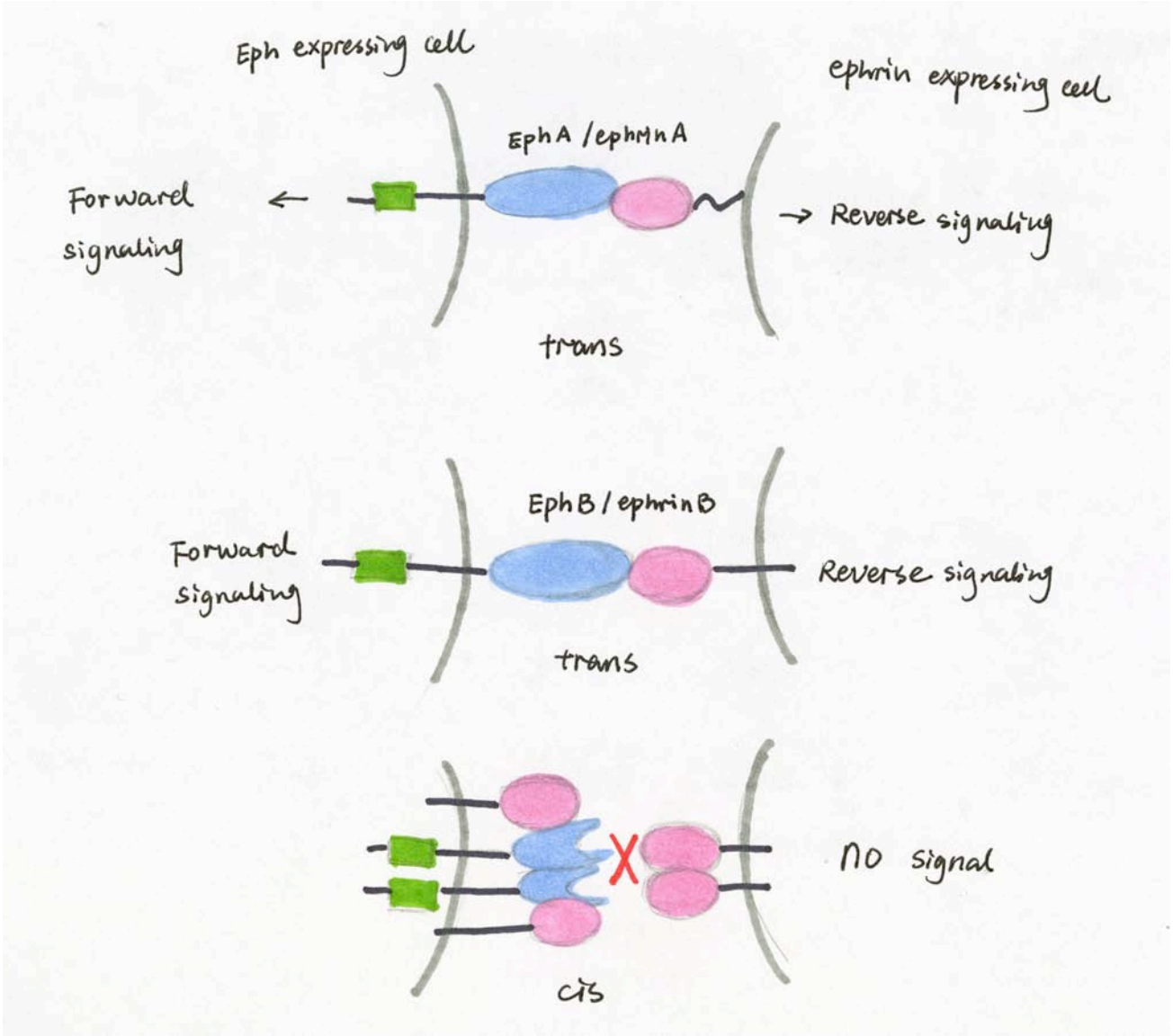
Eph expressing cell
ephrin expressing cell
EphA / ephrinA
Forwarel signaling
Reverse signaling
trans
EphB / ephrinB
Forward signaling
Reverse signaling
trans
No signal
cis

Eph receptors and ephrins are implicated in a variety of processes, such as regulation of cell proliferation, survival, migration, cell-cell adhesion, axon guidance, and insulin secretion (reviewed by Zhao et al., 2006; Himanen et al., 2007; Kuijper et al., 2007; Merlos-Suarez et al., 2008). The best-characterized effect of Eph receptor signaling is retraction of cells upon contact with ephrin-expressing cells (reviewed by Halloran and Wolman 2006). In the central nervous system, cell-cell contact of Eph-expressing cells and ephrin-expressing cells regulates cell-cell attraction/repulsion, migration and adhesion during development. These interactions also participate in synaptic functions in adult animals. There are several hypotheses about how contact of Eph receptor-expressing cells with ephrin-expressing cells could result in cell-cell repulsion. One well-accepted theory invokes proteolytic cleavage (Fig. 16). Upon EphA receptor binding to ephrinA, the metalloprotease ADAM10 and other proteases cleave the extracellular portion of the ephrin. The shedding of ephrinAs releases the molecular tethering between the cells and causes termination of cell-cell adhesion (Mancia and Shapiro, 2005; Janes et al., 2005) (Fig. 16). Another popular theory about how cell-cell attraction switches to cell-cell repulsion is that rapid internalization removes ephrin-Eph complexes from the cell surface and enables the detachment of cells (Fig. 16). Cell culture assays suggest that the interaction of cells expressing EphB receptors with cells expressing ephrinBs results in the rapid formation of intracellular vesicles containing ephrinB-EphB complexes in both cell populations (Zimmer et al., 2003, Marston et al., 2003, Cowan et al., 2005, Irie et al., 2005). The EphB receptor kinase domain regulates the internalization of ephrinB-EphB into EphB-expressing cells. Whereas, the internalization of ephrinB-EphB into ephrinB-expressing cells is mediated by the cytoplasmic tail of ephrinB. Truncation of

the ephrinB intracellular domain leads to preferential internalization of ephrinB-EphB into Eph-expressing cells, whereas the truncation of EphB intracellular kinase domain causes preferential internalization of ephrinB-EphB complex into ephrin-expressing cells. Blocking *trans*endocytosis by C-terminal truncation of both EphB2 and ephrinB1 causes prolonged cell adherence and reduces cell repulsion (Marston et al., 2003; Zimmer et al., 2003). Currently, very little is known about what proteins regulate endocytosis of ephrinB-EphB complexes. Actin polymerization, Rac activity, and the Rac exchange factor Vav have been suggested to be required for internalization of ligand-receptor complex and cell retraction (Marston et al., 2003; Cowan et al., 2005). One report suggests that clathrin-mediated endocytosis accounts for the internalization of ephrin-Eph complexes by ephrin-expressing cells (Parker et al., 2004). Another report indicates that caveolin-1 regulates endocytosis of ephrin-Eph complexes into Eph-expressing cells (Vihanto et al., 2006). These studies also suggest that the Eph receptor and its effectors may signal from an intracellular compartment after endocytosis (Marston et al., 2003; Zimmer et al., 2003). However, it is unclear in which compartment Eph receptors generate their signal, and how intracellular trafficking regulates Eph receptor downstream signaling. Interestingly, my study of VAB-1/Eph receptor signaling during oocye meiotic maturation in *C. elegans* indicates that intracellular trafficking is the key mechanism that regulates VAB-1/Eph function as a negative regulator. I found that the VAB-1/Eph receptor functions within or in transit to the endocytic recycling compartment. Blocking VAB-1/Eph exit from the endocytic recycling compartment by inactivating cellular trafficking regulators like *rab-11* or *rme-1* results in constitutive inhibition of oocyte meiotic maturation even in the presence of the VAB-1 antagonist MSP.

Figure16. Two models of how Eph receptor regulates cell-cell attraction turns to cell-cell repulsion

A. Endocytosis model. Ephrin-expressing cells contact Eph-expressing cells can result in bidirectional endocytosis of the ligand-receptor complex, which leads to the cell-cell adhesion switch to cell-cell repulsion.
B. Protease cleavage model. Ephrin-expressing cells contact with Eph-expressing cells causes ADAM10 metalloproteinase cleavage of the extrallular portion of ephrin, blocks the cell-cell attractions resulting in cell-cell repulsion. Reprinted from Egea and Klein, 2007.

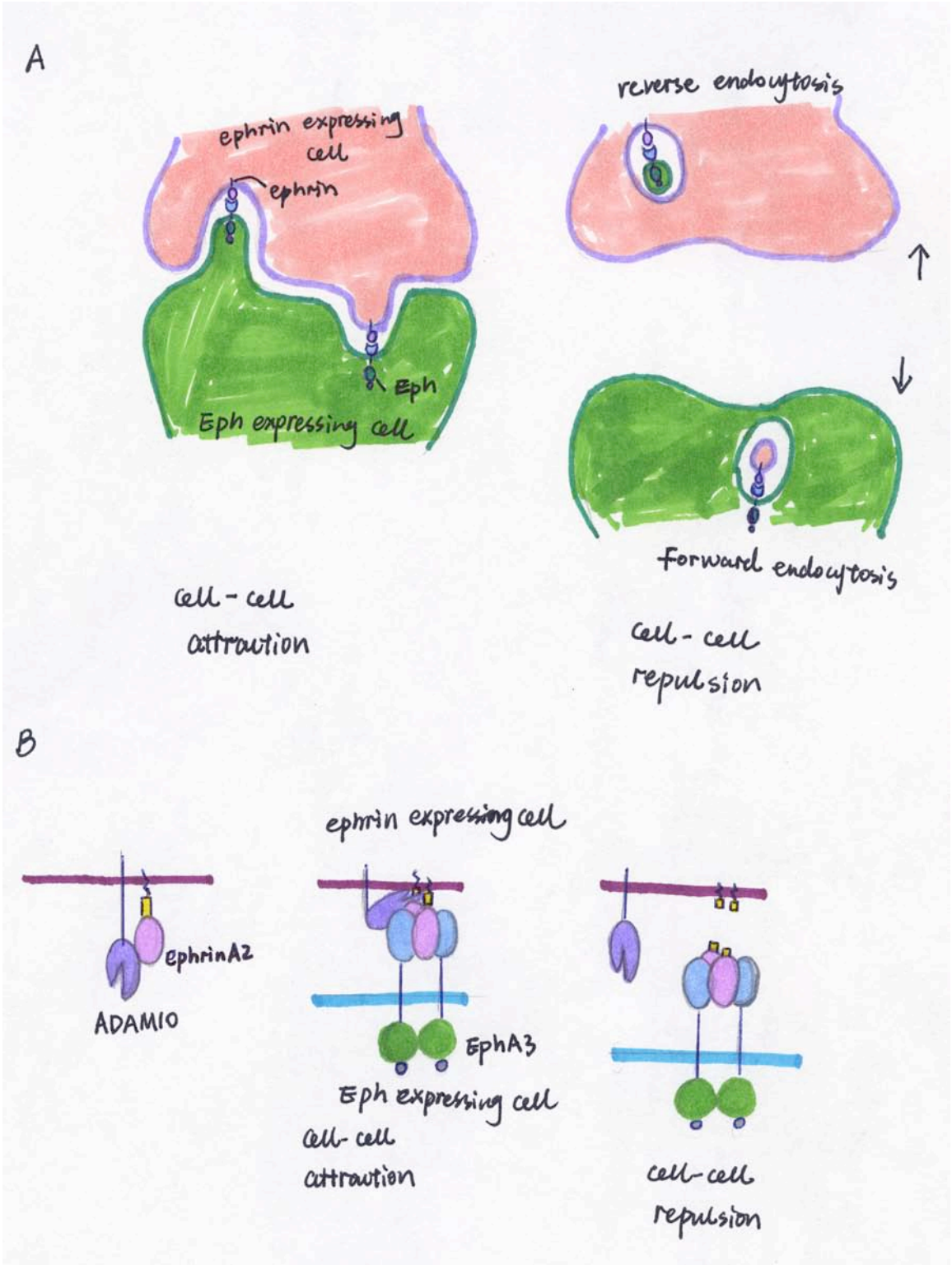
A
ephrin expressing cell
ephrin
Eph
Eph expressing cell
reverse endocytosis
Forward endocytosis
Cell - cell attraction
Cell - cell repulsion
B
ephrin expressing cell
ephrinA2
ADAM10
EphA3
Eph expressing cell
Cell-cell attraction
cell-cell repulsion

Surprisingly, VAB-1/Eph internalization is independent of ephrins, as depletion all the four ephrins in *C. elegans* does not affect VAB-1/Eph localization.

Eph receptors play critical roles in tumorigenesis and metastasis, and high Eph receptor levels positively correlate with angiogenesis in many tumor types, including lung and breast. Eph receptors were identified in carcinoma cells, which suggests a role in tumorigenesis (Hirai et al., 1987). EphA1 overexpression has been reported in various carcinoma cell lines, including lung, and ovary cancers (Hafner et al., 2004; Herath et al., 2006). EphA2 and ephrinA2 have been suggested as transcriptional targets of the tumor suppressor proteins p53, and EphA2 overexpression has been associated with pancreatic adenocarcinoma invasion (Dohn et al., 2001; Duxbury et al., 2004). EphB2 overexpression correlates with ovarian and breast cancer, suggesting that EphB2 is involved in tumorigenesis (Wu et al., 2004; 2006). Interestingly, the EphB4 receptor has both tumor-suppressing and tumor-promoting functions (Noren et al., 2006; Davalos et al., 2006; Stephenson et al., 2001). EphB4 can prevent tumor progression by inhibiting cell motility and invasion and by facilitating apoptosis (Noren et al., 2006). On the other hand, EphB4 receptor can trigger angiogenesis, which promotes tumor growth (Stephenson et al., 2001). Recently, Ephrin-Eph signaling has also been shown to regulate insulin secretion. While, ephrin-A reverse signaling stimulates insulin secretion, Eph A forward signaling inhibits insulin secretion (Konstantinoval et al 2007).

Although ephrins are the well-known ligands for Eph receptors in some cases, Eph receptors can function independently and appear to signal in concert with other pathways, for example, the fibroblast growth factor (FGF) pathway. Overexpression of EphA4 in *Xenopus* embryos induces ectopic posterior protrusions, and inactivation of

FGF rescues this phenotype, which indicates that FGF could be involved in the EphA4 signaling. (Park et al. 2004). Wnt proteins can antagonize EphB function during axon guidance; and it has been suggested that the Wnt pathway terminates Eph receptor signaling by endocytosis of Eph receptors. Wnt may also upregulate Eph receptors and downregulate ephrin ligands (Schmitt et al., 2006). Eph receptors and calcium channels also interact with each other and facilitate reciprocal communication. Eph receptors can interact with calcium channel- NMDA receptor, and can promote NMDA receptor clustering (Takasu et al., 2002). On the other hand, increased intracellular calcium promotes Eph degradation. Interesting, Corrigan et al., (2005) report that there is crosstalk between NMDA and VAB-1/Eph signaling during oocyte meiotic maturation in *C. elegans*.

There is also crosstalk between Eph receptors and MAPK signaling during cell adhesion and cytoskeletal plasticity. Different Eph receptor family members have been implicated in activation or inhibition of MAPK in different cell types. EphA2 activation of the MAPK pathway plays critical roles in cell detachment in breast and prostate cancer cell lines (Pratt et al., 2002). However, EphB2 inhibits MAPK signaling, and this inhibition is necessary for ephrin-induced neurite retraction in mammals (Elowe et al., 2001). EphA2 inhibits the MAPK pathway when it is expressed in endothelial and epithelial cell lines (Miao et al., 2001). The integration of Eph and MAPK signaling pathways is highly conserved as supported by studies of the Eph receptor in *C. elegans*. In *C. elegans,* VAB-1/Eph receptor inhibits MAPK activation in the oocytes in the absence of MSP/sperm (Miller et al., 2003; Govindan et al., 2006).

Eph receptor also exhibits crosstalk with G protein signaling in *C. elegans*. Govindan et al., (2006) demonstrated that somatic G protein pathways regulate oocyte meiotic maturation (see Chapter II for details). In the absence of MSP/sperm, $G\alpha_{o/i}$ signaling inhibits oocyte meiotic maturation in parallel to VAB-1/Eph signaling. In the presence of MSP/sperm, $G\alpha_s$ promotes oocyte meiotic maturation. Interesting, I found that somatic G proteins regulate VAB-1/Eph trafficking. In the absence of MSP/sperm, $G\alpha_{o/i}$ promotes VAB-1/Eph trafficking into the endocytic recycling compartment. By contrast, in the presence of MSP/sperm, $G\alpha_s$ inhibits VAB-1/Eph traffikcking into endocytic recycling compartment, where VAB-1/Eph functions to inhibit oocyte meiotic maturation. Since G protein signaling is part of the story of my dissertation, I will give a very brief introduction about G protein signaling.

G Protein Signaling

Guanine nucleotide-binding proteins are called G proteins, and they function in intercellular signaling by regulating second messenger cascades. G proteins are active when bound to guanosine triphosphate (GTP), and are inactivate when bound to guanosine diphosphate (GDP) (Fig. 17). G proteins and their cellular roles were first discovered by Gilman and Rodbell, who shared the Nobel Prize in Physiology or Medicine in 1994. Gilman and Rodbell found that G-proteins act as signal transducers, which transmit and modulate signals in cells. G proteins receive multiple signals from the exterior, integrate them and thus control fundamental life processes in cells. (Rodbell 1971; Northup at el., 1980). Stimulatory G proteins, Gs, are activated by ligand binding

to a G-protein coupled receptor, and this activation produces a second messenger, cyclic AMP. G proteins consist of two distinct protein families: heterotrimeric G proteins, and small GTPases. Heterotrimeric G proteins, also known as large G proteins are made of three subunits: alpha (α), beta (β), and gamma (γ). β and γ subunit form a dimer that function as a unit and can only be dissociated by denaturation. The α subunit has a high affinity binding site for GDP/GTP. In the GDP bound state, the α subunit binds to a βγ subunit and is inactive, whereas the GTP bound form of the α subunit dissociates from the βγ subunit and serves to regulate effector proteins. GPCRs activate G protein by exchange of GDP to the GTP bound form of G protein, which activates downstream signal transduction pathways (Fig. 16). Small GTPases are monomeric G proteins, and are homologous to the α subunit of large G proteins.

GPCR-associated G proteins are bound to the intracellular surface of plasma membrane and consist of Gα and the tightly associated Gβγ subunits. Ligand binding to the GPCR results in a conformational change and the Gα subunit becomes bound with GTP in place of GDP (Reviewed by Oldham and Hamm, 2007 and 2008). The GTP binding to the Gα subunit causes a conformation change of Gα, which results in the dissociation of Gα from the Gβγ subunit. In terms of Gs protein, the free Gα subunit then binds to and activates different effectors and downstream signal transduction cascades including adenylyl cyclase (Marrari et al., 2007, Sprang et al., 2007). Adenylyl cyclase hydrolyzes ATP to produce cAMP (Fig. 16). cAMP acts as a second messenger that interacts and activates protein kinase A (PKA), which can phosphorylate downstream targets.

Figure 17. G protein signaling

In the inactive state, GDP bound Gα associates with Gβγ. When a ligand binds to G protein coupled receptor (GPCR), GDP changes to GTP, which results in a conformational change of Gα subunit. This conformation change causes dissociation of Gα from Gβγ. Free GTP bound Gα actives adenylyl cyclase, which catalytes the production of cAMP. Adapted from Steve Cook, 2002-2008. http://www.steve.gb.com/images/science/g_protein_coupled_receptor.png

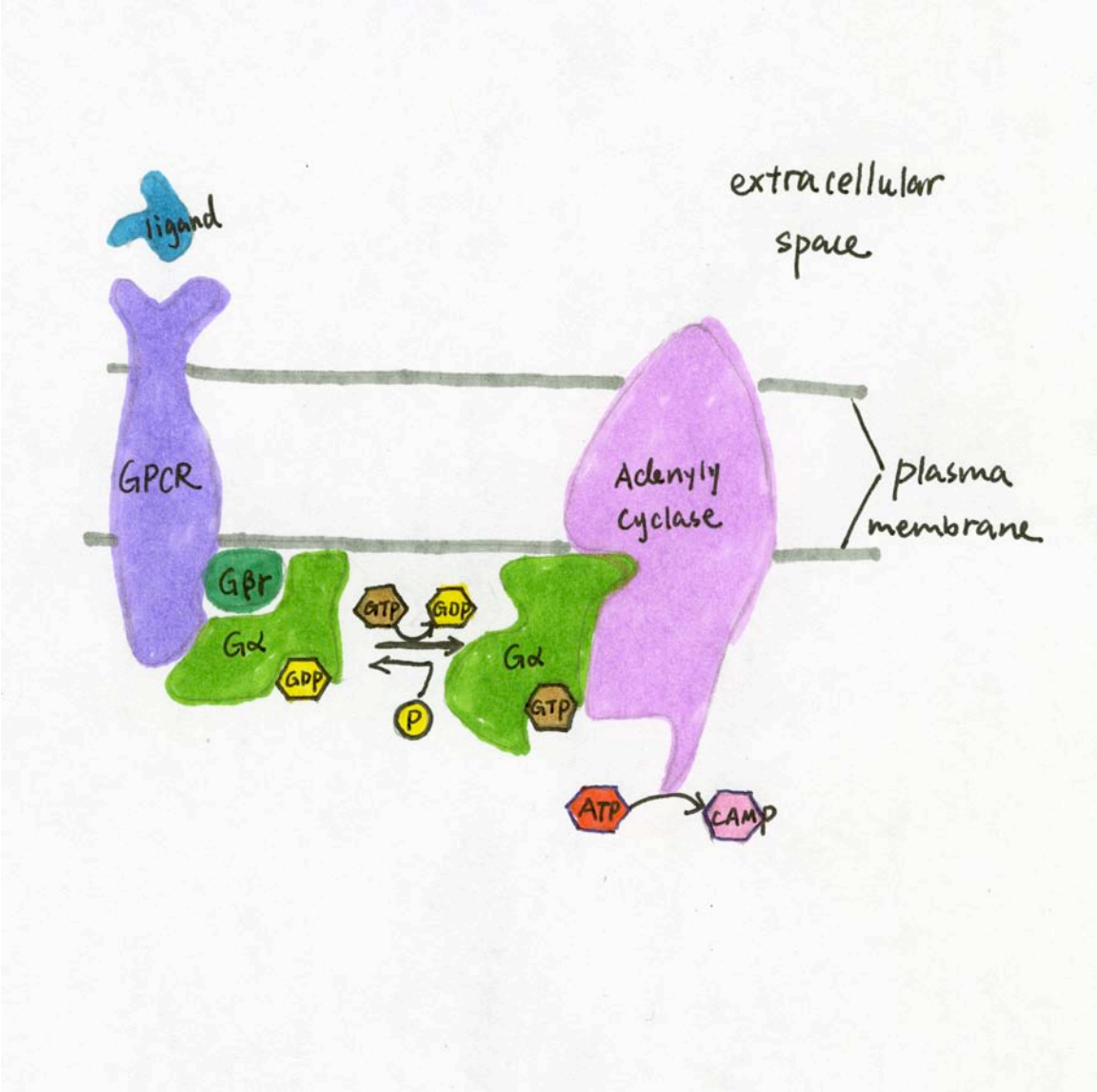
ligand
extracellular space
GPCR
Adenyly cyclase
plasma membrane
Gβr
Gα
GDP
GTP
GDP
P
Gα
GTP
ATP
cAMP

Four general types of Gα subunits that have been elucidated to date, $G\alpha_s$, $G\alpha_i$, $G\alpha_{q/11}$, and $G\alpha_{12/13}$ (reviewed by Gilman 1994). These four types of Gα subunits share a common mechanism but activate different downstream targets and cause different signaling outputs (Lambert et al., 2008, Penn and Benovic, 2008). Whereas $G\alpha_s$ stimulates production of cAMP, $G\alpha_{o/i}$ inhibits the production of cAMP from ATP. $G\alpha_{q/11}$ stimulates membrane-bound phospholipase C β that cleaves PIP2 into two second messengers, IP3 and diacylglycerol (DAG). $G\alpha_{12/13}$ is involved in Rho family GTPase signaling to control cell migration (Lambert et al., 2008, Penn and Benovic, 2008). In *C. elegans*, twenty-one Gα, two Gβ, and two Gγ have been reported to date. Among them, *gsa-1* encodes a $G\alpha_s$, *goa-1* encodes a $G\alpha_{i/o}$, *egl-30* or *gqa-1* encodes a $G\alpha_q$, and *gpa-12* encodes a $G\alpha_{12/13}$ (Brundage et al., 1996; Jansen et al., 1999; Korswagen et al., 1997; Park et al., 1997; Segalat et al.,1995). Adenylyl cyclase also activates the GTPase activity of the Gα subunit. The activated Gα subunit then hydrolyzes GTP to GDP. GDP bound Gα subunit then recycles back to the Gβγ dimer to restore the original heterotrimer and waits for a new signaling cycle. The GTP-bound α subunit can interact with the GPCR and thereby reduce its affinity for ligand. The ligand is then released from the receptor, and the system is back to the resting state (Gilman, 1994). The ability of the heterotrimeric G protein to bind the GPCR is dependent on sites located within all three subunits of the G proteins (Gilman, 1994). Four types of Gα, and five types G_β and seven types G_γ subunits have been reported so far. The different Gα subunit and Gβγ subunit determines which of G protein coupled to which particular type of receptor (Gilman, 1994).

Studies from my dissertation suggest that G proteins play a major role in regulating VAB-1/Eph receptor trafficking. Govindan et al., (2006) reported that somatic $G\alpha_{o/i}$ inhibits oocyte meiotic maturation in parallel with VAB-1/Eph in the absence of sperm and that $G\alpha_s$ promotes oocyte meiotic maturation in the presence of MSP/sperm (please see details in Chapter II). I found that there is crosstalk between the somatic G protein pathway and the oocyte VAB-1/Eph receptor pathway during oocyte meiotic maturation: somatic G proteins regulate VAB-1/Eph trafficking in the oocytes. These findings enhance our understanding of the mechanisms that regulate oocyte meiotic maturation. Because of its involvement in VAB-1/Eph signaling, an overview of intracellular trafficking is presented in the next.

Receptor Trafficking and Signaling

Receptor trafficking regulates signaling

In my dissertation work, I found that intracellular trafficking is a key mechanism that regulates intracellular signaling by the VAB-1/Eph receptor. To provide a background for understanding my experiments, I will start with a general description of how intracellular trafficking is involved in receptor signaling.

Receptor trafficking can affect intercellular signaling at many levels. In some cases, endocytosis and endosomal trafficking can attenuate signaling (Le Roy and Wrana 2005). In the other cases, endocytic trafficking regulates ligand and receptor activation

(reviewed by Gonzalez-Gaitan, 2003a; 2003b; Fischer et al., 2006). In some signaling pathways, ligand/receptor complexes signal from endosomes. For instance, binding of TGF-β to the TGF β receptor induces heterodimerization of type I and type II receptors. Formation of the ligand/receptor complexes triggers a serial phosphorylation event, in which the type II receptor phosphorylates the type I receptor, which then phosphorylates R-Smad (Xu 2006). Phosphorylation of R-Smad causes its nuclear translocation. The phosphorylation of R-Smad occurs in endosomes, and this action needs the assistance of Sara (Smad anchor for receptor activation). An endosome-associated protein, Sara is an adaptor that links type I TGF receptors and R-Smads (Tsukazaki et al. 1998). Internalization of type I receptor is critical for bringing it to Sara and R-Smad in endosome, once phosphorylated in the endosome, Smad then moves into the nucleus wehre it generates transcriptional complexes on the basis of specific DNA-binding (Massague 1998) (Fig. 18).

Hedgehog (Hh) signaling is another example of how endocytosis is involved in intercellular communication. Hh binding to Patched (Ptc) removes the inhibition of activity of smoothened (Smo) protein resulting in downstream signaling (reviewed by Hooper and Scott 2005). Endocytosis has been proposed to be involved in Hh signaling. In the absence of the Hh ligand, Smo is mainly localized to endosomes, whereas Ptc can be found on endosomes and on the plasma membrane. Upon Hh binding to Ptc, Ptc trafficks into lysosomes for degradation, while Smo shuttles to the plasma membrane and is activated (Denef et al., 2000; Incardona et al., 2002; Zhu et al., 2003) (Fig. 19). Translocation of Smo is important for its activation since a mutant Smo that is localized

to the plasma membrane constantly, is constitutively active (reviewed by Ingham and McMahon, 2001).

The Notch signaling pathway provides another example of how endocytosis in one cell affects signaling in neighboring cells. In the *Drosophila* peripheral nervous system, the sensory organ precursor (SOP) cell undergoes a mitotic division to generate a neural precursor cell (pIIb) and a nonneural cell (pIIa) (Emery et al., 2005). The cell fates of pIIb and pIIa are determined by Notch signaling. The Notch receptor is a single transmembrane protein whose ligand is Delta. Asymmetrical distribution of endocytic components in a SOP cell determines the fates of its daughter cells. The cell that internalizes becomes a signal-sending cell, pIIb, whereas its neighboring cell becomes a signaling-receiving cell, pIIa (Emery et al. 2005). Endocytosis of Delta in signaling cells is critical for Notch signal activation in receiving cells. Mutations that block Delta internalization in the signaling cell pIIb fail to activate Notch signaling in the receiving cell pIIa. Delta binding to Notch receptor results in protease cleavage of the Notch receptor: the extracellular domain is cleaved by an ADAM protease, and the intracellular domain is cleaved by the γ–secretase complex. After being cleaved by proteases, the Notch receptor intracellular domain is released and transported into the nucleus to activate target gene expression (reviewed by Le Borgne et al. 2005). The mechanism by which Delta internalization in the signal-sending pIIb cell regulates Notch signaling in the signal receiving pIIa cell has been revealed and two hypotheses have been proposed. One model proposes that internalization of the Delta/Notch receptor complex in the pIIb cell facilitates the cleavage of the extracellular domain of the Notch receptor in the pIIa cell (Parks et al. 2000) (Fig. 20)

Figure 18. Endocytic trafficking regulates TGFβ signaling

TGF-β binding the TGFβ receptor induces heterodimerization of type I and type II receptors. Formation of ligand/receptor complex triggers phosphorylation of both type II and type I receptors. Phosphorylated receptor dimmers are then internalized into the cell, and phosphorylated Smad in the endosomes with the assistance of Sara, protein that links the TGFβ receptor dimer to the Smad. Phosphorylation of R-Smad causes its nuclear translocation, where it regulates transcription. Modified from Fischer et al., 2006.

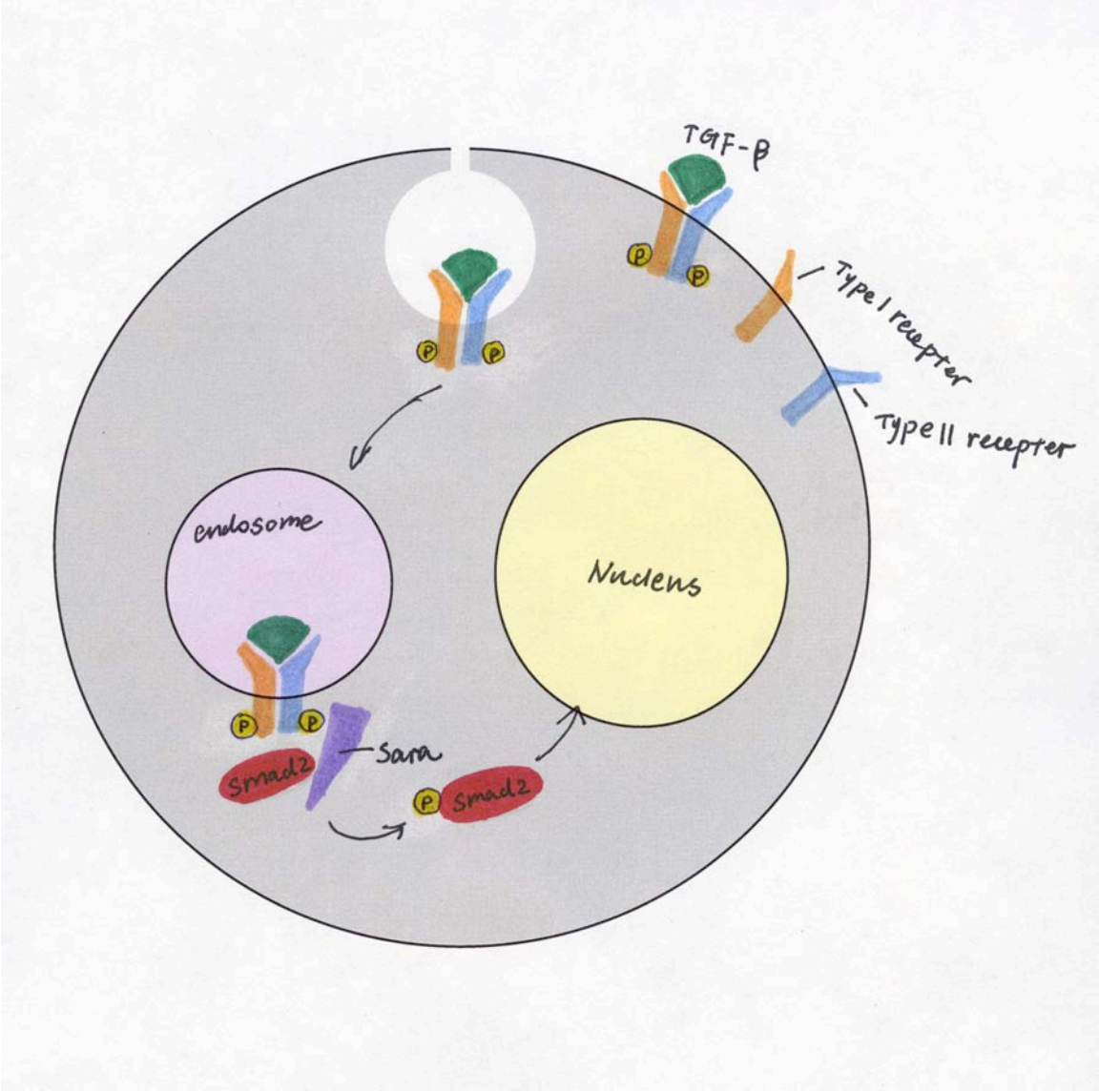
TGF-β
Type I receptor
Type II receptor
endosome
Nucleus
P
P
P
P
P
P
Smad2
Sara
P
Smad2

Figure 19. Intracellular trafficking regulates Hedgehog (Hh) signaling

In the absence of the Hh ligand, Smo is mainly localized to endosomes, whereas Ptc distributes to endosomes and to the plasma membrane. Upon Hh binding to Ptc, Ptc traffics into lysosomes for degradation, while Smo shuttles to the plasma membrane and is activated. Modified from Fischer et al., 2006.

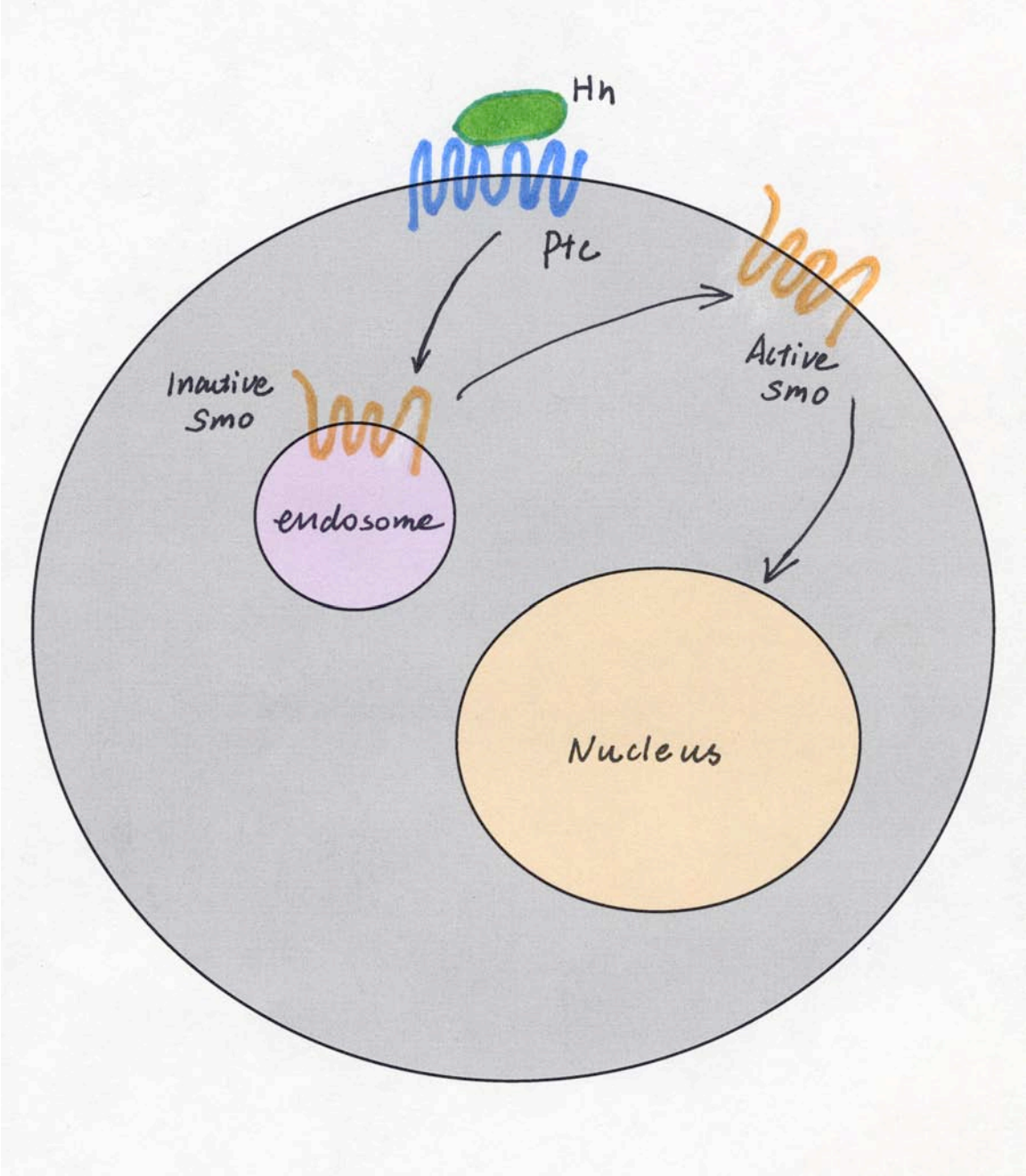
Hh
Ptc
Inactive Smo
endosome
Active Smo
Nucleus

Figure 20. Intracellular trafficking regulates Notch signaling

Addition of ubiquitin to the Delta C-terminal region results in internalization of Delta. Internalized Delta sorts into recycling endosomes and further recycles back to the plasma membrane. This recycled Delta is activated. The active Delta binds to Notch receptor resulting in protease cleavage of the Notch receptor. The extracellular domain of Notch is cleaved by an ADAM protease, and the intracellular domain is cleaved by the γ–secretase complex. The Notch receptor intracellular domain is then released and transported into the nucleus, where it function in transcription regulation. Modified from Fischer et al., 2006.

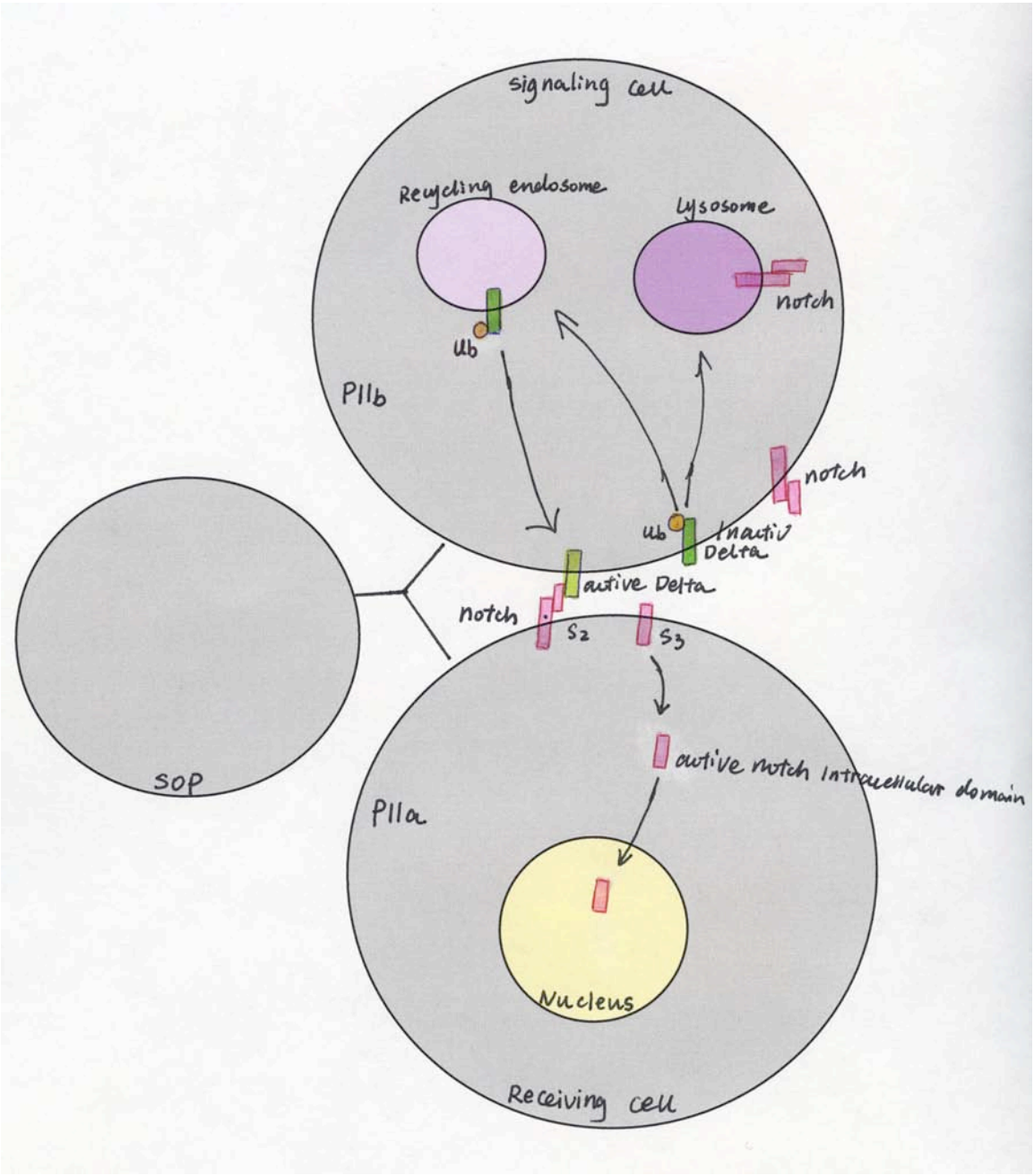
signaling cell
Recycling endosome
Lysosome
notch
Ub
PIIb
notch
Ub
Inactiv
Delta
active Delta
notch
S2
S3
SOP
active notch intracellular domain
PIIa
Nucleus
Receiving cell

Another model proposes that internalization and further endosome processing of Delta in the pIIb cell activates Delta, and this activated Delta then recycles back to the plasma membrane to activate Notch receptor in the pIIa cell (Wang and Struhl 2004; Emery et al. 2005, Jafar-Nejad et al 2005) (Fig. 20). Blocking recycling of Delta in the signal sending pIIb cell prevents activation of Notch signaling in the receiving cell pIIa (Emery et al., 2005).

Endocytosis and intracellular trafficking

How does a cell surface receptor like Eph gets internalized into an intracellular compartments, and how is this intracellular trafficking regulated? To help you understand my dissertation work on intracellular trafficking of the Eph receptor, I will briefly describe how a cell-surface receptor gets internalized into the cell interior by introducing the two major modes of endocytic trafficking. Then I am going to introduce the mechanisms that regulate intracellular vesicle sorting and fusion.

Clathrin-dependent endocytosis and its signaling

One way a cell surface receptor is internalized into the cell interior is through clathrin-dependent endocytosis (reviewed by Ungewickell and Hinrichsen 2007; Mayor and Pagano 2007). To understand how clathrin-dependent endocytosis occurs and how vesicles are formed from the plasma membrane and bud off to form free vesicles, I will describe clathrin and its accessory proteins, such as adaptor protein AP2 and the disabled homolog Dab2. Then, I will describe how clathrin is assembled on the cell surface to form a clathrin-coated vesicle and what mechanisms regulate this process.

The life of a clathrin-coated vesicle starts with the recruitment of clathrin, adaptor proteins and other accessory proteins, such as a cell surface receptor, to a particular region of plasma membrane (Santini et al., 2002; Fig. 21). After flat lattices assemble, the lattices curve into coated pits, which then pinch off from the plasma membrane by a process called fission forming coated-vesicles form. Soon thereafter clathrin and the adaptor proteins are released from the vesicle, forming an uncoated vesicles, which fuses with the early endosome. The contents inside the vesicles usually get passed into lysosomes for degradation, and the receptor on the endosome sometimes gets transported into recycling endosomes for recycling back to the plasma membrane. The released soluble clathrin and adaptor proteins can become engaged in a new round of coated vesicle assembly (reviewed by Ungewickell and Hinrichsen 2007, Benmerah and Lamaze 2007, Mousavi et al., 2004, Johannes and Lamaze 2002) (Fig. 21).

Two main proteins found in coated pits are clathrin and the heterotrimeric protein AP-2. Clathrin contains a three-legged structure with three heavy and three light chains, called a triskelion (Schmid et al., 1997; Greene et al., 2000; Fig. 22) The heavy chain of clathrin regulates binding of clathrin to adaptor proteins, and is necessary for establishing clathrin into an enclosed basket structure, while the light chain modulates the assembly state of the clathrin triskelion (Greene et al., 2000; Ybe et al., 1998). Clathrin interacts with some endocytic proteins mostly through their clathrin box motif, such as the LLNLD sequence of AP-2 (Ter Haar et al., 2000). Clathrin is essential for clathrin-dependent endocytosis, depletion of clathrin blocks uptake of certain extracellular molecules, such as low density lipoprotein (Fielding and Fielding 1996).

Figure 21. Clathrin and AP2

A. Schematic representation of Clathrin-dependent endocytosis. Epsin binding to PIP_2 induces membrane invagination. Ligand binding to the receptor recruits AP-2 and other adaptor proteins such as AP180, which mediate the assembly of a clathrin-coated structure. The budding of deeply invaginated clathrin pits is regulated by dynamin and actin filaments. Adapted from Mousavi et al., 2004.
B. A closer view of the fission of the clathrin-coated vesicle. Adapted from Ungewickell and Hinrichsen, 2007.

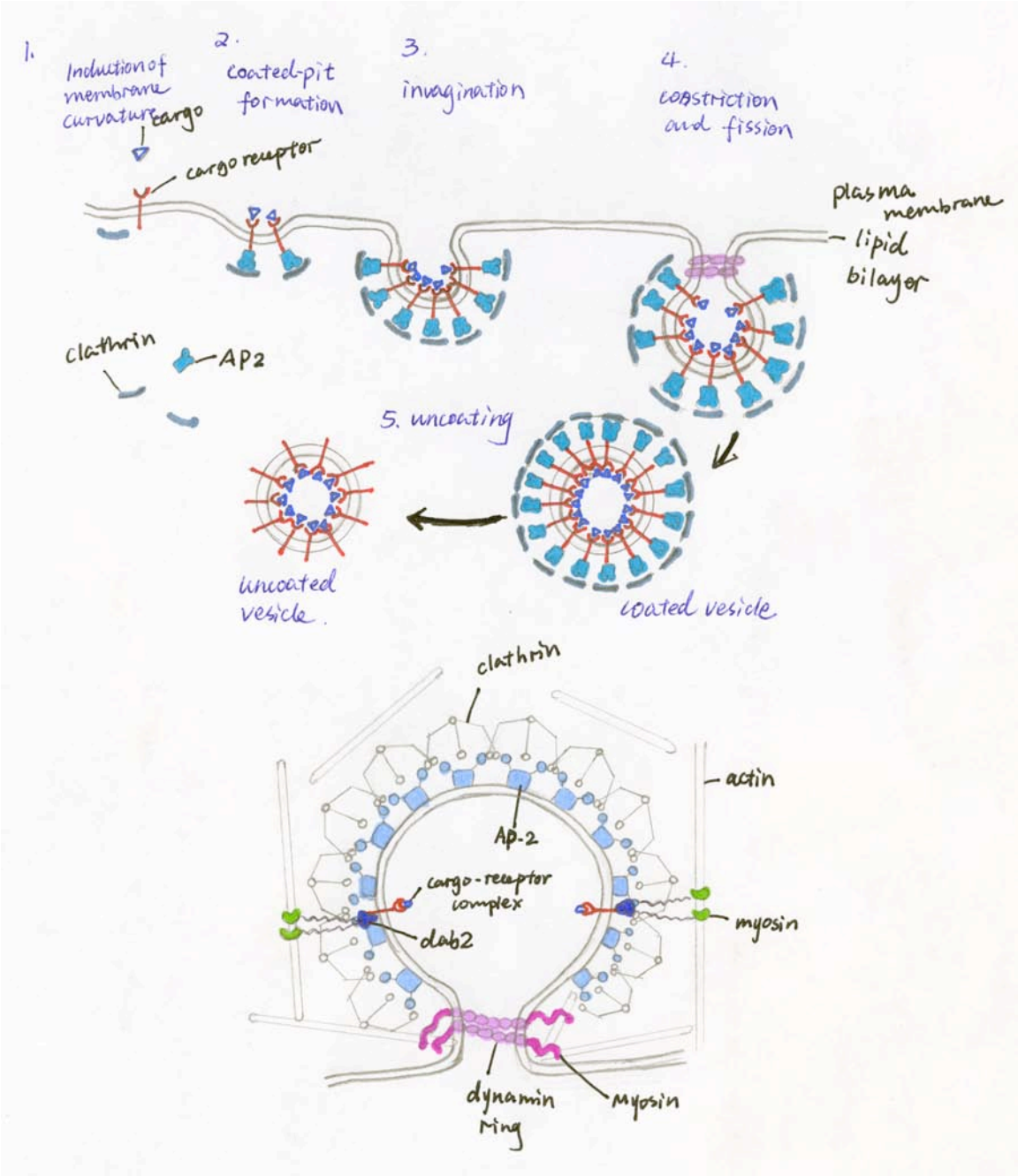
1.
Induction of membrane curvature
cargo
2.
coated-pit formation
3.
invagination
4.
constriction and fission
cargo receptor
plasma membrane
lipid bilayer
clathrin
AP2
5. uncoating
uncoated vesicle
coated vesicle
clathrin
actin
Ap-2
cargo-receptor complex
dab2
myosin
dynamin ring
myosin

Figure 22. Clathrin and AP2.

A. EM image of clathrin-coated pits. Reprinted from Molecular Biology of the Cell, Garland publishing, NY, 1998.
B. Schematic of clathrin cage. One clathrin is shown in light blue. Reprinted from Johnson and Goodsell, 2007.
C. Schematic representation of clathrin and AP2 domain structure. Adapted from Mousavi et al., 2004.

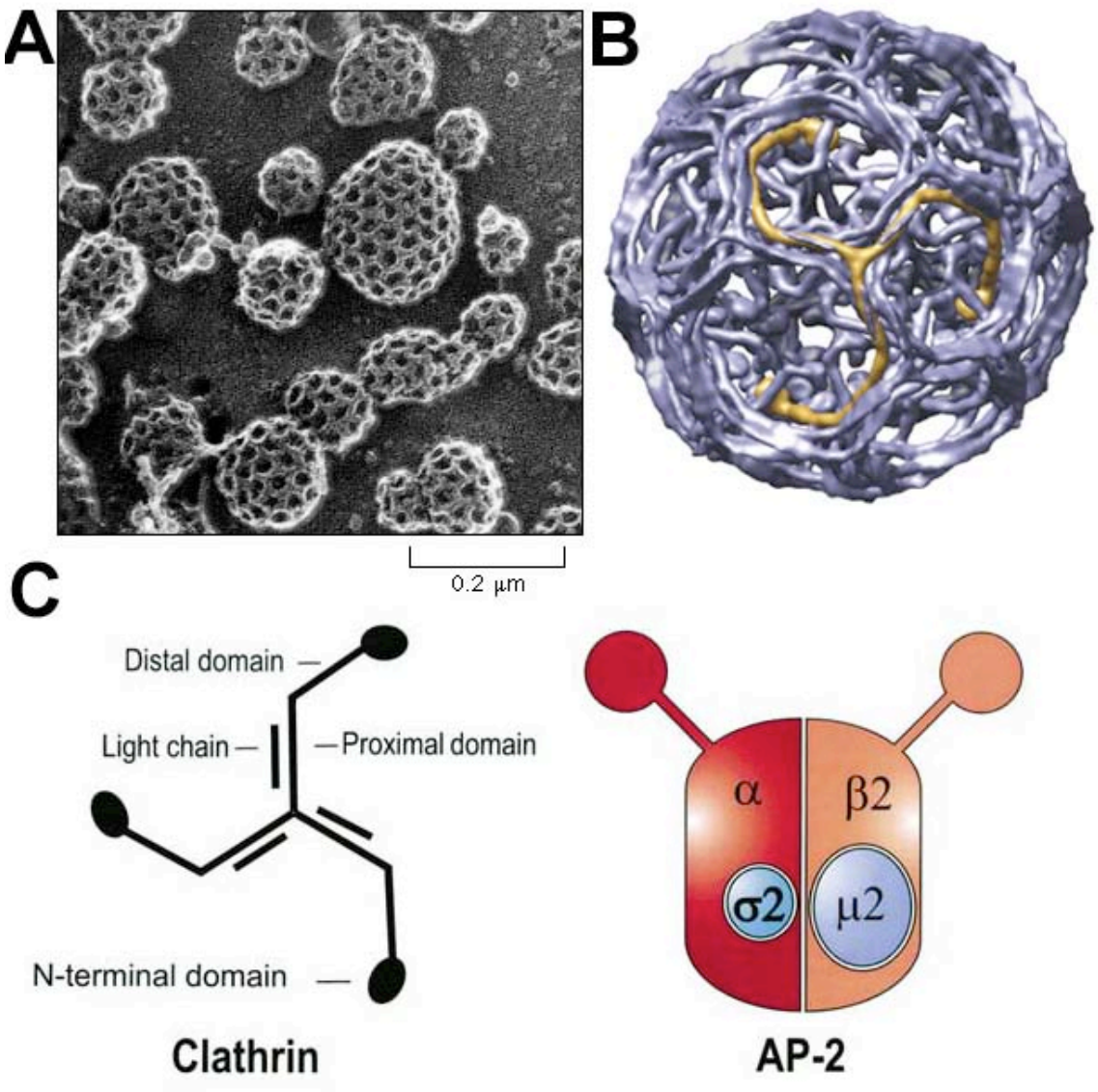
A
B
0.2 μm
C
Distal domain
Light chain
Proximal domain
N-terminal domain
Clathrin
α
β2
σ2
μ2
AP-2

AP-2 is a large adaptor protein for clathrin-dependent endocytosis and contains four subunits: α, β2, μ2, δ (Heuser and Keen 1988)(Fig. 22). The α subunit of AP-2 functions in targeting the AP-2 complex to the plasma membrane; it also binds certain endocytic proteins bearing DPF or DPW motifs. The β2 subunit helps the complex bind clathrin, and this binding promotes clathrin lattice assembly. The β2 subunit also functions to specifically select cargo for endocytosis (Owen et al., 2000). The μ2 subunit contributes to recognition and sorting of the cargos and binds to β2 subunits to assist assembly of the AP-2 complex (Aguilar et al., 1997). In addition, AP-2 specifies the localization of clathrin assembly by interacting with phosphoinositides of the plasma membrane and subsequently recruits and promotes polymerization of clathrin (Page and Robinson 1995). The AP2 adaptor protein can also associate with other endocytic accessory proteins and holds its central position among all the endocytic proteins. Cell-culture studies suggest that the AP2 adaptor is associated with all the coated structures at the plasma membrane. In addition, disruption of AP eliminates most of the clathrin-coated structures and blocks the uptake of certain intracellular ligand proteins. More importantly, inactivation of AP in *C. elegans*, *Drosophila*, and mice causes lethality of the animals.

Other adaptor proteins have been reported to be present in clathrin-coated pits, such as AP180/CALM (clathrin assembly lymphoid myeloid leukaemia), Epsin (Eps15-interacting protein), Eps15, Dab2, and Numb (Ye and Lafer 1995; Kalthoff et al., 2002; Salcini et al., 1999; Morris et al., 2002; Santolini et al., 2000). These proteins bind to clathrin and the AP2 adaptor complex, and they also promote assembly of clathrin (Fig. 22). In addition, Dab2 may have a role in receptor sorting as well as being part of the

general endocytic machinery. Dab2 protein is a putative tumor suppressor protein that is implicated in cell surface receptor turnover. Dab2 is a complex molecule with an N terminal phosphotyrosine binding (PTB) domain, which binds to multiple cell-surface receptors bearing FxNPxY motifs (Mishra et al., 2002). Dab2 also bears a DFP motif, which is sufficient for targeting Dab2 to clathrin-coated pits. Dab2 binds to phosphoinositides and AP2 through its DFP motif (Morris and Cooper 2001). Moreover, a recombinant Dab2 is sufficient to initiate the formation of clathrin-coated vesicles from phosphoinositide-containing lipids (Mishra et al., 2002). Dab2 has been found to associate with members of the LDL receptor family and it is involved in internalization of the LDL receptor-like protein megalin (Morris and Cooper 2001). Analysis of conditional knockout Dab2 mice indicates that the structure of clathrin-coated pits is decreased in renal tubule cells, and mutant mice display defects of amino acid and vitamin uptake, which is also a characteristic feature of megalin mutants (Morris et al., 2002).

Coated pits have a basket-like appearance with pentagonal or hexagonal lattices formed from polymerized clathrin (Heuser, 1980; Fig. 21). Clathrin coated pits occupy ~0.5-2% of the area of the plasma membrane (Brown and Peterson 1999). The specific sites that clathrin coated pits assemble are called coated-pit zones, and the number of these sites is limited. The size of the clathrin-coated pits is ~100 nm in diameter and is dependent on the amount of polymerized clathrin in the coated pits. There are two mechanisms that have been suggested for the assembly of the clathrin triskelion into the coat of a budding vesicle (reviewed by Mousavi et al., 2004). The most common view suggests that clathrin triskelions form a flat hexagonal lattice first, then transform into closed spheres by converting hexagons to pentagons (Heuser et al., 1980, Reviewed by

Pearse and Bretscher,1981; Pearse and Crowther,1987; Santini and Keen, 2002). This view is consistents with the idea that flat lattices serve as precursors of coated pits. An alternative view, however, is that a flat lattice functions as a reserved site for quickly recruiting more clathrin (Kirchhausen, 2000a,b). Coated pits are assembled by incorporating cytosolic clathrins into the growing lattice, and recruiting hexagon and pentagon into the right location. Therefore, no tranformation between hexagons and pentagons is required.

Several membrane lipids, such as PtdIns(4,5)P_2 and PtdIns(3,4,5)P_3, have been proposed to be involved in vesicle formation (reviewed by Haucke, 2005, Simonsen et al., 2001). The inner shell of the coated pits is composed of a layer of adaptor proteins which connect to the plasma membrane and clathrin (Vigers et al., 1986). Epsin, for example, can insert a short helix into the cytoplasmic leaflet of the plasma membrane in association with PtdIns(4,5)P_2.This action results in membrane bending and subsequent coated pit formation (Ford et al., 2002). In addition to phosphoinositide and adaptor proteins, cell surface receptors, which are targeted for internalization, may also contribute to specifying the nucleation site of clathrin (Martin, 2001). The internalized receptors could specify the nucleation sites of clathrin by recruiting AP-2 or other adaptor proteins, then subsequently assembling clathrin to form coated pits. Alternatively, the receptors could incorporate into the clathrin flat lattice and serve as the nucleation site for recruiting more clathrin into the lattice and further assemble coated pits (Pearse and Crowther, 1987) (Fig. 21). Besides receptors, other cell surface proteins, such as synaptotagmins, have been suggested for serving as the binding site of AP-2 at the plasma membrane (Pearse and Crowther, 1987).

AP180/CALM and AP-2 have been suggested to play a critical role in regulating the size of the coated pits (Ye and Lafer 1995, Tebar et al., 1999). Endocytic adaptor proteins induce the initiation of membrane budding, with clathrin then stabilizing the budding membrane. Once the budding membrane is stabilized, the coated pits can serve as the recruiting site for selecting more cargos for internalization. Coated pits can also recruit motor proteins and fusion factors that can subsequently regulate the mobility and fate of the vesicles once endocytosed (Tebar et al., 1999; Ford et al., 2001; Zaremba and Keen, 1983).

After the clathrin lattice has assembled, the shallow coated pits forms (Fig. 20). Several observations suggest that clathrin-coat assembly can provide the driving force for membrane invagination to form shallow coated pits (Larkin et al., 1986; Mahaffey et al., 1989; Lin et al., 1991). First, purified clathrin can assemble into coated vesicles *in vitro*, and the size of the coated structure is similar to that of the endogenous coated vesicles (Mahaffey et al., 1989; Moore et al., 1987). Second, the energy needed to bend a clathrin lattice is similar to the energy needed for invaginating the plasma membrane (Jin and Nossal, 1993). Other investigators, however, disagree with this model and suggest that there are many other mechanisms involved in this process. This view favors the possibility that clathrin stabilizes the budding structure rather than initiating the invagination (Farge et al., 199; Sheetz and Singer, 1974).

Deeply invaginated coated pits form from the shallow coated pits. The characteristic feature of deeply coated pits is the presence of a neck structure, which is also the specific site of fission (Fig. 21). The formation of deeply coated pits involves endophilin and dynamin (Takei et al., 1999, Muhlberg et al., 1997). Dynamin is recruited

to the shallow coated pits in its GDP-bound form; GDP exchange to GTP causes dynamin molecules to form a helical collar structure at the neck of coated pits. Dynamin then hydrolyzes GTP using its GTPase activity. This GTP hydrolysis action can cause the tightening of the dynamin ring around the necks of deeply invaginated coated pits, and causes vesicle fission to form free vesicles (Takei et al., 1995; Sever et al., 1999; Sweitzer et al., 1998). Dab2 disabled protein has also been reported to be involved in the formation of deep coated pits (Morris et al., 2002). Endophilin interacts with dynamin and functions as a downstream effector of dynamin. HIP1/R protein, which gets recruited into the growing coated structure, connects the clathrin coat to actin filaments (Schmidt et al., 1999). Dynamin's GTPase activity is critical for actin assembly at the endocytic site. In order to form a free vesicle, deeply invaginated pits need to bud off from the plasma memrbane. This fission event involves endophilin, dynamin, and actin polymerization (Farsad et al., 2001; Morris et al., 2002). The actin motor protein myosin can also attach to the coated structure and pull the dynamin ring towards the plasma membrane, and the vesicles towards the cytoplasm (Morris et al., 2002). Once the neck structure is established, boundary forces at the lipid interface will aid the fission as well.

There are two mechanisms by which surface receptors can be internalized by coated pits. One way is by constitutive endocytosis: surface receptors are accidently brought into the coated pits by lateral diffusion of the lipid bilayer. Once there, the receptors are captured by the components of the coated pits (reviewed by Ungewickell and Hinrichsen 2007; Mayor and Pagano, 2007). In constitutive endocytosis, receptors undergo continuous internalization and recycling (Waterman et al., 2001). Thus, most constitutive endocytosis is ligand-independent (Bretscher and Pearse, 1984). This

internalization takes up marcromolecules and viruses from extracellular spaces, and it also regulates the amount of the surface receptor. Adaptor proteins recognize and bind to these types of receptors and incorporate these receptors into coated pits. The interaction of adaptor proteins and endocytic receptors is mediated by internalization signals, which are localized in the cytoplasmic tails of the receptors. Alternatively, a ubiquitin (Ub) polypeptide can be added to the cytoplasmic domain of the receptors during posttranslational modification. This Ub polypeptide can server as the internalization signal sequence of the receptor (Collawn et al., 1990; Oleinikov et al., 2000; Weissman et al., 2001).

Another type of endocytosis is ligand-induced internalization, in which the surface receptors are selected into the coated pits. Ligand binding to these receptors, such as EGF binding to the EGF receptor, triggers a conformational change of the receptor, which results in receptor dimerization (Lemmon et al., 1997). Dimerization of the receptor subsequently activates receptor auto-phosphorylation, and the phosphorylated receptor then recruits adaptor proteins to the cytoplasmic tail of the receptors. The associated adaptor proteins then trigger the assembly of clathrin, and a clathrin-coated struture forms. This type of internalization can regulate receptor signaling by regulating the postendocytic fate of the receptor.

Clathrin-dependent endocytosis has been reported to be involved in internalization of various receptors and extracellular ligands. Receptor tyrosine kinase-family members, such as the EGF receptor and the Eph receptors, are internalized through clathrin-dependent endocytosis. Cytokine receptors, such as growth hormone receptors, are also internalized by clathrin-dependent endocytosis (Irie et al., 2005).

Certain types of G protein coupled receptors are brought into the cell by clathrin-mediated internalization (Wolfe and Trejo 2007; Hanyaloglu and von Zastrow 2008). The internalization of all of these receptors plays a critical role for their downstream signal transduction, since blocking endocytosis results in constitutive signaling.

My analysis of Eph receptor trafficking indicates that the internalization of the Eph receptor is partially dependent on clathrin-dependent endocytosis. In the absence of MSP/sperm, VAB-1/Eph largely localizes to the endocytic recycling compartment of the oocyte; there is no detectable level of VAB-1/Eph on the plasma membrane. However, depleting clathrin-dependent endocytosis pathway components such as clathrin, DAB-1, which is the *C. elegans* Dab2 homolog, or dynamin results in a small portion of the VAB-1/Eph receptors localizing to the plasma membrane in female worms (see details in Chapter III).

Caveolae-mediated endocytosis

Another well-characterized pathway that can internalize cell surface receptors is caveolae-mediated endocytosis (Gong et al., 2008; Lajoie and Nobi, 2007; Mayor and Pagano, 2007; Cheng et al., 2006) Caveolae are small flask-shaped invaginations (~50 to 80 nm in diameter) on the cell surface. The reason that I present caveolae-mediate endocytosis here is that Scheel et al., (1999) reported that caveolin-1 (*cav-1*), a component of caveolae (see below for details), is involved in meiotic progression in *C. elegans*, based on RNAi findings. This report suggests that inactivation of *cav-1* causes germ cells to progress through meiotic prophase more rapidly. However, the *cav-1*

potential null mutant does not display these phenotypes, which makes their conclusions somewhat doubtable. Interestingly, Sato et al., (2006) described the germline CAV-1::GFP expression, which shows a similar localization pattern as VAB-1::GFP in the *C. elegans* adult hermaphrodite gonad. CAV-1::GFP localizes to intracellular vesicles that are distribute throughout the oocyte cytoplasm (Sato et al., 2006). In addition, a study of Eph receptor signaling in CHO-EphB1 cells suggests that EphB1and EphA2 interact with caveolin-1 upon ephrin stimulation and that EphB1 localizes in the caveolae structures. These three findings led me to test whether VAB-1/Eph is internalized into the oocyte through caveolae-mediated endocytosis. I found that VAB-1/Eph receptor localization is unaffected by the presence and absence of *cav-1*. To help you understand how caveolin-1 might regulates caveolae-mediated endocytosis, and what is caveolae, I will very briefly explain caveolae-mediate endocytosis.

Caveolae were first identified in 1950s in the heart endothelium, and were named because of their cave-looking shape (Palade, 1953). Caveolae were subsequently found in most cell types, and the shape of caveolae is dynamic, varying from cell to cell, and is also dependent on the physical status of the cell. Caveola is a striated coated vesicle which is composed of caveolins (Glenney 1993; reviewed by Gong et al., 2007; Lajoie and Nobi, 2007; Ishikawa et al., 2005). There are three types of caveolin: caveolin 1, caveolin 2, and caveolin 3 (Parton 1996; Parton and Simons, 2007). Caveolin-1 is expressed in various cell types and is the key component of the caveolae coat and essential for caveolae formation (Mora et al., 1999; Drab et al., 2001). Besides its essential role in caveolae biogenesis, caveolin-1 is also involved in lipid uptake and regulation, transcellular transport, cellular signaling, and the entry of viruses (reviewed

by Goetz et al., 2008; Shatz and Liscovitch, 2008). Caevolin-2 is associated with caveolin-1 in many cell types and it can form a heteroligomer with Caevolin-1 (Das et al., 1999). Caevolin-2 can not form caveolae by itself *in vitro*, and removal of caveolin 2 does not affect the expression of caveolae *in vivo* (Razani et al., 2002). Caveolin-2 needs the assistance of caveolin 1 to generate caveolae, and the protein stability of caveolin-2 is dependent on caveolin 1 (Li et al., 1998). Caveolin-3 is only present in muscle cells, and it can drive caveolae formation by itself in *vitro* (Song et al., 1996; Tang et al., 1996). Besides caveolin proteins, caveolae are also enriched in steroid and sphingolipids. Thus, caveolae are involved in lipid rafts (reviewed by Lajore and Nabi, 2007). Cholesterol is a key component of lipid rafts and is essential for caveolae formation. Cholesterol binds caveolin-1, and this binding triggers caveolin-1 oligomerization. Cholesterol also upregulates caveolin-1 transcription, and depletion of cholesterol causes reduced caveolae formation (Rothberg et al., 1992).

Caveolae can localize protein complexes such as GPCRs (Ostrom and Insel, 2004; Insel et al., 2005). The interaction of GPCRs and caveolin is important for localization of GPCR to the caveolae and critical for subsequently GPCR sorting and trafficking to the plasma membrane. G proteins are enriched in caveolae and directly interact with caveolin 1. The interaction of G protein and caveolin 1 is very important for keeping Gα proteins in the inactive GDP-bound state. Agonist stimulation causes Gα redistribution to the cytosol by exchanging GTP for GDP. Thus, segregation of Gα subunits in caveolae and interaction with caveolin 1 determine the initiation of cell-specific G protein pathways. Several steroid hormone receptors also localize in the caveolae. The compartmentalization of steroid hormones in caveolae facilitates their interaction with

steroid hormonal receptors, which are essential for estrogen-induced downstream signaling.

Vesicle Transport and Trafficking

In my dissertation work, I found that VAB-1/Eph mainly localizes in the intracellular vesicles of the oocyte in *C. elegans*. In the absence of sperm, VAB-1/Eph receptor mainly localizes in the endocytic recycling compartment, while in the presence of sperm, VAB-1/Eph receptor is largely excluded from the endocytic recycling compartment. Thus, it is quite necessary to explain about recycling endosomes, and how the endocytic vesicles traffic to the recycling endosomes or some other compartments, such as lysosomes, and what mechanism regulates these trafficking events.

After internalizing into the cell, these clathrin-dependent and caveolae-mediated endocytic vesicles traffic inwardly into the cell. Vesicle transport plays a critical role in trafficking molecules from one compartment to another (reviewed by Corbeel and Freson, 2008; Kummel and Heinemann, 2008; Vassilieva and Nustrat, 2008). The selectivity of molecule trafficking is key for maintaining the functional organization of the cell. If the selectivity of trafficking is lost, the cell can not carry out its normal cellular function. After budding off from the plasma membrane, the vesicle loses its coat very quickly. Once the vesicle is decoated, the target-target interaction signal is exposed, and the uncoated vesicles can interact with other cellular compartments, such as early endosomes (Fig. 23).

Figure 23. Endocytic trafficking

A schematic representation of endocytitc trafficking. After internalization into the cell, the clathrin-coated vesicle very quickly loses its clathrin coat. After decoating, the vesicle fuses with early endosome. Then the ingested contents either get recycled back to the plasma membrane, or transport into lysosome for degradation. Modified from Sorkin and von Zastrow, 2002.

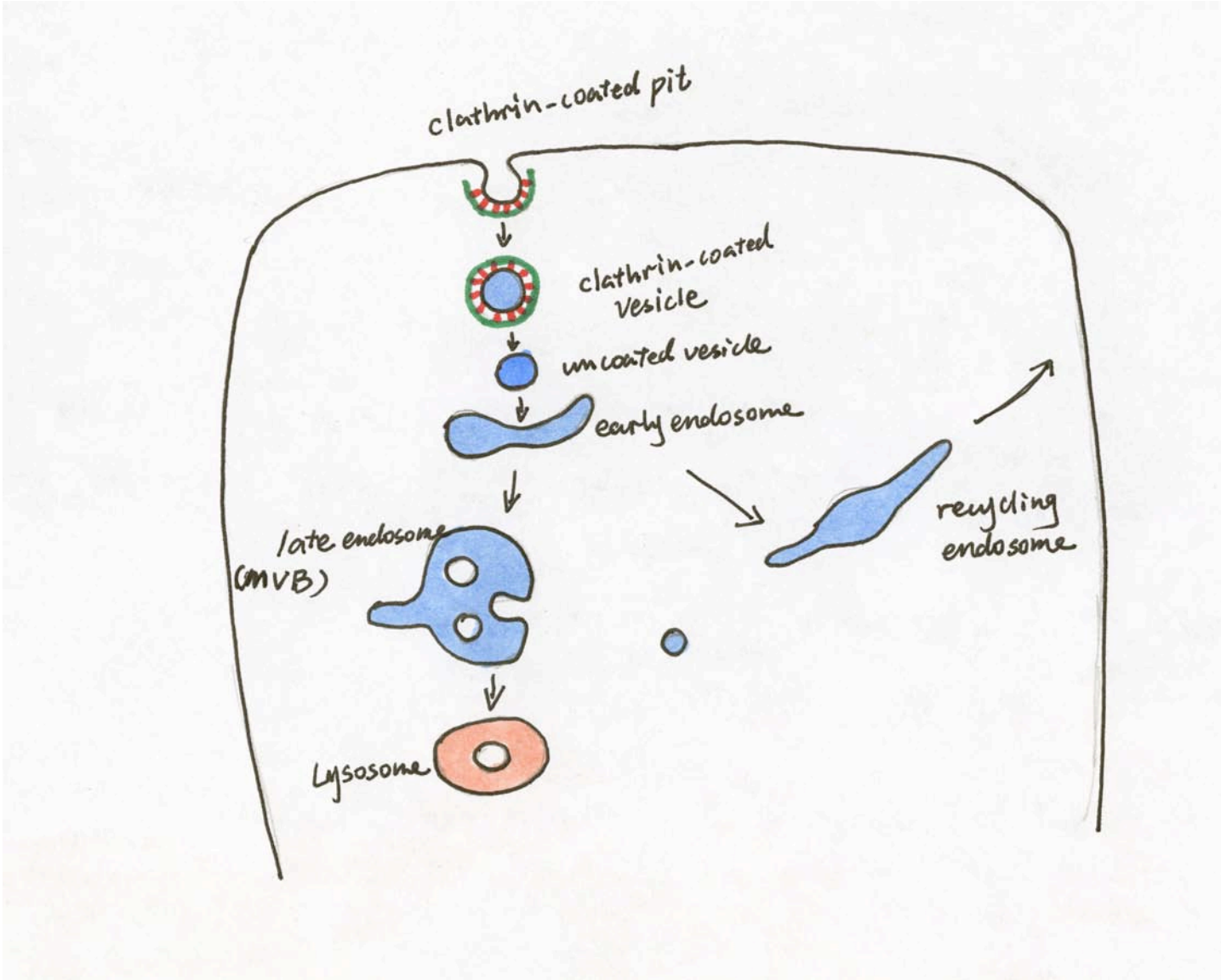
clathrin-coated pit
clathrin-coated vesicle
uncoated vesicle
early endosome
recycling endosome
late endosome (MVB)
Lysosome

After fusing with the early endosomes, which is the sorting vesicle, the internalized protein either get shuttled into recycling endosomes and sent back to the plasma membrane, or it gets targeted into multivesicular bodies and enters late endosomes, and finally transported into lysosomes for degradation or trafficking into exosomes for further secretion (reviewed by Vassilieva and Nustrat, 2008; Fig. 23). The vesicles move by diffusion over short distances, and move by motor proteins (kinesins or dynein) along micrutubules over long distances. Due to constant flux of the membrane material, organelles of the endomembrane system constantly lose their own characteristic protein marker and constantly receive proteins markers that may change the organelle's fate (reviewed by Corbeel and Freson 2008). Therefore, coordinated budding and fusion of each organelle and between organelles is essential for maintaining the function of a cell.

Docking of the vesicles to the accepter compartment is specific, and this docking involves SNARE proteins. There are two types of SNAREs, vesicle SNAREs (v-SNARE) and target SNAREs (t-SNARE) (reviewed by Quick; 2006). v-SNARE is incorporated into the vesicle membrane, whereas t-SNARE is incorporated into the target membrane (reviwed by Bunger, 2005; Fig. 24). The specific binding of v-SNAREs and t-SNAREs regulates the docking of the vesicles to its target compartment (Fig. 24). Once the vesicles dock on the target membrane, several other proteins join the SNARE complex to form fusion complexes, and this action results in the fusion of the vesicles with the target membrane (reviewed by Hong, 2005).

Ras-associated binding (Rab) proteins also play important roles in vesicle trafficking, including vesicle formation, motility, tethering, and fusion to target membrane (Wickner and Schekman, 2008; Fig. 24). To date, more than 60 human Rabs

are identified. Rab proteins interact with different Rab-associated proteins that regulate Rab conformation changes and mobility (Kawasaki et al., 2005). GEF (guanine nucleoide-exchange factors) and GAPs (GTPase activating proteins) regulate the Rab cycle between active GTP-bound and inactive GDP-bound forms. The cycle of Rab proteins between GTP- and GDP- bound forms regulates the ability of Rabs to bind their downstream effectors. Rabs are synthesized as soluble cytoplasmic proteins, which are inactive in their GDP bound form. REP (Rab escort protein) binding to Rab-GDP results in addition of two geranylgeranyl groups to the Rab C-terminus. The addition of these prenyl groups on Rabs allows Rabs to attach into the lipid bilayer of the organelle. To bind to the organelle membrane, GDF needs to displace GDI, and this membrane attachment can be fixed by converting Rab-GDP to Rab-GTP with the assistance of GEF (Guanine nucleotide exchange factor). The membrane attached GTP bound Rabs then can bind to its effector proteins that promote vesicle docking and fusion. After completing their function, Rabs hydrolyze GTP through their intrinsic GTPase activity, which is stimulated by GAP (GTPase activating protein). Subsequently, Rab-GDP is extracted from the membranes by RabGDI (GDP dissociation inhibitor) and locates into the cytosol again as GDP-bound form. Therefore, Rab proteins continuously cycle between the cytosol and different membranes. Different Rabs are associated with different endosomes, and they regulate endosome-endosome or endosome-plasma membrane fusion (reviewed by Zerial and Mcbride 2001; Corbeel and Freson, 2008; Grosshans et al., 2006; Markgraf et al., 2007; table 1). Rab-5 is associated with early endosomes, Rab-4 is associated with sorting endosomes and recycling endosomes, Rab-11 is associated with recycling endosomes, and Rab-7 is associated with late endosomes and lysosomes.

Figure 24. Vesicle fusion

A. Schematic graph of vesicle fusion process. Adapted from courses.bio.psu.edu/.../tutorials/tutorial6.htm
B. Schematic graph of the mechanism controls vesicle fusion. Adapted from http://www.steve.gb.com/science/protein_targeting.html

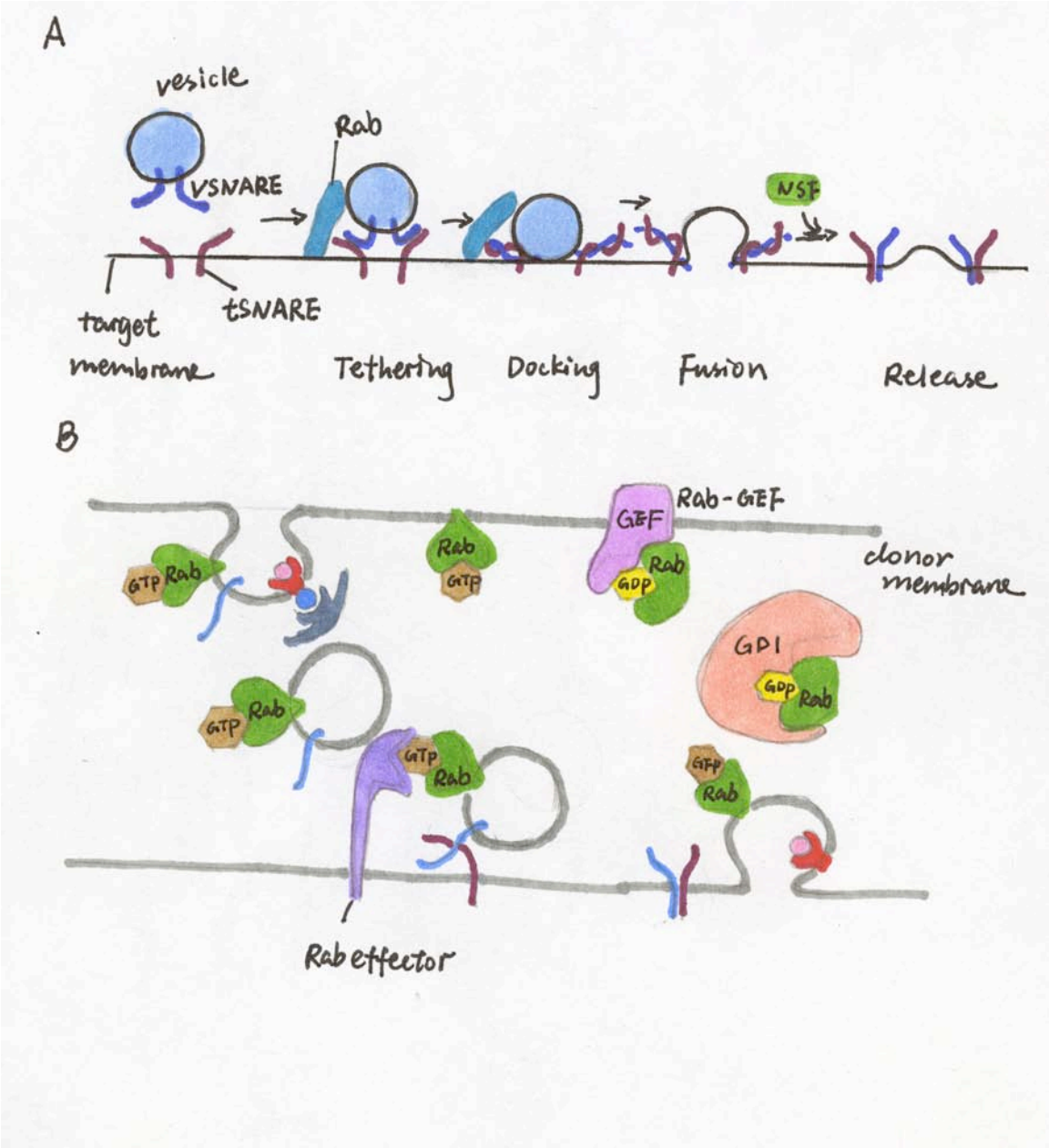
A
vesicle
Rab
VSNARE
NSF
tSNARE
target membrane
Tethering
Docking
Fusion
Release
B
Rab-GEF
GEF
Rab
GTP
GDP
donor membrane
GDI
Rab effector

Tabel 1. Localization and function of Ran proteins

Rab	Rab localization	Rab function
Rab-4	EE, RE, PM	EE-PM sorting/ recycling
Rab-5	CCV, EE, PM	Formation of CCV from PM, regulate CCV-EE and EE-EE homotypic fusion, EE motility
Rab-7	LE and Lys	Required for EE-LE transport and LE-Lys fusion
Rab-9	LE, TGN	LE -TGN transport
Rab-11	RE, TGN, PM	Recycling through perinuclear RE, exocytosis from TGN to PM, implicated in polarization of the Drosiphila oocyte

Modified from Miguel et al., 2002.

These Rab proteins not only serve as the characteristic marker for these endosomes, they also regulate endosomal fusion. Rab-5 regulates cargo segregation into clathrin-coated vesicle (CCV) and together with their effectors promoting vesicle mobility and homotypic early endosomal fusion. In contrast to Rab-5, Rab-15 inhibits cargo transport into early endosomes. Rab-4 regulates early endosomal-recycling endosomal fusion. In early endosomes, molecules, which are destined to be recycled, get sorted into Rab-4 enriched microdomains and then recycles quickly back to the plasma membrane. Rab-11 regulates recycling endosomal and plasma membrane fusion. Rab-7 regulates molecules, which are destined for degradation, to be transported from Rab-5 positive early endosomes into Rab-7 positive late endosomes. In addition, Rab-7 also functions to transport proteins from late endosomes to lysosomes. Rab-9 regulates recycling of certain molecules, such as mannose 6'-phosphae receptor, from late endosomes to *trans*-Golgi network. Therefore, the association of Rab proteins with organelles is dynamic during protein trafficking. Rab proteins mediate intracellular vesicle trafficking by serving as scaffolding platforms to temporally and spatially control protein transportation. How a cargo is transported from one endosome compartment to another, such as from Rab-5 positive endosomes to rab-7 positive late endosome, is not very clear. One hypothesis is the endosome maturation theory. In this view, Rab-5 positive early endosomes grow in size and gradually lose their Rab-5 and effectors (early endosome associated proteins), and at the same time acquires Rab-7 and effector proteins. By this Rab conversion reaction, endosomes mature from early endosomes to late endosomes.

CHAPTER II

IDENTIFICATION OF NEGATIVE REGULATORS OF OOCYTE MEIOTIC MATURATION

Introduction

Oocytes of most sexually reproducing animals arrest in meiotic prophase and actively maintain their arrest for prolonged periods–up to fifty years in humans. In response to hormonal signaling, oocytes resume meiosis in the highly conserved process of meiotic maturation, which prepares the oocyte for fertilization (Voronina and Wessel, 2003; Yamamoto et al., 2006). Oocyte meiotic maturation is defined by the transition between diakinesis and metaphase of meiosis I, and is accompanied by nuclear envelope breakdown, cortical cytoskeletal rearrangement, meiotic spindle assembly, and chromosome congression. Chromosome missegregation in female meiosis I represents the leading cause of human birth defects (e.g., Down syndrome). Because advanced maternal age is the most significant risk factor (Hassold and Hunt, 2001), the mechanisms that maintain meiotic diapause and preserve oocyte vitality are of intense interest.

Great strides have been made in understanding the control of cell-cycle progression during the meiotic maturation process, culminating in the discovery of the Maturation Promoting Factor (Cdk1/cyclin B; Masui, 2001). Mitogen-activated protein kinase (MAPK) cascades also play an important role in controlling meiotic progression (Fan and Sun, 2004). By contrast, comparatively less information is available about the

intercellular signaling pathways that regulate meiotic resumption. Unifying conclusions from studies in vertebrate and invertebrate systems are that soma-germline interactions play a crucial role and that regulation involves both positively- and negatively-acting pathways (Voronina and Wessel, 2003). As meiotic maturation signals have been characterized in several invertebrate systems, studies in these organisms may offer both comparative and mechanistic insights.

In *C. elegans*, sperm export the major sperm protein (MSP) by a vesicle budding mechanism to trigger oocyte MAPK activation and meiotic maturation (Fig. 33A; Miller et al., 2001; Miller et al., 2003; Kosinski et al., 2005). MSP is also the key cytoskeletal element required for the actin-independent amoeboid locomotion of nematode spermatozoa (Bottino et al., 2002). Since hermaphrodites produce only a fixed number of sperm, meiotic maturation rates are initially high for the first two days of adulthood, but decline as sperm are used for fertilization and the MSP signal disappears (Kosinski et al., 2005; McCarter et al., 1999). Similarly, in sex-determination mutants of *C. elegans*, which fully feminize the hermaphrodite gonad (e.g., *fog-2* or *fog-3*), oocytes arrest until sperm are supplied by mating. In *C. elegans*, the vital processes of meiotic maturation and ovulation are tightly coupled to sperm availability through a complex regulatory network involving both negative and positive controls. Parallel genetic pathways defined by *vab-1*, which encodes an ephrin receptor, and *ceh-18*, which encodes a POU-homeoprotein expressed in gonadal sheath cells but not oocytes, together compose an MSP-sensing control mechanism that inhibits meiotic maturation, MAPK activation, and ovulation when sperm are not present in the reproductive tract (Fig. 33A; Miller et al., 2003). Negative regulators of meiotic maturation, such as *vab-1* and *ceh-18*,

are identified by RNAi knockdown or loss-of-function mutations that cause females to mature oocytes in the absence of the MSP signal. In contrast, positive regulators, such as *oma-1* and *oma-2*, which encode two TIS-11 zinc-finger proteins expressed in the germ line (Detwiler et al., 2001), are identified by RNAi knockdown or loss-of-function mutations that reduce or block meiotic maturation in hermaphrodites in the presence of the MSP signal.

In collaboration with J. Amaranath Govindan, a former graduate student in our lab, we report the results of a comprehensive RNAi screen undertaken to identify regulators of meiotic diapause in the absence of the MSP signal. This genome-wide RNAi screen identified 16 new negative regulators of meiotic maturation. Four conserved proteins, DAB-1, PQN-19, PKC-1, and VAV-1, function with the VAB-1 MSP/Eph receptor in oocytes. In parallel to the VAB-1 MSP/Eph receptor pathway, antagonistic $G\alpha_{o/i}$ and $G\alpha_s$ signaling pathways define negatively- and positively-acting somatic cell inputs, respectively. $G\alpha_s$ signaling is necessary and sufficient to trigger oocyte MAPK activation and meiotic maturation, which it does in part by antagonizing inhibitory sheath/oocyte gap-junctional communication. This finding, together with the results from mammalian systems (Jamnongjit and Hammes 2003; Mehlmann, 2005), suggest that the involvement of the $G\alpha_s$ pathway may be an ancestral feature of meiotic maturation signaling.

Material and methods

Genetics

Standard culture and genetic techniques were carried out (Brenner, 1974) at 20 °C, except where indicated otherwise. Alleles used are described in WormBase (http://www.wormbase.org). The strains used were described (Miller et al., 2003), or as follows (all alleles in DG strains have been outcrossed at least 3 time with the wild type): DG1859 [*gsa-1(pk75)/hT2(qIs48)I*], KG421 [*gsa-1(ce81*gf*)I*], KG524 [*gsa-1(ce94*gf*)I*], DG1848 [*gsa-1(ce81*gf*)fog-3(q443)/hT2(qIs48)I*], DG1847 [*gsa-1(ce94*gf*)fog-3(q443)/hT2(qIs48)I*], DG1803 [*inx-22(tm1661)*]; DG1852 [*pqn-19(ok406) I*], DG1856 [*goa-1(sa734)I*], MT2426 [*goa-1(n1134*rf*)I*], DG1813 [*goa-1(sa734)fog-3(q443)/hT2(qIs48)I*], DG1865 [*goa-1(n1134*rf*)fog-3(q443)/hT2(qIs48)I*], DG1853 [*dab-1(gk291)II*], DG1804 [*dab-1(gk291)/mIn1II;fog-2(q71)V*], DG1841 [*vab-1(dx31)dab-1(gk291)/mIn1II;fog-2(q71)V*], PS1493 [*dpy-20(e1362)IV;syIs9(*pMH86 + pJMG$_o$QL)], DG1854 [*pkc-1(ok563)V*], KG532 [*kin-2(ce179*rf*)X*], DG1849 [*kin-2(ce179*rf*)X;fog-3(q443)/hT2(qIs48)I*].

RNA Interference

Genome-wide RNAi screening employed a modification of the method of Kamath et al. (Kamath et al., 2003). HT115(DE3) bacterial strains were grown overnight in 500 µl LB media containing 50 µg/ml ampicillin and 30 µl of each culture was plated per well

onto M9-NGM medium (42.3 mM Na_2HPO_4, 22.1 mM KH_2PO_4, 8.6 mM NaCl, 18.7 mM NH_4Cl, 1 mM $CaCl_2$, 1 mM $MgSO_4$, 0.5 % casamino acids, 2 % agar, 0.2 % β-lactose, 5 μg/ml cholesterol, 25 μg/ml carbenicillin) and incubated overnight at 22°C for induction of dsRNA. Five L3-stage *fog-2(q71)* female worms were placed in each well (35 mm) and incubated at 22°C. Twenty four hours later, any males that were inadvertently plated were removed from the cultures. Each screening experiment utilized *unc-22* as a positive control for RNAi efficacy, and the empty vector (L4440) as a negative control. Cultures were screened on the second day of adulthood for the presence of unfertilized oocytes on the bacterial lawn or within the uteri of the adults. All Class I clones were rescreened and confirmed in more than five experiments; whereas all Class II clones were confirmed by rescreening at least twice. The insert DNA of class I clones was sequenced to verify gene identity.

Phenotypic Analysis and Immunofluorescence

Oocyte meiotic maturation rates and MAPK activation were analyzed as described (Miller et al., 2001). Oocyte meiotic maturation, ovulation, and sheath cell contractions were observed by time-lapse videomicroscopy, and gonads were dissected, fixed, and stained for immunofluorescence microscopy as described (Rose et al., 1997). Wide-field fluorescence and DIC microscopy employed a Zeiss Axioskop microscope using 40X, 63X, or 100X (NA1.4) objective lenses. Images were acquired with an ORCA ER (Hamamatsu) charge-coupled device camera using OpenLab (Improvision) software. All exposures were in the dynamic range of the detector and each individual

photograph in a montage employed the same exposure time. The following antibodies were used: Anti-DAB-1 antibody (Kamikura and Cooper 2003), Anti-GOA-1 antibody (kindly provided by Michael Koelle), anti-MSP (Kosinski et al., 2005), and Cy2- or Cy3-conjugated secondary antibody (Jackson ImmunoResearch Laboratories). Student's t-Test was used to assess statistical significance as indicated.

MSP-VAB-1 Eph Receptor Interaction

The sequence encoding VAB-1ECT (residues 1-558) was amplified using the PCR and subcloned into the pcDNA3.1D TOPO (Invitrogen). The sequence of VAB-1ECT-6His was confirmed by DNA sequencing. The expression vector was introduced into 293F cells by transfection with 293fectin (Invitrogen) according to the manufacturer's instructions. Cell culture supernatants were collected 72 hours after transfection and VAB-1ECT-6His was precipitated with ammonium sulfate (30% saturation). The protein pellet was dissolved in 50 mM sodium phosphate (pH 8.0); 300 mM NaCl and purified on Ni-NTA agarose (Qiagen). MSP-142 was purified as described (Baker et al., 2002). Binding reactions were carried out in 100 µl volumes containing 100 nM MSP-142 and 14 nM VAB-1ECT-6His for 2 hours at 4°C. Two methods were used to isolate the MSP-VAB-1ECT complex. In method 1, 2 µg of an N-terminal-specific MSP polyclonal antibody was added and incubated for another 2 hours at 4°C, followed by addition of 5 µl of Protein-A Sepharose (Amersham Biosciences). Following an additional incubation of 1.5 hours at 4°C, beads were washed four times with RIPA buffer (10mM Tris pH7.4, 150mM NaCl, 5mM EDTA, and 0.25% NP40),

and processed for western blotting with monoclonal anti-MSP antibodies, or anti-V5 antibodies (Invitrogen) for detecting VAB-1ECT. In method 2, the MSP-VAB-1ECT6His complex was isolated with 5 µl Ni-NTA agarose beads with an incubation of 1.5 hours at 4°C.

Results

Identification of Negative Regulators of MSP Signaling Using a Genome-Wide RNAi Screen

MSP promotes oocyte meiotic maturation by antagonizing two parallel negative regulatory circuits: an oocyte VAB-1 Eph receptor pathway and a somatic gonadal sheath cell pathway defined by the POU-homeoprotein CEH-18 (Fig. 25A; Miller et al., 2003). We reasoned that additional components of the VAB-1 and CEH-18 pathways were likely to function as negative regulators and we sought to identify them using a genome-wide RNAi screen (Figure 25B). J. Amaranath Govindan performed this screen using a *fog-2(q71)* female sterile strain in which oocytes arrest at prophase of meiosis I and are retained in the gonad arm due to the absence of MSP. We screened for rare RNAi clones in which meiotic maturation and ovulation occur at elevated rates and unfertilized oocytes are laid onto the bacterial lawn in increased numbers despite the absence of MSP (Figure 25B and Table 2).

We identified 175 clones that fell into two categories depending on their consequence for gonadal structure: class I (17 clones) had no appreciable effects;

whereas class II (158 clones) caused defects in gonadal morphology. The disruption of gonadal integrity observed following RNAi of class II clones limits our ability to study their roles in MSP signaling to varying degrees. Thus, here we focus on the seventeen class I positive clones (Table 2). Class I genes encode several proteins with well characterized intercellular signaling functions, such as components of multiple G-protein signaling pathways (*goa-1*, *kin-2*, *gpb-1*, and *gsa-1*), protein kinase C (*pkc-1*), a 14-3-3 protein (*par-5*), and a disabled homolog (*dab-1*). RNAi to class I genes had no apparent effects on germline sex determination, yet we verified the absence of MSP by immunostaining in all cases (Table 2). The fact that *ceh-18* was identified validates the rationale and effectiveness of the screen. This screen did not identify *vab-1*, *nmr-1*, and *itr-1*, three known negative regulators of meiotic maturation (Miller et al., 2003; Corrigan et al., 2005). Within class I, the level of derepression of meiotic maturation differed between clones (Table 2). Remarkably, RNAi of *goa-1* and *kin-2* resulted in approximately 60% of the wild-type rate in the presence of sperm. MSP is sufficient to activate MAPK in female gonads when assessed with antibodies to the diphosphorylated activated form of MPK-1 MAPK (MAPK-YT; Miller et al., 2001). RNAi to six genes (*goa-1*, *kin-2*, *gpb-1*, *inx-14*, *inx-22*, and *ptc-1*) resulted in MAPK activation in the absence of MSP (Table 2 and Figure 26). These results thus define new negative regulators of the meiotic maturation process and highlight the complexity of the signaling pathways involved.

Figure 25. A genome-wide RNAi screen for negative regulators of oocyte Meiotic maturation

A. Oocytes undergo meiotic maturation in an assembly-line fashion in response to MSP signaling. The oocyte VAB-1 Eph receptor pathway and a sheath cell pathway, defined by CEH-18, negatively regulate oocyte MAPK activation and meiotic maturation. MSP antagonizes these inhibitory inputs to promote meiotic maturation.
B. Flowchart for the genome-wide RNAi screen in a *fog-2(q71)* female-sterile background. Most clones have no effect on meiotic arrest (panel at lower left), whereas RNAi of 17 clones results in MSP-independent meiotic maturation without disrupting gonadal morphology (panel at lower right).

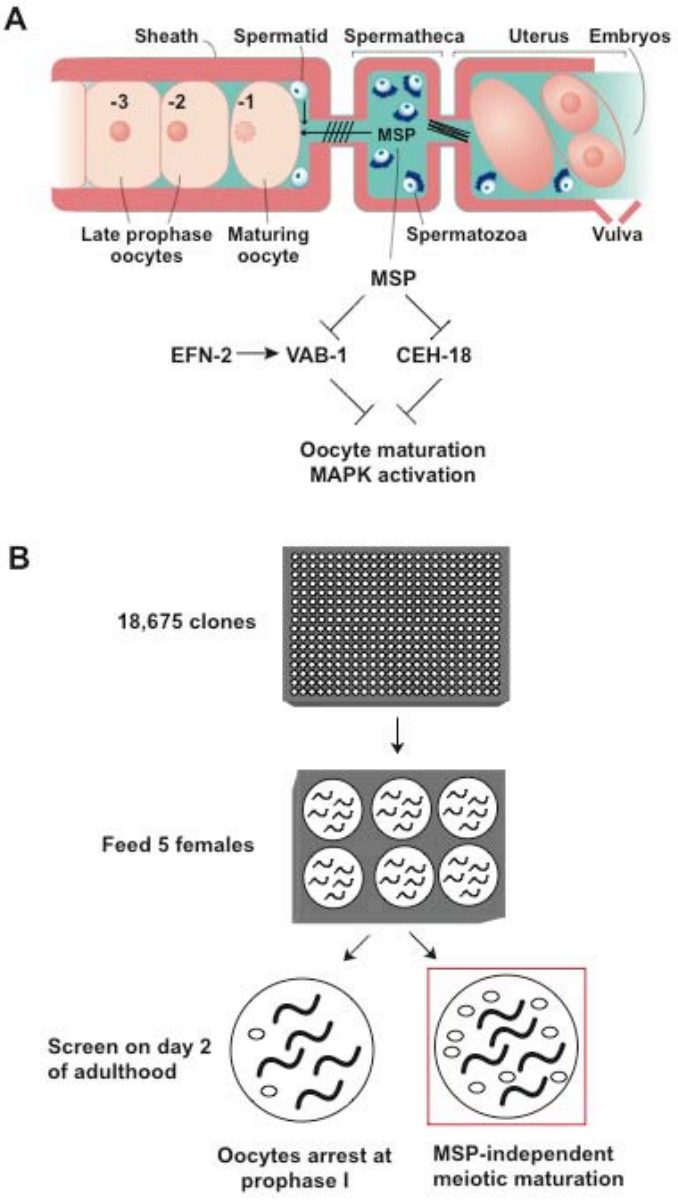
A
Sheath
Spermatid
Spermatheca
Uterus
Embryos
-3
-2
-1
MSP
Late prophase oocytes
Maturing oocyte
Spermatozoa
Vulva
MSP
EFN-2
VAB-1
CEH-18
Oocyte maturation
MAPK activation
B
18,675 clones
Feed 5 females
Screen on day 2 of adulthood
Oocytes arrest at prophase I
MSP-independent meiotic maturation

Figure 26. RNAi to several negative regulators causes MSP-independent MAPK activation in oocytes

(A-F). Fluorescence micrographs showing MAPK-YT staining (red) in oocytes. MAPK-YT staining is observed in the most proximal oocyte of wild-type hermaphrodites (A), but not in *fog-2(q71)* females (B). By contrast MAPK-YT staining is observed in *fog-2(q71)* females following *goa-1(RNAi)* (C), *kin-2(RNAi)*, (D), *inx-14(RNAi)* (E), and *gpb-1(RNAi)* (F). *goa-1(RNAi)* or *goa-1(null)* females exhibit expanded MAPK-YT staining to distal oocytes, though the specific pattern of relative staining intensities, such as the alternating peaks of staining in panel (C) can be variable. *inx-22(RNAi)* and *ptc-1(RNAi)* also result in MSP-independent MAPK activation (Table 2). Scale bar represents 10 μm.

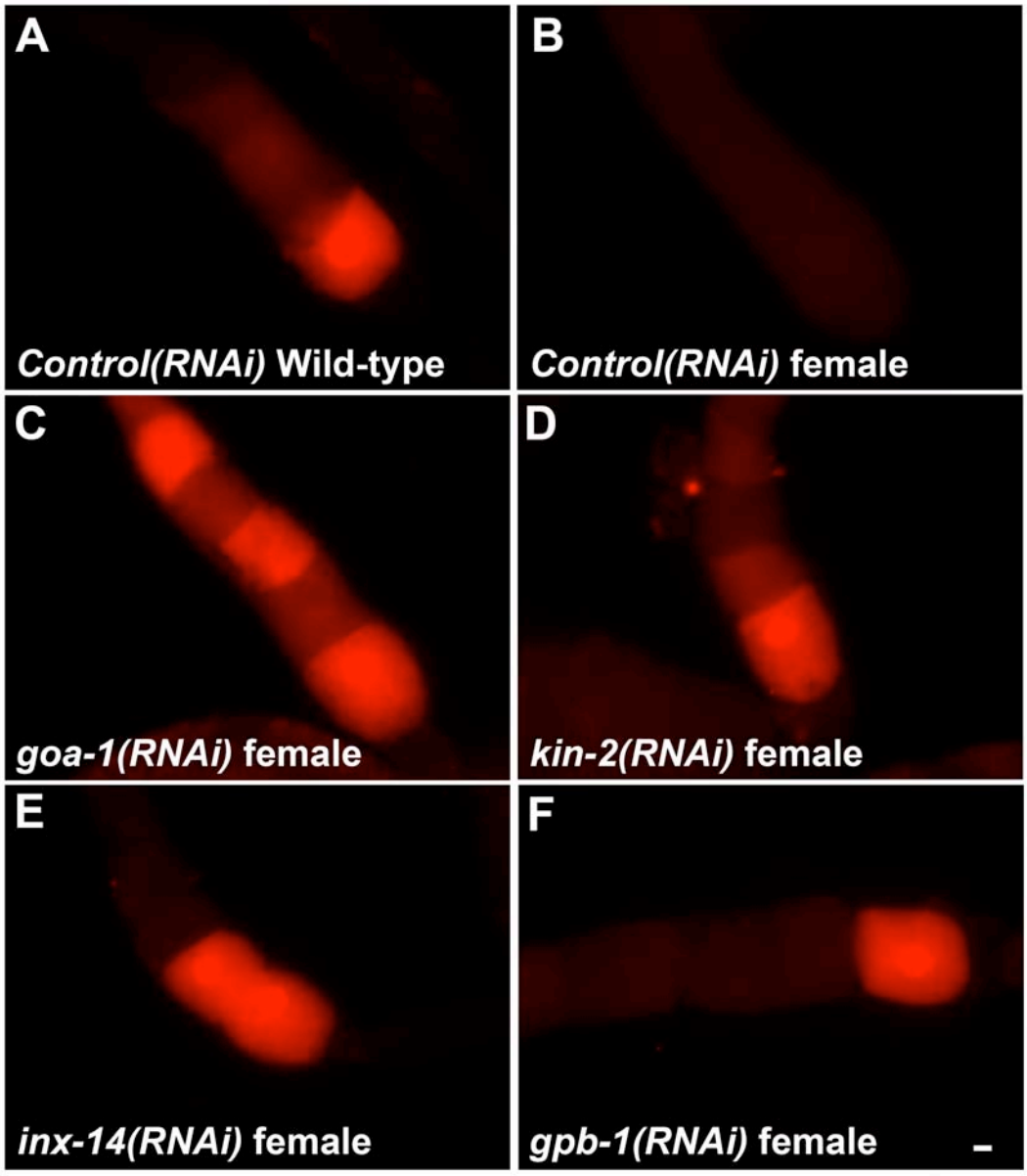
A
Control(RNAi) Wild-type
B
Control(RNAi) female
C
goa-1(RNAi) female
D
kin-2(RNAi) female
E
inx-14(RNAi) female
F
gpb-1(RNAi) female

Table 2. Negative Regulators of Meiotic Maturation Identified in a Genome-Wide RNAi Screen

Gene[a]	Description	MSP[b]	Oocyte Maturation Rate in Females (hr^{-1} gonad arm^{-1})[c]	MAPK Activation[d]
Control	Wild-type hermaphrodite	+	2.50 ± 0.41 (17)	25/25 (+)
Control[e]	*fog-2(q71)* unmated female	–	0.16 ± 0.10 (17)	1/20 (–)
Control	*fog-2(q71)* mated female	+	2.42 ± 0.35 (14)	18/18 (+)
goa-1	Heterotrimeric $G_{o/i}$ α protein subunit	–	1.67 ± 0.38 (36)[f]	14/15 (+)
kin-2	cAMP-dependent protein kinase (regulatory subunit)	–	1.50 ± 0.30 (9)[f]	9/13 (+)
gpb-1	Heterotrimeric G_{β} protein subunit	–	0.88 ± 0.24 (21)[f]	13/18 (+)
gsa-1	Heterotrimeric $G_s\alpha$ protein subunit	–	0.37 ± 0.18 (12)[g]	1/19 (–)
rpt-3	Component of 26S proteasome[h]	–	0.44 ± 0.15 (25)[f]	1/14 (–)
inx-14	Gap junction protein (innexin family)	–	0.99 ± 0.30 (21)[f]	17/17 (+)
inx-22	Gap junction protein (innexin family)	–	0.90 ± 0.36 (30)[f]	15/18 (+)
ran-1	Ran GTPase	–	0.72 ± 0.13 (6)[f]	0/18
ceh-18	POU-Homeo domain transcription factor	–	0.45 ± 0.18 (12)[f, i]	1/17 (+)
arf-1.1	Arf-family GTP binding protein	–	0.64 ± 0.28 (10)[f]	1/19 (–)
ptc-1	Patched receptor	–	0.60 ± 0.27 (18)[f, j]	12/15 (+)
phi-11	Splicing factor 3B, subunit 1[k]	–	0.50 ± 0.15 (10)[f]	0/15
par-5	Encodes 14-3-3 protein	–	0.49 ± 0.20 (28)[f]	0/17
pqn-19	Signal-transducing adaptor molecule (STAM)	–	0.48 ± 0.34 (12)[g]	0/17
pkc-1	Protein kinase C	–	0.44 ± 0.11 (9)[f]	1/17 (–)
vav-1	Vav-GEF proto-oncogene homolog	–	0.42 ± 0.13 (15)[f]	0/16
dab-1	Disabled homolog	–	0.38 ± 0.14 (15)[f]	0/16

[a], Shown are class I positive clones, RNAi of which does not appreciably alter gonadal morphology. The identity of the clones was verified by DNA sequencing.
[b], The absence of MSP in unmated female gonads was confirmed by staining with monoclonal anti-MSP antibodies.
[c], Oocyte maturation rates are expressed as the number of maturations per gonad arm per hour and were measured in two-day-old adult *fog-2(q71)* females (excepting the wild-type hermaphrodite control). The number of worms scored is given in the parentheses.
[d], The fraction of gonads arms showing MAPK-YT staining. MAPK activation was further classified according to whether the observed staining was strong or weak, indicated by (+) or (–), respectively.
[e], Mock RNAi using the empty vector, L4440, served as a control.
[f], $P<0.001$ compared to *control(RNAi)* in *fog-2(q71)* females.
[g], $P<0.01$ compared to *control(RNAi)* in *fog-2(q71)* females.
[h], RNAi of many 26S proteasome components resulted in gonadal defects and scored as class II positives in the screen.
[i], *ceh-18(mg57);fog-2(q71)* females have a maturation rate of 0.75 ± 0.32.
[j], *ptc-1(ok122) unc-4(e120);fog-2(q71)* females have a maturation rate of 0.56 ± 0.26.
[k], Many splicing factors were identified as class II positives.

Germline and Somatic Pathways Regulate Meiotic Maturation

The somatic cells surrounding the oocyte play a key role in negatively regulating meiotic progression in mammals and *C. elegans* (Miller et al., 2001; Pincus and Enzmann, 1935). In *C. elegans*, the gonadal sheath cells form gap junctions with oocytes and these gap junctions are rare or absent in *ceh-18* mutants (Rose et al., 1997; Hall et al., 1999), suggesting their importance. Gap-junctional communication between sheath cells and oocytes are a critical aspect of the negative control of meiotic maturation, as our screen identified two innexin components (*inx-14* and *inx-22*) of invertebrate gap junctions (Starich et al., 2003). To determine whether negative regulators function in the soma or the germ line, we conducted RNAi analysis in an *rrf-1(null)* mutant background (Table 3). *rrf-1* encodes an RNA-dependent RNA polymerase (RdP) that is required for normal RNAi responses in many somatic cells (Sijen et al., 2001), but is dispensable for germline RNAi, which employs the EGO-1 RdP (Smardon et al., 2000). Thus, an RNAi response in an *rrf-1(null)* female background is indicative of a germline function, whereas a significantly reduced response suggests gene function in the soma. As a control, we conducted *ceh-18(RNAi)* and observed elevated meiotic maturation rates in the female background, but not in *rrf-1* females (Table 3), consistent with the idea that *ceh-18* is required for normal sheath cell differentiation and function (Rose et al., 1997). By contrast, *vab-1* functions in the germ line using this test (Miller et al., 2003). The *rrf-1* RNAi test suggests that the function of eleven genes, including *inx-14* and *inx-22*, is needed in the germ line for full repression of meiotic maturation (Table 3). By contrast, the function of four genes (*goa-1*, *kin-2*, *gpb-1*, and *rpt-3)* is predominantly somatic using this test (Table 3). This observation suggests that control of meiotic maturation in *C.*

elegans involves somatically acting $G\alpha_{o/i}$ and $G\alpha_s$ signaling pathways, an idea that we explore further below. The slight RNAi responses observed in *rrf-1(null)* females for *goa-1*, *kin-2*, *gpb-1*, and *rpt-3* might be due to residual somatic effects, as under our conditions, *unc-22(RNAi)* produces overt muscle twitching and weak uncoordination in 5.3% of *rrf-1(null)* animals (n=228). Nonetheless, we cannot exclude the possibility that these genes may also have some germline functions. Genetic mosaic analysis of *goa-1* and *kin-2* in a female background will be needed to test this possibility.

DAB-1, a Disabled Homolog, Functions in the VAB-1 Eph/MSP Receptor Signal Transduction Pathway for the Control of Meiotic Maturation

Previous data using an *in situ* binding assay indicated that labeled MSP binds specifically and saturably to *C. elegans* gonads and that *vab-1(null)* gonads exhibit a significant reduction in MSP binding (Miller et al., 2003). VAB-1 was similarly shown to be sufficient for conferring specific MSP binding to cultured mammalian cells following transient transfection (Miller et al., 2003). These data, coupled with the finding that *vab-1* is required in the germ line for full repression of meiotic maturation in the absence of MSP, led to the hypothesis that VAB-1 is one of several oocyte and sheath cell receptors that respond to the MSP signal. To more fully test the hypothesis that VAB-1 is an MSP receptor, I examined whether MSP directly binds the VAB-1 ectodomain *in vitro* at submicromolar concentrations. The VAB-1 ectodomain (VAB-1ECT) was expressed as a 6His-fusion in mammalian cells using its endogenous secretion signal peptide and purified from the culture supernatant (Figure 27A and B).

Table 3. Parsing the Function of Negative Regulators to the Germ Line or Soma.

RNAi	Oocyte Maturation Rate in Females[a] (N)	Oocyte Maturation Rate in *rrf-1(null)* Females[b] (N)
Control	0.17 ± 0.14 (15)	0.20 ± 0.10 (12)
ceh-18	0.44 ± 0.16 (11)[c]	0.21 ± 0.10 (10)[f]
goa-1	1.51 ± 0.20 (10)[d]	0.50 ± 0.20 (16)[g]
kin-2	1.45 ± 0.60 (12)[d]	0.54 ± 0.16 (15)[g]
gpb-1	1.03 ± 0.20 (12)[d]	0.44 ± 0.22 (16)[g]
gsa-1	0.37 ± 0.22 (13)[e]	0.21 ± 0.20 (10)[f]
rpt-3	0.51 ± 0.16 (12)[c]	0.30 ± 0.18 (12)[f]
inx-14	1.03 ± 0.22 (12)[e]	0.88 ± 0.34 (12)[g]
inx-22	0.84 ± 0.13 (12)[e]	1.00 ± 0.31 (16)[g]
ran-1	1.00 ± 0.30 (6)[e]	1.39 ± 0.32 (5)[g]
arf-1.1	0.53 ± 0.20 (9)[e]	0.45 ± 0.28 (12)[h]
ptc-1	0.63 ± 0.13 (12)[e]	0.74 ± 0.17 (14)[g]
phi-11	0.50 ± 0.20 (12)[e]	0.58 ± 0.30 (11)[g]
par-5	0.80 ± 0.29 (11)[e]	0.71 ± 0.29 (14)[g]
pqn-19	0.46 ± 0.17 (12)[e]	0.47 ± 0.14 (13)[g]
pkc-1	0.48 ± 0.16 (12)[e]	0.40 ± 0.10 (7)[g]
vav-1	0.44 ± 0.11 (11)[e]	0.48 ± 0.20 (14)[g]
dab-1	0.39 ± 0.15 (11)[e]	0.43 ± 0.10 (8)[g]

[a], Meiotic maturation rates were measured in a *fog-3(q443)* female background.

[b], Meiotic maturation rates were measured in *rrf-1(pk1417);fog-3(q443)* double mutant females.

[c], $P<0.01$ compared to the rate following RNAi in the *rrf-1(null*) female background.

[d], $P<0.001$ compared to the rate following RNAi in the *rrf-1(null*) female background.

[e], $P>0.1$ compared to the rate following RNAi in the *rrf-1(null)* female background.

[f], $P>0.1$ compared to the rate following control RNAi in the *rrf-1(null)* female background.

[g], $P<0.001$ compared to the rate following control RNAi in the *rrf-1(null*) female background.

[h], $P<0.01$ compared to the rate following control RNAi in the *rrf-1(null*) female background.

I assessed the binding by incubating MSP with VAB-1ECT-6His and isolating the complex by immunoprecipitation with anti-MSP N-terminal-specific antibodies or using Ni-NTA agarose.Using this test, MSP and VAB-1ECT-6His exhibit direct binding (Figure 27C), with approximately 10% of the MSP bound under the binding conditions used. These data add further support to the idea that meiotic maturation is controlled in part by a VAB-1 MSP/Eph receptor signal transduction pathway.

To identify genes that play a major role in the *vab-1* pathway, we set three stringent genetic and phenotypic criteria. First, the RNAi inactivation of a *vab-1* pathway gene should derepress meiotic maturation to a similar extent as a *vab-1(null)* mutant. Second, the RNAi inactivation of a *vab-1* pathway gene should not exhibit additive or synergistic interactions with a *vab-1(null)* mutant. Finally, the RNAi inactivation of a *vab-1* pathway gene should synergize with a *ceh-18(null)* mutant. We considered the eleven genes (*inx-14*, *inx-22*, *ran-1*, *arf-1.1*, *ptc-1*, *phi-11*, *par-5*, *pqn-19*, *pkc-1*, *vav-1*, and *dab-1*), whose activity is needed in the germ line for full repression of meiotic maturation, as candidates for functioning in the VAB-1 MSP/Eph receptor signal transduction pathway. Four of these genes meet these initial criteria, DAB-1, a disabled homolog, PKC-1, a protein kinase C homolog, PQN-19 a STAM homolog, and VAV-1, a Rho-family guanine-nucleotide exchange factor (Figure 27D and E; Table 6). Of these four genes, only *vav-1* was previously implicated in Eph receptor signaling by the finding that Rho family GEF Vav2 interacts with the EphA4 receptor and promotes ephrin-triggered endocytosis (Cowan et al., 2005).

As a further test that *dab-1*, *vav-1*, *pkc-1*, and *pqn-19* function as part of the *vab-1* pathway, we examined the effect of null mutants and RNAi of these genes on oocyte

MAPK activation in hermaphrodites (Fig. 35F-K and data not shown). *vab-1(null)* hermaphrodites exhibit an expanded pattern of MAPK activation in which MAPK-YT staining extends to distal oocytes (Fig. 35G; Miller et al., 2003). Similarly, *dab-1(gk291* or *RNAi)*, *pkc-1(ok563* or *RNAi)*, *pqn-19(ok406* or *RNAi)*, and *vav-1(RNAi)* hermaphrodites display expanded patterns of MAPK-YT staining in oocytes (Fig. 35H-K), suggesting that these genes, like *vab-1*, function as germline negative regulators of MAPK activation. We only analyzed *vav-1* using RNAi because a *vav-1(null)* mutation is lethal (Norman et al., 2005). Additionally, *vab-1* functions in parallel to *ceh-18* in the negative control of oocyte MAPK activation: *vab-1(null); ceh-18(null)* females show MAPK-YT staining in oocytes despite the absence of MSP (Miller et al., 2003). By this criteria, *dab-1*, *vav-1*, *pkc-1*, and *pqn-19* behave similarly to *vab-1*, as MAPK-YT staining is observed when RNAi is carried out for these genes in a *ceh-18(null)* mutant female background (Figure 31).

Because strong conclusions regarding genetic pathways are not possible without phenotypic analysis of null mutations, I analyzed meiotic maturation phenotypes in deletions alleles of *dab-1*, *pkc-1*, and *pqn-19*, which are predicted to significantly reduce or eliminate gene function. To further explore the involvement of *dab-1* disabled, I analyzed meiotic maturation rates in females homozygous for a *dab-1* null mutation, *gk291*, which deletes exons two and three, including the phosphotyrosine-binding domain (Kamikura and Cooper, 2003; 2006). These *dab-1(gk291)* null mutant females exhibit increased meiotic maturation rates [0.42 ± 0.14 (n=22)] compared to normal females [0.16 ± 0.1(n=17), $P<0.001$]. This increase in meiotic maturation rate is similar to that observed in *vab-1(null)* mutant females [0.38 ± 0.25 (n=18)].

Figure 27. Genetic and biochemical analysis of the VAB-1 Eph/MSP receptor pathway

(A-C) MSP binds the VAB-1 ectodomain (VAB-1ECT). (A) VAB-1ECT with its endogenous signal peptide and V5 and 6-His epitope tags was expressed in 293F cells. (B) Western blot probed with anti-V5 antibodies showing VAB-1ECT secretion into the culture medium. (C) *In vitro* interaction between MSP and VAB-1ECT. Purified MSP-142 (100 nM) was incubated with partially purified VAB-1ECT (14 nM) and the complex was isolated by immunopreciptation with MSP antibodies and protein-A Sepharose (lanes 1-4) or using Ni-NTA agarose (lanes 5-7).
(D-K) Evidence that PQN-19, PKC-1, DAB-1, and VAV-1 function with the VAB-1 Eph/MSP receptor. (D) Organization of signaling domains in VAB-1 pathway proteins. PQN-19 contains VHS (VPS-27/Hrs/STAM), UIM (ubiquitin-interaction motif), and SH3 domains. PKC-1 contains C1, C2, kinase, and a protein kinase C domains. DAB-1 contains a phosphotyrosine-binding (PTB) domain. VAV-1 contains CH (calponin homology), C1, RhoGEF, SH2, and SH3 domains. (E) Measurement of oocyte meiotic maturation rates following *dab-1*, *vav-1*, *pqn-19*, *pkc-1*, or control RNAi in *fog-2(q71)*, *vab-1(dx31);fog-2(q71)*, or *ceh-18(mg57);fog-2(q71)* female genetic backgrounds. Each of the four genes synergize with *ceh-18* but not *vab-1*. Error bars represent s.d. (F-K) Fluorescence micrographs showing MAPK-YT staining (red) in oocytes. In wild-type hermaphrodites (F), MSP-dependent MAPK-YT staining is observed in proximal oocytes (typically oocytes –1 through –3). (G) MAPK-YT staining is extended to three to eight proximal oocytes in *vab-1(null)* hermaphrodites, consistent with the idea that *vab-1* is a negative regulator of meiotic maturation and MAPK activation in oocytes [7]. Similarly, *dab-1(null)* (H), *pqn-19(null)* (I), *pkc-1(null)* (J), and *vav-1(RNAi)* hermaphrodites (K) exhibit an extended MAPK-YT staining pattern similar to that of *vab-1(null)* hermaphrodites (G).
(L-O) DAB-1 is expressed in oocytes. Western blot detection of DAB-1 (53 kDa) in the wild-type, but not *dab-1(gk291)* hermaphrodites (L). Fluorescent detection of DAB-1 in oocytes from wild-type hermaphrodites (M) and *fog-2(q71)* females (N), but not *dab-1(gk291)* hermaphrodites (O). DAB-1 is cortically enriched when sperm are present.

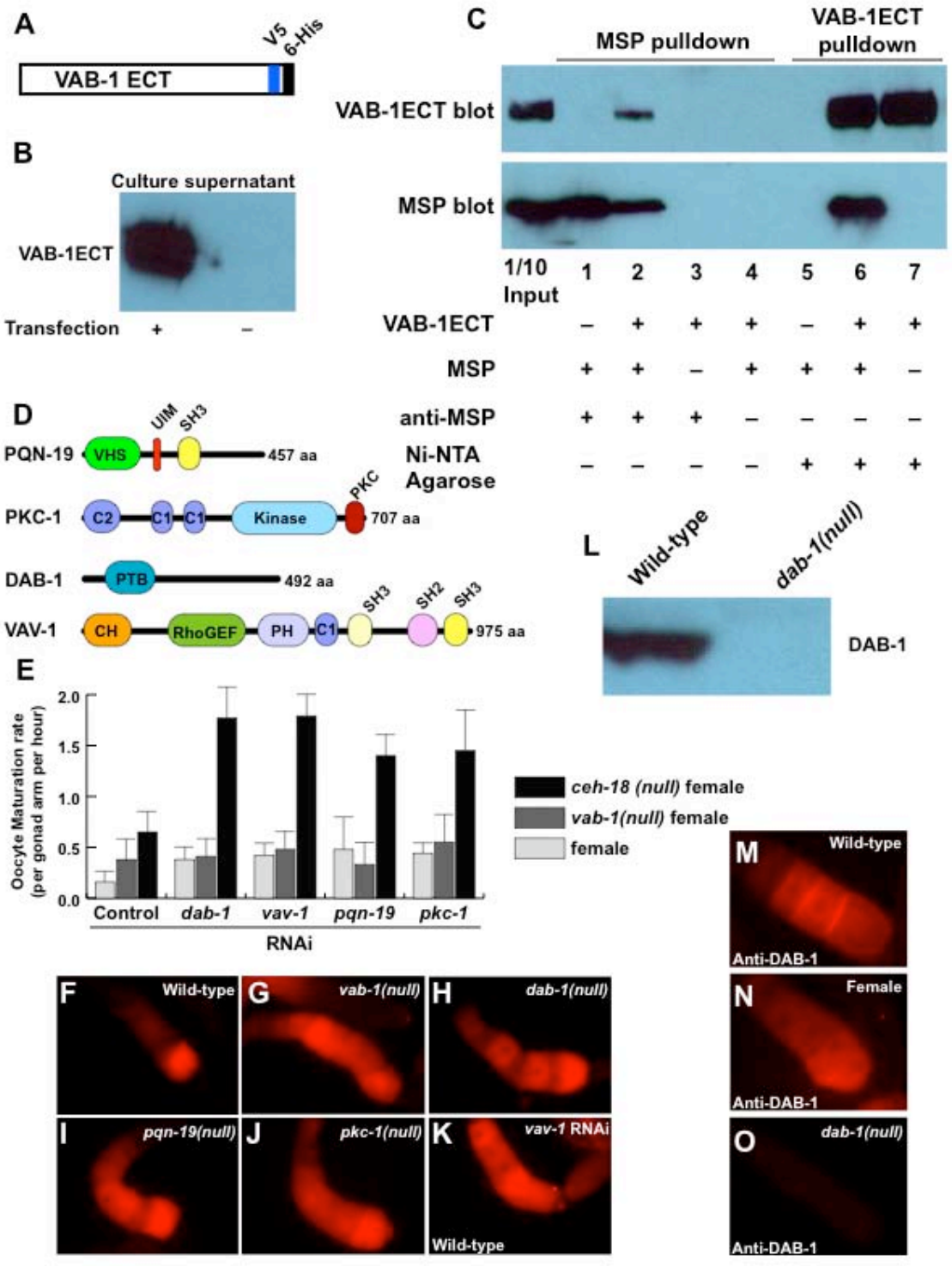
A
V5
6-His
VAB-1 ECT
B
Culture supernatant
VAB-1ECT
Transfection + –
C
MSP pulldown
VAB-1ECT pulldown
VAB-1ECT blot
MSP blot
1/10 Input 1 2 3 4 5 6 7
VAB-1ECT – + + + – + +
MSP + + – + + + –
anti-MSP + + + – – – –
Ni-NTA Agarose – – – – + + +
D
UIM
SH3
PQN-19 VHS 457 aa
PKC
PKC-1 C2 C1 C1 Kinase 707 aa
DAB-1 PTB 492 aa
SH3
SH2
SH3
VAV-1 CH RhoGEF PH C1 975 aa
L
Wild-type
dab-1(null)
DAB-1
E
Oocyte Maturation rate (per gonad arm per hour)
2.0
1.5
1.0
0.5
0.0
Control
dab-1
vav-1
pqn-19
pkc-1
RNAi
ceh-18 (null) female
vab-1(null) female
female
F Wild-type
G vab-1(null)
H dab-1(null)
I pqn-19(null)
J pkc-1(null)
K vav-1 RNAi
Wild-type
M Wild-type
Anti-DAB-1
N Female
Anti-DAB-1
O dab-1(null)
Anti-DAB-1

Further, *vab-1(null)dab-1(null)* double mutant females exhibit a meiotic maturation rate of 0.43 ± 0.19 (n=22), consistent with the idea that these two genes function in a common pathway. Additional evidence supporting the idea that *dab-1* functions in an oocyte pathway comes from the finding that DAB-1 protein localizes to the oocyte cytoplasm and is enriched at the oocyte cell cortex between oocytes (Fig. 27M) in a pattern similar to VAB-1::GFP (Miller et al., 2003). Strikingly, DAB-1 protein localization is altered in the absence of sperm, no longer exhibiting cortical enrichment between oocytes (Figure 27N). Recent data indicate that DAB-1 physically interacts with the VAB-1 intracellular domain *in vitro* (Cheng et al., 2008, see chapter III). In contrast to *dab-1*, I did not observe elevated meiotic maturation rates in *pqn-19(ok406)fog-3(q443)* females, which displayed rates (0.10 ± 0.15; n=22) similar to unmated female controls. Likewise, meiotic maturation rates in *pkc-1(ok563);fog-3(q443)* females, though slightly elevated (0.18 ± 0.20; n=24), were significantly lower than those of *vab-1* females ($P<0.001$). Thus, for *pqn-19* and *pkc-1*, the analysis of meiotic maturation rates in a female background led to a different conclusion from the RNAi and MAPK activation studies described above. To reconcile this discrepancy, I analyzed oocyte meiotic maturation by time-lapse videomicroscopy and noticed that *pqn-19(ok406)* and *pkc-1(ok563)* hermaphrodites exhibited an incompletely penetrant (~33%) delay in nuclear envelope breakdown during oocyte meiotic maturation. I made the same observation in *dab-1(gk291)* hermaphrodites and similar data were published for *vav-1(null)* mutant hermaphrodites for which the lethal pharyngeal defects were transgenically rescued (Norman et al., 2005). Since this delay in nuclear envelope breakdown is not observed in *vab-1(null)* mutants, I conclude

that *dab-1*, *pkc-1*, *pqn-19*, and *vav-1* may also have redundant functions as positive regulators of meiotic maturation, through *vab-1*-independent pathways.

Necessity and Sufficiency of Somatic $G\alpha_{o/i}$ Signaling in the Control of Meiotic Maturation and Oocyte MAPK Activation

The strongest negative regulator of meiotic maturation identified in the RNAi screen is *goa-1*, which encodes a heterotrimeric $G\alpha_{o/i}$ protein previously shown to regulate locomotion, egg-laying, and male mating behaviors (Mendel et al., 1995; Segalat et al., 1995). *goa-1(RNAi)* in a female background triggers meiotic maturation and MAPK activation in oocytes despite the absence of MSP (Table 2 and Figure 28C). Extending these RNAi results using genetics, we found that *goa-1(sa734)* null mutant females exhibited significantly higher meiotic maturation rates than control females and they showed MSP-independent MAPK activation in oocytes (Table 4, compare lines 4 and 2, and Figure 28C, $P<0.001$). The *goa-1(n1134)* reduction-of-function (rf) allele behaved similarly (Table 4, compare lines 6 and 2, and Figure 28E, $P<0.001$). Meiotic maturation rates were lower in *goa-1(sa734)* null mutant females compared to *goa-1(RNAi)* females, however, most likely because the *goa-1(sa734)* females appeared starved and produced fewer oocytes. Consistent with this interpretation, *goa-1(n1134*rf*)* females were healthier and exhibited higher meiotic maturation rates than null mutant females, and *goa-1(sa734)* hermaphrodites had lower rates than the wild type (Table 4, compare lines 1-7).

Figure 28. $G\alpha_{o/i}$ and $G\alpha_s$ signaling antagonistically regulate oocyte MAPK activation

(A-L) Fluorescent micrographs showing MAPK-YT staining (red) in oocytes following the indicated genetic or RNAi perturbations of the $G\alpha_{o/i}$ and $G\alpha_s$ pathways in hermaphrodites (A, G, H, I, L) or females (B-F, J, K). Scale bars represent 10 μm.

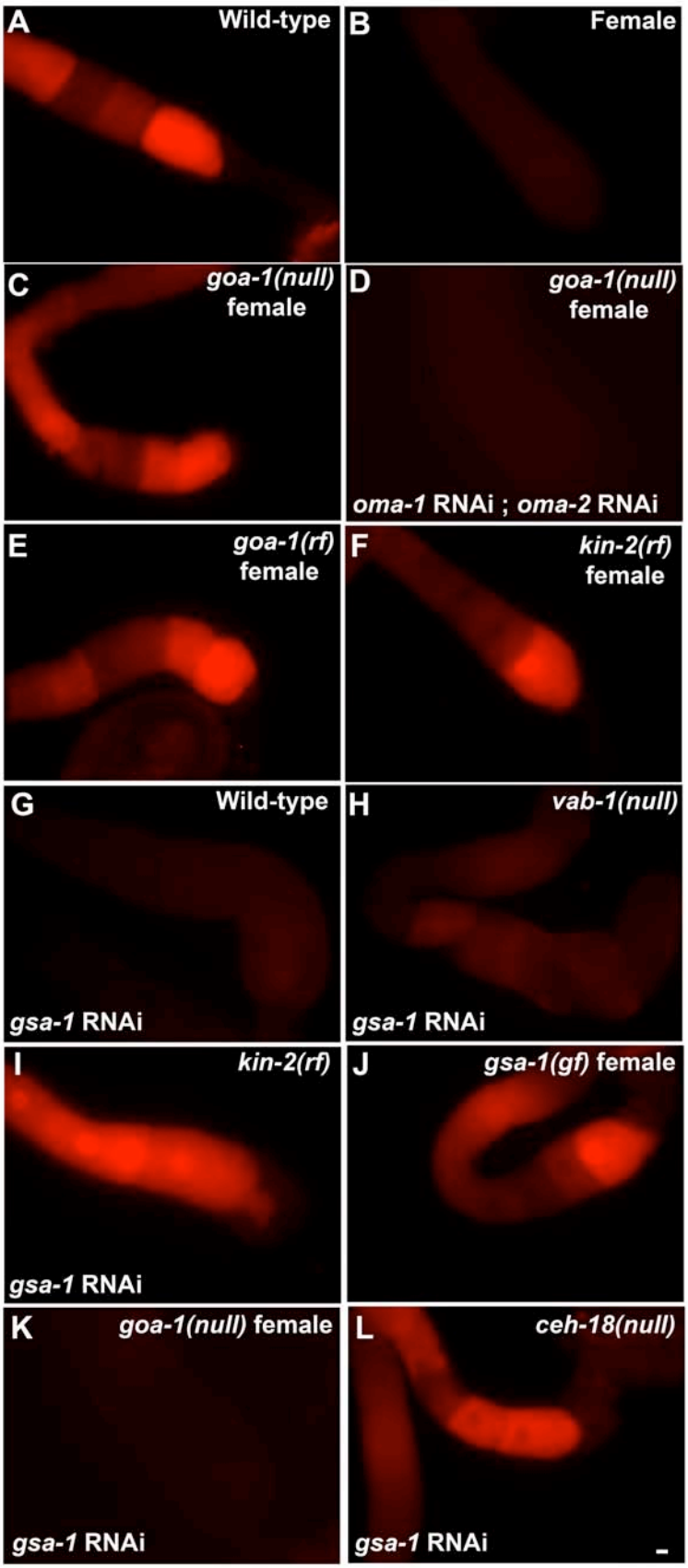
A
Wild-type
B
Female
C
goa-1(null)
female
D
goa-1(null)
female
oma-1 RNAi ; oma-2 RNAi
E
goa-1(rf)
female
F
kin-2(rf)
female
G
Wild-type
gsa-1 RNAi
H
vab-1(null)
gsa-1 RNAi
I
kin-2(rf)
gsa-1 RNAi
J
gsa-1(gf) female
K
goa-1(null) female
gsa-1 RNAi
L
ceh-18(null)
gsa-1 RNAi

Table 4 Genetic analysis of G-protein signaling

	Genotype[a]	Sperm (yes/no)	Oocyte Maturation Rate[b]	MAPK Activation[c]
1.	Wild-type hermaphrodite	yes	2.50 ± 0.41 (16)	on
2.	*fog-3(q443)* unmated	no	0.17 ± 0.14 (15)	off
3.	*fog-3(q443)* mated	yes	2.29 ± 0.43 (20)	on
4.	*goa-1(sa734) fog-3(q443)* female	no	0.47 ± 0.17 (30)	on
5.	*goa-1(sa734)*hermaphrodite	yes	1.23 ± 0.18 (15)	on
6.	*goa-1(n1134)fog-3(q443)* female	no	1.06 ± 0.25 (16)	on
7.	*goa-1(n1134)* hermaphrodite	yes	2.55 ± 0.40 (18)	on
8.	*oma-1(RNAi);oma-2(RNAi)* hermaphrodite	yes	0.06 ± 0.07 (13)	off
9.	*oma-1(RNAi);oma-2* (RNAi); *goa-1(sa734)fog-3(q443)* female	no	0.00 ± 0.00 (13)	off
10.	*oma-1(RNAi);oma-2* (RNAi); *goa-1(sa734)* hermaphrodite	yes	0.00 ± 0.00 (17)	off
11.	*goa-1(gf)* hermaphrodite[d]	yes	0.76 ± 0.62 (19)	on
12.	*kin-2(ce179* rf*);fog-3(q443)* female	no	0.64 ± 0.23 (14)	on
13.	*gsa-1* (RNAi) wild-type hermaphrodite	yes	0.30 ± 0.11 (17)	off
14.	Control (RNAi); *vab-1(dx31)* hermaphrodite	yes	2.44 ± 0.60 (15)	on
15.	*gsa-1* (RNAi); *vab-1(dx31)* hermaphrodite	yes	0.20 ± 0.17 (15)	off
16.	Control (RNAi); *kin-2(ce179* rf*)* hermaphrodite	yes	1.92 ± 0.59 (12)	on
17.	*gsa-1* (RNAi); *kin-2(ce179* rf*)* hermaphrodite	yes	1.78 ± 0.46 (15)	on
18.	*gsa-1(ce81* gf*) fog-3(q443)* female	no	0.38 ± 0.14 (12)	on
19.	*gsa-1(ce94* gf*) fog-3(q443)* female	no	0.44 ± 0.13 (13)	on
20.	*gsa-1(pk75)/+* hermaphrodite	yes	1.60 ± 0.40 (10)	on
21.	Control (RNAi); *rrf-1(pk1417)* hermaphrodite	yes	2.39 ± 0.50 (12)	on
22.	*gsa-1* (RNAi); *rrf-1(pk1417)* hermaphrodite	yes	2.06 ± 0.40 (15)	on
23.	*gsa-1* (RNAi); *goa-1(sa734)* hermaphrodite	yes	0.14 ± 0.10 (16)	off
24.	*gsa-1* (RNAi); *goa-1(n1134)* hermaphrodite	yes	0.34 ± 0.20 (14)	off
25.	*gsa-1* (RNAi); *goa-1(sa734)fog-3(q443)*	no	0.16 ± 0.10 (10)	off
26.	Control (RNAi); *ceh-18 (mg57)* hermaphrodite	yes	1.76 ± 0.44 (15)	on
27.	*gsa-1* (RNAi); *ceh-18(mg57)* hermaphrodite[e]	yes	1.78 ± 0.36 (16)	on
28.	*oma-1;oma-2* (RNAi); *gsa-1(ce94* gf*)fog-3(q443)* female	no	0.00 ± 0.00 (12)	off

[a] , Genotypes utilized null mutations unless where indicated by "gf" or "rf" for gain-of-function and reduction-of function mutations, respectively. The position and morphology of sheath cell nuclei were unaffected by RNAi of *gsa-1*, *kin-2*, or *goa-1*, or in mutants of these genes.

[b]Meiotic maturation rates were measured in two-day-old adult animals.

[c], MAPK activation was scored as described above, with "on" denoting strong staining in proximal oocytes and "off," an absence of staining.

[d], The PS1493 transgenic strain that expresses constitutively-activated GOA-1($G\alpha_oQL$) under the control of *goa-1* promoter was used.

[e] , *ceh-18* mutant sheath cells respond to RNAi, as *gfp(RNAi)* could silence *lim-7::gfp* expression in a *ceh-18(mg57)* mutant background.

Time-lapse videomicroscopy of meiotic maturation and ovulation in *goa-1(n1134)fog-3(q443)* (n=8) and *goa-1(RNAi);fog-2(q71)* (n=8) females indicated that nuclear envelope breakdown, cortical cytoskeletal rearrangement, and ovulation all occurred normally despite the absence of MSP.

MSP-dependent MAPK activation and meiotic maturation require the downstream action of OMA-1 and OMA-2, two TIS-11 zinc-finger proteins expressed in the germ line (Detwiler et al., 2001). No MAPK activation or meiotic maturation is observed in *goa-1(sa734);oma-1(RNAi);oma-2(RNAi)* or *goa-1(n1134);oma-1(RNAi);oma-2(RNAi)* hermaphrodites and females (Fig. 27D, Table 3, lines 9 and 10, and Fig. 32). Thus, $G\alpha_{o/i}$ likely functions upstream or in parallel with OMA-1/OMA-2 to repress meiotic maturation in the absence of the MSP signal, with the caveat that RNAi is not necessarily equivalent to null mutations in genetic epistasis experiments. To test whether GOA-1 activity is sufficient to repress meiotic maturation, we measured meiotic maturation rates in hermaphrodites expressing constitutively-activated GOA-1(Q205L) under control of the *goa-1* promoter (Mendel et al., 1995) and observed that meiotic maturation rates were reduced by 70% despite the presence of MSP (Table 4, line 11). These results suggest that *goa-1* activity is needed to fully repress meiotic maturation in the absence of MSP and that it is also sufficient to partially repress meiotic maturation in the presence of MSP. Since transgenes are ordinarily silenced in the germ line (Kelly et al., 1997), this data constitutes a further line of evidence suggesting *goa-1* functions in the soma.

The analysis of *goa-1(RNAi)* in an *rrf-1* mutant female background described above suggests that *goa-1* functions in the somatic control of oocyte meiotic maturation (Table 3).

Figure 29. Expression of GOA-1 in the soma is sufficient to inhibit MAPK activation in oocytes

(A-E) Fluorescent micrographs of dissected gonads stained for GOA-1 (red) and DNA (blue). GOA-1 is expressed in sheath cells, oocytes, and spermathecal cells of wild-type hermaphrodites (A) and *fog-2(q71)* (B) and *fog-3(q443)* (not shown) females. In females, GOA-1 is cortically enriched between oocytes (B). No GOA-1 staining is observed in *goa-1(sa734)* mutants (C). GOA-1 staining in oocytes is significantly reduced following *goa-1(RNAi)* in an *rrf-1(null)fog-3(q443)* mutant female background (D). Note, GOA-1 staining between oocytes is reduced in the medial focal plane, comparing panels (D) and (B), yet staining in the sheath (Sh) and spermatheca (Sp) persists. GOA-1 staining also persists when viewed in superficial focal planes (E) in *goa-1(RNAi);rrf-1(null)fog-3(q443)* females with punctate staining possibly corresponding to the sheath cell processes (arrowheads).
(F) Fluorescence micrograph of MAPK-YT staining following *goa-1(RNAi)* in a *rrf-1(null)fog-3(q443)* mutant female background. MAPK-YT staining is not observed, suggesting that GOA-1 expression in the soma (D and E) is sufficient to repress MAPK activation in oocytes.

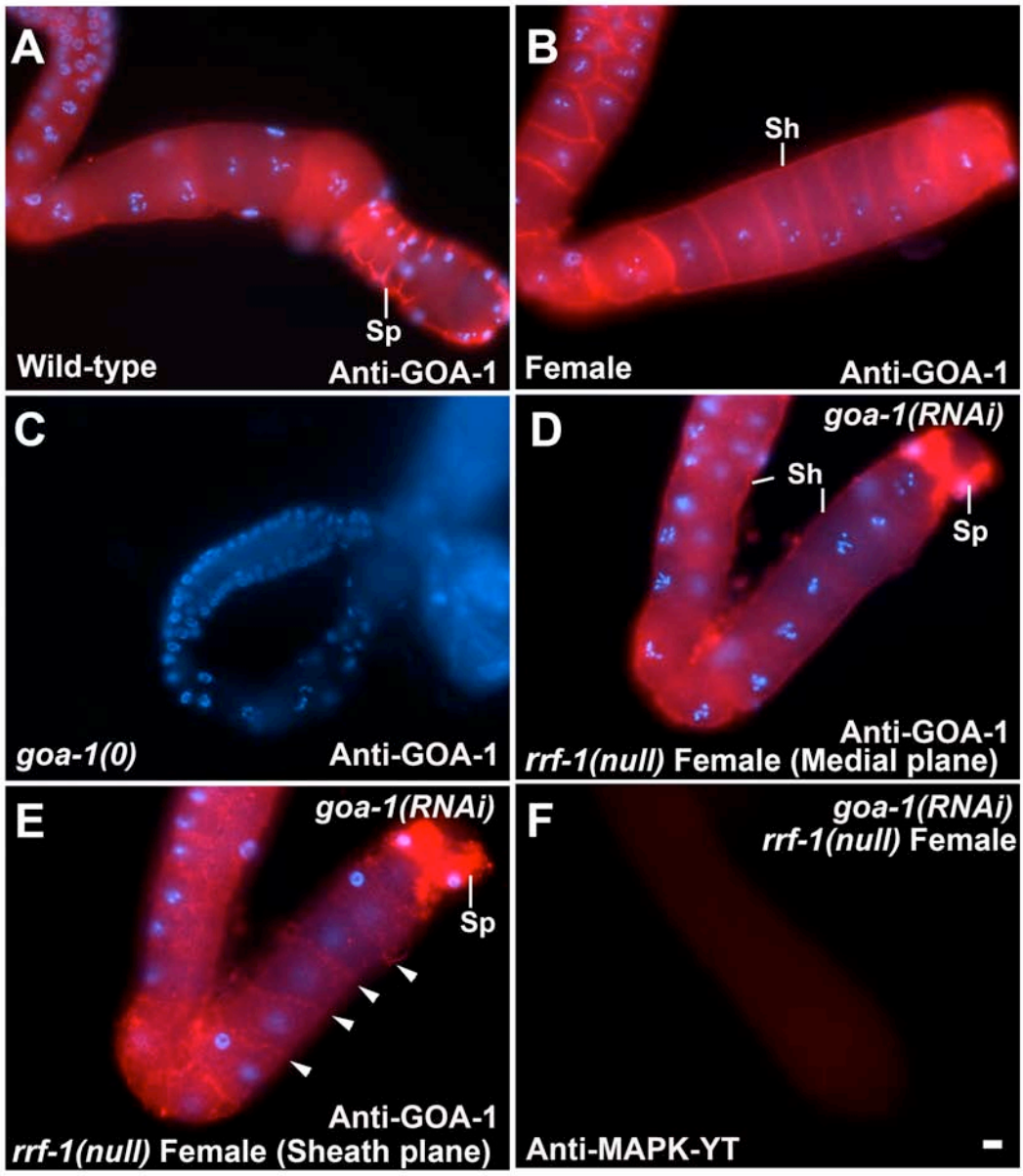
A
Sp
Wild-type
Anti-GOA-1
B
Sh
Female
Anti-GOA-1
C
goa-1(0)
Anti-GOA-1
D
goa-1(RNAi)
Sh
Sp
Anti-GOA-1
rrf-1(null) Female (Medial plane)
E
goa-1(RNAi)
Sp
Anti-GOA-1
rrf-1(null) Female (Sheath plane)
F
goa-1(RNAi)
rrf-1(null) Female
Anti-MAPK-YT

Since *goa-1* is maternally required for positioning mitotic spindles in embryonic blastomeres (Bastiani and Mendel, 2006), we examined the expression of GOA-1 in dissected gonads of hermaphrodites and females using specific antibodies (Figure 29). In hermaphrodites, we observed cytoplasmic staining in oocytes as well as staining that appeared to be in the surrounding sheath (Figure 29A). No staining was observed in *goa-1(sa734)* null mutants or following *goa-1(RNAi)*, confirming the specificity of the antibodies (Fig. 29C and data not shown). In dissected gonads from females, we observed cortical enrichment of GOA-1 between oocytes as well as staining that appeared to be in the sheath (Figure 29B). Since sheath cell and oocyte plasma membranes are in close apposition and the sheath cells are extremely thin (~0.2 μm; Hall et al., 1999), we needed a way to visualize GOA-1 expression in sheath cells separately from oocytes. Thus, we reduced the expression of GOA-1 in the germ line by performing *goa-1* RNAi on *rrf-1* females and stained the dissected gonads with anti-GOA-1 antibody. In these *goa-1(RNAi);rrf-1* female gonads, cortical GOA-1 staining between oocytes is significantly reduced through medial focal planes, yet staining persists in the thin layer surrounding oocytes, consistent with sheath cell expression (Figure 29, D and E). The gonadal sheath cells insert finger-like projections between oocytes that can only be resolved by electron microscopy (Hall et al., 1999). In these *goa-1(RNAi);rrf-1* female gonads, punctate staining is observed between oocytes mainly in superficial focal planes, suggesting that GOA-1 may be present in the sheath cell processes (Figure 29E).

Table 5. Effect of *vab-1* and *ceh-18* mutations on meiotic maturation rates following RNAi of class I genes in the absence of sperm

Gene (RNAi)	Oocyte Maturation Rate in Females[a] (N)	Oocyte Maturation Rate in *vab-1(null)* Females[b] (N)	Oocyte Maturation Rate in *ceh-18(null)* Females[c] (N)
Control[d]	0.16 ± 0.10 (17)	0.38 ± 0.25 (18)	0.65 ± 0.25 (12)
goa-1	1.67 ± 0.38 (36)	2.19 ± 0.35 (17)	0.92 ± 0.30 (19)
gpb-1	0.88 ± .24 (21)	1.63 ± 0.36 (15)	0.64 ± 0.21 (27)
inx-22	0.90 ± 0.36 (30)	1.90 ± 0.25 (10)	0.99 ± 0.30 (22)
inx-14	0.99 ± 0.30 (26)	1.94 ± 0.28 (21)	0.67 ± 0.25 (11)
par-5	0.49 ± 0.20 (28)	0.80 ± 0.25 (26)	0.82 ± 0.28 (17)
kin-2[e]	1.50 ± 0.30 (9)	1.70 ± 0.26 (15)	0.83 ± 0.47 (17)
rpt-3	0.44 ± 0.15 (25)	0.82 ± 0.19 (5)	0.45 ± 0.18 (15)
arf-1.1	0.64 ± 0.28 (10)	0.44 ± 0.14 (13)	0.73 ± 0.19 (14)
ptc-1	0.60 ± 0.27 (18)	0.75 ± 0.24 (10)	0.59 ± 0.09 (7)
gsa-1	0.37 ± 0.18 (12)	0.52 ± 0.25 (12)	0.79 ± 0.22 (9)
ran-1	0.72 ± 0.13 (6)	0.80 ± 0.19 (6)	1.30 ± 0.23 (12)
phi-11	0.50 ± 0.15 (10)	0.44 ± 0.20 (10)	0.53 ± 0.21 (12)
dab-1	0.38 ± 0.14 (15)	0.41 ± 0.24 (10)	1.77 ± 0.32 (18)
vav-1	0.42 ± 0.13 (15)	0.48 ± 0.18 (10)	1.79 ± 0.20 (10)
pkc-1	0.44 ± 0.11 (9)	0.55 ± 0.28 (13)	1.45 ± 0.40 (18)
pqn-19	0.48 ± 0.34 (12)	0.33 ± 0.20 (13)	1.40 ± 0.16 (12)

[a], Meiotic maturation rates were measured in a *fog-2(q71)* female background.
[b], Meiotic maturation rates were measured in a *vab-1(dx31);fog-2(q71)* females.
[c], Meiotic maturation rates were measured in a *ceh-18(mg57);fog-2(q71)* females. *ceh-18* mutant sheath cells respond to RNAi, as *gfp(RNAi)* could silence *lim-7::gfp* expression in a *ceh-18(mg57)* mutant background.
[d], Mock RNAi using the empty vector, L4440, served as a control.
[e], Worms fed *kin-2(RNAi)* become lethargic and bloated with unfertilized oocytes on the second day of adulthood.

We stained dissected gonads from these *goa-1(RNAi);rrf-1* mutant females with MAPK-YT antibodies and observed an absence of MAPK activation in the proximal gonad, suggesting that *goa-1* activity might be sufficient in the soma to negatively regulate MAPK activation in oocytes (Figure 29F). Since the sheath cells mediate the *ceh-18*-dependent inhibition of MAPK activation and meiotic maturation, which in turn is antagonized by MSP (Miller et al., 2003), we tested whether *ceh-18* and *goa-1* genetically interact.

The high meiotic maturation rate (1.67 ± 0.38) observed following *goa-1(RNAi)* in a *fog-2(q71)* background depends on *ceh-18(+)* function because *goa-1(RNAi)* in a *ceh-18(null);fog-2(q71)* background results in a lower meiotic maturation rate (0.92 ± 0.30; see Table 5). This result is consistent with a model in which *goa-1* functions in the sheath cell control of meiotic maturation or acts in parallel to *ceh-18*. A role for *goa-1* in the soma is additionally suggested by the observation that the basal sheath cell contraction rate is elevated in *goa-1(n1134)fog-3(q443)* and *goa-1(RNAi);fog-2(q71)* females (data not shown). Genetic epistasis analysis between $G\alpha_{o/i}$, $G\alpha_s$, *ceh-18*, and innexins (see below) further supports a role for *goa-1* in regulating sheath/oocyte communication.

A Somatic $G\alpha_s$ Signaling Pathway is Necessary and Sufficient to Promote Meiotic Maturation

In canonical $G\alpha_s$ signaling, activated $G\alpha_s$ stimulates adenylyl cyclase resulting in production of cAMP, which binds the regulatory subunit of cAMP-dependent PKA thereby releasing the active catalytic subunit (Cabrera-Vera et al., 2003). We identified

kin-2, which encodes the regulatory subunit of cAMP-activated protein kinase, as a strong negative regulator of meiotic maturation and found that *kin-2* functions somatically to inhibit meiotic maturation and MAPK activation in oocytes (Table 2 and Table 4, and Figure 26D, and data not shown). Time-lapse videomicroscopic analysis of *kin-2(RNAi)* in *fog-2(q71)* females (n=4) indicates that meiotic maturation occurs normally and that basal sheath cell contractions are elevated despite the absence of MSP. Consistent with the RNAi results, *kin-2(ce179*rf*)* females exhibit increased meiotic maturation rates compared to control females (Table 4, compare lines 12 and 2, $P<0.001$), and they display MAPK activation in proximal oocytes (Figure 28F). These results predict that *gsa-1*, which encodes cAMP-stimulatory $G\alpha_s$, should function to promote meiotic maturation. Surprisingly, our RNAi screen identified *gsa-1* as a weak negative regulator of meiotic maturation in the absence of sperm (Table 2).

To resolve this paradox, we reasoned that *gsa-1* might have an MSP-dependent function in promoting meiotic maturation through the canonical pathway and a weak MSP-independent function in inhibiting meiotic maturation through a non-canonical pathway. Importantly, our RNAi screen could not reveal a positive role for *gsa-1* because it was conducted in the absence of the MSP signal. Consistent with this hypothesis, *gsa-1(RNAi)* in a wild-type hermaphrodite background results in a 90% reduction in the meiotic maturation rate (Table 4, compare lines 13 and 1), and strikingly blocks MAPK activation in proximal oocytes (Figure 28G). Further, *gsa-1(RNAi)* can block meiotic maturation and MAPK activation in the *vab-1(null)* mutant hermaphrodite background where MAPK activation is ordinarily expanded to distal oocytes (Table 4, compare lines 14 and 15 and Figure 28H). $G\alpha_s$ signals through the canonical pathway to

promote meiotic maturation because *gsa-1(RNAi);kin-2(ce179*rf*)* hermaphrodites undergo meiotic maturation at 93% of the rate of *kin-2(ce179*rf*)* hermaphrodites treated with control RNAi, and their proximal oocytes contain activated MAPK (Table 4, compare lines 16 and 17, and Figure 28I). Since the *gsa-1(pk75)* null mutant is a larval lethal (Korswagen et al., 1997), we examined *gsa-1 (pk75)/+* heterozygous hermaphrodites and observed a significant 36% reduction in the meiotic maturation rates (Table 4, compare lines 20 and 1, $P<0.001$). We also noted that *gsa-1(pk75)/+* hermaphrodites moved slowly and were slightly egg-laying defective but were otherwise healthy and well-fed, suggesting that *gsa-1* is haploinsufficient for multiple phenotypes. We performed *gsa-1(RNAi)* in *rrf-1(null)* hermaphrodites and observed similar meiotic maturation rates and MAPK activation as *rrf-1(null)* hermaphrodites treated with control RNAi (Table 4, compare lines 21 and 22), suggesting that *gsa-1* function may be sufficient in the soma and dispensable in the germ line. Consistent with these data, we found that extrachromosomal arrays bearing transcriptional and translational *gsa-1::gfp* reporter constructs are expressed in the somatic sheath cells (data not shown). Recently, Seongseop Kim, a graduate student in our lab, generated rescuing gsa-1 fusion and found that gsa-1 expresses in the somatic sheath cells (Kim S. and Greenstein D. unpublished results).

To examine whether *gsa-1* activity is sufficient to promote meiotic maturation, we examined two dominant gain-of-function (gf) *gsa-1* alleles, *ce94*gf and *ce81*gf, which are predicted to stabilize the GTP-bound form of $G\alpha_s$ through G45R and R182C substitutions, respectively (Schade et al., 2005). *gsa-1(ce94*gf*)* and *gsa-1(ce81*gf*)* females display elevated meiotic maturation rates and MAPK activation in oocytes

despite the absence of MSP (Table 4, compare lines 18, 19, and 2, and Figure 28J). No MAPK activation or meiotic maturation was observed in *oma-1(RNAi);oma-2(RNAi);gsa-1(ce94*gf*)* hermaphrodites or females (Table 4, compare lines 19 and 28, and data not shown), suggesting that $G\alpha_s$ is either an upstream regulator, or functions in parallel. These data are consistent with a model in which somatic *gsa-1* activity is necessary and sufficient for promoting meiotic maturation and MAPK activation in oocytes.

$G\alpha_{o/i}$ Antagonizes $G\alpha_s$ Signaling to Repress Meiotic Maturation in the Absence of MSP

Since $G\alpha_{o/i}$ activity is required for repressing meiotic maturation in the absence of MSP, and $G\alpha_s$ signaling is necessary and sufficient to promote meiotic maturation, we asked whether *goa-1* negatively regulates *gsa-1* in analogy to the regulation of the $G\alpha_q$ *egl-30* pathway by *goa-1* in neurons (Bastiani and Mendel, 2006). We performed *gsa-1(RNAi)* on *goa-1(sa734)* and *goa-1(n1134)* hermaphrodites and females and observed low meiotic maturation rates and an absence of MAPK activation in proximal oocytes despite the presence of MSP (Table 4, lines 23-25, Figure 28K). This result suggests that the important function of $G\alpha_{o/i}$ in blocking meiotic maturation when sperm are unavailable for fertilization operates via the control of $G\alpha_s$ signaling, or through the regulation of a parallel pathway.

A key clue of how *gsa-1* might promote meiotic maturation comes from the observation that *gsa-1(RNAi);ceh-18(null)* hermaphrodites exhibit normal meiotic

maturation rates and show MAPK activation in oocytes (Table 4, compare lines 26 and 27, Figure 28L). How might *gsa-1*'s function to promote meiotic maturation become dispensable in the absence of *ceh-18* activity? In *ceh-18(null)* mutants, sheath cells and oocytes are not in close apposition and sheath/oocyte gap junctions are rare or absent (Rose et al., 1997; Hall et al., 1999). Our RNAi screen identified *inx-14* and *inx-22* as germline negative regulators of meiotic maturation and MAPK activation in the absence of sperm (Table 2, Figure 26D and Table 3). Since oocytes have only been observed to form gap junctions with sheath cells (Hall et al., 1999), *inx-14* and *inx-22* likely encode oocyte components of sheath/oocyte gap junctions. Since sheath/oocyte gap junctions must be lost when oocytes lose contact with sheath cells during ovulation, we considered the possibility that $G\alpha_s$ signaling promotes meiotic maturation in part by destabilizing inhibitory sheath/oocyte gap junctions. To test this possibility, we conducted *gsa-1;inx-14* double RNAi experiments in wild-type and *inx-22(tm1661)* backgrounds under conditions in which we could verify that both RNAi treatments were effective (Table 3). Whereas meiotic maturation was blocked following *gsa-1(RNAi)* in the wild type and *inx-22(tm1661)* backgrounds, meiotic maturation occurred normally following *gsa-1(RNAi);inx-14(RNAi)* in the *inx-22(tm1661)* background. Importantly, meiotic maturation was blocked following *gsa-1(RNAi) inx-14(RNAi)* in the wild type. This result suggests that reduction of both *inx-14* and *inx-22* function is needed to bypass the requirement for *gsa-1* for normal meiotic maturation. Taken together, these data suggest that $G\alpha_s$ signaling may promote meiotic maturation in part by affecting the synthesis or stability of sheath/oocyte gap junctions, or through action in a parallel pathway (Figure 30).

Table 5. Effect of *vab-1* and *ceh-18* mutations on meiotic maturation rates following RNAi of class I genes in the absence of sperm

Gene (RNAi)	Oocyte Maturation Rate in Females[a] (N)	Oocyte Maturation Rate in *vab-1(null)* Females[b] (N)	Oocyte Maturation Rate in *ceh-18(null)* Females[c] (N)
Control[d]	0.16 ± 0.10 (17)	0.38 ± 0.25 (18)	0.65 ± 0.25 (12)
goa-1	1.67 ± 0.38 (36)	2.19 ± 0.35 (17)	0.92 ± 0.30 (19)
gpb-1	0.88 ± .24 (21)	1.63 ± 0.36 (15)	0.64 ± 0.21 (27)
inx-22	0.90 ± 0.36 (30)	1.90 ± 0.25 (10)	0.99 ± 0.30 (22)
inx-14	0.99 ± 0.30 (26)	1.94 ± 0.28 (21)	0.67 ± 0.25 (11)
par-5	0.49 ± 0.20 (28)	0.80 ± 0.25 (26)	0.82 ± 0.28 (17)
kin-2[e]	1.50 ± 0.30 (9)	1.70 ± 0.26 (15)	0.83 ± 0.47 (17)
rpt-3	0.44 ± 0.15 (25)	0.82 ± 0.19 (5)	0.45 ± 0.18 (15)
arf-1.1	0.64 ± 0.28 (10)	0.44 ± 0.14 (13)	0.73 ± 0.19 (14)
ptc-1	0.60 ± 0.27 (18)	0.75 ± 0.24 (10)	0.59 ± 0.09 (7)
gsa-1	0.37 ± 0.18 (12)	0.52 ± 0.25 (12)	0.79 ± 0.22 (9)
ran-1	0.72 ± 0.13 (6)	0.80 ± 0.19 (6)	1.30 ± 0.23 (12)
phi-11	0.50 ± 0.15 (10)	0.44 ± 0.20 (10)	0.53 ± 0.21 (12)
dab-1	0.38 ± 0.14 (15)	0.41 ± 0.24 (10)	1.77 ± 0.32 (18)
vav-1	0.42 ± 0.13 (15)	0.48 ± 0.18 (10)	1.79 ± 0.20 (10)
pkc-1	0.44 ± 0.11 (9)	0.55 ± 0.28 (13)	1.45 ± 0.40 (18)
pqn-19	0.48 ± 0.34 (12)	0.33 ± 0.20 (13)	1.40 ± 0.16 (12)

[a], Meiotic maturation rates were measured in a *fog-2(q71)* female background.
[b], Meiotic maturation rates were measured in a *vab-1(dx31);fog-2(q71)* females.
[c], Meiotic maturation rates were measured in a *ceh-18(mg57);fog-2(q71)* females. *ceh-18* mutant sheath cells respond to RNAi, as *gfp(RNAi)* could silence *lim-7::gfp* expression in a *ceh-18(mg57)* mutant background.
[d], Mock RNAi using the empty vector, L4440, served as a control.
[e], Worms fed *kin-2(RNAi)* become lethargic and bloated with unfertilized oocytes on the second day of adulthood.

Figure 30. A model for the parallel control of meiotic maturation in *C. elegans* by antagonistic G protein signaling from the soma and an oocyte MSP/Eph receptor pathway

The germline and soma meiotic maturation control network is depicted in two states, according to whether the MSP signal is absent (left panel) or present (right panel). $G\alpha_{o/i}$ negatively regulates meiotic maturation and oocyte MAPK activation and antagonizes a $G\alpha_s$ pathway that promotes maturation. The $G\alpha_s$ pathway is drawn showing the involvement of the regulatory subunit (KIN-2) of cyclic-AMP-dependent protein kinase A (PKA) and adenylate cyclase (ACY). Genetic evidence is presented here for the involvement of *kin-2*, both *acy-4(ok1806)* and *acy-4(tm2510)* null mutant allele are sterile, which suggest that ACY-4 is required for oocyte meiotic maturation(J.A.G. and D.G., unpublished results). Unidentified sheath cell GPCRs are proposed to receive the MSP signal in parallel to VAB-1 on the oocyte, such that GPCR's coupled to $G\alpha_{o/i}$ are antagonized by MSP, whereas $G\alpha_s$-coupled receptors are stimulated by MSP. The $G\alpha_s$ pathway is proposed to directly destabilize the inhibitory sheath/oocyte gap junctions, but a parallel function is equally consistent with current genetic data. The CEH-18 POU-homeoprotein localizes to sheath cell nuclei where it functions in the control of sheath cell differentiation and function, in part, by directly or indirectly affecting the assembly of sheath/oocyte gap junctions. DAB-1 and VAV-1 function in the VAB-1 MSP/Eph receptor pathway in the germ line.

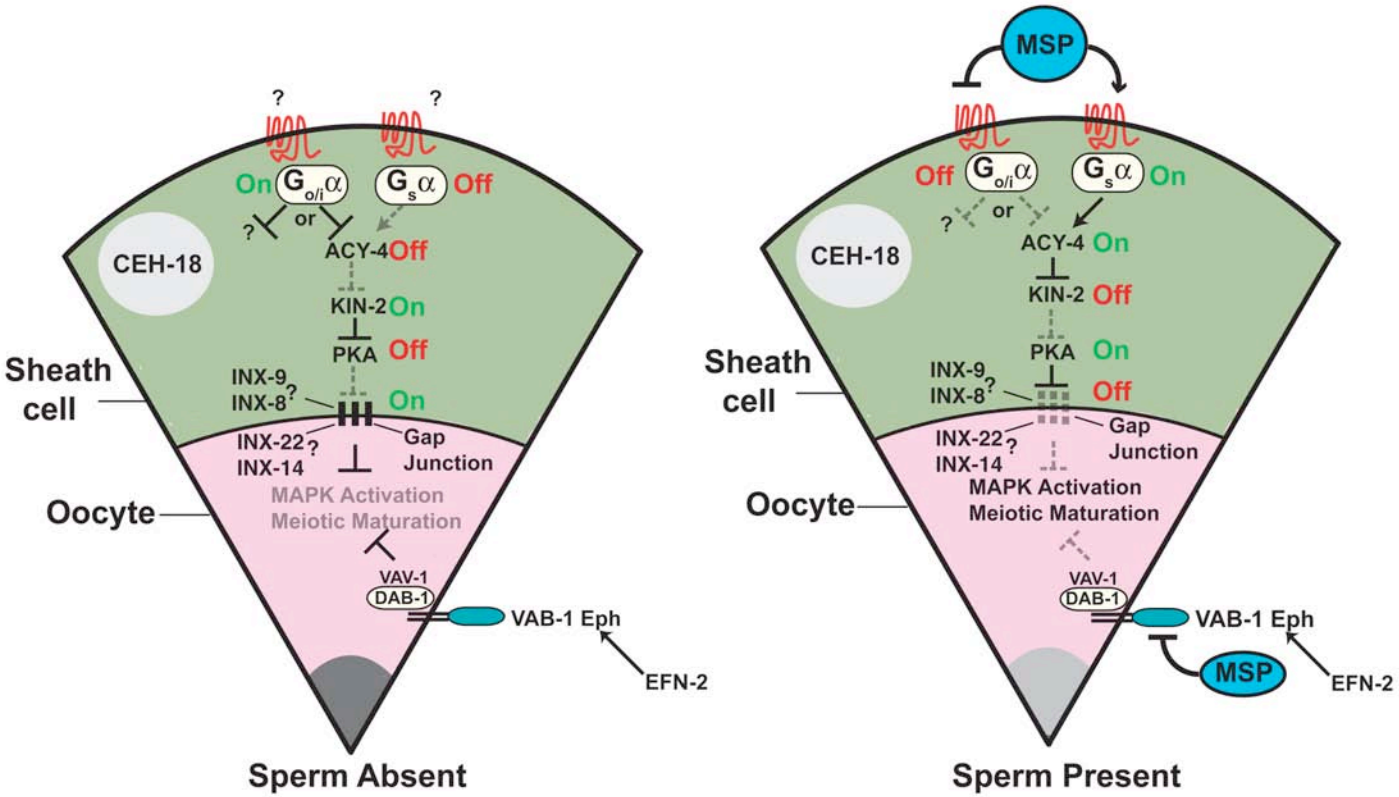
?
?
On
$G_{o/i}\alpha$
$G_s\alpha$
Off
?
or
CEH-18
ACY-4 Off
KIN-2 On
PKA Off
Sheath cell
INX-9
INX-8?
On
INX-22?
INX-14
Gap Junction
Oocyte
MAPK Activation
Meiotic Maturation
VAV-1
DAB-1
VAB-1 Eph
EFN-2
Sperm Absent
MSP
Off
$G_{o/i}\alpha$
$G_s\alpha$
On
?
or
CEH-18
ACY-4 On
KIN-2 Off
PKA On
Sheath cell
INX-9
INX-8?
Off
INX-22?
INX-14
Gap Junction
Oocyte
MAPK Activation
Meiotic Maturation
VAV-1
DAB-1
VAB-1 Eph
MSP
EFN-2
Sperm Present

Figure 31. *vav-1,pqn-19, pkc-1,* and *dab-1* negatively regulate oocyte MAPK activation in parallel to *ceh-18*

(A-E) Fluorescence micrographs showing MAPK-YT staining (red) in oocytes. No MAPK-YT staining is seen in oocytes in *ceh-18(mg57);fog-2(q71)* females following control RNAi (A), however, MAPK-YT staining is observed following *vav-1(RNAi)* (B), *pqn-19(RNAi)* (C), *pkc-1(RNAi)* (D), and *dab-1(RNAi)* (E) in the *ceh-18(mg57); fog-2(q71)* background (D). Scale bar, represents 10 μm.

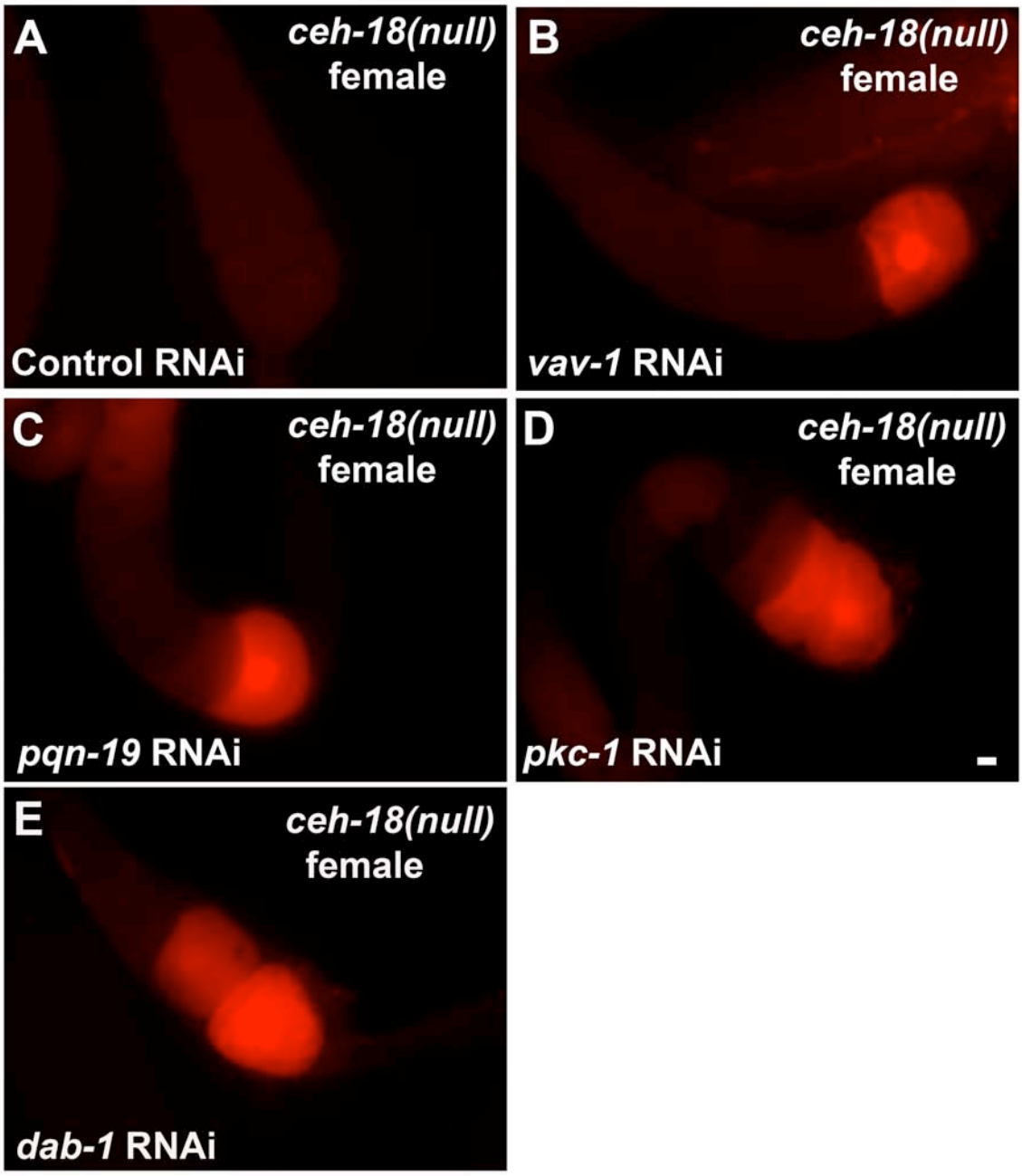
A
ceh-18(null)
female
Control RNAi
B
ceh-18(null)
female
vav-1 RNAi
C
ceh-18(null)
female
pqn-19 RNAi
D
ceh-18(null)
female
pkc-1 RNAi
E
ceh-18(null)
female
dab-1 RNAi

Figure 32. Oocyte MAPK activation in *goa-1(n1134)* hermaphrodites and females is dependent on OMA-1/OMA-2 function

(A-F) Fluorescence micrographs showing MAPK-YT staining (red) in oocytes from hermaphrodites (A-D) and females (E and F) of the indicated genotypes. *oma-1(RNAi); oma-2(RNAi)* prevents MAPK activation in wild-type (B), *goa-1(n1134)* (D), and *goa-1(n1134)fog-3(q443)* (F) genetic backgrounds. Scale bar represents 10 μm.

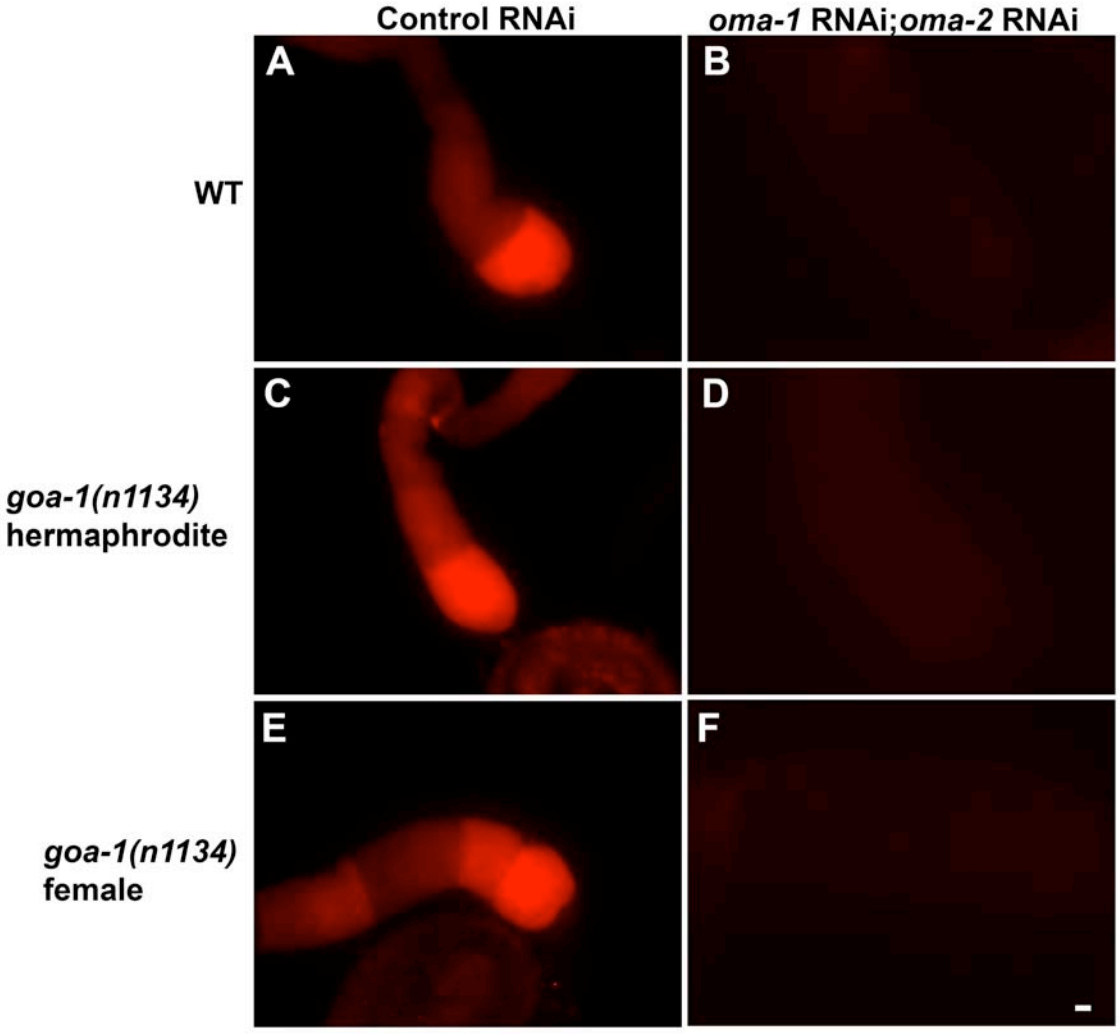
Control RNAi
oma-1 RNAi;oma-2 RNAi
A
B
WT
C
D
goa-1(n1134)
hermaphrodite
E
F
goa-1(n1134)
female

Table 7. Oocyte meiotic maturation rate measurements

RNAi	Oocyte maturation rate in females[a] (N)	
fog-3(q443)	0.05±0.105	(23)
pqn-19(ok406);fog-3(q443)	0.10±0.150	(22)
pkc-1(ok563);fog-3(q443)	0.182±0.20	(24)

While further studies will be needed to test this model at cell biological and ultrastructural levels, these data are consistent with studies in several systems, which show that G protein signaling can promote the assembly or disassembly of gap junctions (Lampe et al., 2001; Ouyang et al., 2005; Somekawa et al., 2005).

Discussion

Previous studies demonstrate that somatic and germline regulatory pathways work in concert to control oocyte meiotic maturation (Yamamoto et al., 2006; Mehlmann, 2005). Here we employed a genome-wide RNAi screen to define new regulators of oocyte meiotic maturation in *C. elegans*. The set of regulators defined in this screen comprises 17 highly conserved proteins (Table 2), which mediate meiotic maturation signaling functions in the somatic gonadal sheath cells or oocytes. The RNAi screen identified four genes (*dab-1*, *vav-1*, *pqn-19*, and *pkc-1*) satisfying multiple genetic criteria expected of genes functioning in the *vab-1* Eph receptor pathway (Figure 30). *vab-1* was previously shown to be necessary for complete MSP binding to gonads using an *in situ* binding assay and also to be sufficient to confer specific MSP binding activity to cultured mammalian cells (Miller et al., 2003). Data presented here showing that the VAB-1 ectodomain directly binds MSP, taken together with functional genetic analyses, provide strong evidence that MSP promotes meiotic maturation in part by antagonizing an Eph receptor signaling pathway in oocytes as proposed (Miller et al., 2003). Recently, it was suggested that VAB-1 may switch from a negative regulator to a redundant positive regulator of meiotic maturation upon binding MSP (Corrigan et al., 2005). Consistent

with the possibility that negative regulators of meiotic maturation may also have redundant activating functions, we found that mutations in *dab-1*, *pqn-19*, and *pkc-1* confer an incompletely penetrant delay in nuclear envelope breakdown during meiotic maturation and a similar observation was made previously for *vav-1* (Norman et al., 2005). The maturation-promoting redundant functions of *dab-1*, *pqn-19*, *pkc-1*, and *vav-1* are likely through a *vab-1*-independent pathway because *vab-1(null)* mutations do not exhibit delays in nuclear envelope breakdown. The mechanisms by which the *vab-1* pathway represses meiotic maturation and MAPK activation in oocytes in the absence of MSP will take additional work to decipher. Nonetheless, the conserved *vab-1* pathway genes described here are likely to mediate analogous signaling functions in mammals. In fact, a recent study of Eph receptor signaling during axonal guidance in mammals found a critical role for a homolog of VAV-1, the Rho family guanine nucleotide exchange factor Vav2 (Cowan et al., 2005).

Our findings suggest that antagonistic $G\alpha_s$ and $G\alpha_{o/i}$ protein signaling pathways play a predominant role in mediating the control of meiotic maturation likely by the gonadal sheath cells. $G\alpha_{o/i}$ defines a negatively acting pathway, whereas $G\alpha_s$ defines a positively acting pathway (Fig. 30). In part, $G\alpha_s$ may promote meiotic maturation by antagonizing inhibitory sheath/oocyte gap-junctional communication. Since *gsa-1(RNAi)* is epistatic to *goa-1(null)* mutations, $G\alpha_{o/i}$ signaling might inhibit the $G\alpha_s$ pathway at some level, perhaps by interfering with the activation of $G\alpha_s$ or possibly through inhibition of adenlyate cyclase. Alternatively, $G\alpha_s$ and $G\alpha_{o/i}$ may converge at some point far downstream, in effect, defining parallel regulatory inputs. Nonetheless, these results lead us to suggest that the gonadal sheath cells have the dual function of inhibiting

meiotic maturation in the absence of MSP, and promoting it in the presence of MSP. We speculate that unidentified MSP receptors (Miller et al., 2003) may be G-protein-coupled receptors (GPCRs) expressed in the gonadal sheath cells (Fig. 30). Our results illustrate that the control of meiotic diapause in *C. elegans* involves multiple layers of control involving both the soma and the germ line. This multi-tiered control mechanism may be important for tightly repressing meiotic maturation when sperm are unavailable, while also enabling graded responses that match the meiotic maturation rate to the number of sperm in the reproductive tract.

Our findings highlight interesting parallels and underscore fundamental differences between the control of meiotic maturation in *C. elegans* and mammals. In both cases, the somatic gonad may function to promote or inhibit meiotic progression depending on the hormonal status of the organism. For example, the removal of oocytes from large antral follicles causes meiotic resumption in most mammals (Pincus and Enzmann, 1935; Edwards, 1965). At the same time, luteinizing hormone (LH) receptor signaling in the mural granulosa cell compartment of the ovary promotes meiotic maturation in part through the triggered release of EGF-like ligands that induce meiotic resumption (Park et al., 2004). The LH receptor is $G\alpha_s$-coupled GPCR, and thus in mammals and *C. elegans*, $G\alpha_s$ signaling in somatic cells has a meiotic maturation-promoting function. In contrast, $G\alpha_s$ signaling within oocytes involving the GPR3 orphan GPCR plays a critical role in promoting meiotic arrest in mice (Mehlmann et al., 2002; Mehlmann et al., 2004; Kalinowski et al., 2004). In mammals, these multiple levels of control, involving the somatic gonad and the germ line, may serve to maintain oocyte homeostasis during the prolonged meiotic arrest, while at the same time

integrating the behaviors of the somatic gonad and the germ line so as to coordinate nuclear and cytoplasmic meiotic maturation events with ovulation. In humans, defects in female meiosis I represent the leading cause of congenital birth defects and miscarriage and the frequency of these meiotic errors increases with maternal age (Hassold and Hunt 2001). In the aging ovarian environment, defective hormonal signaling responses may be a factor underlying the high rate of aneuploidy (Hodges et al., 2002; 2005). Since *goa-1(null)* mutations cause non-disjunction during female meiosis (J. A. G. and D. G., unpublished results), signaling defects may also contribute to aneuploidy in *C. elegans*. The conserved regulatory genes described here are therefore expected to facilitate an understanding of how perturbations in hormonal signaling might contribute to aneuploidy. We defined germline and somatic signaling pathways that maintain meiotic arrest of *C. elegans* oocytes in the absence of the MSP signal. The underlying logic of meiotic diapause control in *C. elegans* and mammals is remarkably similar–both utilize multiple layers of control involving the soma and the germ line and G protein signaling can promote or repress meiotic maturation depending on cellular context.

CAPTER III

REGULATED TRAFFICKING OF THE MSP/EPH RECEPTOR DURING OOCYTE MEIOTIC MATURATION IN *CAENORHABDITIS ELEGANS*

Introduction

Studies of several conserved signal transduction pathways reveal a close connection between receptor trafficking and signaling output (González-Gaitán, 2003; von Zastrow and Sorkin, 2007). For example, internalization of ligand-bound EGF receptor via clathrin-mediated endocytosis is a known mechanism for desensitization. Other observations suggest that endocytosis of the EGF receptor is important for signaling (Vieira et al., 1996) and that signaling within endosomal compartments may be critical (Wunderlich et al., 2001). In the Delta/Notch signaling pathway, endocytosis and recycling of Delta in signaling cells is required for Notch activation in responding cells (Seugnet et al., 1997; Wang and Struhl, 2004; Emery et al., 2005; Jafar-Nejad et al., 2005; Fischer et al., 2006). Epsin-dependent trafficking through Rab11-positive recycling endosomes is apparently required to convert the Delta ligand to an active form (Wang and Struhl, 2004; Emery et al., 2005). Studies of intercellular signaling during axonal guidance show that endocytosis of ephrin/Eph receptor complexes, dependent on the Vav2 Rho-family GEF, is required for a switch from contact-mediated adhesion to repulsion (Marston et al., 2003; Zimmer et al., 2003; Cowan et al., 2005). Here I examine the role of Eph receptor trafficking during meiotic maturation signaling in *Caenorhabditis elegans*.

In *C. elegans*, oocyte meiotic maturation, a necessary step for ovulation and fertilization, is coupled to sperm availability (Fig. 33). In the absence of sperm, oocytes arrest in meiotic prophase for prolonged periods, whereas in the presence of abundant sperm, meiotic maturation, ovulation, and fertilization occur at a rapid pace (McCarter et al., 1999). Meiotic maturation rates are tightly linked to the number of sperm present; hermaphrodites produce a fixed number of sperm, and when they are consumed by fertilization, meiotic maturation rates progressively decline (Kosinski et al., 2005). Available evidence is consistent with the hypothesis that extracellular MSP, which forms a graded distribution in the proximal gonad of hermaphrodites and mated females, is the signal that provides the basis for the tight regulation of meiotic maturation (Kosinski et al., 2005; Miller et al., 2001; Miller et al., 2003; Govindan et al., 2006; Harris et al., 2006; Corrigan et al., 2005). MSP is sufficient to trigger activation of oocyte mitogen-dependent protein kinase (MAPK) activation in proximal oocytes (Miller et al., 2001), a conserved step in the regulation of meiotic maturation (Lee et al., 2007; Liang et al., 2007). Oocytes and sheath cells sense MSP/sperm through an oocyte MSP/Eph receptor and unidentified receptors (Miller et al., 2003). MSP-domain proteins are highly conserved and recently the MSP-domain protein VAPB, which is mutated in Amyotrophic Lateral Sclerosis type 8 (Nishimura et al., 2004), was shown to be a ligand for Eph receptors in *Drosophila* and mammals (Tsuda et al., 2008). The VAB-1 MSP/Eph receptor negatively regulates oocyte meiotic maturation in the absence of sperm, and MSP counteracts this regulation (Miller et al., 2003; Govindan et al., 2006; Corrigan et al., 2005). $G\alpha_s$ signaling is required for oocyte meiotic maturation and functions in the somatic gonad as indicated by cell-specific RNAi experiments (Govindan

et al., 2006) and genetic mosaic analysis (J. A. G. and D.G., unpublished results). Somatic $G\alpha_s$ signaling functions in part to antagonize sheath/oocyte gap-junctional communication (Govindan et al., 2006). A key unanswered question is how oocyte and sheath cell pathways function coordinately to produce appropriate meiotic maturation responses to graded MSP distributions. Here I show that the presence of MSP/sperm has a major effect on VAB-1 localization, which may be part of the cellular mechanism underlying the meiotic maturation response.

In this study, I use a functional VAB-1::GFP fusion expressed in *C. elegans* oocytes to evaluate the connection between receptor trafficking and signaling. I present several lines of evidence suggesting that a recycling VAB-1 Eph receptor inhibits oocyte meiotic maturation in the absence of the MSP ligand. Further, we provide evidence that the accumulation of VAB-1::GFP in the RAB-11-positive endocytic recycling compartment is inhibited by non-cell autonomous $G\alpha_s$ signaling in the presence of MSP/sperm. The modulation of VAB-1 MSP/Eph receptor trafficking in oocytes by $G\alpha_s$ signaling in the gonadal sheath cells might contribute to coordinating meiotic maturation rates with sperm availability.

Figure 33. A Model for the control of meiotic maturation in *C. elegans* by an oocyte MSP/Eph receptor pathway and antagonistic G-protein signaling from the soma

The germline and soma meiotic maturation control network is depicted in two states, according to whether the MSP signal is absent (left) or present (right). DAB-1 and VAV-1 function in the VAB-1 MSP/Eph receptor pathway in the germ line. $G\alpha_{o/i}$ negatively regulates meiotic maturation and oocyte MAPK activation and antagonizes a $G\alpha_s$ pathway that promotes maturation. The $G\alpha_s$ pathway is drawn showing the involvement of the regulatory subunit (KIN-2) of cyclic-AMP-dependent protein kinase A (PKA) and adenylate cyclase-4 (ACY-4). Unidentified sheath cell G-protein-coupled receptors (GPCRs) are proposed to receive the MSP signal in parallel to VAB-1 on the oocyte, such that GPCR's coupled to $G\alpha_{o/i}$ are antagonized by MSP, whereas $G\alpha_s$-coupled receptors are stimulated by MSP. The $G\alpha_s$ pathway is proposed to antagonize inhibitory sheath/oocyte gap junctions (See details in Chapter II; Whitten and Miller, 2007). The CEH-18 POU-homeoprotein localizes to sheath cell nuclei where it functions in the control of sheath cell differentiation and function, in part, by directly or indirectly affecting the assembly of sheath/oocyte gap junctions.

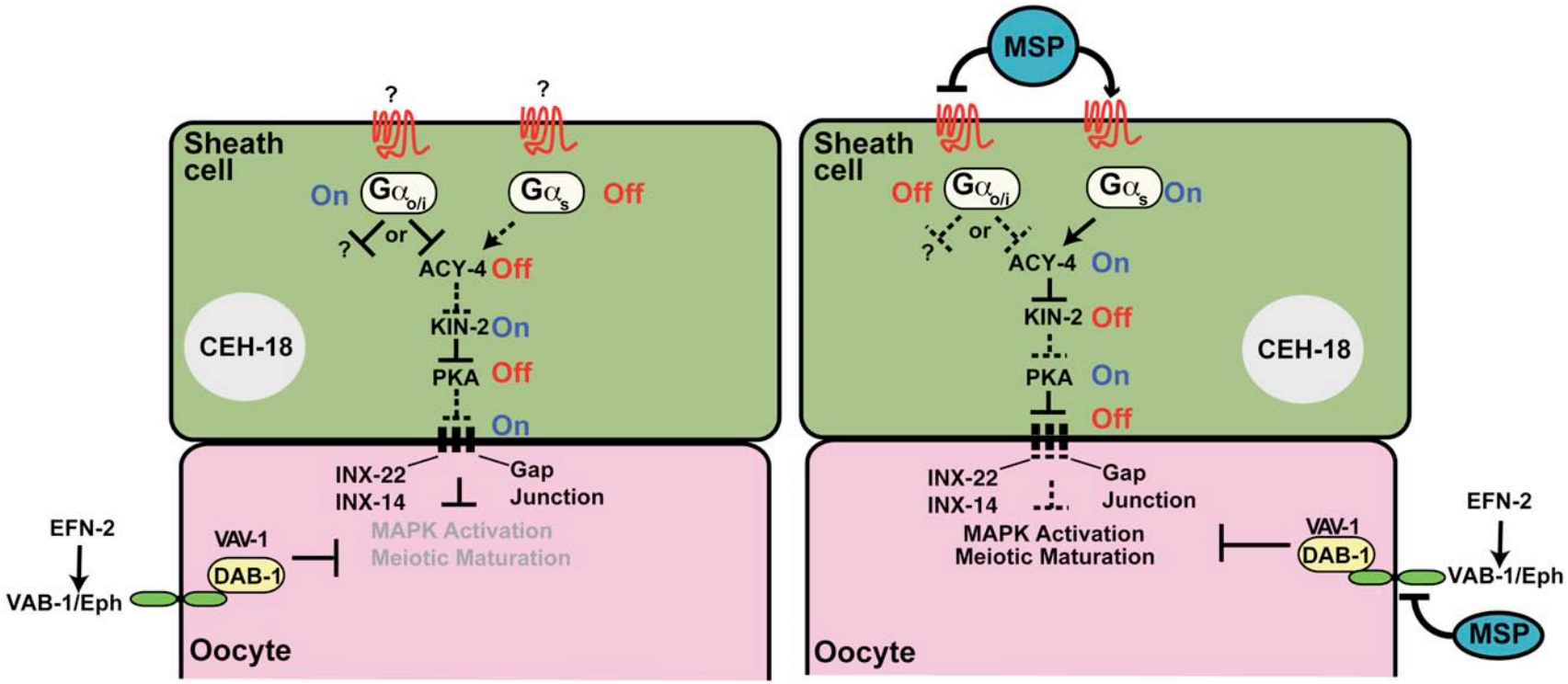
Sheath cell
On
Gαo/i
Gαs
Off
?
or
ACY-4 Off
KIN-2 On
PKA Off
On
CEH-18
INX-22
INX-14
Gap Junction
MAPK Activation
Meiotic Maturation
EFN-2
VAV-1
DAB-1
VAB-1/Eph
Oocyte
MSP/Sperm Absent
MSP
Sheath cell
Off
Gαo/i
Gαs
On
?
or
ACY-4 On
KIN-2 Off
PKA On
Off
CEH-18
INX-22
INX-14
Gap Junction
MAPK Activation
Meiotic Maturation
VAV-1
DAB-1
EFN-2
VAB-1/Eph
MSP
Oocyte
MSP/Sperm Present

Materials and methods

Nematode Culture, Genetics, and Strains

Standard culture and genetic techniques were carried out (Brenner, 1974) at 20°C, except transgenic lines were maintained at 25°C to reduce the potential of transgene silencing. The presence of mutations in *cav-1*, *efn-2*, and *efn-3* was confirmed by PCR. Genes, alleles, and balancer chromosomes are described in WormBase (http://www.wormbase.org). The following strains were used: CZ337 *vab-1(dx31)II,* DG1612 *vab-1(dx31)/mIn1[dpy-10(e128) mIs14]II; fog-2(q71)V,* DG1853 *dab-1(gk291)II*, DG1804 *dab-1(gk291)/mIn1[dpy-10(e128) mIs14]II; fog-2(q71)V,* CZ2611 *vab-2(ju1) efn-2(ev658)IV; efn-3(ev696)X,* RB1679 *cav-1(ok2089)V*, DH1201 *rme-1(b1045)V,* DG2305 *vab-1(dx31)II; rme-1(b1045)V,* BC277 *unc-46(e177) dpy-11(e224)V,* DG2100 *tnIs12* [*pie-1p-vab-1::gfp* + *rol-6(su1006)*], DG2102 *unc-119(ed3)III*; *tnIs13V* [*pie-1p-vab-1::gfp* + *unc-119(+)*], DG2101 *vab-1(dx31)II; fog-2(q71)/+V; tnIs12*, DG2190 *fog-3(q443)/hT2(qIs48)I; tnIs13V*, OD70 *unc-119(ed3)III; ltIs44V [pie-1p-mCherry::PH(PLC1delta1) + unc-119(+)]* (Kachur et al., 2008, a gift of Anjon Audhya and Karen Oegema), DG2189 *fog-3(q443)/hT2(qIs48)I; tnIs13 ltIs44V,* DG2148 *vab-1(dx31)/mIn1[dpy-10(e128) mIs14]II; tnIs13/+ fog-2(q71)V*, DG2161 *dab-1(gk291)II; tnIs13V,* DG2199 *dab-1(gk291)/mIn1[dpy-10(e128) mIs14]II; tnIs13/+ fog-2(q71)V*, DG2158 *cav-1(ok2089)IV; tnIs13V*, DG2200 *rme-1(b1045) tnIs13V*, DG2160 *tnIs13 ltIs44V*, DG2147 *tnIs13/+ fog-2(q71)V,* DG2431 *vab-2(ju1) efn-2(ev658)IV; tnIs13 fog-2(q71)/+V; efn-3(ev696)X,* DG2448 *vab-2(ju1) efn-2(ev658)IV; fog-*

2(q71)/+V; efn-3(ev696)X, RT201 *pwIs40 [pie-1p-mRFP::rab-7 + unc-119(+)],* a gift of Barth Grant, DG2390 *pwIs40; tnIs13 fog-2(q71)/+V,* RT193 *pwIs39[pie-1p-mRFP::rab-11 + unc-119(+)],* from Barth Grant, DG2391 *pwIs39/+; tnIs13/+ fog-2(q71)/+*.

RNA Interference and Phenotypic Analysis

RNA interference (RNAi) experiments were conducted at 22°C as described (Govindan et al., 2003), except *rab-11.1(RNAi)* was conducted by injecting double-stranded RNA into the intestine of L4 hermaphrodites and females. To prepare *rab-11.1* double-stranded RNA, a complementary DNA template was prepared using the PCR from *C. elegans* first-strand cDNA using the primers:

rab-11F1 5'-ATGGGCTCTCGTGACGATGAATAC-3'

rab-11R1 5'-ACACTGCTTCTTTGGTGGGTCGGA-3'

To introduce T7 promoter sequences at both ends, a second round of the PCR was conducted using the primers T7rab-11F2 and T7rab-11R2:

5'-TAATACGACTCACTATAGGGAGGGGTTGTTCTGATTGGAGACTCAGG-3'

5'-TAATACGACTCACTATAGGGAGGCGCTGGCGAAGGAATGATTGT-3'

In vitro transcription was conducted using the MEGAscript RNAi kit (Ambion). DNA sequencing was used to confirm the identities of RNAi clones from the Ahringer library (Kamath et al., 2003). The control for the RNAi feeding experiments was bacteria containing the L4440 vector. For injection RNAi experiments double-stranded RNA for

T26G10.4 served as a control as this treatment had no effect on the meiotic maturation rate. Oocyte meiotic maturation rates were measured and MSP injections were conducted as described (Miller et al., 2001; Miller et al., 2003) except that MSP was expressed and purified from *E. coli* using the method of (Baker et al., 2002). Meiotic maturation rates were measured on day one of adulthood (24 hours after L4 at 20°C). All staining and injection experiments were repeated at least twice and at least forty animals or gonads were examined. Student's t-test was used to assess statistical significance.

efn-4(RNAi) in an *efn-1(ju1); efn-2(ev658) efn-3(ev696)* background results in a large oocyte phenotype, which is not observed in *vab-1(dx31)* null mutants (Sarah Moseley and Andrew Chisholm, pers. comm.). Their result suggests that ephrins can have *vab-1*-independent functions in germline development. I observed this large oocyte phenotype after conducting *efn-4(RNAi)* in an *efn-1(ju1); efn-2(ev658) efn-3(ev696)*; *tnIs13* background, confirming that the *efn-4(RNAi)* treatment was efficacious. Previously it was reported that *efn-2(ev658); fog-2(q71)* unmated females have an elevated meiotic maturation rate compared to *fog-2(q71)* females, but they exhibit lower meiotic maturation rates than *vab-1(dx31); fog-2(q71)* females (Miller et al., 2003). To determine whether other ephrins might contribute to the *vab-1*-mediated inhibition of oocyte meiotic maturation, I examined *efn-1(ju1); efn-2(ev658) efn-3(ev696); fog-2(q71)* females; these animals exhibited a meiotic maturation rate of 0.11 ± 0.12 meiotic maturations per gonad arm per hour (n=11). While the basis for this effect is unclear, as these animals are sickly, one possibility is that ephrins may have maturation-inhibiting and -promoting functions or there could be additional *vab-1* ligands. This possibility is

consistent with the results of Sarah Moseley and Andrew Chisholm (pers. comm.) that ephrins can have *vab-1*-independent functions during germline development.

Corrigan et al. (Corrigan et al., 2005) reported that UNC-43 Ca2+/calmodulin-dependent protein kinase II (CaMKII) activation, as detected by anti-phospho CamKII (pThr286, Sigma), is dependent on MSP/sperm, *vab-1*, and *nmr-1*. No staining was observed in oocytes from *unc-43(n1186)* and *unc-43(e408)* mutants (Corrigan et al., 2005). To examine the effect of endocytic recycling on *vab-1* signaling, we attempted to evaluate the effects of *rab-11.1*, *rme-1*, *dab-1*, and *ran-1* on the UNC-43 phosphorylation. I used two staining methods, the procedure used in (Corrigan et al., 2005) and the method of (Kramer et al., 1990), as modified below. I used anti-phospho CamKII antibodies purchased from Sigma and also provided by Michael Miller. Both sources of antibody produced the same staining patterns. For wild-type hermaphrodite gonads, the staining patterns I observed matched those previously reported [19], however, I also observed identical staining patterns in *unc-43(e408)* hermaphrodites, *vab-1(dx31)* hermaphrodites, *nmr-1(ak4)* hermaphrodites, and *fog-2(q71)* females, which were previously reported not to stain (Corrigan et al., 2005). The basis for this discrepancy is unclear.

Generation of Transgenic C. elegans Strains Expressing VAB-1::GFP in the Germ Line

The plasmid (pHC12-23), which encodes a C-terminal GFP fusion to VAB-1 using the *pie-1* promotor, was constructed in several steps. At each step of this and all plasmid constructions, DNA sequencing confirmed that no unwanted mutations were

introduced during site-directed mutagenesis and PCR. First, site-directed mutagenesis was used to introduce an *Asc*I restriction site in the full-length *vab-1* cDNA clone (pCZ64) near the 3' end of the gene (the *Xho*I site at genomic position 4590476) to produce pHC6-4. The primers used for site direct mutagenesis were:

CAscIF1 5'-

AGAACGACGAGACCGCCTGGCGCGCCGCGAGAAGAGGGATTCTTT-3'

and CAscIR1 5'-

AAAGAATCCCTCTTCTCGCGGCGCGCCAGGCGGTCTCGTCGTTCT-3'.

Second, a GFP coding sequence with synthetic introns was amplified by PCR from plasmid pPD9577 (a gift of Andy Fire), such that an in frame *Asc*I site was introduced at both ends, using the primers: GFPF1 5'-AAGGCGCGCCGATGAGTAAAGGAGAAGAA-3' and GFPR1 5'-AACGGCGCGCCTAGTTCATCCATGCCATG-3'. The amplified *gfp* fragment was introduced into pHC6-4 to produce pHC8-41.

Third, the VAB-1::GFP coding segment with the synthetic introns from pHC8-41 was amplified, such that *attB1* and *attB2* sites were introduced at the 5'- and 3'-ends, respectively, using primers: B1VF1 and B2VR1

5'-

GGGGACAAGTTTGTACAAAAAAGCAGGCTATACCATGCGGTTGTACAATTCG

-3'

5'-GGGGACCACTTTGTACAAGAAAGCTGGGTCTAAACAAAGAATCCCTC-3'

The Gateway recombination BP reaction was used to introduce the *attB1 vab-1::gfp attB2* fragment into the entry vector pDONR221(Invitrogen) to produce pHC10-1. Finally, *vab-1::gfp* was inserted into the *pie-1* promoter destination vector pID2.02 (a gift of Geraldine Seydoux) using the Gateway LR reaction to generate the expression clone, pHC12-23. Transgenic lines were generated by microinjection (Kelly et al., 1997) and microparticle bombardment (Praitis et al., 2001). For the generation of complex arrays, microinjections employed 60 µg/ml *Pvu*II-digested genomic DNA, 5 µg/ml *Eco*RI-digested pRF4 (Kramer et al., 1990), and 2 µg/ml *Sna*BI-digested pHC12-23. Using microinjection, six out of twenty-six transgenic lines expressed VAB-1::GFP in the germ line. One of these, *tnIs12*, was a spontaneous integrant; the site of insertion was not mapped. Using bombardment, five of five transgenic lines expressed VAB-1::GFP in the germ line. One of these, *tnIs13*, was integrated into LGV, as shown by linkage to *unc-46* and *dpy-11*.

Immunostaining and Fluorescence Microscopy

Fluorescence microscopy employed a Zeiss motorized Axioplan 2 microscope with a 63x PlanApo (NA1.4) objective lens and an apotome adaptor. Fluorescence images were acquired with an AxioCam MRm camera and Axiovision acquisition software (Zeiss). eGFP and mCherry were imaged using 49002ET and 49008ET filter sets (Chroma), respectively. All exposures were within the dynamic range of the detector and there was no cross talk between fluorophores. Pixel intensities were measured in arbitrary fluorescent units. DNA was detected with DAPI. For mRFP::RAB-7 /VAB-

1::GFP and mRFP::RAB-11/VAB-1::GFP samples, images were acquired using a Nikon Eclipse TE200 inverted microscope equipped with the PerkinElmer confocal imaging system (PerkinElmer Life and Analytical Sciences, Boston, MA), and Hamamatsu's Orca-ER digital camera with a 60X PlanApo (NA1.4) objective.

Immunohistochemistry of dissected gonad preparations was performed as described (Rose et al., 1997) except that short fixations were employed to preserve the GFP fluorescence. Briefly, gonads were dissected and fixed with 2% paraformaldehyde for 5 minutes at room temperature. Methanol post-fixation was not used, as it caused a significant loss of the GFP signal. Primary and secondary antibody (Cy3-conjugated anti-rabbit antibodies; Jackson ImmunoResearch; 1:5000) incubations were performed at room temperature for four and two hours, respectively. Antibodies used were as follows: RAB-11 and RAB-7 (Poteryaev et al., 2007); a gift of A. Spang; both used at 1:100); RAB-5 (Audhya et al., 2007; Poteryaev et al., 2007); gifts of A. Audhya and K. Oegema and A. Spang; used at 1:100); RME-1, RME-2, and EEA-1 (Sato et al., 2006; Gran et al., 2001; Grant et al., 1999); gifts from Barth grant; used at 1:50); monoclonal anti-MSP 4A5 (Kosinski et al., 2005). and monoclonal anti-Ran (Clone ARAN1, Sigma, used at 1:200 in Fig. 37D and 1:1000 overnight in Fig. 43). Staining with succinylated wheat germ agglutinin (WGA, Vector Laboratories; 25 μg/ml) was for four hours at room temperature.

Biochemical Purification of VAB-1-ICD-interacting Proteins

The VAB-1 intracellular domain (residues 583-1122) was expressed as a C-terminal fusion to Maltose-binding protein (MBP). Inclusion of the first two residues of the intracellular domain (KK, residues 581-582) resulted in proteolysis, and thus these were deleted. The VAB-ICD was amplified from pCZ64, such that *Fse*I and *Asc*I sites were introduced at the 5'- and 3'-ends, respectively. Primers used were:

VMPF2: 5'-ATTGGCCGGCCGTCGAAGAATCGGAAACAGATGAGC-3'

VMPR1: 5'-AAGGCGCGCCCTAAACAAAGAATCCCTCTTCTCGAGG-3'.

The amplified fragment was digested with *Fse*I and *Asc*I and ligated to a T7 promoter pMal-derivative (gift of Ethan Lee). The resulting plasmid, 5litcvab-1, was used for MBP-VAB-1-ICD expression in *E. coli* BL21::DE3. Four liter cultures were grown at 37°C in LB containing 100 □g/ml ampicillin to A_{600}=0.6, upon which the culture was induced with 0.5 mM IPTG for four hours. Purification of MBP-VAB-1-ICD was performed using amylose-Sepharose followed by ion-exchange chromatography on a Hitrap™ Q HP column using an AKTA Prime FPLC system (GE Healthcare). FPLC purification was required to remove degradation products produced in *E. coli*. The resulting MBP-VAB-1-ICD was approximately ~90% pure as evaluated by SDS-PAGE. Maltose-binding protein (MBP) was produced from *E. coli* containing the parent vector and purified using affinity purification. To prepare affinity resins, MBP-VAB-1-ICD (3 mg) was coupled to 2 ml of Sulfolink resin (Pierce) according to the manufacturer's instructions, and MBP (10 mg) was coupled to 4 ml CNBr-activated Sepharose 4B (GE

Healthcare). The efficiency of coupling was confirmed by SDS-PAGE analysis. For the negative control column, I used Sulfolink resin blocked with 50 mM cysteine.

Synchronized day-1 adult hermaphrodites (~30 ml of packed worm pellet) were resuspended in 1X PBS containing complete EDTA-free protease inhibitors (Roche) and 1 mM PMSF. All subsequent steps were performed at 4°C. Worms were lysed using a French Press at 16,000 psi and the lysate was centrifuged at 200,000 x g for 45 minutes. The lysate was loaded onto a MBP-Sepharose column (4 ml) equilibrated with 1 X PBS, and the flow through was loaded onto cysteine-blocked Sulfolink column. Half the flow through was loaded onto a MBP-VAB-1-ICD-Sulfolink column (2 ml; experimental column) and half was loaded onto a cysteine-blocked Sulfolink column (2 ml; control column). Both experimental and control columns were washed successively with 10 column volumes of the following buffers: 1 X PBS; 1 mM EDTA (buffer 1), followed by buffer 1; 500 mM NaCl, followed by buffer 1; 1 M NaCl, followed by 100 mM glycine pH 7.0. Bound proteins from experimental and control columns were eluted with 100 mM glycine pH 2.0 and precipitated with 5% trichloracetic acid. Peak protein fractions from the MBP-VAB-1-ICD column, as identified by SDS-PAGE and silver staining, and the corresponding fractions from the control column were trypsin-digested and identified by liquid chromatography-tandem mass spectrometry by the Vanderbilt Proteomics Laboratory in the Mass Spectrometry Research Center using the Sequest algorithm and proteins from WormBase. The non-specific background present in the experimental and control columns consisted mainly of ribosomal proteins and *E. coli* contaminants, presumably from the worm food. I recovered two tryptic peptides from RAN-1 (142-

NLQYYDISAK-153 and 153-SNYNFEKPFLWLAR-165) in the experimental column but not the control, representing 11.2% coverage of RAN-1.

Analysis of Protein-protein Interactions

Expression plasmids encoding Glutathione-S-transferase (GST) fusions to DAB-1 fragments were kindly provided by Jonathan Cooper (Kamikura and Cooper, 2006). GST-DAB-1(53-546), GST-DAB-1(53-435), GST-DAB-1(53-252), and GST were expressed in *E. coli* BL21::DE3 and purified using Glutathione-Sepharose (a gift of Ethan Lee). MBP-VAB-1-ICD (1 μg), or MBP as a negative control, were incubated with individual GST-DAB-1 protein derivatives (~1 μg), or GST as a negative control, in 100 μl volumes containing 50 mM Tris-HCl (pH 7.4); 2 mM EDTA; 150 mM NaCl; 1% NP-40, at 4°C for 2 hours. Glutathione-Sepharose (5 μl) beads were then added to the protein mixtures and incubated for 2 hours at 4°C. Complexes were isolated by centrifugation and washed three times in 1 ml of binding buffer. Western blots were probed with the following antibodies: anti-GST (a gift of Ethan Lee), anti-DAB-1 (Kamikura and Cooper, 2003), anti-MBP (New England Biolabs), and anti-VAB-1(1094-1118)E6450.

The RAN-1 coding sequence was amplified from CEORF clone K01G5.4 (OpenBiosystems) using primers RAN100F and RAN100R:

5’-GAATTCGGATCCATGTCTGGTGGAGACGGC-3’

5’-GAATTCGGATCCTTAAAGATCATCGTCGTCATC-3’

The amplified *ran-1* fragment was digested with *Bam*HI and ligated with *Bam*HI-digested pBG102 vector (provided by the Center for Structural Biology, Vanderbilt University), which provides N-terminal 6His and SUMO epitope tags. 6His-SUMO-RAN-1 and the 6His-SUMO control were expressed in *E. coli* BL21::DE3 and purified on Ni-NTA agaraose (Qiagen) according to the manufacturer's instructions. MBP-VAB-1-ICD (1 μg) or MBP were incubated with 6His-SUMO-RAN-1 (2 μg) or 6His-SUMO in a volume of 100 μl of 1 X PBS buffer at 4°C for 2 hours. Amylose-Sepharose beads (5 μl) were then added to the protein mixture and incubated at 4°C for 2 hours. Protein complexes were isolated by centrifugation and washed with 1 ml of 1 X PBS buffer three times. Western blots were probed with anti-MBP, anti-6His (Invitrogen), and anti-VAB-1.

Results

Sperm-Dependent Localization of the Oocyte MSP/Eph Receptor

To examine the localization and trafficking of the oocyte MSP/Eph receptor, I expressed VAB-1::GFP in the germ line using the germline-specific *pie-1* promoter (Fig. 34). I obtained eleven transgenic lines that express VAB-1::GFP in the germ line in identical patterns (two integrants and nine extrachromosomal arrays). To determine whether the VAB-1::GFP fusions are functional, I tested whether the oocyte meiotic maturation regulatory defects conferred by the *vab-1(dx31)* null mutation were rescued by the VAB-1::GFP in the integrated lines. Previous studies showed that VAB-1 functions as a

negative regulator of oocyte meiotic maturation in the absence of the MSP ligand (Miller et al., 2003). Oocytes arrest at meiotic prophase in the absence of MSP, and thus, *fog-2(q71)* homozygotes, which lack spermatogenesis and are therefore females, display low meiotic maturation rates (0.06 ± 0.07 maturations per gonad arm per hr; n=21; Fig. 34A) relative to that of wild-type hermaphrodites (2.64 ± 0.40 maturations per gonad arm per hr; n=18). In contrast, *vab-1(dx31); fog-2(q71)* females exhibit a moderate derepression in meiotic maturation rates (0.34 ± 0.10 maturations per gonad arm per hr, n=22, $p<0.0005$ compared to unmated females). Since expression of the VAB-1::GFP fusion in the germ line restores the tight regulation of meiotic maturation in the absence of MSP [Fig. 34A; maturation rate=0.06 ± 0.06 maturations per gonad arm per hr, n=18; $p<0.0005$ compared to *vab-1(dx31); fog-2(q71)* females; $p>0.4$ compared to *fog-2* females], I conclude that the VAB-1::GFP fusion is biologically active. I was unsuccessful in generating VAB-1-specific antibodies for immunostaining experiments despite scores of attempts (H.C., and D.G., unpublished results). Besides possessing the ability to rescue a null allele, localization of the VAB-1::GFP fusion is dependent on the *vab-1*-pathway gene *dab-1*, as described below.

The VAB-1::GFP fusion can be visualized throughout the germ line of living adult hermaphrodites (Fig. 34B). In the distal germ line, VAB-1::GFP localizes to the plasma membrane of the syncytial germ cells as visualized using an mCherry::PH domain fusion (Figures 34B and 34E and 39). Thus, the VAB-1::GFP fusion can efficiently traffic to the plasma membrane in distal germ cells.

Figure34. MSP/sperm alters the localization of the VAB-1 MSP/Eph receptor

(A) VAB-1::GFP negatively regulates meiotic maturation in the absence of MSP/sperm. Meiotic maturation rates were measured in *fog-2(q71)* female backgrounds of the indicted genotypes. (B-G) Fluorescence micrographs of VAB-1::GFP in living adult hermaphrodites (B, E), unmated *fog-2(q71)* females (C, F), MSP-injected unmated females (D), and *chc-1(RNAi)* unmated females (G), visualized in central or cortical optical sections [left and right panels, respectively (B-D)]. (E-G) The oocyte plasma membrane (middle panels) was visualized with mCherry::PH(PLC1delta1) (Kachur et al., 2008). in centrally located optical sections. The VAB-1::GFP channels and merged images are shown as indicated. Insets show magnified views of the indicated regions, showing the 0.5-1.0 μm VAB-1::GFP ring-like structures; arrows indicate the oocyte plasma membrane. Note that there is detectable VAB-1::GFP at the oocyte plasma membrane in hermaphrodites (E) and *chc-1(RNAi)* females (G). In unmated females (F), cortical VAB-1::GFP vesicles are located adjacent to the plasma membrane, and the GFP signal at the plasma membrane is below the detection limit. Hermaphrodites and MSP-injected females exhibit a decreased VAB-1::GFP signal, and twice the exposure time was used in (B, D, E) compared to (C, F, G). (H-K) Oocyte membrane proteins visualized in dissected gonad preparations of hermaphrodites (H, J) and unmated females (I, K) using anti-RME-2 antibodies (H, I) and succinylated-WGA (J, K). RME-2 localization is sperm-independent, whereas sperm cause an increase in internal WGA-staining vesicle numbers. Oocytes are numbered, with –1 denoting the most proximal oocyte. Scale bars represent 10 μm.

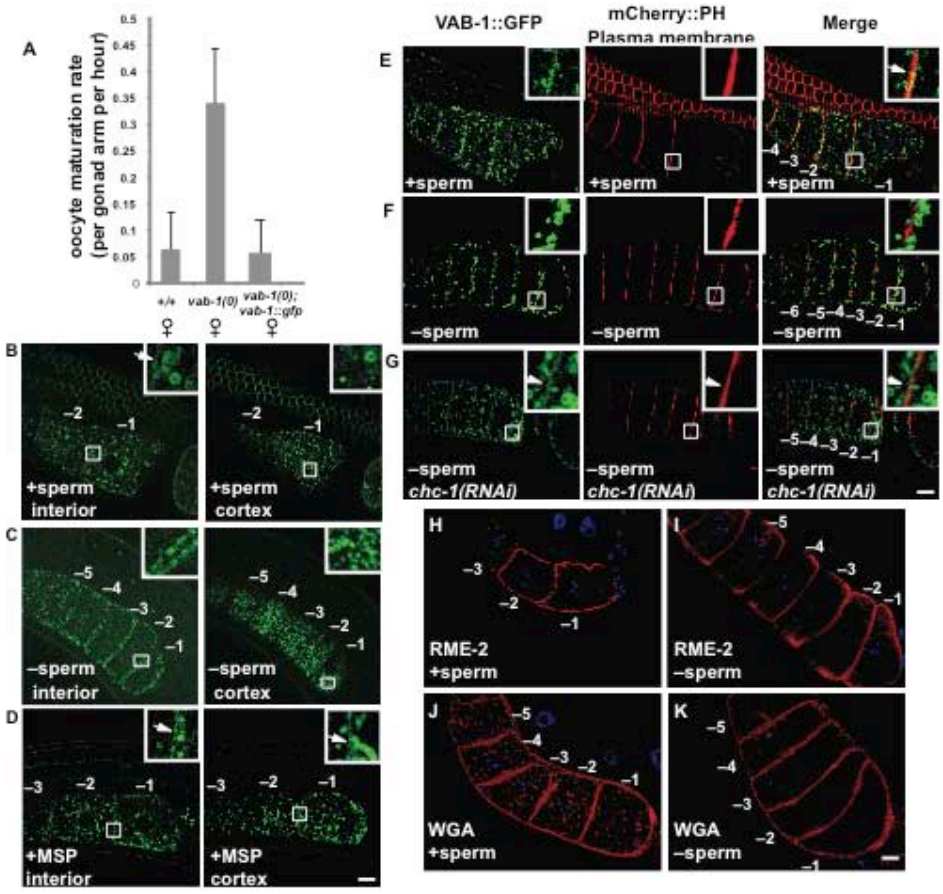
A
oocyte maturation rate (per gonad arm per hour)
0.5
0.45
0.4
0.35
0.3
0.25
0.2
0.15
0.1
0.05
0
+/+
vab-1(0)
vab-1(0); vab-1::gfp
♀
♀
♀
B
+sperm interior
+sperm cortex
C
–sperm interior
–sperm cortex
D
+MSP interior
+MSP cortex
VAB-1::GFP
mCherry::PH Plasma membrane
Merge
E
+sperm
+sperm
+sperm
F
–sperm
–sperm
–sperm
G
–sperm chc-1(RNAi)
–sperm chc-1(RNAi)
–sperm chc-1(RNAi)
H
RME-2 +sperm
I
RME-2 –sperm
J
WGA +sperm
K
WGA –sperm

The plasma membrane localization observed in the distal germ line stands in sharp contrast to the localization observed in proximal oocytes of adult hermaphrodites (Figures 34B and 34E), where it is known that MSP/Eph receptor signaling occurs antagonistically to ephrin/Eph receptor signaling (Miller et al., 2003). In proximal oocytes, VAB-1::GFP is predominantly associated with intracellular vesicles both in the interior and at the cortex (Fig. 34B). The VAB-1::GFP-containing intracellular vesicles vary in size from small puncta to large (0.5-1.0 μm diameter) ring-like structures (Figures 34B and 34E). Cortically localized VAB-1::GFP-containing vesicles abut, or are adjacent to, the plasma membrane (insets, Figures 34B and 34E), and only a small fraction of the VAB-1::GFP signal exhibits colocalization with the mCherry::PH domain plasma membrane marker (insets, Fig. 34E). In unmated *fog-2(q71)* females, VAB-1::GFP is highly enriched in cortically-localized vesicles (Figures 34C and 34F); fewer VAB-1::GFP-containing vesicles are found in the oocyte interior, and detectable levels of the VAB-1::GFP signal fail to accumulate at the plasma membrane in the steady state (insets Fig. 34F). The cortically-localized vesicles are highly enriched just beneath the plasma membrane. The mean fluorescence intensity of the VAB-1::GFP signal at the cortex was higher in females than in hermaphrodites (52.48±7.6 versus 32.14±6.16 arbitrary fluorescence units, respectively, $p<0.0005$, $n=10$). Mated female animals exhibit a VAB-1::GFP localization pattern identical to that of hermaphrodites (Table 8). Here, I analyze VAB-1::GFP localization in multiple genetic backgrounds and experimental situations, which affect either the hermaphrodite or female patterns (a summary of all the VAB-1::GFP localization patterns are found in Table 8).

To determine whether the effects of sperm were specific for VAB-1::GFP, or more general, I examined the localization of the RME-2 yolk receptor. I found that RME-2 localization, as detected in dissected and fixed gonads, was the same in the presence and absence of sperm (Figures 34and 34I). Other receptors and intracellular vesicles may respond to the presence of sperm, however, because I observed that staining with the succinylated lectin wheat germ agglutinin (WGA), which detects N-acetylglucosamine-modified structures, resulted in a markedly different staining pattern in hermaphrodites versus females. In females, oocytes exhibit cortically-enriched WGA-positive structures and reduced internal staining (compare Figures 34J and 34K). To determine whether MSP is sufficient to alter VAB-1::GFP localization, I examined the effects of injecting MSP into the uterus of unmated females. I found that injection of 200 nM MSP into unmated females (n=40) was sufficient to alter the global VAB-1::GFP localization pattern such that it resembled that observed in hermaphrodites (Fig. 34D). The effects of MSP on VAB-1::GFP localization were slow to develop, taking approximately 90 minutes. By contrast, activation of sheath cell contraction, oocyte MAPK activation, and meiotic maturation typically commence within 30-40 minutes post-injection. Since sperm continuously release MSP (Kosinski et al., 2005), the situation following MSP injection differs from that in hermaphrodites or mated females in that the MSP signal is only present transiently. Thus, the relocalization of VAB-1::GFP in oocytes could be part of a chronic response to abundant quantities of MSP/sperm. Consistent with this possibility, I observe that the VAB-1::GFP fusion exhibits progressive cortical enrichment in distal oocytes as sperm become depleted in hermaphrodites (data not shown).

Figure 35. MSP signaling affects the accumulation of VAB-1::GFP in recycling endosomes

(A-G) Fluorescence micrographs of VAB-1::GFP expression and RAB-11 staining in dissected and fixed gonads; insets in the upper right are magnified views of the oocyte cortex, and insets in the lower left are magnified views of the oocyte interior. In wild-type hermaphrodites (A), *dab-1(RNAi) fog-2(q71)* females (D), *ran-1(RNAi) fog-2(q71)* females (E), and *goa-1(RNAi) fog-2(q71)* females (G), VAB-1::GFP is largely excluded from the RAB-11-positive compartment. In *fog-2(q71)* females (B), *rme-1(b1045)* hermaphrodites (C), and *gsa-1(RNAi)* hermaphrodites (F), VAB-1::GFP accumulates in the RAB-11-positive compartment. (H) Spinning disc confocal image of mRFP::RAB-11 and VAB-1::GFP localization in living females (left panel) and hermaphrodites (right panel). Scale bars represent 10 μm.

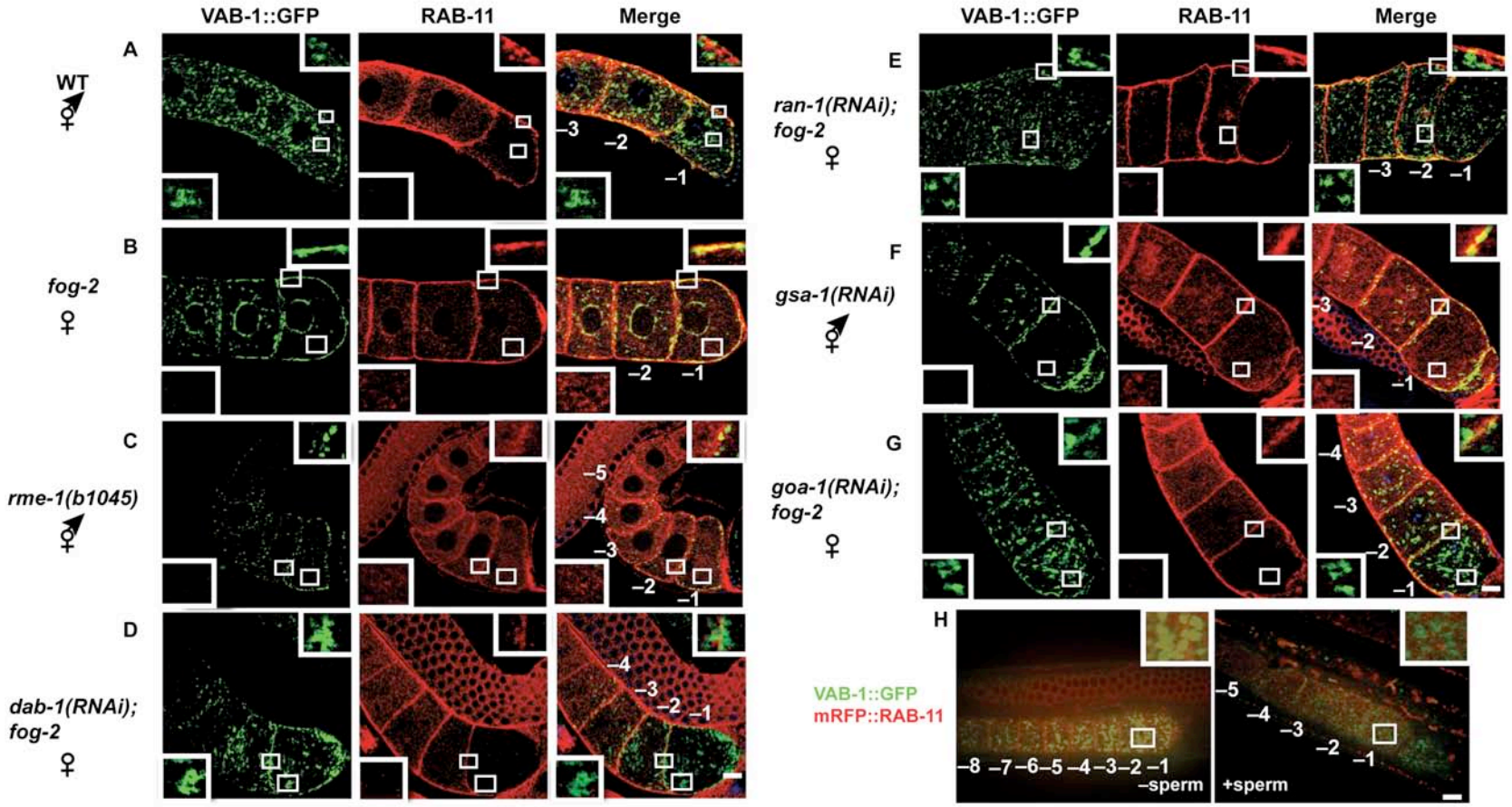
VAB-1::GFP
RAB-11
Merge
A
WT
♀
B
fog-2
♀
C
rme-1(b1045)
♀
D
dab-1(RNAi);
fog-2
♀
E
ran-1(RNAi);
fog-2
♀
F
gsa-1(RNAi)
♀
G
goa-1(RNAi);
fog-2
♀
H
VAB-1::GFP
mRFP::RAB-11
–sperm
+sperm

Figure 39. VAB-1::GFP Localization to Early Endosomes is MSP/sperm-independent

(A) VAB-1::GFP is localized to the plasma membrane in distal germ cells. The oocyte plasma membrane (middle panel) was visualized with mCherry::PH(PLC1delta1) [49]. The VAB-1::GFP and mCherry:PH channels and merged images are shown as indicated. Insets show magnified views of the distal germ cells showing co-localization of the VAB-1::GFP and mCherry::PH signals. (B-C) Fluorescence micrographs of VAB-1::GFP expression and EEA-1 staining in dissected and fixed gonads from hermaphrodites (B) and unmated females (C), visualized in cortical optical sections; insets are magnified views of the indicated regions. (D-E) Fluorescence micrographs of VAB-1::GFP and RAB-5::mCherry expression, visualized in cortical optical sections from living hermaphrodites (D) and unmated females (E); insets are magnified views of the indicated regions. A small fraction of VAB-1::GFP localizes in EEA-1-positive or RAB-5-positive structures in both the presence and absence of MSP/sperm. This result suggests that the steady-state localization of VAB-1::GFP to early endosomes is MSP/sperm independent. We observed no overlap between VAB-1::GFP and EEA-1 or RAB-5::mCherrry in the oocyte interior (data not shown). (F-G) Spinning disc confocal fluorescence micrographs of VAB-1::GFP and mRFP::RAB-7 expression, visualized in interior optical sections from living hermaphrodites (F) and unmated females (G). The mRFP::RAB-7 expression signal exhibits a uniform distribution pattern in oocytes irrespective of the presence of sperm. There is no evidence for enrichment of RAB-7 at sites of VAB-1::GFP accumulation. Similar results were obtained using anti-RAB-7 antibodies (data not shown). Scale bars represent 10 μm.

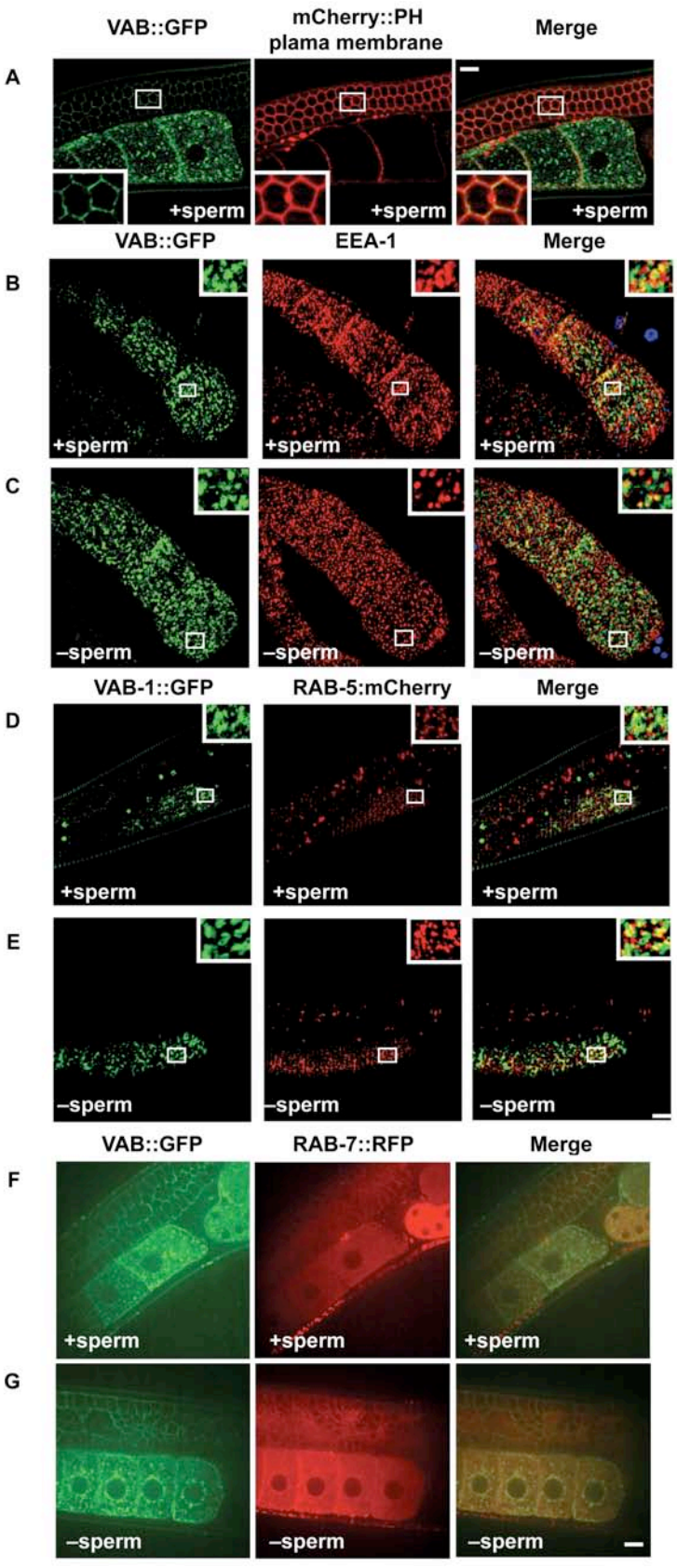
VAB::GFP
mCherry::PH
plama membrane
Merge
A
+sperm
+sperm
+sperm
VAB::GFP
EEA-1
Merge
B
+sperm
+sperm
+sperm
C
–sperm
–sperm
–sperm
VAB-1::GFP
RAB-5:mCherry
Merge
D
+sperm
+sperm
+sperm
E
–sperm
–sperm
–sperm
VAB::GFP
RAB-7::RFP
Merge
F
+sperm
+sperm
+sperm
G
–sperm
–sperm
–sperm

Taken together, these data suggest that the presence of MSP alters VAB-1::GFP trafficking, which could be part of the mechanism by which the continued presence of MSP promotes high rates of meiotic maturation.

VAB-1::GFP is Enriched in the Endocytic Recycling Compartment in the Absence of Sperm

To address the possibility that the sperm-dependent changes in VAB-1::GFP localization might reflect alterations in vesicle trafficking, I used antibodies against RAB-5 (Audhya et al., 2007) and EEA-1 (Sato et al., 2006), RAB-7 (Poteryaev et al., 2007), and RAB-11 (Poteryaev et al., 2007) as markers for early, late, and recycling endosomes, respectively, and asked whether the VAB-1::GFP vesicles might be associated with any of these compartments. (Figures 35 and 39). In unmated females, I observed that VAB-1::GFP and RAB-11 exhibited extensive co-localization at the cortex (Fig. 35B). By contrast, I observed that only a small fraction of the VAB-1::GFP-containing vesicles stained positively for RAB-11 in the presence of sperm (Fig. 35A). I obtained similar results using mRFP::RAB-11 and VAB-1::GFP (Fig. 35H). I did note, however, that the fraction of VAB-1::GFP vesicles that stained positively for RAB-11 increased in more distally localized oocytes (Fig. 35A and data not shown), which are exposed to lower extracellular MSP levels (Kosinski et al., 2005).

I considered the possibility that VAB-1::GFP traffics to the plasma membrane from recycling endosomes in the absence of MSP/sperm but is cleared by endocytosis. Consistent with this possibility, a detectable fraction of the VAB-1::GFP signal at the oocyte cortex exhibits co-localization with the early endocytic markers EEA-

1 and RAB-5 in both the absence and presence of MSP/sperm (Fig. 39). Endocytosis occurs via clathrin-dependent and -independent mechanisms. Thus, I tested whether knocking down the expression of the clathrin heavy chain using RNAi affects VAB-1::GFP localization. When I conducted *chc-1(RNAi)* in a *fog-2(q71)* female background, I observed modest but detectable levels of VAB-1::GFP at the plasma membrane (inset, Fig. 34G), suggesting that VAB-1::GFP can traffic to the plasma membrane in the absence of sperm but is cleared by endocytic processes. Because caveolin has been implicated in endocytic processes (Hommelgaard et al., 2005) and CAV-1::GFP is associated with vesicles in *C. elegans* oocytes (Sato et al., 2006), I analyzed VAB-1::GFP localization in the *cav-1(ok2089)* deletion allele that removes the entire coding sequence of the caveolin-1 homolog. I observed that the localization of VAB-1::GFP was not affected by *cav-1(ok2089)* in the presence of sperm (Table 8). Since RAB-7 exhibits a uniform staining pattern in oocytes in the presence and absence of sperm, when visualized either by anti-RAB-7 antibody staining or using a mRFP::RAB-7 fusion, the co-localization studies were less informative using this marker (Fig. 39 and data not shown). I have not been able to address whether VAB-1::GFP might traffic to lysosomes in the presence of sperm because lysotracker-Red-staining methods are not effective in oocytes. I observed no apparent change in VAB-1::GFP localization in the presence or absence of sperm following RNAi to *vps-28* and *vps-37*, which encode components of the endosomal sorting complex required for transport-I complex that mediates lysosomal degradation of ubiquitinated proteins (Fig. 40). I did note, however, that *vps-28(RNAi)* and *vps-37(RNAi)* delayed VAB-1::GFP degradation in embryos (Fig. 41).

Figure 40. Localization of VAB-1::GFP in hermaphrodites is regulated by *rab-11.1* and *rme-1*

(A-E) Fluorescence micrographs of VAB-1::GFP expression in the following genotypes and experimental situations: *rab-11.1(RNAi)* by injection (A); *rme-1(b1045)* (B); *dab-1(gk291)* (C); *vps-28(RNAi)* (D); *vps-37(RNAi)* (E). Hermaphrodites and unmated females were examined (left, and right panels, respectively). Scale bars represent 10 μm.

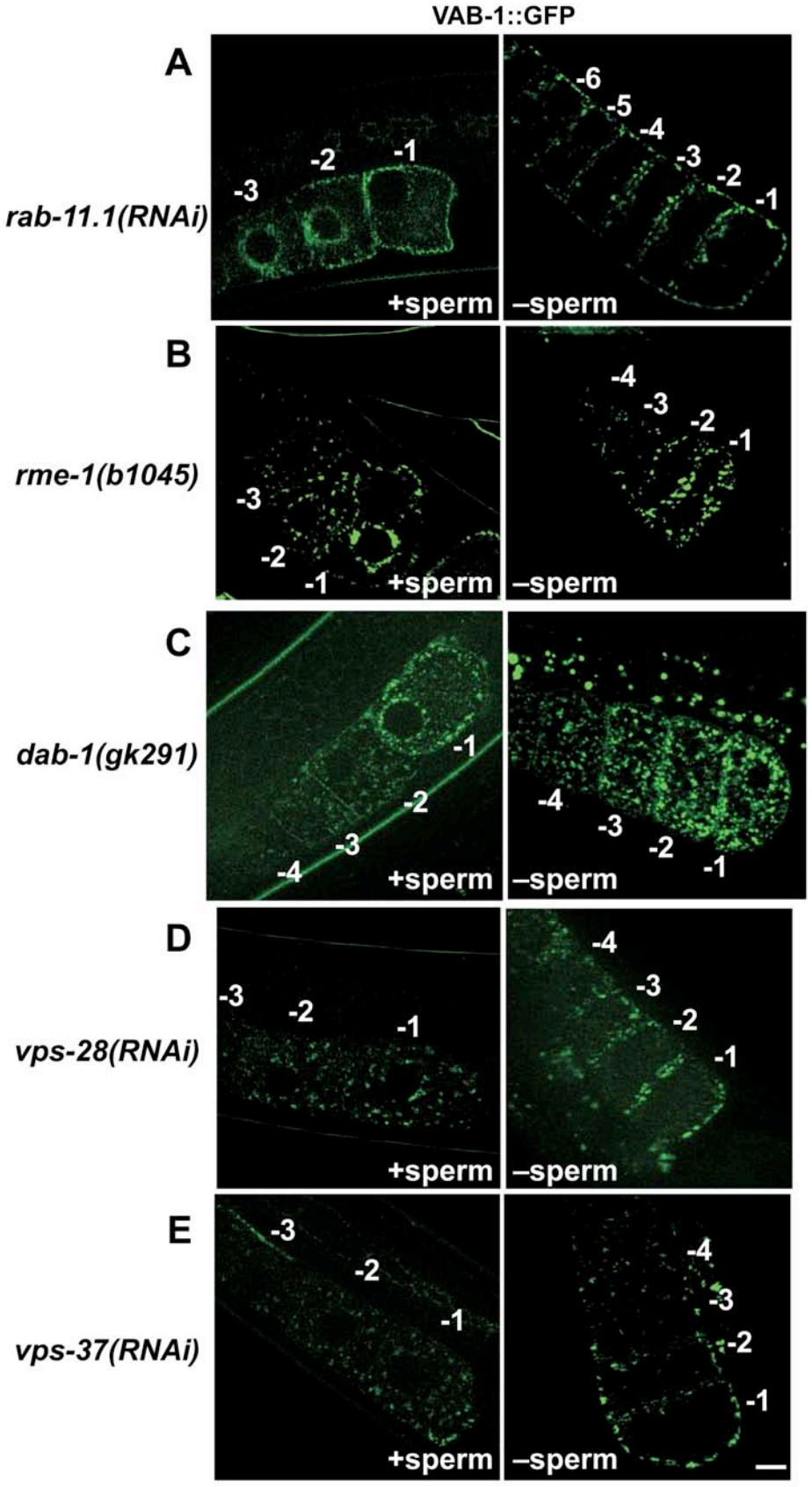
VAB-1::GFP
A
rab-11.1(RNAi)
-3
-2
-1
+sperm
-6
-5
-4
-3
-2
-1
–sperm
B
rme-1(b1045)
-3
-2
-1
+sperm
-4
-3
-2
-1
–sperm
C
dab-1(gk291)
-4
-3
-2
-1
+sperm
-4
-3
-2
-1
–sperm
D
vps-28(RNAi)
-3
-2
-1
+sperm
-4
-3
-2
-1
–sperm
E
vps-37(RNAi)
-3
-2
-1
+sperm
-4
-3
-2
-1
–sperm

Figure 41. *vps-28* and *vps-37* promote VAB-1::GFP degradation in the embryo

Fluorescence micrographs of VAB-1::GFP expression in embryos. The wild-type embryos VAB-1::GFP signal is not apparent after the 4-cell stage. Both *vps-28(RNAi)* and *vps-37(RNAi)* cause VAB-1::GFP to accumulate in large foci that persist in embryos beyond the 16-cell stage. Scale bars represent 10 μm.

Wild type

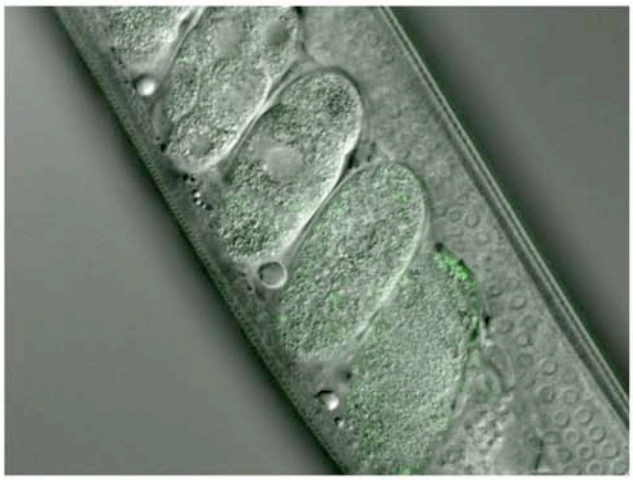

vps-28(RNAi)

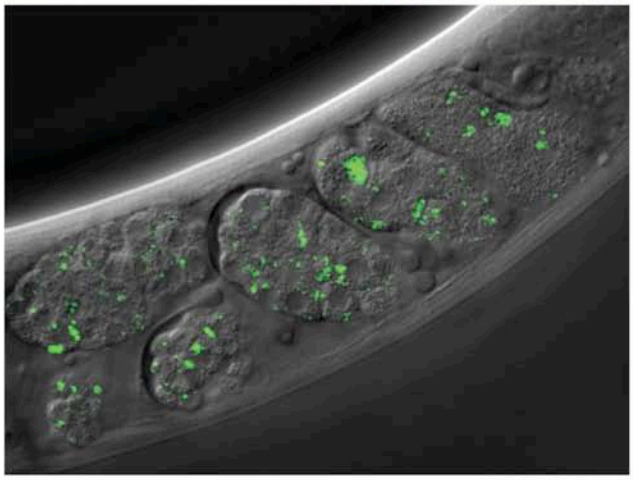

vps-37(RNAi)

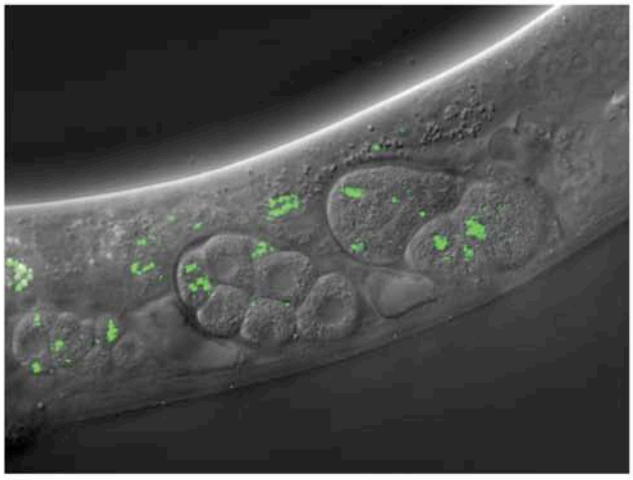

The finding that VAB-1::GFP is enriched in a RAB-11-positive compartment in the absence of sperm raises the possibility that a recycling receptor may be functional in inhibiting oocyte meiotic maturation when MSP is absent. This hypothesis has two key predictions: first, promotion of VAB-1 localization to the endocytic recycling compartment in hermaphrodites should reduce the meiotic maturation rate; and second, genes required for VAB-1 localization to the endocytic recycling compartment in the absence of MSP/sperm should function as negative regulators of oocyte meiotic maturation. Both these predictions have been met. To test the first prediction, I examined *rme-1(b1045)* mutants (the second prediction is tested below). *rme-1* encodes a conserved Eps-15 homology domain-containing protein that is required for normal endocytic recycling in *C. elegans* and mammalian cells (Grant et al., 2001; Lin et al., 2001). In unmated females, RME-1 localizes to the oocyte cortex between the plasma membrane and the cortically-localized VAB-1::GFP vesicles (data not shown). The VAB-1::GFP localization patterns were similar in *rme-1(b1045)* hermaphrodites and females, both resembling the normal female pattern (Fig. 40 and Table 8). Interestingly, in *rme-1(b1045)* mutant hermaphrodites, the VAB-1::GFP and RAB-11 fluorescence signals exhibit an increased overlap at the cortex in comparison to wild-type hermaphrodites (Fig. 35A and 35C). By contrast, the global localization of vesicle-associated proteins, as detected by WGA staining, is unaffected (Fig. 36A and 36C). To examine whether this altered localization might have functional consequences, I measured the oocyte meiotic maturation rate in *rme-1(b1045)* mutant hermaphrodites. I found that *rme-1(b1045)* mutant hermaphrodites display lower oocyte meiotic maturation rates than wild-type hermaphrodites (1.67 ± 0.35 maturations per gonad arm per hr, n=19,

versus 2.64 ± 0.40, n=18, p<0.0005). I tested the possibility that the reduction in meiotic maturation rate in *rme-1(b1045)* hermaphrodites might be caused by a defect in sperm recruitment to the spermatheca (sperm-storage compartment), as this has been observed in mutants defective for the *rme-2* yolk receptor (Kubagawa et al., 2006). This is unlikely to be the case because I observed normal sperm retention in the spermathecae of *rme-1(b1045)* adult hermaphrodites (Fig. 42). In addition, I observed a normal distribution of extracellular MSP within the spermatheca (Fig. 42). Importantly, *vab-1(dx31); rme-1(b1045)* double mutant hermaphrodites exhibit meiotic maturation rates similar to those of *vab-1(dx31)* hermaphrodites (2.05 ± 0.45, n=20; and 2.01 ± 0.23 maturations per gonad arm per hr, n=21, respectively), which are both higher than *rme-1(b1045)* single mutants (p<0.005). Similarly, *dab-1(RNAi)* in an *rme-1(b1045)* mutant background increases the oocyte meiotic maturation rate (data not shown). To further investigate the role of VAB-1 trafficking in the regulation of oocyte meiotic maturation, I used RNAi to deplete *rab-11.1*, which is required for receptor recycling to the plasma membrane from recycling endosomes, and also for trafficking from the trans-Golgi network to the plasma membrane (Sato et al., 2008). RNAi of *rab-11.1* in a hermaphrodite background resulted in a cortical enrichment of VAB-1::GFP resembling that observed in unmated females (Fig. 40). By contrast, *rab-11.1(RNAi)* did not alter VAB-1::GFP localization in unmated females (Fig. 40). In hermaphrodites, *rab-11.1(RNAi)* caused a reduction in the meiotic maturation rate (1.18 ± 0.65 maturations per gonad arm per hr, n=23) compared to the RNAi control (2.41 ± 0.55 maturations per gonad arm per hr, n=20; p<0.0005).

Figure 42. Spermatozoa localize to the spermatheca and release MSP in *rme-1(b1045)* mutants

DIC micrograph of a *rme-1(b1045)* hermaphrodite (top panel); the inset shows spermatozoa in the spermatheca. MSP visualized in the spermatheca (SP) of a *rme-1(b1045)* hermaphrodite using immunofluorescence (bottom panels); spermatozoa stain intensely and extracellular MSP fills the spermathecal lumen surrounding the spermatozoa. Scale bars represent 10 μm.

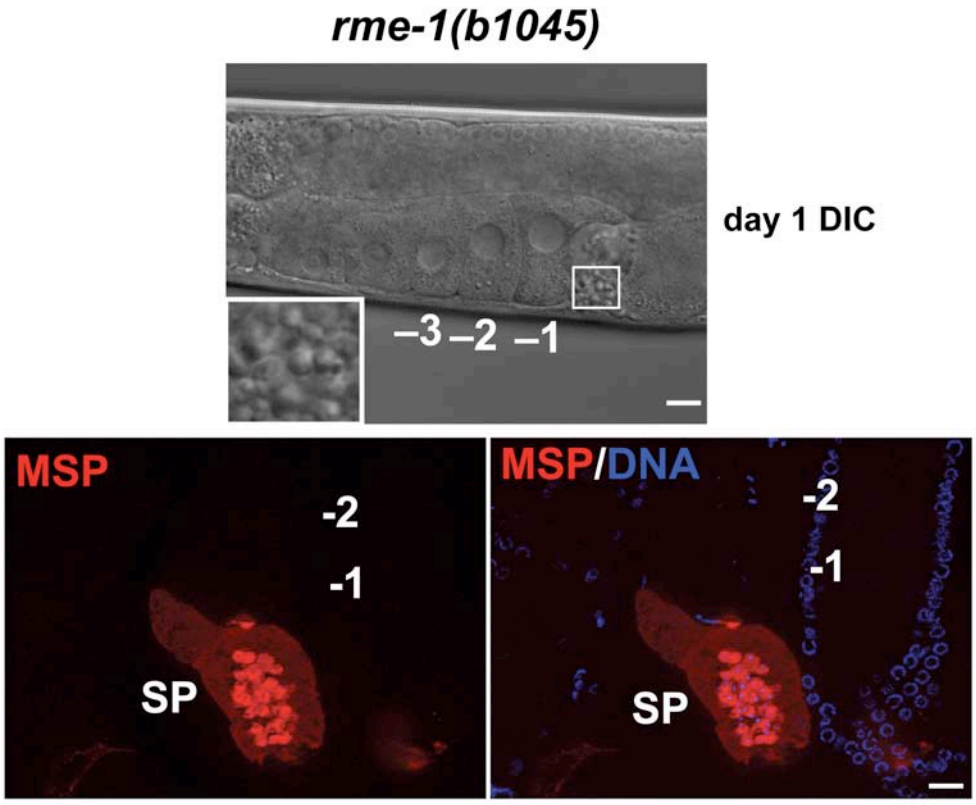
rme-1(b1045)
day 1 DIC
–3 –2 –1
MSP
-2
-1
SP
MSP/DNA
-2
-1
SP

By contrast, *rab-11.1(RNAi)* in *vab-1(dx31)* hermaphrodites had no effect on the meiotic maturation rate (2.01 ± 0.67 maturations per gonad arm per hr, n=20, compared to 2.03 ± 0.42 maturations per gonad arm per hr, n=20 in the RNAi control; p> 0.4). Taken together, these data show that interfering with efficient receptor exit from the endocytic recycling compartment causes a *vab-1*-dependent reduction in the oocyte meiotic maturation rate in hermaphrodites.

DAB-1/Disabled and RAN-1, but not Ephrins, Regulate VAB-1::GFP Trafficking in the Absence of Sperm

To determine whether negative regulators of oocyte meiotic maturation affect VAB-1 localization to the endocytic recycling compartment in females, I began by analyzing genes in the *vab-1* arm of the meiotic maturation signaling pathway. Since ephrin binding can trigger Eph receptor endocytosis in mammalian cells (Cowan et al., 2005), I first asked whether VAB-1::GFP localization is ephrin dependent. *C. elegans* has four ephrin genes (*efn-1*, *efn-2*, *efn-3*, and *efn-4*), but only *efn-1*, *efn-2*, and *efn-3* have been implicated in *vab-1* signaling (Chin-Sang et al., 1999; Wang et al., 1999). By contrast, *efn-4* has been shown to function in semaphorin signaling (Chin-Sang et al., 2002; Ikegami et al., 2004). I analyzed *efn-1(ju1) efn-2(ev658)*; *efn-3(ev696)* triple mutant females and hermaphrodites and found that the VAB-1::GFP localization pattern was unchanged (Fig. 43). Since *efn-4(RNAi)* in these strains led to no further changes in VAB-1::GFP localization (Fig. 43), I conclude that VAB-1::GFP localization in oocytes is ephrin independent; however, I cannot exclude the possibility that VAB-1 trafficking depends on uncharacterized non-ephrin ligands in the absence of sperm.

Previously, I identified *dab-1* as a negative regulator of oocyte meiotic maturation and presented genetic data that are consistent with the interpretation that *vab-1* and *dab-1* function in a common pathway to negatively regulate meiotic maturation in the absence of sperm (Govindan et al., 2006). I analyzed VAB-1::GFP localization following *dab-1(RNAi)* and in *dab-1(gk291)* null mutants in female and hermaphrodite backgrounds. I observed that VAB-1::GFP was no longer enriched in a RAB-11-positive compartment following *dab-1(RNAi)* in a female background (Fig. 35D). The VAB-1::GFP pattern in *dab-1(RNAi)* females resembled that seen in wild-type hermaphrodites with the majority of vesicles localizing in the interior of the oocyte and a small fraction on the plasma membrane (Fig. 35A and 35D). The same result was obtained using *dab-1(gk291)* mutant females (Fig. 40). By contrast, I observed no change in the VAB-1::GFP pattern in *dab-1(RNAi)* or *dab-1(gk291)* hermaphrodites, compared to wild-type hermaphrodites (Fig. 36A and 36E and Fig. 40). Thus, *dab-1* is only required for VAB-1::GFP trafficking in a female background in which the majority of the receptor is recycling. Because *dab-1* and Disabled homologs have been implicated in vesicle trafficking and endocytosis (Morris et al., 2001; Kamikura and Copper 2003; 2006), I examined the effects of *dab-1* on the global localization of vesicle-associated proteins using succinylated-WGA staining. I observed that *dab-1(RNAi)* did not affect the localization of WGA-staining vesicles in the presence or absence of sperm (Fig. 36D and 36E). Interestingly, the VAB-1::GFP vesicles are WGA-negative following *dab-1(RNAi)* only in the absence of sperm (compare Fig. 36D and 36E), suggesting that DAB-1 plays a critical role in promoting the female mode of VAB-1::GFP trafficking.

Figure 43. Localization of VAB-1::GFP is ephrin-independent

(A-E) Fluorescence and DIC micrographs of VAB-1::GFP expression in the following genotypes: *efn-1(ju1) efn-(ev658)2; efn-3(ev696)* triple mutant hermaphrodite (A); *efn-1(ju1) efn-2(ev658); efn-3(ev696); fog-2(q71)* female (B); *efn-1(ju1) efn-2(ev658); efn-3(ev696); efn-4(RNAi)* hermaphrodite (C); *efn-1(ju1) efn-2(ev658);efn-3(ev696); efn-4(RNAi); fog-2(q71)* female (D); and a *mpk-1(ga111*ts*)* hermaphrodite (E). Scale bars represent 10 μm.

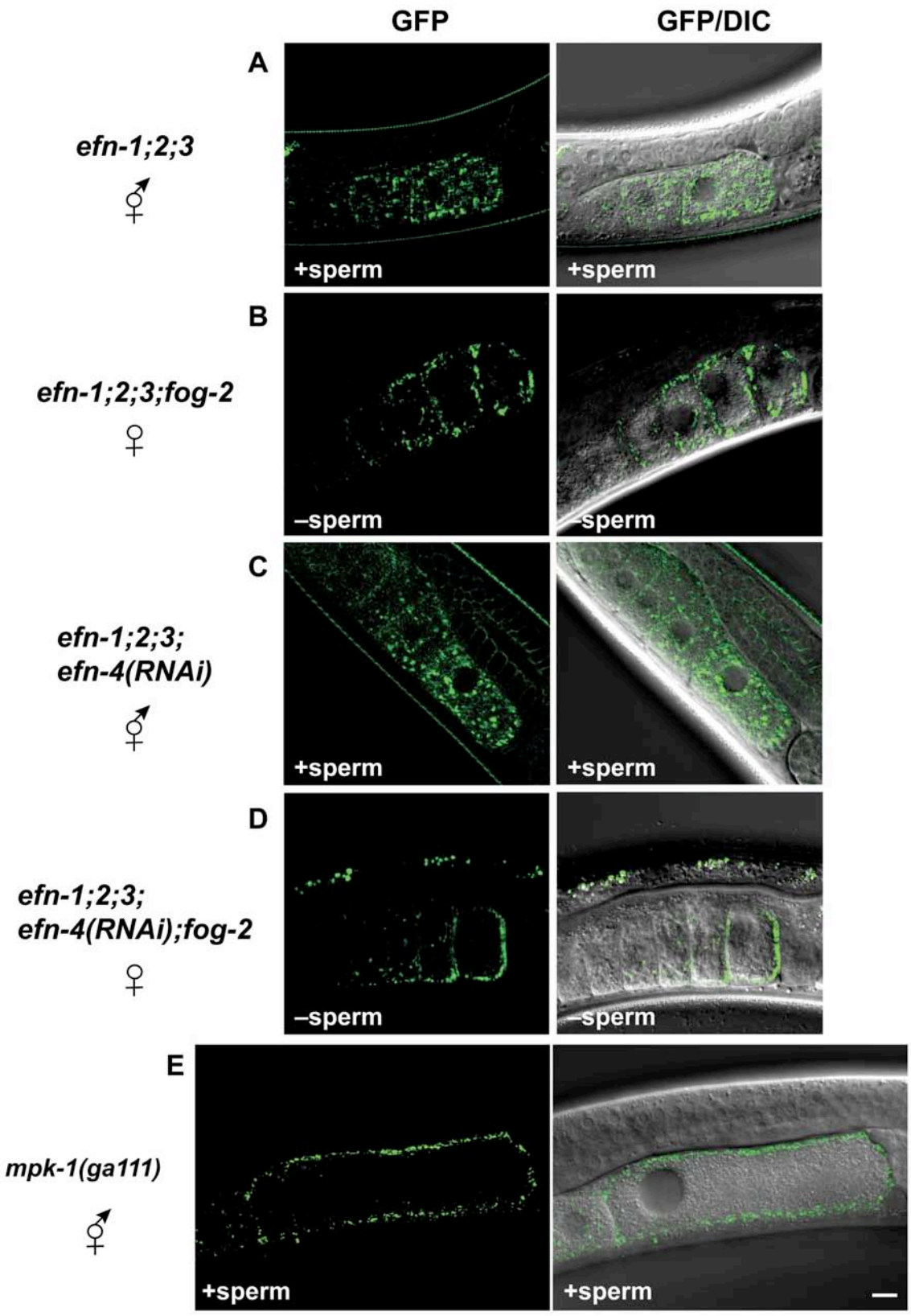
GFP
GFP/DIC
A
efn-1;2;3
♀♂
+sperm
+sperm
B
efn-1;2;3;fog-2
♀
–sperm
–sperm
C
efn-1;2;3;
efn-4(RNAi)
♀♂
+sperm
+sperm
D
efn-1;2;3;
efn-4(RNAi);fog-2
♀
–sperm
–sperm
E
mpk-1(ga111)
♀♂
+sperm
+sperm

Figure 36. DAB-1 and RAN-1 affect VAB-1::GFP trafficking in the absence of MSP/sperm

(A-H) Fluorescence micrographs of VAB-1::GFP expression and WGA staining in dissected and fixed gonads; insets in the upper right are magnified views of the oocyte cortex and insets in the lower left are magnified views of the oocyte interior. VAB-1::GFP mainly localizes to WGA-positive vesicles in wild-type hermaphrodites (A), *fog-2(q71)* females (B), *rme-1(b1045)* hermaphrodites (C), *dab-1(RNAi)* hermaphrodites (E), *gsa-1(RNAi)* hermaphrodites (G), and *goa-1(RNAi) fog-2(q71)* females (H). In contrast, VAB-1::GFP extensively localizes to WGA-negative vesicles in *dab-1(RNAi) fog-2(q71)* females (D) and *ran-1(RNAi) fog-2(q71)* females (F). Scale bars represent 10 μm.

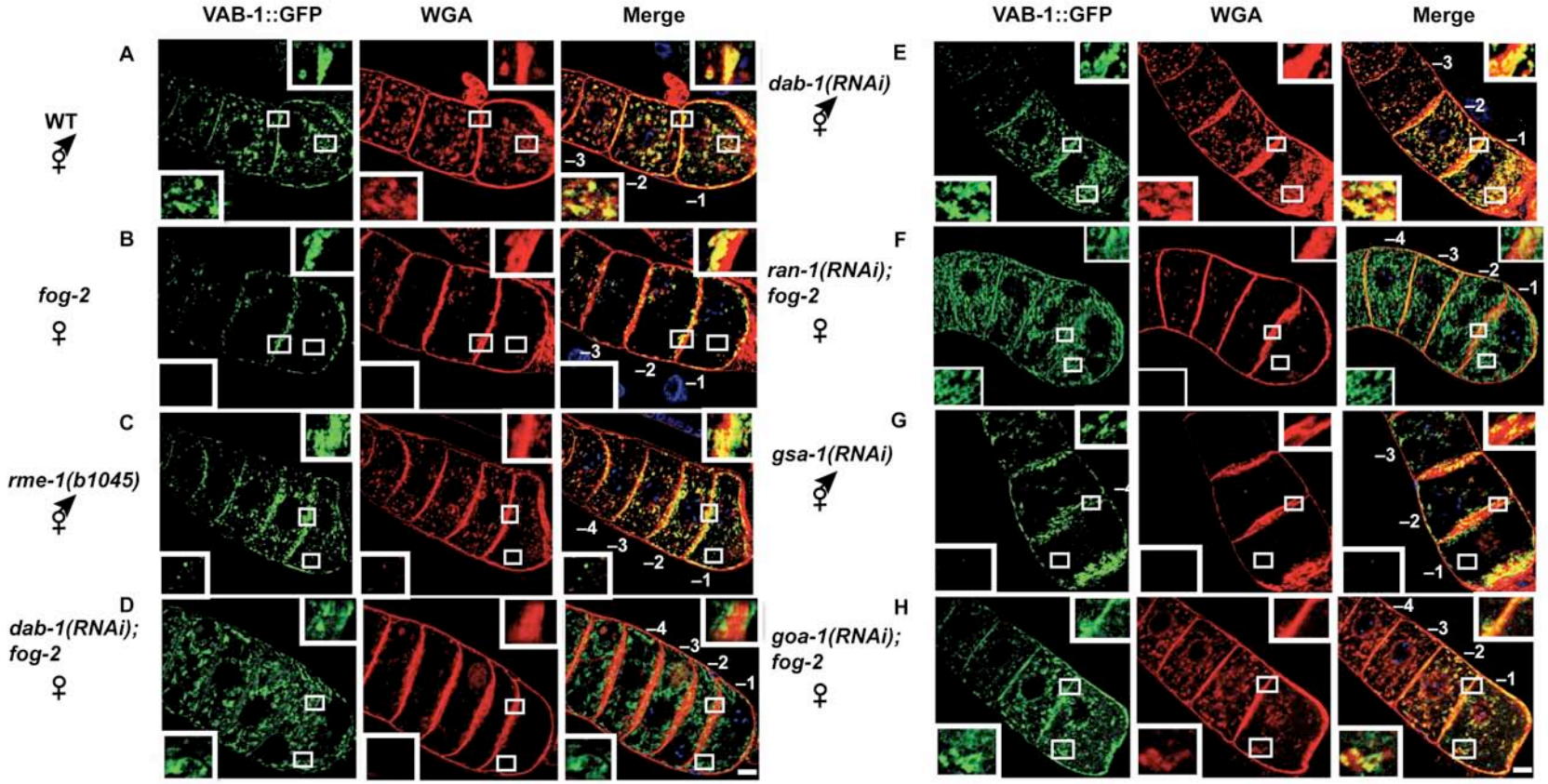
VAB-1::GFP
WGA
Merge
A
WT
♀
B
fog-2
♀
C
rme-1(b1045)
♀
D
dab-1(RNAi);
fog-2
♀
E
dab-1(RNAi)
♀
F
ran-1(RNAi);
fog-2
♀
G
gsa-1(RNAi)
♀
H
goa-1(RNAi);
fog-2
♀
–4
–3
–2
–1

Taken together, these results suggest that *dab-1* is specifically required for VAB-1::GFP to localize to the endocytic recycling compartment in the absence of MSP/sperm. Moreover, when *dab-1* function is disrupted in the absence of sperm, VAB-1::GFP accumulates in an interior vesicular compartment with different characteristics as assessed by WGA staining.

Prior work has shown that the PTB domain of Disabled proteins can bind the intracellular domain of receptor proteins and serve as adaptors (Howell et al., 1999). Thus I examined whether DAB-1 could interact with the VAB-1 intracellular domain (VAB-1-ICD) in vitro. I expressed and purified VAB-1-ICD as an amino-terminal fusion to the maltose binding protein (MBP-VAB-1-ICD) and performed pull-down experiments using DAB-1(53-546) fused to glutathione S-transferase. I found that GST-DAB-1(53-546) can interact with MBP-VAB-1-ICD but not with MBP (Fig. 37A). By contrast, GST does not interact with MBP-VAB-1-ICD (Fig. 37A). Two additional DAB-1-deletion derivatives, GST-DAB-1(53-435) and GST-DAB-1(53-252), also bind MBP-VAB-1-ICD in vitro (data not shown). The DAB-1 PTB domain binds FxNPxY motifs in the intracellular domain of receptors. The VAB-1-ICD has a related motif (GLNHVY), but I have not determined whether this motif is critical for *vab-1* function or DAB-1 binding.

Our prior work suggested that PKC-1, a protein kinase C homolog, PQN-19, a STAM homolog, and VAV-1, a Rho family guanine-nucleotide exchange factor, may function in the *vab-1* pathway to inhibit meiotic maturation when MSP is absent (Govindan et al., 2006). I did not observe any VAB-1::GFP localization changes after *pkc-1(RNAi)*, *pqn-19(RNAi)*, or *vav-1(RNAi)* in females or hermaphrodites (Table 8).

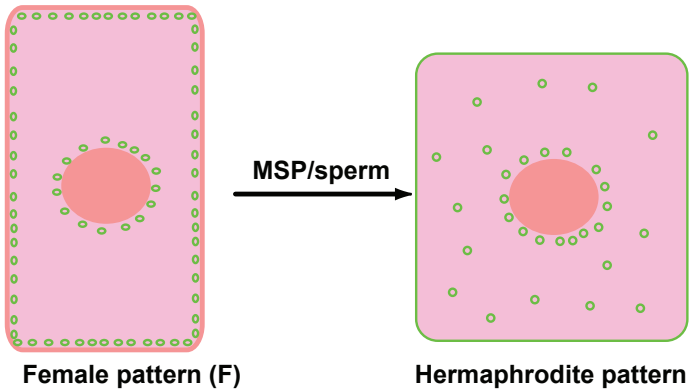

Table 8. Summary of VAB-1::GFP localization patterns

Relevant genotype or experimental treatment[a]	VAB-1::GFP localization pattern in female background[b]	VAB-1::GFP localization pattern in hermaphrodite background
Wild type	F[c-e]	H
Mated female	H[c]	N.A.
cav-1(ok2089)	N.D.	H
Wild type, MSP injection	H[c, d]	N.D.
rme-1(b1045)	F[d]	F
rab-11.1 (RNAi) injection	F[d]	F
vps-28(RNAi)	F[d]	H[f]
vps-37(RNAi)	F[d]	H[f]
efn-1(ju1);efn-2(ev658);efn-3(ev696)	F[c]	H
efn-1(ju1);efn-2(ev658);efn-3(ev696);efn-4(RNAi)	F[c]	H
dab-1(RNAi)	H[c, d, g]	H
dab-1(gk291)	H[c, g]	H
pkc-1(RNAi)	F[c, d]	H
pqn-19(RNAi)	F[c, d]	H
vav-1(RNAi)	F[c, d]	H
ran-1(RNAi)	H[c, d, g]	H
goa-1(RNAi)	H[c, d]	H
inx-22(RNAi)	H[c, d]	H
inx-14(RNAi)	H[c]	H
kin-2(RNAi)	H[c]	H
gsa-1(RNAi)	F[c]	F
oma-1(RNAi);oma-2(RNAi)	N.D.	F
*mpk-1(ga111*ts*)*	N.D.	F

[a]All strains contained *tnIs13*
[b]*fog-2(q71)*, *fog-2(oz40)*, *fog-3(q443)*, *fog-1(q253*ts*)*, or *fem-1(hc17*ts*)* as indicated.
[c]*fog-2(q71)* females were analyzed.
[d]*fog-3(q443)* females were analyzed.
[e]*fog-2(oz40)*, *fog-1(q253*ts*)*, and *fem-1(hc17*ts*)* were also analyzed.
[f]VAB-1::GFP degradation in embryos is delayed.
[g]The VAB-1::GFP-containing compartment is WGA negative.
N.A., not applicable; N.D., not determined.

Figure 37. DAB-1 and RAN-1 bind to the VAB-1 intracellular domain

(A) In vitro interaction of GST-DAB-1(53-546) and MBP-VAB-1-ICD. Complexes were isolated using Glutathione Sepharose. MBP and GST served as negative controls. Western blots were probed with anti-MBP (top panel) and anti-GST (middle and bottom panels). The bottom panel shows the position of GST and breakdown products of GST-DAB-1(53-546). (B) Biochemical purification of VAB-1-ICD-interacting proteins. A flow chart depicts the purification strategy starting with 30 ml of packed adult hermaphrodites. The bottom panel shows the sequence of RAN-1 tryptic peptides that were retained on the MBP-VAB-1-ICD column at high stringency, but were absent from the empty column control. (C) In vitro interaction of 6His-SUMO-RAN-1 and MBP-VAB-1-ICD. Complexes were isolated using Amylose Sepharose. 6His-SUMO and MBP served as negative controls. Western blots were probed with anti-6His (top panel) and anti-MBP (middle and bottom panels). The bottom panel shows the position of MBP and breakdown products of MBP-VAB-1-ICD. (D) Cortical views of VAB-1::GFP expression and RAN-1 staining in dissected and fixed gonads from female (upper panel) and hermaphrodite animals (lower panel); insets in the upper left are magnified views of the indicated regions. Scale bars represent 10 μm.

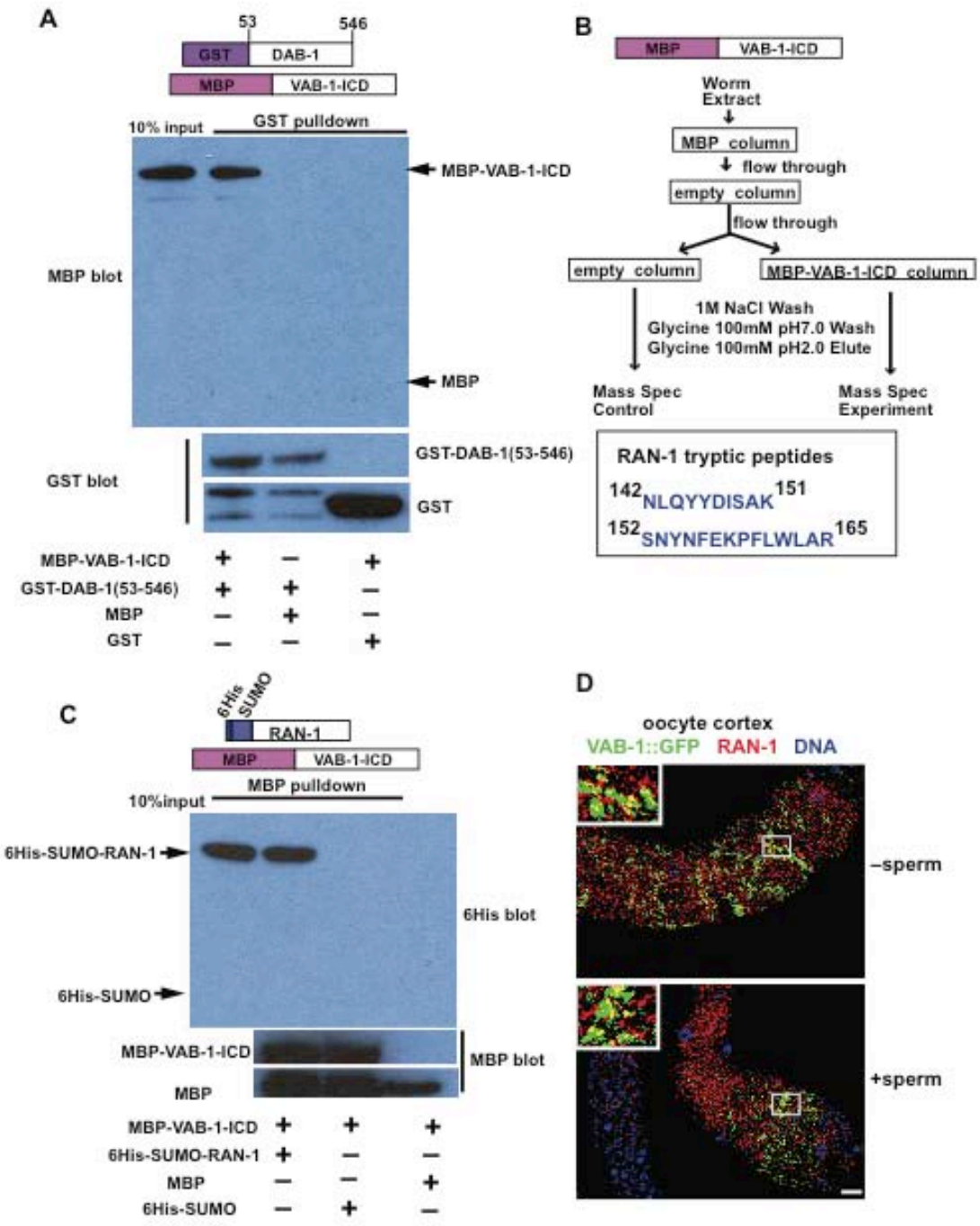
A
53
546
GST
DAB-1
MBP
VAB-1-ICD
10% input
GST pulldown
MBP-VAB-1-ICD
MBP blot
MBP
GST-DAB-1(53-546)
GST blot
GST
MBP-VAB-1-ICD + − +
GST-DAB-1(53-546) + + −
MBP − + −
GST − − +
B
MBP
VAB-1-ICD
Worm Extract
MBP column
flow through
empty column
flow through
empty column
MBP-VAB-1-ICD column
1M NaCl Wash
Glycine 100mM pH7.0 Wash
Glycine 100mM pH2.0 Elute
Mass Spec Control
Mass Spec Experiment
RAN-1 tryptic peptides
142 NLQYYDISAK 151
152 SNYNFEKPFLWLAR 165
C
6His SUMO
RAN-1
MBP
VAB-1-ICD
MBP pulldown
10%input
6His-SUMO-RAN-1
6His blot
6His-SUMO
MBP-VAB-1-ICD
MBP blot
MBP
MBP-VAB-1-ICD + + +
6His-SUMO-RAN-1 + − −
MBP − − +
6His-SUMO − + −
D
oocyte cortex
VAB-1::GFP RAN-1 DNA
−sperm
+sperm

Thus, these three genes might influence *vab-1* signaling in a manner not dependent on trafficking, as apparent by examination of the VAB-1::GFP localization pattern.

I sought new regulators of VAB-1::GFP trafficking using affinity purification of VAB-1-ICD-interacting proteins (Fig. 37B). I reasoned that proteins that bind to VAB-1-ICD at high stringency [retained by 1M NaCl, but not 0.1 M glycine pH(2.0)] might function in VAB-1 signaling or trafficking. Using this method, I specifically recovered two peptides from RAN-1 (Fig. 5B, 11.2% coverage) in the mass spectrometry data from the MBP-VAB-1-ICD column but not the control.The non-specific background largely consisted of ribosomal proteins. Consistent with these data, RAN-1 binds the MBP-VAB-1-ICD but not the MBP control in pull-down assays (Fig. 37C). Previously, We identified *ran-1* as a negative regulator of oocyte meiotic maturation that functions in the germ line (Govindan et al., 2003). Because *ran-1* is an essential gene that functions in many processes, including nucleocytoplasmic transport and microtubule dynamics and organization (Joseph, 2006), I used RNAi to analyze interactions with other negative regulators of meiotic maturation. These data were consistent with the possibility that *ran-1* functions in *vab-1*-dependent and -independent pathways (Govindan et al., 2003). I examined VAB-1::GFP localization following *ran-1(RNAi)* in female and hermaphrodite genetic backgrounds. In these analyses, *ran-1* behaved similarly to *dab-1*: I observed reduced overlap between VAB-1::GFP and RAB-11 at the oocyte cortex in the absence of sperm (Fig. 35E); and VAB-1::GFP localized to an interior WGA-negative compartment (Fig. 36F). By contrast, *ran-1(RNAi)* had no apparent effect on VAB-1::GFP localization and trafficking in hermaphrodites (Table 8). Antibodies raised to the C-terminus of human RAN specifically detect *C. elegans* RAN-1 in immuno-staining

experiments (Fig. 44). I used these antibodies to compare the localization of RAN-1 and VAB-1::GFP. I observed a similar degree of association between VAB-1::GFP and RAN-1 in the presence and absence of sperm (Fig. 37D). Taken together, these data suggest that *ran-1* and *dab-1* promote VAB-1::GFP trafficking into the endocytic recycling compartment in females and this might be part of the mechanism by which they inhibit oocyte meiotic maturation and MAPK activation when MSP is absent.

Somatic G-protein Signaling Influences VAB-1::GFP Localization

Previous data suggested that regulation of oocyte meiotic maturation in *C. elegans* involves the *vab-1* pathway in oocytes (Miller et al., 2003), Govindan et al., 2006; Corrigan et al., 2005) and parallel inputs from $G\alpha_s$ and $G\alpha_{o/i}$ protein signaling pathways from the gonadal sheath cells (Fig. 33; Govindan et al., 2003). A genome-wide screen for negative regulators of oocyte meiotic maturation identified *goa-1*, which encodes $G\alpha_{o/i}$, and *inx-22* and *inx-14*, which encode innexin/pannexin components of gap-junctional channels that function downstream of $G\alpha_s$ signaling (Fig. 33). Since *goa-1* and *inx-22* function to inhibit meiotic maturation when MSP/sperm is absent, I examined VAB-1::GFP localization after conducting RNAi in a female background. In a female background, *goa-1(RNAi)* and *inx-22(RNAi)* causes VAB-1::GFP to be largely excluded from a RAB-11-positive compartment (Fig. 35G and 45), as is typically observed in wild-type hermaphrodites (Fig. 35A).

Figure 44. Specificity of anti-Ran antibodies

Fluorescence micrographs of RAN-1 staining in dissected gonads from control(RNAi) (top panel) and *ran-1(RNAi)* hermaphrodites (bottom panel). L1-stage hermaphrodites were treated with RNAi using the feeding method. No staining was observed following *ran-1(RNAi)*. Because *ran-1(RNAi)* severely disrupts gonadal development, it was formally possible that *ran-1(RNAi)* interferes with the gonadal accumulation of a cross-reacting protein. We tested this possibility by *ran-1(RNAi)* feeding of L3-stage larvae. Under these conditions, oocytes were produced but *ran-1* staining was diminished (data not shown). Scale bars represent 10 μm.

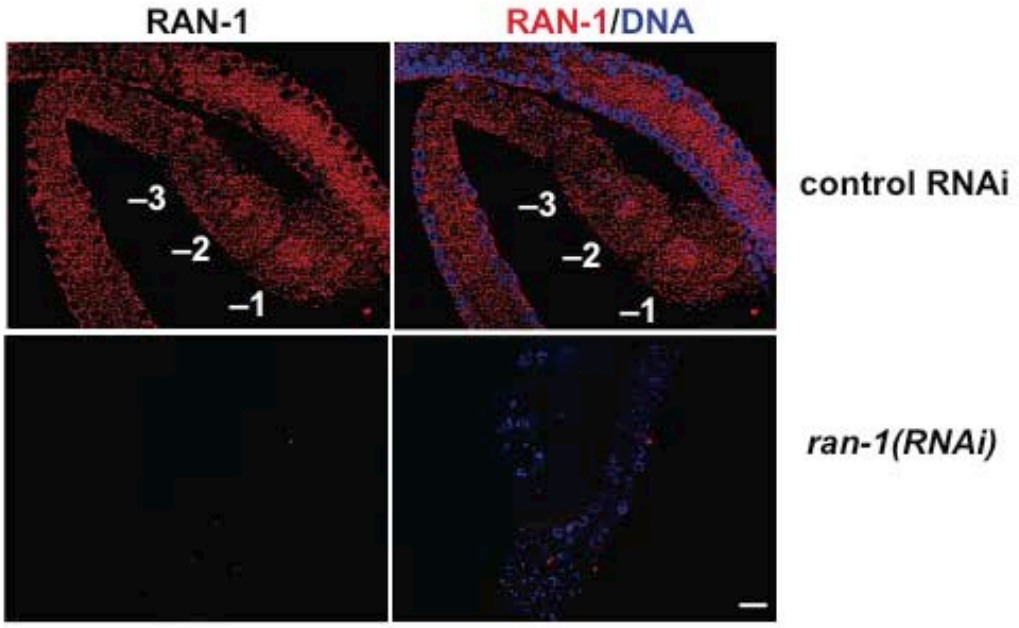
RAN-1
RAN-1/DNA
–3
–2
–1
–3
–2
–1
control RNAi
ran-1(RNAi)

Figure 45. GSA-1, INX-22 and OMA-1/2 affect VAB-1::GFP localization

(A) Fluorescence micrographs of VAB-1::GFP and mCherry::PH expression in living *gsa-1(RNAi)* hermaphrodites. (B-G) Fluorescence micrographs of VAB-1::GFP expression in dissected gonads from *inx-22(RNAi); fog-2(q71)* females (B, F), *oma-1(RNAi); oma-2(RNAi)* hermaphrodites (C, G), and *dab-1(gk291)* hermaphrodites (D) and females (E). RAB-11 (B, C) and WGA (D-G) staining were also examined. Insets show magnified views of the oocyte cortex (upper right) and the interior (lower left). Scale bars represent 10 μm.

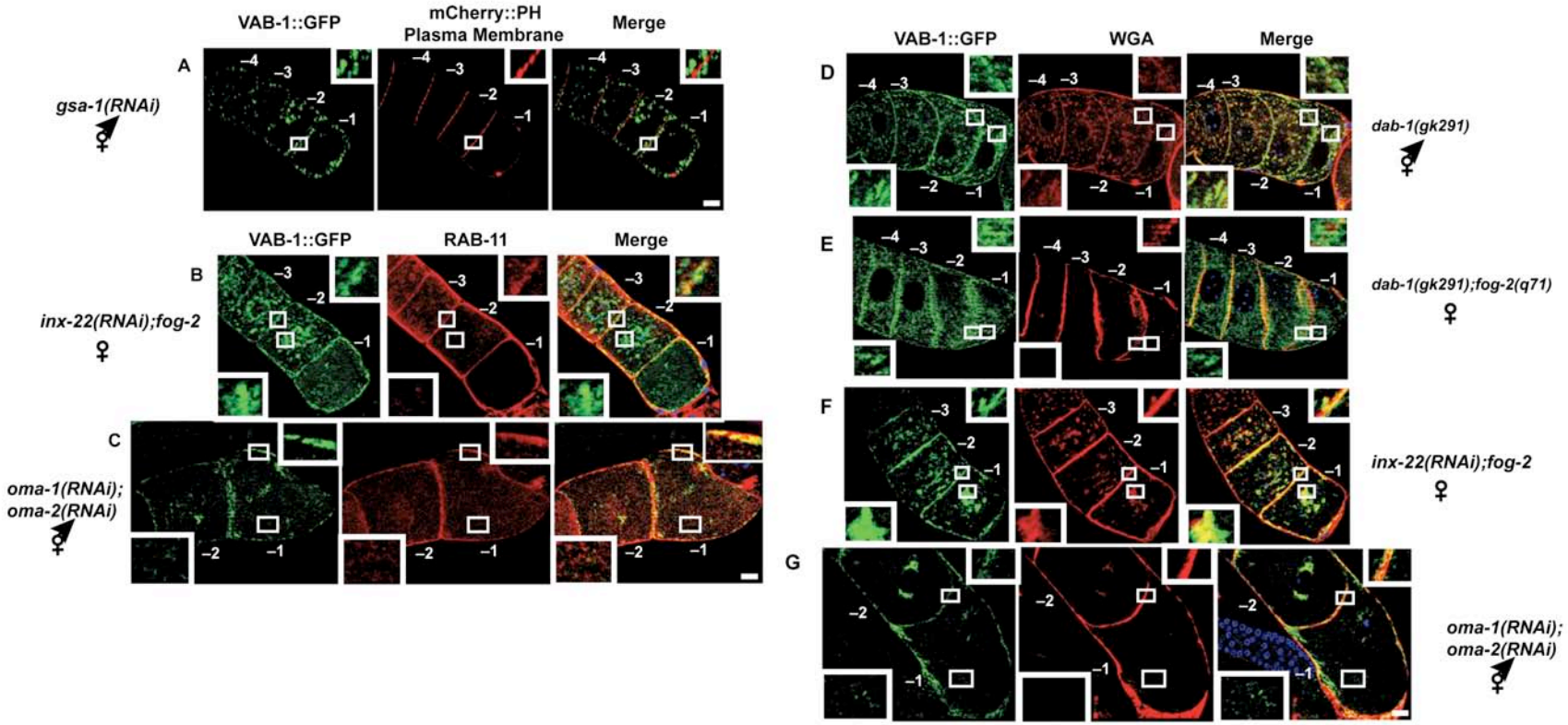
VAB-1::GFP
mCherry::PH
Plasma Membrane
Merge
A
gsa-1(RNAi)
♀
VAB-1::GFP
RAB-11
Merge
B
inx-22(RNAi);fog-2
♀
C
oma-1(RNAi);
oma-2(RNAi)
♀
VAB-1::GFP
WGA
Merge
D
dab-1(gk291)
♀
E
dab-1(gk291);fog-2(q71)
♀
F
inx-22(RNAi);fog-2
♀
G
oma-1(RNAi);
oma-2(RNAi)
♀

Similarly, *goa-1(RNAi)* or *inx-22(RNAi)* in female worms caused the global pattern of vesicle-associated proteins to resemble that typically seen in wild-type hermaphrodites (compare Fig. 36A, 36H, and 45). I also observed similar effects following *inx-14(RNAi)* and *kin-2(RNAi)* in unmated females (Table 8). These results suggest that VAB-1::GFP is actively maintained in the endocytic recycling compartment in the absence of MSP/sperm and this localization is dependent on $G\alpha_{o/i}$ signaling in the gonadal sheath cells and sheath/oocyte gap-junctional communication.

Genetic mosaic analysis now shows that *gsa-1* and *acy-4*, which respectively encode $G\alpha_s$ and adenylate cyclase, are required in the sheath/spermathecal cell lineages for oocyte MAPK activation and meiotic maturation (J. A. G. and D. G., unpublished results). Thus, I examined the effect of $G\alpha_s$ signaling on VAB-1::GFP localization. Following *gsa-1(RNAi)* in a hermaphrodite background, I observed that VAB-1::GFP-containing vesicles were cortically localized in a RAB-11-positive compartment (Fig. 3F), as typically seen in unmated females (Fig. 35B), and detectable levels of VAB-1::GFP were not observed at the plasma membrane, as visualized using the mCherry::PH domain marker (Fig. 45). I observed that *gsa-1(RNAi)* in a hermaphrodite background appears to have a global effect on the localization of vesicle-associated proteins, as revealed by WGA staining (Fig. 36G). This result further indicates that the $G\alpha_s$ signaling in the gonadal sheath cells can regulate membrane protein trafficking in oocytes.

Discussion

Our results suggest a model in which a recycling MSP/Eph receptor functions to inhibit oocyte meiotic maturation in the absence of MSP/sperm (Fig. 38). The localization of VAB-1::GFP to the endocytic recycling compartment is dependent on DAB-1 and RAN-1, which both participate in the negative regulation of meiotic maturation in the absence of MSP/sperm (Govindan et al., 2003) and interact with the VAB-1 intracellular domain. In the absence of DAB-1 or RAN-1, VAB-1::GFP localizes to a new compartment that is defined by its lack of staining with WGA. The requirement of DAB-1 and RAN-1 in VAB-1::GFP trafficking is only observed in the absence of MSP/sperm. For this reason, I favor the hypothesis that DAB-1 and RAN-1 promote VAB-1::GFP endosomal trafficking into the recycling pathway in the absence of MSP/sperm (Fig. 38). In this model, the absence of DAB-1 and RAN-1 excludes VAB-1::GFP from the recycling compartment and favors trafficking to a different compartment in which the modifications detected by WGA staining are removed. Alternatively, DAB-1 and RAN-1 may function in VAB-1::GFP export from the Golgi, as has been proposed for DAB-1 in EGL-17 export (Kamikura et al., 2003). If DAB-1 and RAN-1 are required for efficient VAB-1::GFP export, however, this requirement must be dispensable in the presence of MSP/sperm. Since I purified RAN-1 as a VAB-1-ICD-interacting protein from hermaphrodite protein extracts, I think it unlikely that VAB-1 trafficking in the hermaphrodite mode is regulated at the level of RAN-1 binding.

When MSP/sperm is present, somatic $G\alpha_s$ function is required to exclude VAB-1::GFP from the endocytic recycling compartment.

Figure 38. A model for VAB-1 trafficking and signaling in the control of meiotic maturation

In the absence of MSP/sperm (left panel), VAB-1 traffics to the endocytic recycling compartment (ERC). The accumulation of VAB-1 in the endocytic recycling compartment in the absence of MSP/sperm depends on DAB-1 and RAN-1 and sheath/oocyte gap-junctional communication but not ephrins. VAB-1 is proposed to signal while either in or in transit to the endocytic recycling compartment to inhibit oocyte MAPK activation and meiotic maturation. In the presence of MSP/sperm (right panel), VAB-1 is largely excluded from the endocytic recycling compartment, and traffics away from the oocyte cortex (EE, early endosome; LE, late endosome; L, lysosome). This MSP/sperm-mode of VAB-1 endosomal sorting requires $G\alpha_s$ signaling in the gonadal sheath cells.

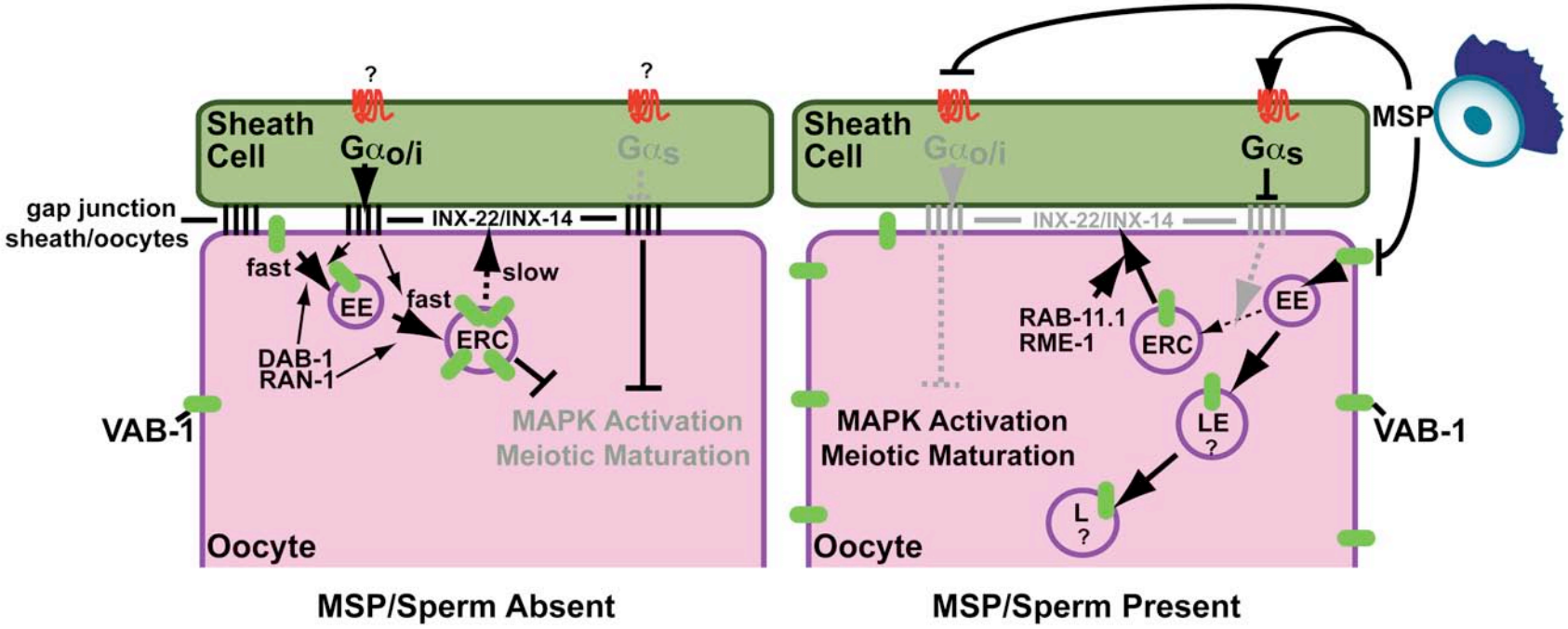
?
?
Sheath Cell
Gαo/i
Gαs
gap junction sheath/oocytes
INX-22/INX-14
fast
slow
fast
EE
ERC
DAB-1
RAN-1
VAB-1
MAPK Activation
Meiotic Maturation
Oocyte
MSP/Sperm Absent
Sheath Cell
Gαo/i
Gαs
MSP
INX-22/INX-14
RAB-11.1
RME-1
ERC
EE
LE
?
L
?
MAPK Activation
Meiotic Maturation
VAB-1
Oocyte
MSP/Sperm Present

The exclusion of VAB-1 from the endocytic recycling compartment is important for an efficient meiotic maturation response as indicated by our analysis of an *rme-1* null mutant and *rab-11.1(RNAi)*. Somatic $G\alpha_s$ signaling is also likely required for the localization of many other oocyte vesicle-associated proteins, as revealed by WGA staining. This result suggests a model in which the sheath cells may play a role as the major sensor of MSP/sperm and regulate the ability of the oocyte to sense and respond to MSP/sperm (Fig. 38). Are the alterations in vesicular trafficking I observe in the presence of MSP/sperm, and which require somatic $G\alpha_s$ signaling, a consequence of meiotic maturation or a regulatory response? At present, I cannot distinguish between these two possibilities. On the one hand, an *rme-1* mutation and *rab-11.1(RNAi)* result in *vab-1*-dependent reductions in the oocyte meiotic maturation rate. Also, depletions of the weak negative regulators *pkc-1*, *pqn-19*, and *vav-1* have no effect on VAB-1::GFP localization, despite the fact that these genes inhibit meiotic maturation in females to similar extents as *dab-1*(Govindan et al., 2003). On the other hand, the CCCH zinc-finger proteins, OMA-1 and OMA-2, which are redundantly required in the germ line for meiotic maturation (Detwiler et al., 2001), affect the global localization of vesicle-associated proteins in the oocyte (Fig. 45). In addition, MSP injection experiments suggest that alterations in VAB-1::GFP localization represent slower responses than MAPK activation. In fact, *mpk-1(ga111*ts*)* mutant hermaphrodites accumulate VAB-1::GFP at the oocyte cortex in the female pattern at the non-permissive temperature (Fig. 43). Whether *oma-1/oma-2* and *mpk-1* affect VAB-1::GFP as a consequence of meiotic maturation or a feedback response is unclear. Possibly, recompartmentalization of negative regulators in the germ line may contribute to sustaining high rates of meiotic maturation when sperm are

plentiful. Interestingly, meiotic maturation results in the translocation of the DYRK-family kinase MBK-2 from the oocyte cortex to the cytoplasm, which is needed for its role in promoting the oocyte-to-embryo transition (Stitzel et al., 2006; 2007; Maruyama et al., 2007). The reorganization of the oocyte during meiotic maturation may occur in a stepwise fashion, first inactivating negative regulators, then promoting the activity of effectors needed for completing meiosis and early embryonic development. MSP signaling has also been shown to reorganize the oocyte microtubule cytoskeleton, and this response requires $G\alpha_s$ and *oma-1/2* (Harris et al., 2006). The coordinate regulation of endosomal recycling and microtubule organization by MSP signaling is intriguing: the importance of the microtubule cytoskeleton in vesicular trafficking is well established; and microtubule dynamics and organization are documented to be affected by *rab-11* (Dollar et al., 2006; Zhang et al., 2008).

Regulated endosomal trafficking of Eph receptors has been shown to be critical for axonal repulsion in the vertebrate nervous system (Marston et al., 2003; Zimmer et al., 2003; Cowan et al., 2005). The ephrin-dependent endocytosis of Eph receptors requires the small GTPase Rac, which plays a major role in reorganizing the actin cytoskeleton during Eph receptor-promoted cell retraction in concert with Rho and Cdc42 (Groeger et al., 2007). The finding that phosphorylated Eph receptors are present in intracellular vesicles following ephrin binding suggests that Eph receptors may signal from intracellular vesicles (Marston et al., 2003; Zimmer et al., 2003). Our finding that a recycling VAB-1 Eph receptor may be active in negatively regulating meiotic maturation in the absence of MSP is consistent with the idea that signaling may continue within the cell after initial ligand engagement. This study reinforces the view that endosomal

trafficking and signaling are intimately linked, as has been found for several other highly conserved signal transduction pathways (González-Gaitán, 2003; von Zastrow and Sorkin, 2007). MSP-domain proteins are highly conserved, and recently the MSP-domain protein VAPB, which is mutated in Amyotrophic Lateral Sclerosis type 8 (Nishimura et al., 2004), was shown to be a secreted ligand for Eph receptors in *Drosophila* and mammals (Tsuda et al., 2008). Therefore, our findings of the regulated trafficking of the MSP/Eph receptor during meiotic maturation of the *C. elegans* oocyte and its modulation by $G\alpha_s$ signaling in the gonadal sheath cells may have wider relevance.

CHAPTER IV

GENERAL DICUSSION AND FUTURE DIRECTIONS

Summary

In most females, oocytes arrest in meiotic prophase I for a prolonged period of time, and resume meiosis in response to hormonal signaling (Masui, 2001). Defects in meiotic processes may result in aneuploid gametes, which would cause infertility, embryonic lethality, or birth defects (Hassold and Hunt 2001). Therefore, understanding the underlying mechanisms controlling oocyte meiotic maturation might help us to identify new therapies for improving human health. In my dissertation work, I used *C. elegans* as a model organism to study this conserved biological process. In *C. elegans*, sperm release MSP via a vesicle budding mechanism to promote oocyte meiotic maturation (Miller et al., 2001; Kosinski et al., 2005). In the absence of sperm, oocyte VAB-1/Eph receptor and somatic sheath cell pathways act in parallel to inhibit oocyte meiotic maturation (Miller et al., 2003). MSP antagonizes VAB-1/Eph receptor and sheath cell inhibitory function to promote oocyte meiotic maturation (Miller et al., 2003). My work addresses the molecular mechanism that regulates VAB-1 function as a negative regulator during oocyte meiotic maturation in the absence of MSP/sperm, and the mechanism by which MSP antagonizes VAB-1 function to promote oocyte meiotic maturation. My work suggests that intracellular trafficking of VAB-1/Eph receptor is the key mechanism that regulates VAB-1/Eph receptor function as an inhibitor of oocyte

meiotic maturation. VAB-1/Eph receptor functions in or in transit to from the recycling endosome to negatively regulate oocyte meiotic maturation in the absence of MSP/sperm. MSP antagonizes VAB-1 entering into recycling endosomes to counteract VAB-1's function. I further provided evidence showing that DAB-1/disabled functions in a common pathway with VAB-1/Eph, and binds VAB-1 intracellular domain *in vitro*, and promotes VAB-1/Eph receptor trafficking into the recycling endosomes in the absence of MSP/sperm. Moreover, I identified a small GTPase RAN-1 in a biochemical purification as a protein that interacts with VAB-1 intracellular domain. RAN-1 functions as a negative regulator of oocyte meiotic maturation, and acts in a common pathway with VAB-1/Eph receptor. RAN-1 also promotes recycling endosomal transport of VAB-1/Eph receptor. In addition, in collaboration with J. Amaranath Govindan, we found that somatic G protein function in the somatic sheath cells to regulate oocyte meiotic maturation. In addition, I found that somatic G protein pathway regulates VAB-1 trafficking through crosstalk. In this section, I present a summary of the major findings and discuss a model how VAB-1 inhibits oocyte meiotic maturation and how MSP antagonizes VAB-1's function. I will also discuss some future studies need for testing my model.

Regulated trafficking controls VAB-1/Eph receptor function during oocyte meiotic maturation

In *C. elegans*, in the presence of sperm, oocytes undergo meiotic maturation in response to a sperm signal, MSP (McCarter et al., 1999, Miller et al., 2001). Whereas, in the absence of sperm, oocytes arrest at meiotic prophase I, and this meiotic arrest is

regulated by the VAB-1 MSP/Eph receptor and a somatic sheath cell pathway (Miller et al., 2003). In order to address how VAB-1 might regulate meiotic arrest, and how MSP might antagonize VAB-1's function, I used genetics, cell biology, and biochemistry to investigate these mechanisms.

In order to identify genes that regulate VAB-1's function, I collaborated with J. Amaranath Govindan, who conducted a genome wide RNAi screen looking for negative regulators of oocyte meiotic maturation. He identified sixteen genes, and four of which function in a common pathway with the VAB-1/Eph receptor. We showed that DAB-1/Disable1, PQN-19/STAM homolog, PKC-1/protein kinase C, and VAV-1/GEF function in the germline to negatively regulate oocyte meiotic maturation in the absence of sperm. In addition, we also identified the somatic G protein pathways that regulate oocyte meiotic maturation. Using a biochemical purification strategy to identify proteins that interact with VAB-1 intracellular domain, I identified that RAN-1 a small GTPase binds to VAB-1 intracellular domain. Govindan also found that RAN-1 functions in the germline and acts in a common pathway with VAB-1.

More importantly, by using a germline expressed biological functional VAB-1::GFP fusion protein, I showed that VAB-1 is enriched in the endocytic recycling compartment in the absence of sperm, and is largely excluded from the endocytic recycling compartment upon the stimulation of MSP/sperm. I also showed that MSP is sufficient for changing VAB-1 localization. Furthermore, I showed that the recycling VAB-1 inhibits oocyte meiotic maturation, because blocking exit of VAB-1 from the endocytic recycling compartment inhibits oocyte meiotic maturation in the presence of MSP/sperm. In addition, I showed that Disabled DAB-1 and RAN-1 GTPase promotes

VAB-1::GFP trafficking into the endocytic recycling compartment in the absence of sperm. Somewhat surprisingly, I found that somatic G protein also regulates VAB-1::GFP trafficking. Taken together, My finding suggest that regulated trafficking is a key mechanism that DAB-1/disabled and RAN-1/GTPase regulate VAB-1/Eph receptor's function as a inhibitor of oocyte meiotic maturation and that MSP antagonizes VAB-1 function by regulating its trafficking.

Further outstanding questions

My findings that regulated trafficking is a key mechanism that regulates oocyte meiotic maturation, raises additional questions. For example, how does VAB-1 inhibit oocyte meiotic maturation in or in transit to from the endocytic recycling compartment? How does MSP regulate VAB-1 trafficking? How do DAB-1 and RAN-1 regulate VAB-1 trafficking? How do somatic G proteins regulate VAB-1 trafficking in the oocytes? How does MSP interact with VAB-1? One question which is not quite related to my findings, but I found to be interesting, is what are the other MSP receptor(s), which are likely to be GPCR? I will now explain the potential strategies that can be used to address these questions.

How does endocytic recycling regulate VAB-1 function as a negative regulator of oocyte meiotic maturation

The most interesting question that I want to ask is how recycling VAB-1/Eph negatively regulates oocyte meiotic maturation. Since VAB-1/Eph is a receptor tyrosine

kinase, one possibility is that VAB-1 gets phosphorylated and becomes activated in the endocytic recycling endosomes, where VAB-1 inhibits oocyte meiotic maturation. VAB-1 inhibits VAB-1 might interact with its effector in recycling endosomes. To test this hypothesis, a specific antibody that can recognize tyrosin phosphorylated VAB-1 is needed to examine whether VAB-1/Eph receptor gets phosphorylated only in the endocytic recycling endosomes. This woud be technically demanding because the in vivo phophorylation sites would forst have to be definded. In addition, VAB-1/Eph receptor might inhibit oocyte meiotic maturation by activating VAB-1 downstream effectors which are localized in the endocytic recycling endosomes. To test this hypothesis, proteins that are associated with VAB-1::GFP vesicles need to be identified. In addition, to understand how VAB-1/Eph receptor functions in the endocytic recycling endosomes and what molecules regulate VAB-1/Eph receptor trafficking, it is also very important to know what links VAB-1/Eph receptor signaling to oocyte meiotic arrest. Oocyte meiotic maturation is regulated by MPF complex in most animals. How VAB-1 inhibits MPF complex activity and what signal cascades lie between VAB-1 and MPF? Since inactivation of MPF is regulated by phosphorylation, and VAB-1/Eph receptor is a tyrosine kinase, it is possible that VAB-1/Eph receptor kinase is activated in the recycling endosomes, then activated VAB-1 triggers a series of phosphorylation events which eventually inactivates MPF. To test all these hypotheses, we need to know what proteins are associated with VAB-1 vesicles.

Recently, I did some preliminary experiment to purify the VAB-1 vesicles. I homogized the 15 ml *C. elegans* adult female worms that carrying VAB-1::GFP.

Figure 46. Fractionation of VAB-1::GFP vesicle

A. Strategy of fractionation of VAB-1::GFP vesicle. 30 ml packed female worms carrying VAB-1::GFP were homogenized then were roughly fractionationed by centrifugation. The pellet of 30,000xg were collected and resuspended in buffer, then were applied to centrifugation on a sucrose gradient (10%-40%). Centrifugation fractions were analyzed by using anti-VAB-1 and anti-RAB-11 antibodies.
B. VAB-1::GFP cofractionations with RAB-11. VAB-1::GFP were pelleted in fraction with relative high sucrose concentration. Endogenous VAB-1 is associated with VAB-1::GFP in this fractionation strategy. RAB-11 is also enriched in fractions containing VAB-1::GFP.

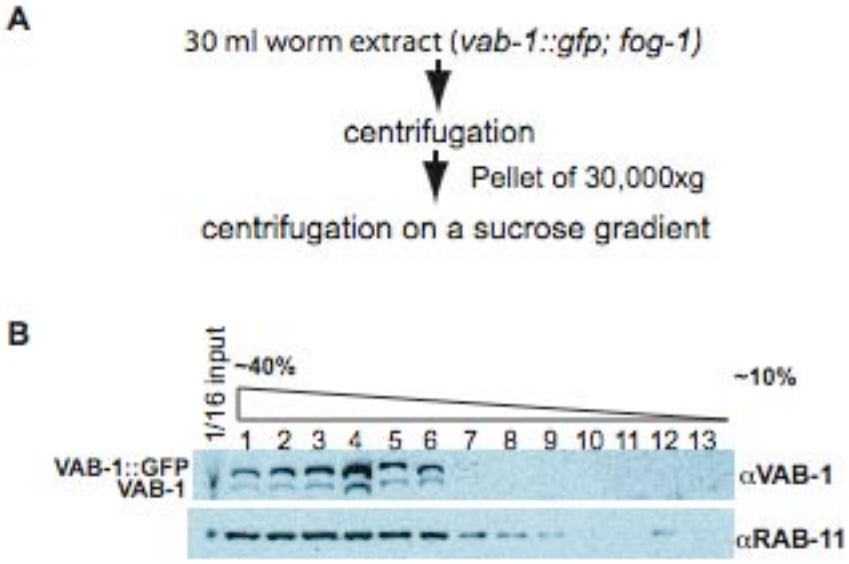
A
30 ml worm extract (vab-1::gfp; fog-1)
centrifugation
Pellet of 30,000xg
centrifugation on a sucrose gradient
B
1/16 input
~40%
~10%
1 2 3 4 5 6 7 8 9 10 11 12 13
VAB-1::GFP
VAB-1
αVAB-1
αRAB-11

Then I performed fractionation of this worm extract by centrifugation and I found that most VAB-1::GFP and endogenous VAB-1 are distributed in a fraction that pellet at ~30,000 xg centrifugation force. I further purified VAB-1::GFP vesicles by centrifugation on a sucrose gradient (10%-40%) and found that VAB-1::GFP and endogenous VAB-1 are enriched in fractions of higher sucrose concentration (Fig. 46). Then I used an anti-VAB-1 specific antibody to immunoprecipitate VAB-1::GFP vesicles. My preliminary results suggest that endogenous VAB-1 is always associated with VAB-1::GFP fractions and endocytic recycling marker RAB-11 is always associated with VAB-1::GFP fraction as well. To further identify the VAB-1::GFP vesicle components, I will scale up my purification and use mass spectrometry strategy to identify the proteins that associated with VAB-1::GFP vesicles. I can also test the VAB-1::GFP phophorylation status in this vesicles by mass spectrometry. I expect some of the proteins that associate with VAB-1::GFP vesicles are negative regulators of oocyte meiotic maturation, and they are activated by VAB-1. To test this hypothesis, once I have the protein list of VAB-1::GFP vesicles, I will inactivate those candidate gene in female background by RNAi or use the genetic null mutants if they are available. Then I am going to examine whether those gene candidates are negative regulators of oocyte meiotic maturation. Alternatively, VAB-1 could inhibit oocyte meiotic maturation by inactivating some positive regulators, to test this hypothesis, I will examine the gene candidates that associate with VAB-1::GFP vesicles to see whether they promote oocyte meiotic maturation in the *vab-1(0)* female background.

Another interesting questions is what regulates VAB-1 trafficking. In my dissertation work I found that *rab-11* and *rme-1* promotes VAB-1::GFP recycling in the

presence of sperm. endocytic trafficking is a quite complex process, and endocytic trafficking proteins need to function in a orchestra to regulate these processes. Since RAB-11 is associated with the endocytic recycling compartment, I hypothesize that some other trafficking proteins that regulate VAB-1 localization must be associated with VAB-1::GFP vesicles as well. To test this hypothesis, I will analyze the proteins candidates that associate with VAB-1::GFP vesicles to test whether they affect endocytic recycling. I will conduct a VAB-1::GFP localization analysis after inactivating the VAB-1::GFP vesicle gene candidates by RNAi or use genetic null mutants in the presence/absence of sperm. In addition, I will test whether these gene candidates affect general trafficking process by examing whether they regulate oocyte yolk uptake.

How MSP regulate VAB-1 trafficking

The enrichment of VAB-1::GFP in the endocytic recycling compartment in the absence of sperm or in the absence of $G\alpha_s$ allows me to ask whether MSP regulates VAB-1 trafficking indirectly.How MSP antagonizes VAB-1 from entering into the endocytic recycling compartment appears not to be due to changes in the general endocytic machinery in presence/absence of sperm, since the endocytic trafficking component proteins (e.g. RAB-11, RAB-5, EEA-1, RAB-7, clathrin, caveolin-1) do not change their localization in the presence or absence of sperm (Grant et al., 1999; Grant et al., 2001; Sato et al., 2006;). Thus the presence of MSP must change VAB-1 structure somehow to expose VAB-1 to some trafficking regulators that are not accessible to VAB-1 in the absence of sperm. Alternatively, MSP might activate or inactivate some VAB-1-

specific trafficking regulators. To test my hypothesis, it is very important to know what is associated with VAB-1::GFP vesicles in the presence of sperm. Then I could test whether these proteins affect VAB-1::GFP trafficking in the presence or absence of sperm. If they promotes VAB-1::GFP trafficking into its functional endocytic recycling compartment in the presence of sperm, it suggests that MSP antagonizes their trafficking function. If these protein candidates inhibit VAB-1 entering into its functional endocytic recycling compartment in the presence of sperm, it suggests that the MSP activates the trafficking function of these endocytic proteins.

How do DAB-1 and RAN-1 regulates VAB-1 trafficking

My dissertation work suggests that DAB-1/disabled promotes VAB-1 trafficking in the absence of sperm. DAB-1 is a homolog of mammalian Dab2 protein, which is a putative tumor suppressor protein implicated in cell surface receptor turnover. Dab2 is a complex molecule with N terminal phosphotyrosine binding (PTB) domain, which binds to multiple cell-surface receptors bearing FxNPxY motif. Multiple studies suggest that the tyrosine residue of this FxNPxY motif is essential for Dab2 binding. I found a similar motif GLNHVY at the intracellular portion of VAB-1/Eph receptor, and I confirmed that DAB-1 interacts with VAB-1 intracellular domain *in vitro*. However, whether GLNHVY of VAB-1 is required for DAB-1 binding and VAB-1 internalization is unclear. To answer this question, a VAB-1 mutation without GLNHVY motif needs to be generated to test the binding activity with DAB-1 protein. If this GLNHVY motif is required for VAB-1 binding to DAB-1, a mutant VAB-1::GFP which does not bear the GLNHVY

motif can be generated and analyzed for its localization. If this mutant VAB-1::GFP localizes only at the oocyte membrane, this would suggest that the GLNHVY motif of VAB-1 is required for its internalization. If this mutant VAB-1::GFP, which does not bear GLNHVY motif, displays a hermaphrodite pattern, this result would suggest that DAB-1 is not required for VAB-1 internalization but is required for VAB-1 to enter the endocytic recycling compartment.

Very interestingly, I found that localization of DAB-1 is dependent on sperm. In the absence of sperm, DAB-1 distributes uniformly throughout the oocyte (female pattern, Fig. 27), however, in the presence of sperm, DAB-1 is highly enriched at the oocyte cortex (hermaphrodite pattern, Fig. 27). This localization change is probably due to endocytosis, since blocking the endocytic process by incubating female worms at 4ºC for 1 hour alters DAB-1 localization from the female pattern to hermaphrodite pattern. These observations suggest that the MSP/sperm signal might alter DAB-1 trafficking mode.

I identified RAN-1, a small GTPase, in a biochemical purification as a protein that interacts with the VAB-1 intracellular domain. RAN-1 is a negative regulator of oocyte meiotic maturation that acts in a common pathway with VAB-1. Ran is well know for its regulatory role during nuclear transport. Ran has also been implicated in mitotic spindle assembly. Studies suggest that RanGTP can induce assembly of both microtubule asters and spindle-like structures in the egg extracts in the absence of chromatin and centrosomes. (carazo-salas et al., 2001, Wilde et al., 2001) and increased RanGTP can override the spindle checkpoint and activates the APC/C in *Xenopus* egg extract. By contrast, increasing hydyolysis of RanGTP restores the checkpoint activity (Carazo-Salas

et al., 2001; Wilde et al., 2001). Ran has also been implicated in regulating nuclear envelope assembly (Askjaer et al., 2002; Clarke and Zhang 2001; Hetzer et al., 2005). My studies suggest that Ran is also involved in vesicle trafficking. How Ran regulates VAB-1/Eph receptor trafficking is unclear. RCC1, a guanine nucleotide exchange factor (GEF), is associated with chromatin, where it catalyses Ran to exchange its GDP for GTP. RanGAP is enriched in cytoplasm where it stimulates Ran hydrolyzing GTP to GDP. Ran binding protein 1 is also enriched in the cytoplasm and it regulates Ran transport cargoes from nucleus to the cytosol. Therefore, RanGTP is highly concentrated in the nucleus, and RanGDP is concentrated in the cytoplasm. Since VAB-1 localizes in the vesicles in the cytoplasm, I propose a hypothesis in which RanGAP and RanBP1 might be required for RAN's function in regulating VAB-1 localization. To test this hypothesis, analysis of VAB-1::GFP localization needs to be conducted after depleting Ran cycling proteins: such as ran-2/RanGAP, npp-9/RanBP1 using RNAi

How do somatic G proteins regulate VAB-1 trafficking in oocytes

It was somewhat surprising that I found somatic G protein pathways affect VAB-1 trafficking in the oocytes. Govindan found that somatic G protein pathways play a major role for regulating oocyte meiotic maturation in response to sperm signaling (Chaptor II; Govindan J.A. and Greenstein, D. unpublished results). This finding might explain how VAB-1 functions in concert with G proteins to regulate a fully on/off oocyte maturation when sperm is abundant/absent, and the moderate rate of oocyte maturtion in between (Kosinski et al., 2005). How G protein signaling from somatic cells affect

VAB-1::GFP trafficking is an intriguing question to me. Interestingly, MSP signaling has also been shown to reorganize the oocyte microtubule cytoskeleton, and this response requires $G\alpha_s$ (Harris et al., 2000). Moreover, the importance of the microtubule cytoskeleton in vesicular trafficking is well established; and microtubule dynamics and organization are documented to be affected by *rab-11*. (Dollar et al., 2002; Zhang et al., 2008). Thus, it seems likely that G protein signaling regulates microtubule dynamics, which facilitate VAB-1 vesicle trafficking. Since cytoskeletal elements (ie. actin or microtubule) are critical for vesicle trafficking, I predict that disrupting the cytoskeleton will change VAB-1 localization. However, I am more interested in the specific mechanism by which signaling reorganizes microtubule in oocytes.

How does MSP interacts with VAB-1

The interaction between MSP domain containing protein and Eph receptor is evolutionary conserved. Human VAPB, a MSP domain containing protein, is associated with Amyotrophic lateral sclerosis (ALS), and the MSP domains of VAP proteins are cleaved and secreted to function as ligands for Eph receptors (Tsuda et al., 2008). However, how MSP binds to VAB-1 is still unclear. Although the crystal structure of MSP suggests that MSP has an immunoglobulin-like fold (Bullock et al., 1996), mammalian Eph receptor crystal structure has been revealed as well. But how MSP interacts with VAB-1/Eph receptor is still unclear. Which amino acids of MSP are required for VAB-1 interaction; which parts of VAB-1 interact with MSP? To address these questions, the crystal structure of MSP-VAB-1 complex needs to be analyzed, and

analysis of interaction of MSP mutations to VAB-1 ectodomain needs to be conducted. Analysis of VAB-1 mutations that interact with MSP protein to test which domain of VAB-1 binds MSP can be performed as well. Studies suggest that MSP can antagonize ephrin ligand binding to Eph receptor, and the crystal structure of ephrin-Eph complex suggest that ephrin inerts its loop into Eph receptor channel. I predict that in the MSP-VAB-1 crystal structure, MSP binds to Eph using the same Eph receptor channel that ephrins use.

What are the other MSP receptor(s)

This question is quite intriguing to me although is not derived from my dissertation work. VAB-1 is a MSP receptor in the oocyte, however, multiple lines of evidence suggest there are other receptors for MSP. The identification of G protein signaling in sheath cells that function as regulators of oocyte meiotic maturation suggests that multiple GPCR, which couple to $G\alpha_s$, $G\alpha_{o/i}$ and $G\alpha_q$ are involved (Govindan and Greenstien, unpublished results). These GPCRs are predicted to be expressed in sheath cells.

REFERENCES

Abrieu, A., Brassac, T., Galas, S., Fisher, D., Labbé, J. C., and Dorée, M. (1998). The Polo-like kinase Plx1 is a component of the MPF amplification loop at the G2/M-phase transition of the cell cycle in Xenopus eggs. *J Cell Sci* **111,** 1751-1757

Agarwal, S. and Roeder, G.S. (2000). Zip3 provides a link between recombination enzymes and synaptonemal complex proteins. *Cell* **102**, 245-255

Aguilar, R. C., Ohno, H., Roche, K. W. and Bonifacino, J. S. (1997). Functional domain mapping of the clathrin-associated adaptor medium chains mu1 and mu2. *J Biol Chem* **272**, 27160–6

Anderson, E. and Albertini, D. F. (1976). Gap junctions between the oocyte and companion follicle cells in the mammalian ovary. *J Cell Biol.* **71**,680-686

Araki, K., Naito, K., Haraguchi, S., Suzuki, R., Yokoyama, M., Inoue, M., Aizawa, S., Toyoda, Y., and Sato, E. (1996). Meiotic abnormalities of c-mos knockout mouse oocytes: activation after first meiosis or entrance into third meiotic metaphase. *Biol. Reprod* **55**,1315-1324

Aoto, J. and Chen, L. (2007). Bidirectional ephrin/Eph signaling in synaptic functions. *Brain Res* **1184**, 72-80.

Audhya, A., Desai, A., and Oegema, K. (2007). A role for Rab5 in structuring the endoplasmic reticulum. *J Cell Biol* **178***,* 43-56.

Baker, A. M., Roberts, T. M., and Stewart, M. (2002). 2.6 Å resolution crystal structure of helices of the motile major sperm protein (MSP) of *Caenorhabditis elegans*. *J Mol Biol* **319**, 491-499

Bailis, J. M. and Roeder, G. S. (1998). Synaptonemal complex morphogenesis and sister-chromatid cohesion require Mek1-dependent phosphorylation of a meiotic chromosomal protein. *Genes Dev* **12**, 3551-3563.

Bastiani, C. and Mendel, J. (2006). Heterotrimeric G-proteins in *C. elegans*. *WormBook* http://www.wormbook.org.

Benmerah, A. and Lamaze, C. (2007). Clathrin-coated pits: vive la différence? *Traffic* **8**, 970-982.

Bickel, S. E., Orr-Weaver, T. L., and Balicky, E. M. (2002). The sister-chromatid cohesion protein ORD is required for chiasma maintenance in Drosophila oocytes. *Curr Biol* **12**, 925-9.

Binns, K. L., Taylor, P. P., Sicheri, F., Pawson, T., and Holland, S.J. (2000). Phosphorylation of tyrosine residues in the kinase domain and juxtamembrane region regulates the biological and catalytic activities of Eph receptors. *Mol Cell Biol.* **20**, 4791-4805

Bishop, D. K., Nikolski, Y., Oshiro, J., Chon, J., Shinohara, M., and Chen, X. (1999). High copy number suppression of the meiotic arrest caused by a dmc1 mutation: REC114 imposes an early recombination block and RAD54 promotes a DMC1-independent DSB repair pathway. *Genes Cells* **4**, 425-444

Börner, G. V., Kleckner, N., and Hunter, N. (2004). Crossover/noncrossover differentiation, synaptonemal complex formation, and regulatory surveillance at the leptotene/zygotene transition of meiosis. *Cell* **117**, 29-45.

Bornslaeger, E.A. and Schultz, R.M. (1985). Regulation of mouse oocyte maturation: effect of elevating cumulus cell cAMP on oocyte cAMP levels. *Biol Reprod* **33**, 698-704.

Bottino, D., Mogilner, A., Roberts, T., Stewart, M., and Oster, G. (2002). How nematode sperm crawl. *J Cell Sci* 115, 367-384.

Boyd, A.W. and Lackmann, M. (2001). Signals from Eph and ephrin proteins: a developmental tool kit. *Sci STKE* **2001**, RE20

Brenner, S. (1974). The genetics of *Caenorhabditis elegans*. *Genetics* **77**, 71-94.

Bretscher, M. S. and Pearse, B. M. (1984) Coated pits in action. *Cell* **38**, 3–4

Brown, C. M. and Petersen, N. O. (1999) Free clathrin triskelions are required for the stability of clathrin-associated adaptor protein (AP-2) coated pit nucleation sites. *Biochem. Cell Biol* **77**, 439–448

Buonomo, S. B., Clyne, R. K., Fuchs, J., Loidl, J., Uhlmann, F., and Nasmyth, K. (2000). Disjunction of homologous chromosomes in meiosis I depends on proteolytic cleavage of the meiotic cohesin Rec8 by separin. *Cell* **103**, 387-398

Brunet, S. and Maro, B. (2005). Cytoskeleton and cell cycle control during meiotic maturation of the mouse oocyte: integrating time and space. *Reproduction* **130**, 801-811

Rrunger, A. T. (2005). Structure and function of SNARE and SNARE-interacting proteins. *Q Rev Biophys* **38**, 1-47.

Cabrera-Vera, T. M., Vanhauwe, J., Thomas, T. O., Medkova, M., Preininger, A., Mazzoni, M. R., and Hamm, H. E. (2003). Insights into G protein structure, function, and regulation. *Endocr Rev* **24**, 765-781.

Carpenter, G. and Cohen, S. (1990). Epidermal growth factor. *J Biol Chem*. **265**, 7709-12

Carvalho, R. F., Beutler, M., Marler, K. J., Knöll, B., Becker-Barroso, E., Heintzmann, R., Ng, T., and Drescher, U. (2006). Silencing of EphA3 through a *cis* interaction with ephrinA5. *Nat Neurosci* **9**, 322-330.

Champion, M. D. and Hawley, R. S. (2002). Playing for half the deck: the molecular biology of meiosis. *Nat Cell Biol* **4**, 50-56.

Cheng, Z. J., Singh, R. D., Marks, D. L., and Pagano, R. E. (2006). Membrane microdomains, caveolae, and caveolar endocytosis of sphingolipids. *Mol Membr Biol* **23**, 101-110.

Chikashige, Y., Ding, D. Q., Funabiki, H., Haraguchi, T., Mashiko, S., Yanagida, M., and Hiraoka, Y. (1994). Telomere-led premeiotic chromosome movement in fission yeast. *Science* **264**, 270-273.

Chikashige, Y., Ding, D. Q., Imai, Y., Yamamoto, M., Haraguchi, T., and Hiraoka, Y. (1997). Meiotic nuclear reorganization: switching the position of centromeres and telomeres in the fission yeast *Schizosaccharomyces pombe*. *EMBO J* **16**, 193-202.

Chin-Sang, I. D., George, S. E., Ding, M., Moseley, S. L., Lynch, A. S., and Chisholm, A. D. (1999). The ephrin VAB-2/EFN-1 functions in neuronal signaling to regulate epidermal morphogenesis in *C. elegans*. *Cell*. **99**, 781-90

Chin-Sang, I. D., Moseley, S. L., Ding, M., Harrington, R.J., George, S.E., and Chisholm, A. D. (2002). The divergent C. elegans ephrin EFN-4 functions inembryonic morphogenesis in a pathway independent of the VAB-1 Eph receptor. *Development* **129**, 5499-5510

Chrencik, J. E., Brooun, A., Kraus, M. L., Recht, M. I., Kolatkar, A. R., Han, G. W., Seifert, J.M., Widmer, H., Auer, M., and Kuhn, P. (2006). Structural and biophysical characterization of the EphB4*ephrinB2 protein-protein interaction and receptor specificity. *J Biol Chem* **281**, 28185-28192.

Cho, W. K., Stern, S., and Biggers, J. D. (1974). Inhibitory effect of dibutyryl cAMP on mouse oocyte maturation in vitro. *J Exp Zool* **187**, 383-386.

Chua, P. R. and Roeder, G. S. (1998). Zip2, a meiosis-specific protein required for the initiation of chromosome synapsis. *Cell* **93**, 349-359.

Cohen, Y., Dardalhon, M., and Averbeck, D. (2002). Homologous recombination is essential for RAD51 up-regulation in Saccharomyces cerevisiae following DNA crosslinking damage. *Nucleic Acids Res* **30**, 1224-1232.

Collawn, J. F., Stangel, M., Kuhn, L. A., Esekogwu, V., Jing, S. Q., Trowbridge, I. S. and Tainer, J. A. (1990) Transferrin receptor internalization sequence YXRF implicates a tight turn as the structural recognition motif for endocytosis. *Cell* **63**, 1061–1072

Conti, M., Andersen, C. B., Richard, F., Mehats, C., Chun, S. Y., Horner, K., Jin, C., and Tsafriri, A. (2002). Role of cyclic nucleotide signaling in oocyte maturation. *Mol Cell Endocrinol* **187**,153-159.

Cooper, J. P, Watanabe, Y., and Nurse, P. (1998). Fission yeast Taz1 protein is required for meiotic telomere clustering and recombination. *Nature* **392**, 828-831.

Corbeel, L. and Freson, K. (2008). Rab proteins and Rab-associated proteins: major actors in the mechanism of protein-trafficking disorders. *Eur J Pediatr*. **167**, 723-729.

Corrigan, C., Subramanian, R., and Miller, M. A. (2005). Eph and NMDA receptors control Ca^{2+}/calmodulin-dependent kinase II activation during *C. elegans* oocyte meiotic maturation. *Development* **132**, 5225-5237.

Cowan, C. A., and Henkemeyer, M. (2001). The SH2/SH3 adaptor Grb4 transduces B-ephrin reverse signals. *Nature* **413**, 174-179.

Cowan, C.W., Shao, Y.R., Sahin, M., Shamah, SM., Lin, MZ., Greer, P.L., Gao, S., Griffith, E.C., Brugge, J.S., and Greenberg, M.E. (2005). Vav family GEFs link activated Ephs to endocytosis and axon guidance. *Neuron* **46***,* 205-217.

Cowan, C. A., Yokoyama, N., Saxena, A., Chumley, M. J., Silvany, R. E., Baker, L. A., Srivastava, D., and Henkemeyer. M. (2004). Ephrin-B2 reverse signaling is required for axon pathfinding and cardiac valve formation but not early vascular development. *Dev Biol* **271,** 263-271.

Cromie, G. A. and Smith, G. R. (2007). Branching out: meiotic recombination and its regulation. *Trends Cell Biol* **17**, 448-455.

Das, K., Lewis, R. Y., Scherer, P. E., Lisanti, M. P. (1999). The membrane-spanning domains of caveolins-1 and -2 mediate the formation of caveolin hetero-oligomers. Implications for the assembly of caveolae membranes in vivo. *J Biol Chem* **274**, 18721–18728.

Davalos, V., Dopeso, H., Castaño, J., Wilson, A. J., Vilardell, F., Romero-Gimenez, J., Espín, E., Armengol, M., Capella, G., Mariadason, J. M., Aaltonen, L. A.,

Schwartz, S. Jr., and Arango, D. (2006). EPHB4 and survival of colorectal cancer patients. *Cancer Res* **66**, 8943-8948.

Davis, S., Gale, N. W., Aldrich, T. H., Maisonpierre, P. C., Lhotak, V., Pawson, T., Goldfarb, M., and Yancopoulos, G. D. (1994). Ligands for EPH-related receptor tyrosine kinases that require membrane attachment or clustering for activity. *Science* **266**, 816-819

Davy, A., Aubin, J., and Soriano, P. (2004). Ephrin-B1 forward and reverse signaling are required during mouse development. *Genes Dev* **18**, 572-583.

Davy, A. and Soriano, P. (2005). Ephrin signaling in vivo: look both ways. *Dev Dyn* **232**, 1-10

Denef, N., Neubuser, D., Perez, L., and Cohen, S. M. (2000). Hedgehog induces opposite changes in turnover and subcellular localization of Patched and Smoothened. *Cell* **102**, 521–531

Dernburg, A. F., McDonald, K., Moulder, G., Barstead, R., Dresser, M., and Villeneuve, A. M. (1998). Meiotic recombination in *C. elegans* initiates by a conserved mechanism and is dispensable for homologous chromosome synapsis. *Cell* **94**, 387-398.

Detwiler, M. R., Reuben, M., Li, X., Rogers, E., and Lin, R. (2001). Two zinc finger proteins, OMA-1 and OMA-2, are redundantly required for oocyte maturation in *C. elegans*. *Dev Cell* **1**, 187-199.

Ding, D. Q., Yamamoto, A., Haraguchi, T., and Hiraoka, Y. (2004). Dynamics of homologous chromosome pairing during meiotic prophase in fission yeast. *Dev Cell* **6**, 329-341

Dohn, M., Jiang, J., and Chen, X. (2001). Receptor tyrosine kinase EphA2 is regulated by p53-family proteins and induces apoptosis. *Oncogene* **20**, 6503-6515.

Dollar, G., Struckhoff, E., Michaud, J., and Cohen, R.S. (2002). Rab11 polarization of the *Drosophila* oocyte: a novel link between membrane trafficking, microtubule organization, and *oskar* mRNA localization and translation. *Development* **129**, 517-526.

Dong, H. and Roeder, G. S. (2000). Organization of the yeast Zip1 protein within the central region of the synaptonemal complex. *J Cell Biol* **148**, 417-426

Drab, M., Verkade, P., Elger, M., Kasper, M., Lohn, M., Lauterbach, B., Menne, J., Lindschau, C., Mende, F., Luft, F. C., Schedl, A., Haller, H., and Kurzchalia, T. V. (2001). Loss of caveolae, vascular dysfunction, and pulmonary defects in caveolin-1 gene-disrupted mice. *Science* **293**, 2449–2452.

Drescher, U. (2002). Eph family functions from an evolutionary perspective. *Curr Opin Genet Dev* **12**, 397-402

Dresser, M. E., Ewing, D. J., Conrad, M. N., Dominguez, A. M., Barstead, R., Jiang, H., and Kodadek, T. (1997). DMC1 functions in a Saccharomyces cerevisiae meiotic pathway that is largely independent of the RAD51 pathway. *Genetics* **147**, 533-544.

Duckworth, B. C., Weaverm, J. S., and Ruderman, J. V. (2002). G2 arrest in Xenopus oocytes depends on phosphorylation of cdc25 by protein kinase A. *Proc Natl Acad Sci* **99**, 16794-16799.

Duxbury, M. S., Ito, H., Zinner, M. J., Ashley, S. W., and Whang, E. E. (2004). Ligation of EphA2 by Ephrin A1-Fc inhibits pancreatic adenocarcinoma cellular invasiveness. *Biochem Biophys Res Commun* **320**, 1096-1102

Ecker, R. E. and Smith, L. D. (1971). Influence of exogenous ions on the events of maturation in Rana pipiens oocytes. *J Cell Physiol* **77**, 61-70.

Edwards, R. G. (1965). Maturation *in vitro* of mouse, sheep, cow, pig, rhesus monkey and human ovarian oocytes. *Nature* **208,** 349-351.

Egea, J. and Klein, R. (2007). Bidirectional Eph-ephrin signaling during axon guidance.

Trends Cell Biol **17**, 230-238.

Ellis, R. and Schedl, T. (2007). Sex determination in the germ line. *WormBook* **5**, 1-13.

Elowe, S., Holland, S. J., Kulkarni, S., and Pawson, T. (2001). Downregulation of the Ras-mitogen-activated protein kinase pathway by the EphB2 receptor tyrosine kinase is required for ephrin-induced neurite retraction. *Mol Cell Biol* **21**, 7429-7441.

Emery, G., Hutterer, A., Berdnik, D., Mayer, B., and Wirtz-Peitz, F., Gaitan, M. G., and Knoblich, J. A. (2005). Asymmetric Rab11 endosomes regulate Delta recycling and specify cell fate in the *Drosophila* nervous system. *Cell* **122**:763–773

Fan, H. Y. and Sun, Q. Y. (2004). Involvement of mitogen-activated protein kinase cascade during oocyte maturation and fertilization in mammals. *Biol Reprod* **70**, 535-547.

Farge, E., Ojcius, D. M., Subtil, A., and Dautry-Varsat, A. (1999). Enhancement of endocytosis due to aminophospholipid transport across the plasma membrane of living cells. *Am J Physiol* **276**, 725-733

Farsad, K., Ringstad, N., Takei, K., Floyd, S. R., Rose, K. and De Camilli, P. (2001) Generation of high curvature membranes mediated by direct endophilin bilayer interactions. *J Cell Biol* **155**, 193–200

Fielding, P. E. and Fielding, C. J. (1996). Intracellular transport of low density lipoprotein derived free cholesterol begins at clathrin-coated pits and terminates at cell surface caveolae. *Biochemistry* **35**, 14932-14938

Fischer, J. A., Eun, S. H., and Doolan, B. T. (2006). Endocytosis, endosome trafficking, and the regulation of *Drosophila* development. *Annu Rev Cell Dev Biol* **22**, 181-206.

Ford, M. G., Mills, I. G., Peter, B. J., Vallis, Y., Praefcke, G. J., Evans, P. R. and McMahon, H. T. (2002) Curvature of clathrin-coated pits driven by epsin. *Nature* **419**, 361–366

Ford, M. G., Pearse, B. M., Higgins, M. K., Vallis, Y., Owen, D. J., Gibson, A., Hopkins, C. R., Evans, P. R., and McMahon, H. T. (2001). Simultaneous binding of PtdIns(4,5)P2 and clathrin by AP180 in the nucleation of clathrin lattices on membranes. *Science* **291**, 1051-1055

Gallo, C. J., Hand, A. R., Jones, T. L., and Jaffe, L. A. (1995). Stimulation of Xenopus oocyte maturation by inhibition of the G-protein alpha S subunit, a component of the plasma membrane and yolk platelet membranes. *J Cell Biol* **130**, 275-284

Gautier, J., Minshull, J., Lohka, M., Glotzer, M., Hunt, T., and Maller, J. L. (1990). Cyclin is a component of maturation-promoting factor from Xenopus. *Cell* **60**, 487-494.

Gautier, J., Norbury, C., Lohka, M., Nurse, P., and Maller, J. (1988). Purified maturation-promoting factor contains the product of a Xenopus homolog of the fission yeast cell cycle control gene cdc2+. *Cell* **54**, 433-439.

George, S. E., Simokat, K., Hardin, J., and Chisholm, A. D. (1998). The VAB-1 Eph receptor tyrosine kinase functions in neural and epithelial morphogenesis in *C. elegans*.

Cell **92**, 633-643

Gerton, J. L. and Hawley, R. S. (2005). Homologous chromosome interactions in meiosis: diversity amidst conservation. *Nat Rev Genet* **6**, 477-487.

Giroux, C. N., Dresser, M. E., and Tiano, H. F. (1989). Genetic control of chromosome synapsis in yeast meiosis. *Genome* **31**, 88-94.

Glenney, J. R. Jr. (1992). The sequence of human caveolin reveals identity with VIP21, a component of transport vesicles. *FEBS Lett* **314**, 45-48

Goetz, J. G., Lajoie, P., Wiseman, S. M., and Nabi, I. R. (2008). Caveolin-1 in tumor progression: the good, the bad and the ugly. *Cancer Metastasis Rev* **27**, 715-35.

Gong, Q., Huntsman, C., and Ma, D. (2007). Clathrin-independent internalization and recycling. *J Cell Mol Med* **12**, 126-144.

González-Gaitán, M. (2003). Endocytic trafficking during *Drosophila* development. *Mech Dev* **120**, 1265-1282.

Gould, K. L. and Nurse, P. (1989). Tyrosine phosphorylation of the fission yeast cdc2+ protein kinase regulates entry into mitosis. *Nature* **342**, 39-45

Gonzalez-Gaitan, M. (2003)a. Endocytic trafficking during *Drosophila* development. *Mech Dev* **120**:1265–1282

Gonzalez-Gaitan M. (2003)b. Signal dispersal and transduction through the endocytic pathway. *Nat Rev Mol Cell Biol* **4**:213–224

Grant, B. and Hirsh, D. (1999). Receptor-mediated endocytosis in the *Caenorhabditis elegans* oocyte. *Mol Biol Cell* **10***,* 4311-4326.

Grant, B., Zhang, Y., Paupard, M.C., Lin, S.X., Hall, D.H., and Hirsh, D. (2001). Evidence that RME-1, a conserved *C. elegans* EH-domain protein, functions in endocytic recycling. *Nat Cell Biol* **3***,* 573-579.

Greene, B., Liu, S. H., Wilde, A. and Brodsky, F. M. (2000) Complete reconstitution of clathrin basket formation with recombinant protein fragments: adaptor control of clathrin self-assembly. *Traffic* **1**, 69–75

Groeger, G., and Nobes, C.D. (2007). Co-operative Cdc42 and Rho signalling mediates ephrinB-triggered endothelial cell retraction. *Biochem J* **404***,* 23-29.

Grosshans, B. L., Ortiz, D., and Novick, P. (2006). Rabs and their effectors: achieving specificity in membrane traffic. *Proc Natl Acad Sci* **103**, 11821-11827.

Gumienny, T. L., Lambie, E., Hartwieg, E., Horvitz, H. R., and Hengartner, M. O. (1999). Genetic control of programmed cell death in the *Caenorhabditis elegans* hermaphrodite germline. *Development* **126**, 1011-1022.

Hafner, C., Schmitz, G., Meyer, S., Bataille, F., Hau, P., Langmann, T., Dietmaier, W., Landthaler, M., and Vogt, T. (2004). Differential gene expression of Eph receptors and ephrins in benign human tissues and cancers. *Clin Chem* **50**, 490-499.

Hall, D. H., Winfrey, V. P., Blaeuer, G., Hoffman, L. H., Furuta, T., Rose, K. L., Hobert, O., and Greenstein, D. (1999). Ultrastructural features of the adult

hermaphrodite gonad of *Caenorhabditis elegans*: relations between the germ line and soma. *Dev Biol* **212**, 101-123.

Halloran, M. C. and Wolman, M. A. (2006). Repulsion or adhesion: receptors make the call. *Curr Opin Cell Biol* **18**, 533-540

Han, S. J. and Conti, M. (2006). New pathways from PKA to the Cdc2/cyclin B complex in oocytes: Wee1B as a potential PKA substrate. *Cell Cycle* **5**, 227-231.

Hanyaloglu, A. C. and von Zastrow, M. (2008). Regulation of GPCRs by endocytic membrane trafficking and its potential implications. *Annu Rev Pharmacol Toxicol* **48**, 537-568.

Harris, J. E., Govindan, J. A., Yamamoto, I., Schwartz, J., Kaverina, I., and Greenstein, D. (2006). Major sperm protein signaling promotes oocyte microtubule reorganization prior to fertilization in *Caenorhabditis elegans*. *Dev Biol* **299***,* 105-121.

Hassold, T. and Hunt, P. (2001). To err (meiotically) is human: the genesis of human aneuploidy. *Nat Rev Genet* **2**, 280-291.

Haucke, V. (2005). Phosphoinositide regulation of clathrin-mediated endocytosis.

Biochem Soc Trans **33**, 1285-1289.

Hayase, A., Takagi, M., Miyazaki, T., Oshiumi, H., Shinohara, M., and Shinohara, A. (2004). A protein complex containing Mei5 and Sae3 promotes the assembly of the meiosis-specific RecA homolog Dmc1. *Cell* **119**, 927-940.

Herath, N. I., Spanevello, M. D., Sabesan, S., Newton, T., Cummings, M., Duffy, S., Lincoln, D., Boyle, G., Parsons, P.G., and Boyd, A. W. (2006). Over-expression of Eph and ephrin genes in advanced ovarian cancer: ephrin gene expression correlates with shortened survival. *BMC Cancer* **6**, 144.

Heuser, J. (1980) Three-dimensional visualization of coated vesicle formation in fibroblasts. *J. Cell Biol* **84**, 560–583

Heuser, J. E. and Keen, J. (1988) Deep-etch visualization of proteins involved in clathrin assembly. *J Cell Biol* **107**, 877–886

Hillers, K. J., and Villeneuve, A. M. (2003). Chromosome-wide control of meiotic crossing over in C. elegans. *Curr Biol* **13**, 1641-1647

Himanen, J. P., Chumley, M. J., Lackmann, M., Li, C., Barton, W. A., Jeffrey, P. D., Vearing, C., Geleick, D., Feldheim, D. A., Boyd, A. W., Henkemeyer, M., and

Nikolov, D. B. (2004). Repelling class discrimination: ephrin-A5 binds to and activates EphB2 receptor signaling. *Nat Neurosci* **7**, 501-509.

Himanen, J. P., Henkemeyer, M., and Nikolov, D. B. (1998). Crystal structure of the ligand-binding domain of the receptor tyrosine kinase EphB2. *Nature* **396**, 486-4891.

Himanen, J. P. and Nikolov, D. B. (2002). Purification, crystallization and preliminary characterization of an Eph-B2/ephrin-B2 complex. *Acta Crystallogr D Biol Crystallogr* **58**, 533-535.

Himanen, J. P. and Nikolov, D. B. (2003). Eph signaling: a structural view. *Trends Neurosci* **26**, 46-51.

Himanen, J. P. and Nikolov, D. B. (2003). Eph receptors and ephrins. *Int J Biochem Cell Biol* **35**, 130-134.

Himanen, J. P., Saha, N., and Nikolov, D. B. (2007). Cell-cell signaling via Eph receptors and ephrins. *Curr Opin Cell Biol* **19**, 534-542

Hirai, H., Maru, Y., Hagiwara, K., Nishida, J., and Takaku, F. (1987). A novel putative tyrosine kinase receptor encoded by the eph gene. *Science* **238**, 1717-1720.

Hodges, C. A., Ilagan, A., Jennings, D., Keri, R., Nilson, J., and Hunt, P.A. (2002). Experimental evidence that changes in oocyte growth influence meiotic chromosome segregation. *Hum Reprod* **17**, 1171-1180.

Hodges, C. A., Revenkova, E., Jessberger, R., Hassold, T. J., and Hunt, P. A. (2005). SMC1b-deficient female mice provide evidence that cohesins are a missing-link in age-related nondisjunction. *Nat Genet* **37**, 1351-1355.

Hodgkin, J. and Herman, R. K. (1998). Changing styles in C. elegans genetics. *Trends Genet* **14**, 352-357.

Holland, S. J., Gale, N. W., Gish, G. D., Roth, R. A., Songyang, Z., Cantley, L. C., Henkemeyer, M., Yancopoulos, G. D, and Pawson, T. (1997). Juxtamembrane tyrosine residues couple the Eph family receptor EphB2/Nuk to specific SH2 domain proteins in neuronal cells. *EMBO J* **16**, 3877-3888.

Hollingsworth, N. M., Goetsch, L., and Byers, B. (1990). The HOP1 gene encodes a meiosis-specific component of yeast chromosomes. *Cell* **61**, 73-84

Hommelgaard, A.M., Roepstorff, K., Vilhardt, F., Torgersen, M L., Sandvig, K., and van Deurs, B. (2005). Caveolae: stable membrane domains with a potential for internalization. *Traffic* **6**, 720-724.

Hong W. (2005). SNAREs and traffic. *Biochim Biophys Acta* **1744**, 493-517.

Howell, B.W., Lanier, L.M., Frank, R., Gertler, F.B., and Cooper, J.A. (1999). The disabled 1 phosphotyrosine-binding domain binds to the internalization signals of transmembrane glycoproteins and to phospholipids. *Mol Cell Biol* **19,** 5179-5188.

Joseph, J. (2006). Ran at a glance. *J Cell Sci* **119***,* 3481-3484.

Hubbard, E. J. and Greenstein, D. (2000). The Caenorhabditis elegans gonad: a test tube for cell and developmental biology. *Dev Dyn* **218**, 2-22

Huchon, D., Ozon, R., Fischer, E. H., and Demaille, J. G. (1981). The pure inhibitor of cAMP-dependent protein kinase initiates Xenopus laevis meiotic maturation. A 4-step scheme for meiotic maturation. *Mol Cell Endocrinol* **22**, 211-222.

Huse, M. and Kuriyan, J. (2002). The conformational plasticity of protein kinases. *Cell* **109**, 275-282.

Ikegami, R., Zheng, H., Ong, S.H., and Culotti, J. (2004). Integration of semaphorin-2A/MAB-20, ephrin-4, and UNC-129 TGF-beta signaling pathways regulates sorting of distinct sensory rays in *C. elegans*. *Dev Cell* **6***,* 383-395.

Incardona, J. P., Gruenberg, J., and Roelink, H. (2002). Sonic hedgehog induces the segregation of Patched and Smoothened in endosomes. *Curr Biol* **12**:983–995

Ingham, P. W. and McMahon, A. P. (2001). Hedgehog signaling in animal development: paradigms and principles. *Genes Dev* **15**, 3059-3087

Irie, F., Okuno, M., Pasquale, E. B., and Yamaguchi, Y. (2005). EphrinB-EphB signalling regulates clathrin-mediated endocytosis through tyrosine phosphorylation of synaptojanin 1. *Nat Cell Biol* **7**, 501-509

Insel, P. A., Head, B. P., Patel, H. H., Roth, D. M., Bundey, R. A., and Swaney, J. S. (2005). Compartmentation of G-protein-coupled receptors and their signalling components in lipid rafts and caveolae. *Biochem Soc Trans* **33**, 1131-1134.

Ishikawa, Y., Otsu, K., and Oshikawa, J. (2005). Caveolin; different roles for insulin signal? *Cell Signal* **17**, 1175-1182.

Ishiguro, K. and Watanabe, Y. (2007). Chromosome cohesion in mitosis and meiosis.

J Cell Sci **120**, 367-369.

Jafar-Nejad, H., Andrews, H. K., Acar, M., Bayat, V., Wirtz-Peitz, F., et al. (2005). Sec15, a component of the exocyst, promotes Notch signaling during the asymmetric division of *Drosophila* sensory organ precursors. *Dev Cell* **9**:351–363

Jamnongjit, M., and Hammes, S. R. (2005). Oocyte maturation: the coming of age of a germ cell. *Semin Reprod Med* **23**, 234-241.

Janes, P. W., Saha, N., Barton, W. A., Kolev, M. V., Wimmer-Kleikamp, S. H., Nievergall, E., Blobel, C. P., Himanen, J. P., Lackmann, M., and Nikolov, D. B. (2005). Adam meets Eph: an ADAM substrate recognition module acts as a molecular switch for ephrin cleavage in *trans*. *Cell* **123**, 291-304.

Jansen, G., Thijssen, K. L., Werner, P., van der Horst, M., Hazendonk, E., and Plasterk, R H. (1999). The complete family of genes encoding G proteins of *Caenorhabditis elegans*. *Nat Genet* 21, 414-419.

Jin, A. J. and Nossal, R. (1993) Topological mechanisms involved in the formation of clathrin-coated vesicles. *Biophys J* **65**, 1523–1537

Johannes, L. and Lamaze, C. (2002). Clathrin-dependent or not: is it still the question?

Traffic 3, 443-451

Kachur, T.M., Audhya, A., and Pilgrim, D.B. (2008). UNC-45 is required for NMY-2 contractile function in early embryonic polarity establishment and germline cellularization in *C. elegans*. *Dev Biol 314,* 287-299.

Kalinowski, R. R., Berlot, C. H., Jones, T. L., Ross, L. F., Jaffe, L. A., and Mehlmann, L M. (2004). Maintenance of meiotic prophase arrest in vertebrate oocytes by a G_s protein-mediated pathway. *Dev Biol* **267**, 1-13.

Kalo, M.S. and Pasquale, E.B. (1999). Signal transfer by Eph receptors. *Cell Tissue Res* **298**, 1-9.

Kalthoff, C., Alves, J., Urbanke, C., Knorr, R. and Ungewickell, E. J. (2002) Unusual structural organization of the endocytic proteins AP180 and Epsin 1. *J Biol Chem* **277**, 8209–8216

Kamath, R. S., Fraser, A. G., Dong, Y., Poulin, G., Durbin, R., Gotta, M., Kanapin, A., Le Bot, N., Moreno, S., Sohrmann, M., Welchman, D. P., Zipperlen, P., and Ahringer, J. (2003). Systematic functional analysis of the *Caenorhabditis elegans* genome using RNAi. *Nature* **421**, 231-237.

Kamikura, D. M. and Cooper, J. A. (2003). Lipoprotein receptors and a disabled family cytoplasmic adapter protein regulate EGL-17/FGF export in *C. elegans*. *Genes Dev* **17**, 2798-2811.

Kamikura, D. M. and Cooper, J. A. (2006). Clathrin interaction and subcellular localization of Ce-DAB-1, an adaptor for protein secretion in *Caenorhabditis elegans*. *Traffic* **7**, 324-336.

Kapoor TM, Mayer TU, Coughlin ML, Mitchison TJ. (2000). Probing spindle assembly mechanisms with monastrol, a small molecule inhibitor of the mitotic kinesin, Eg5. *J Cell Biol* **150**, 975-988.

Karaiskou, A., Perez, L. H., Ferby, I., Ozon, R., Jessus, C., and Nebreda, A. R. (2001). Differential regulation of Cdc2 and Cdk2 by RINGO and cyclins. *J Biol Chem* **276**, 36028-36034.

Kawasaki, M., Nakayama, K., and Wakatsuki, S. (2005). Membrane recruitment of effector proteins by Arf and Rab GTPases. *Curr Opin Struct Biol* **15**, 681-689.

Keeney, S., Giroux, C. N., and Kleckner, N. (1997). Meiosis-specific DNA double-strand breaks are catalyzed by Spo11, a member of a widely conserved protein family. *Cell* **88**, 375-384.

Kelly, W., Xu, S., Montgomery, M., and Fire, A. (1997). Distinct requirements for somatic and germline expression of a generally expressed *Caernorhabditis elegans* gene. *Genetics* **146**, 227-238.

Klein, F., Mahr, P., Galova, M., Buonomo, S.B., Michaelis, C., Nairz, K., and Nasmyth, K. (1999). A central role for cohesins in sister chromatid cohesion, formation of axial elements, and recombination during yeast meiosis. *Cell* **98**, 91-103

Kirchhausen, T. (2000) Clathrin. *Annu Rev Biochem* **69**, 699–727

Kirchhausen, T. (2000) Three ways to make a vesicle. *Nat Rev Mol Cell Biol* **1**, 187–198

Koehler, K. E., Hawley, R. S., Sherman, S., and Hassold, T. (1996). Recombination and nondisjunction in humans and flies. *Hum Mol Genet* **5**, 1495-1504.

Konstantinova I, Nikolova G, Ohara-Imaizumi M, Meda P, Kucera T, Zarbalis K, Wurst W, Nagamatsu S, Lammert E. (2007). EphA-Ephrin-A-mediated beta cell communication regulates insulin secretion from pancreatic islets. *Cell* **129**, 359-370

Koolpe, M., Burgess, R., Dail, M., and Pasquale, E. B. (2005). EphB receptor-binding peptides identified by phage display enable design of an antagonist with ephrin-like affinity. *J Biol Chem* **280**, 17301-17311.

Korswagen, H. C., Park, J. H., Ohshima, Y., Plasterk, R. H. (1997). An activating mutation in a Caenorhabditis elegans Gs protein induces neural degeneration. *Genes Dev* **11**, 1493-1503.

Korswagen, H. C., Park, J. H., Oshima, Y., and Plasterk, R. H. A. (1997). An activating mutation in *Caenorhabditis elegans* G_s protein induces neural degeneration. *Genes Dev* 11, 1493-1503.

Kosinski, M., McDonald, K., Schwartz, J., Yamamoto, I., and Greenstein, D. (2005). *C. elegans* sperm bud vesicles to deliver a meiotic maturation signal to distant oocytes. *Development* **132,** 3357-3369.

Kramer, J. M., French, R.P., Park, E. C., and Johnson, J.J. (1990). The *Caenorhabditis elegans rol-6* gene, which interacts with the *sqt-1* collagen gene to determine organismal morphology, encodes a collagen. *Mol Cell Biol* **10***,* 2081-2089.

Kubagawa, H. M., Watts, J. L., Corrigan, C., Edmonds, J. W., Sztul, E., Browse, J., and Miller, M. A. (2006). Oocyte signals derived from polyunsaturated fatty acids control sperm recruitment in vivo. *Nat Cell Biol* **8**, 1143-1148.

Kümmel, D. and Heinemann, U. (2008). Diversity in structure and function of tethering complexes: evidence for different mechanisms in vesicular transport regulation. *Curr Protein Pept Sci* **9**, 197-209.

Kuijper, S., Turner, C. J., and Adams, R. H. (2007). Regulation of angiogenesis by Eph-ephrin interactions. *Trends Cardiovasc Med* **17**, 145-151

Labrador, J.P., Brambilla, R., and Klein, R. (1997). The N-terminal globular domain of Eph receptors is sufficient for ligand binding and receptor signaling. *EMBO J* **16**, 3889-3897.

Lackmann, M., Oates, A.C., Dottori, M., Smith, F.M., Do, C., Power, M., Kravets, L., and Boyd, A. W. (1998). Distinct subdomains of the EphA3 receptor mediate ligand binding and receptor dimerization. *J Biol Chem* **273**, 20228-20237.

Lajoie, P. and Nabi, I. R. (2007). Regulation of raft-dependent endocytosis. *J Cell Mol Med* **11**, 644-53.

Lambert, N. A. (2008). Dissociation of heterotrimeric g proteins in cells. *Sci Signal* **1**, re5.

Larkin, J. M., Donzell, W. C., and Anderson, R. G. (1986). Potassium-dependent assembly of coated pits: new coated pits form as planar clathrin lattices. *J Cell Biol* **103**, 2619-2627.

Lampe, P. D., Qiu, Q., Meyer, R. A., TenBroek, E. M., Walseth, T. F., Starich, T. A., Grunenwald, H. L., and Johnson, R. G. (2001). Gap junction assembly: PTX-sensitive G proteins regulate the distribution of connexin43 within cells. *Am J Physiol Cell Physiol* **281**, 1211-1222.

Le Borgne R, Bardin A, Schweisguth F. (2005). The roles of receptor and ligand endocytosis in regulating Notch signaling. *Development* **132**:1751–1762

Le Roy, C., Wrana, J. L. (2005). Clathrin- and non-clathrin-mediated endocytic regulation of cell signalling. *Nat Rev Mol Cell Biol* **6**, 112-126.

Lee, M.H., Ohmachi, M., Arur, S., Nayak, S., Francis, R., Church, D., Lambie, E., and Schedl, T. (2007). Multiple functions and dynamic activation of MPK-1 extracellular signal-regulated kinase signaling in *Caenorhabditis elegans* germline development. *Genetics* **177**, 2039-2062.

Lemmon, M. A., Bu, Z., Ladbury, J. E., Zhou, M., Pinchasi, D., Lax, I., Engelman, D. M. and Schlessinger, J. (1997) Two EGF molecules contribute additively to stabilization of the EGFR dimer. *EMBO J* **16**, 281–294

Leu, J. Y., Chua, P. R., Roeder, G. S. (1998). The meiosis-specific Hop2 protein of S. cerevisiae ensures synapsis between homologous chromosomes. *Cell* **94**, 375-386

Li, S., Galbiati, F., Volonte, D., Sargiacomo, M., Engelman, J.A., Das, K., Scherer PE, Lisanti MP. (1998). Mutational analysis of caveolin-induced vesicle formation. Expression of caveolin-1 recruits caveolin-2 to caveolae membranes. *FEBS Lett* **434**, 127–134.

Liang, C.G., Su, Y.Q., Fan, H.Y., Schatten, H., and Sun, Q.Y. (2007). Mechanisms regulating oocyte meiotic resumption: roles of mitogen-activated protein kinase. *Mol Endocrinol* **21***,* 2037-2055.

Liebe, B., Alsheimer, M., Höög, C., Benavente, R., Scherthan, H. (2004). Telomere attachment, meiotic chromosome condensation, pairing, and bouquet stage duration are modified in spermatocytes lacking axial elements. *Mol Biol Cell* **15**, 827-837.

Lichten, M. and Goldman, A. S. (1995). Meiotic recombination hotspots. *Annu Rev Genet* **29**:423-444

Lin, H. C., Moore, M. S., Sanan, D. A., and Anderson, R. G. (1991). Reconstitution of clathrin-coated pit budding from plasma membranes. *J Cell Biol* **114**, 881-891

Lin, S.X., Grant, B., Hirsh, D., and Maxfield, F.R. (2001). Rme-1 regulates the distribution and function of the endocytic recycling compartment in mammalian cells. *Nat Cell Biol* **3***,* 567-572.

Lohka, M. J., Hayes, M. K., and Maller, J. L. (1988). Purification of maturation-promoting factor, an intracellular regulator of early mitotic events. *Proc Natl Acad Sci* **85**, 3009-3013

Lohka, M. J. and Maller, J. L. (1985). Induction of nuclear envelope breakdown, chromosome condensation, and spindle formation in cell-free extracts. *J Cell Biol* **101**, 518-523.

Loidl, J., Klein, F., and Scherthan, H. (1994). Homologous pairing is reduced but not abolished in asynaptic mutants of yeast. *J Cell Biol* **125**, 1191-1200.

Lorca, T., Castro, A., Martinez, A. M., Vigneron, S., Morin, N., Sigrist, S., Lehner, C., Dorée, M., and Labbé, J. C. (1998). Fizzy is required for activation of the APC/cyclosome in *Xenopus* egg extracts. *EMBO J* **17**, 3565-3575.

Lorca, T., Cruzalegui, F. H., Fesquet, D., Cavadore, J. C., Méry, J., Means, A., Dorée, M. (1993). Calmodulin-dependent protein kinase II mediates inactivation of MPF and CSF upon fertilization of Xenopus eggs. *Nature* **366**, 270-273.

Lorca, T., Galas, S., Fesquet, D., Devault, A., Cavadore, J. C., and Dorée, M. (1991). Degradation of the proto-oncogene product p39mos is not necessary for cyclin proteolysis and exit from meiotic metaphase: requirement for a Ca(2+)-calmodulin dependent event. *EMBO J* **10**, 2087-2093.

Mahaffey, D.T., Moore, M.S., Brodsky, F.M., Anderson, R.G. (1989). Coat proteins isolated from clathrin coated vesicles can assemble into coated pits. *J Cell Biol* **108**, 1615-1624.

Maller, J.L. and Krebs, E.G. (1977). Progesterone-stimulated meiotic cell division in Xenopus oocytes. Induction by regulatory subunit and inhibition by catalytic subunit of adenosine 3':5'-monophosphate-dependent protein kinase. *J Biol Chem* **252**, 1712-1718.

Mancia, F. and Shapiro, L. (2005). ADAM and Eph: how Ephrin-signaling cells become detached. *Cell* **123**, 185-187

Markgraf, D.F., Peplowska, K., and Ungermann, C. (2007). Rab cascades and tethering factors in the endomembrane system. *FEBS Lett* **581**, 2125-2130.

Marrari, Y., Crouthamel, M., Irannejad, R., Wedegaertner, P. B. (2007). Assembly and trafficking of heterotrimeric G proteins. *Biochemistry* **46**, 7665-7677.

Marston, D.J., Dickinson, S., and Nobes, C.D. (2003). Rac-dependent trans-endocytosis of ephrinBs regulates Eph-ephrin contact repulsion. *Nat Cell Biol* **5***,* 879-888.

Martin, T. M. J. (2001) PI(4,5)P_2 regulation of surface membrane traffic. *Curr Opin Cell Biol* **13**, 493–499

Maruyama, R., Velarde, N.V., Klancer, R., Gordon, S., Kadandale, P., Parry, J.M., Hang, J.S., Rubin, J., Stewart-Michaelis, A., and Schweinsberg, P., et al. (2007). EGG-3 regulates cell-surface and cortex rearrangements during egg activation in *Caenorhabditis elegans*. *Curr Biol* **17***,* 1555-1560.

Massagué, J. (1998). TGF-beta signal transduction. *Annu Rev Biochem*. **67**, 753-791.

Masui, Y. (1967). Relative roles of the pituitary, follicle cells, and progesterone in the induction of oocyte maturation in Rana pipiens. *J Exp Zool.* **166**, 365-375

Masui, Y. (2001). From oocyte maturation to the in vitro cell cycle: the history of discoveries of Maturation-Promoting Factor (MPF) and Cytostatic Factor (CSF). *Differentiation* **69**, 1-17.

Masui, Y. and Markert, C. L. (1971). Cytoplasmic control of nuclear behavior during meiotic maturation of frog oocytes. *J Exp Zool* **177**, 129-145

Mayor, S. and Pagano, R. E. (2007). Pathways of clathrin-independent endocytosis.

Nat Rev Mol Cell Biol **8**, 603-612.

McCarter, J., Bartlett, B., Dang, T., and Schedl, T. (1999). On the control of oocyte meiotic maturation and ovulation in *C. elegans*. *Dev Biol* **205**, 111-128.

McKee, B. D., Habera, L., and Vrana, J. A. (1992). Evidence that intergenic spacer repeats of Drosophila melanogaster rRNA genes function as X-Y pairing sites in male meiosis, and a general model for achiasmatic pairing. *Genetics* **132**, 529-544

McKee, B. D. and Karpen, G. H. (1990). Drosophila ribosomal RNA genes function as an X-Y pairing site during male meiosis. *Cell* **61**, 61-72

McKim, K. S. and Hawley, R. S. (1995). Chromosomal control of meiotic cell division. *Science* **270**, 1595-1601.

McKim, K. S and Hayashi-Hagihara, A. (1998). mei-W68 in Drosophila melanogaster encodes a Spo11 homolog: evidence that the mechanism for initiating meiotic recombination is conserved. *Genes Dev* **12**, 2932-2942.

McKim, K. S., Howell, A. M., and Rose, A. M. (1988). The effects of translocations on recombination frequency in Caenorhabditis elegans. *Genetics* **120**, 987-1001.

McKim, K. S., Peters, K., and Rose, A. M. (1993). Two types of sites required for meiotic chromosome pairing in *Caenorhabditis elegans*. *Genetics* **134,** 749-68.

Mehlmann, L. M. (2005). Stops and starts in mammalian oocytes: recent advances in understanding the regulation of meiotic arrest and oocyte maturation. *Reproduction* **130**, 791-799.

Mehlmann, L. M., Jones, T. L., and Jaffe, L. A. (2002). Meiotic arrest in the mouse follicle maintained by a G_s protein in the oocyte. *Science* **297**, 1343-1345.

Mehlmann, L. M., Saeki, Y., Tanaka, S., Brennan, T. J., Evsikov, A. V., Pendola, F. L., Knowles, B. B., Eppig, J. J., and Jaffe, L. A. (2004). The G_s-linked receptor GPR3 maintains meiotic arrest in mammalian oocytes. *Science* **306**, 1947-1950.

Mendel, J. E., Korswagen, H. C., Liu, K. S., Hajdu-Cronin, Y. M., Simon, M. I., Plasterk, R. H., and Sternberg, P. W. (1995). Participation of the protein G_o in multiple aspects of behavior in *C. elegans*. *Science* **267**, 1652-1655.

Meneely, P. M. and Herman, R. K. (1979). Lethals, steriles and deficiencies in a region of the X chromosome of *Caenorhabditis elegans. Genetics* **92**, 99-115.

Meneely, P. M., Farago, A. F., Kauffman, T. M. (2002). Crossover distribution and high interference for both the X chromosome and an autosome during oogenesis and spermatogenesis in *Caenorhabditis elegans*. *Genetics* **162,** 1169-1177.

Merlos-Suárez, A. and Batlle, E. (2008). Eph-ephrin signalling in adult tissues and cancer. *Curr Opin Cell Biol* **20**, 194-200.

Metz, C.W. (1926). Genetic Evidence of a Selective Segregation of Chromosomes in Sciara (Diptera). *Proc Natl Acad Sci* **12**, 690-692.

Miao, H., Wei, B. R., Peehl, D. M., Li, Q., Alexandrou, T., Schelling, J. R., Rhim, J. S., Sedor, J.R., Burnett, E., and Wang, B. (2001). Activation of EphA receptor tyrosine kinase inhibits the Ras/MAPK pathway. *Nat Cell Biol*. **3**, 527-30

Miller, M. A., Nguyen, V. Q., Lee, M.-H., Kosinski, M., Schedl, T., Caprioli, R. M., and Greenstein, D. (2001). A sperm cytoskeletal protein that signals oocyte meiotic maturation and ovulation. *Science* **291**, 2144-2147.

Miller, M. A., Ruest, P. J., Kosinski, M., Hanks, S. K., and Greenstein, D. (2003). An Eph receptor sperm-sensing control mechanism for oocyte meiotic maturation in *Caenorhabditis elegans*. *Genes Dev* **17**, 187-200.

Miller, M. A., Cutter, A., Yamamoto, I., Ward, S., and Greenstein, D. (2004). Clustered organization of reproductive genes in the *C. elegans* genome. *Curr Biol* **14**, 1284-1290.

Mishra, S. K., Keyel, P. A., Hawryluk, M. J., Agostinelli, N. R., Watkins, S. C. and Traub, L. M. (2002) Disabled-2 exhibits the properties of a cargo-selective endocytic clathrin adaptor. *EMBO J* **21**, 4915–4926

Moore, M. S., Mahaffey, D. T., Brodsky, F. M., and Anderson, R. G. (1987). Assembly of clathrin-coated pits onto purified plasma membranes. *Science* **236**, 558-563.

Mora, R., Bonilha, V. L., Marmorstein, A., Scherer, P. E., Brown, D., Lisanti, M. P., and Rodriguez-Boulan, E. (1999). Caveolin-2 localizes to the golgi complex but redistributes to plasma membrane, caveolae, and rafts when co-expressed with caveolin-1. *J Biol Chem* **274**: 25708–25717.

Morris, S. M. and Cooper, J. A. (2001) Disabled-2 colocalizes with the LDLR in clathrin-coated pits and interacts with AP-2. *Traffic* **2**, 111–123

Morris, S. M., Tallquist, M. D., Rock, C. O. and Cooper, J. A. (2002) Dual roles for the Dab2 adaptor protein in embryonic development and kidney transport. *EMBO J* **21**, 1555–1564

Mousavi, S. A., Malerød, L., Berg, T., and Kjeken, R. (2004). Clathrin-dependent endocytosis. *Biochem J* **377**, 1-16.

Mueller, P. R., Coleman, T. R., and Dunphy, W. G. (1995). Cell cycle regulation of a Xenopus Wee1-like kinase. *Mol Biol Cell* **6**, 119-134.

Muhlberg, A. B. and Warnock, D. E., and Schmid, S. L. (1997). Domain structure and intramolecular regulation of dynamin GTPase. *EMBO J* **16**, 6676-6683

Murai, K. K. and Pasquale EB. (2002). Can Eph receptors stimulate the mind? *Neuron* **33**, 159-162.

Brundage, L., Avery, L., Katz, A., Kim, U. J., Mendel, J. E., Sternberg, P. W., Simon, M. I. (1996). Mutations in a *C. elegans* Gqalpha gene disrupt movement, egg laying, and viability. *Neuron* **16**, 999-1009

Nakajo, N., Yoshitome, S., Iwashita, J., Iida, M., Uto, K., Ueno, S., Okamoto, K., and Sagata, N. (2000). Absence of Wee1 ensures the meiotic cell cycle in Xenopus oocytes. *Genes Dev* **14**, 328-338

Nikolov, D. B., Li, C., Barton, W. A., and Himanen, J. P. (2005). Crystal structure of the ephrin-B1 ectodomain: implications for receptor recognition and signaling. *Biochemistry* **44**, 10947-10953.

Nikolov, D., Li, C., Lackmann, M., Jeffrey, P., Himanen, J. (2007). Crystal structure of the human ephrin-A5 ectodomain. *Protein Sci* **16**, 996-1000.

Nimmo, E. R., Pidoux, A. L., Perry, P.E., Allshire, R. C. (1998). Defective meiosis in telomere-silencing mutants of Schizosaccharomyces pombe. *Nature* **392**, 825-828.

Nishimura, A.L., Mitne-Neto, M., Silva, H.C., Richieri-Costa, A., Middleton, S., Cascio, D., Kok, F., Oliveira, J.R., Gillingwater, T., Webb, J., et al. (2004). A mutation in the vesicle-trafficking protein VAPB causes late-onset spinal muscular atrophy and amyotrophic lateral sclerosis. *Am J Hum Genet* **75***,* 822-831.

Niu, H., Wan, L., Baumgartner, B., Schaefer, D., Loidl, J., and Hollingsworth, N. M. (2005). Partner choice during meiosis is regulated by Hop1-promoted dimerization of Mek1. *Mol Biol Cell* **16**, 5804-5818.

Noren, N. K., Foos, G., Hauser, C. A., Pasquale, E. B. (2006). The EphB4 receptor suppresses breast cancer cell tumorigenicity through an Abl-Crk pathway. *Nat Cell Biol* **8**, 815-825.

Noren, N. K. and Pasquale, E. B. (2004). Eph receptor-ephrin bidirectional signals that target Ras and Rho proteins. *Cell Signal* **16**, 655-666.

Norman, K. R., Fazzio, R. T., Mellem, J. E., Espelt, M. V., Strange, K., Beckerle, M. C., and Maricq, A. V. (2005). The Rho/Rac-family guanine nucleotide exchange factor VAV-1 regulates rhythmic behaviors in *C. elegans*. *Cell* **123**, 119-132.

Northup, J. K., Sternweis, P. C., Smigel, M. D., Schleifer, L. S., Ross, E. M., Gilman, A. G. (1980). Purification of the regulatory component of adenylate cyclase.

Proc Natl Acad Sci **77**, 6516-6520.

Nurse, P. (1990). Universal control mechanism regulating onset of M-phase. *Nature* **344**, 503-508.

Ohsumi, K., Koyanagi, A., Yamamoto, T. M., Gotoh, T., Kishimoto, T. (2004). Emi1-mediated M-phase arrest in Xenopus eggs is distinct from cytostatic factor arrest. *Proc Natl Acad Sci* **101**, 12531-12536.

Oldham, W. M. and Hamm, H. E. (2007). How do receptors activate G proteins? *Adv Protein Chem***74**, 67-93.

Oldham, W. M. and Hamm, H. E. (2008). Heterotrimeric G protein activation by G-protein-coupled receptors. *Nat Rev Mol Cell Biol* **9**, 60-71.

Oleinikov, A. V., Zhao, J. and Makker, S. P. (2000) Cytosolic adaptor protein Dab2 is an intracellular ligand of endocytic receptor gp600/megalin. *Biochem J* **347**, 613–621

Ostrom, R. S. and Insel, P. A. (2004). The evolving role of lipid rafts and caveolae in G protein-coupled receptor signaling: implications for molecular pharmacology. *Br J Pharmacol* **143**, 235-245.

Ouyang, X., Winbow, V. M., Patel, L. S., Burr, G. S., Mitchell, C. K., and O'Brien, J. (2005). Protein kinase A mediates regulation of gap junctions containing connexin 35 through a complex pathway. *Mol Brain Res* **135**, 1-11.

Owen, D. J., Vallis, Y., Pearse, B. M., McMahon, H. T. and Evans, P. R. (2000) The structure and function of the beta 2-adaptin appendage domain. *EMBO J* **19**, 4216–4227

Page, S. L., and Hawley, R. S. (2003). Chromosome choreography: the meiotic ballet.

Science **301**, 785-789.

Page, L. J. and Robinson, M. S. (1995) Targeting signals and subunit interactions in coated vesicle adaptor complexes*. J Cell Biol* **131**, 619–630

Palmer, A. and Nebreda, A. R. (2000). The activation of MAP kinase and p34cdc2/cyclin B during the meiotic maturation of Xenopus oocytes. *Prog Cell Cycle Res* **4**:131-143.

Park, E. K., Warner, N., Bong, Y. S., Stapleton, D., Maeda, R., Pawson, T., Daar, I. O. (2004). Ectopic EphA4 receptor induces posterior protrusions via FGF signaling in Xenopus embryos. *Mol Biol Cell* **15**, 1647-1655.

Park, J. H., Ohshima, S., Tani, T., and Ohshima, Y. (1997). Structure and expression of the gsa-1 gene encoding a G protein alpha(s) subunit in *C. elegans*. *Gene* **194**, 183-190.

Park, J. Y., Su, Y. Q., Ariga, M., Law, E., Jin, S. L., Conti, M. (2004). EGF-like growth factors as mediators of LH action in the ovulatory follicle. *Science* **303**, 682-684.

Parker, M., Roberts, R., Enriquez, M., Zhao, X., Takahashi, T., Pat Cerretti, D., Daniel, T., and Chen, J. (2004). Reverse endocytosis of transmembrane ephrin-B ligands via a clathrin-mediated pathway. *Biochem Biophys Res Commun* **323**, 17-23.

Pasquale, E. B. (2004).Eph-ephrin promiscuity is now crystal clear. *Nature Neuroscience* **7**, 417 - 418

Pasquale, E. B. (2005). Eph receptor signalling casts a wide net on cell behaviour. *Nat Rev Mol Cell Biol* 6, 462-475.

Pasquale, E. B. (2008). Eph-ephrin bidirectional signaling in physiology and disease.

Cell **133**, 38-52.

Peter, M., Castro, A., Lorca, T., Le Peuch, C., Magnaghi-Jaulin, L., Dorée, M., Labbé. J. C. (2001). The APC is dispensable for first meiotic anaphase in Xenopus oocytes. *Nat Cell Biol* **3**, 83-87.

Pearse, B. M. and Bretscher, M. S. (1981). Membrane recycling by coated vesicles. *Annu Rev Biochem*. **50**, 85-101

Pearse, B. M. and Crowther, R. A. (1987) Structure and assembly of coated vesicles. Annu. Rev. Biophys. Biophys. *Chem* **16**, 49–68

Penn, R. B. and Benovic, J. L. (2008). Regulation of heterotrimeric G protein signaling in airway smooth muscle. *Proc Am Thorac Soc* **5**, 47-57.

Peters, J. M. (2006). The anaphase promoting complex/cyclosome: a machine designed to destroy. *Nat Rev Mol Cell Biol* **7**, 644-656.

Petukhova, G. V., Romanienko, P. J., and Camerini-Otero, R. D. (2003). The Hop2 protein has a direct role in promoting interhomolog interactions during mouse meiosis. *Dev Cell* **5**, 927-936.

Pincus, G. and Enzmann E. V. (1934). Can Mammalian Eggs Undergo Normal Development in Vitro? *Proc Natl Acad Sci* **20**, 121-122.

Pincus, G., and Enzmann, E. V. (1935). The comparative behavior of mammalian eggs *in vivo* and *in vitro*. I. The activation of ovarian eggs. *J Exp Med* **62**, 655-675.

Pont, S. J., Robbins, J. M., Bird, T. M., Gibson, J. B., Cleves, M. A., Tilford, J. M., and Aitken, M. E. (2006). Congenital malformations among liveborn infants with trisomies 18 and 13. *Am J Med Genet A* **140**, 1749-1756

Poteryaev, D., Fares, H., Bowerman, B., and Spang, A. (2007). *Caenorhabditis elegans* SAND-1 is essential for RAB-7 function in endosomal traffic. *EMBO J* **26**, 301-312.

Praitis, V., Casey, E., Collar, D., and Austin, J. (2001). Creation of low-copy integrated transgenic lines in *Caenorhabditis elegans. Genetics* **157**, 1217-1226.

Pratt, R. L. and Kinch, M. S. (2002). Activation of the EphA2 tyrosine kinase stimulates the MAP/ERK kinase signaling cascade. *Oncogene* **21**, 7690-7699

Qian, Y. W., Erikson, E., Taieb, F. E, and Maller, J. L. (2001). The polo-like kinase Plx1 is required for activation of the phosphatase Cdc25C and cyclin B-Cdc2 in Xenopus oocytes. *Mol Biol Cell* **12**, 1791-1799

Quick, M. W. (2006). The role of SNARE proteins in trafficking and function of neurotransmitter transporters. *Handb Exp Pharmacol* **175**, 181-196.

Rabitsch, K.P., Tóth, A., Gálová, M., Schleiffer, A., Schaffner, G., Aigner, E., Rupp, C., Penkner, A. M., Moreno-Borchart, A. C., Primig, M., Esposito, R. E., Klein, F., Knop, M., and Nasmyth, K. (2001). A screen for genes required for meiosis and spore formation based on whole-genome expression. *Curr Biol* **11**, 1001-1009.

Rasmussen, S. W. and Holm, P. B. (1984). The synaptonemal complex, recombination nodules and chiasmata in human spermatocytes. *Symp Soc Exp Biol* **38**, 271-292.

Razani, B., Wang, X. B., Engelman, J. A., Battista, M., Lagaud, G., Zhang, X. L., Kneitz, B., Hou, H. Jr, Christ, G. J., Edelmann, W., and Lisanti, M. P. Caveolin-2-deficient mice show evidence of severe pulmonary dysfunction without disruption of caveolae. *Mol Cell Biol* **22**, 2329–2344.

Reimann, J.D., Freed, E., Hsu, J. Y., Kramer, E. R., Peters, J. M., and Jackson, P. K. (2001). Emi1 is a mitotic regulator that interacts with Cdc20 and inhibits the anaphase promoting complex. *Cell* **105**, 645-655.

Reimann, J. D. and Jackson, P. K. (2002). Emi1 is required for cytostatic factor arrest in vertebrate eggs. *Nature* **416**, 850-854.

Reinke, V., Smith, H. E., Nance, J., Wang, J., Van Doren, C., Begley, R., Jones, S. J., Davis, E. B., Scherer, S., Ward, S., and Kim, S. K. (2000). A global profile of germline gene expression in *C. elegans*. *Mol Cell* **6**, 605-616

Richards, J. S., Russell, D. L., Ochsner, S., Hsieh, M., Doyle, K. H., Falender, A. E., Lo, Y. K., and Sharma, S. C. (2002). Novel signaling pathways that control ovarian follicular development, ovulation, and luteinization. *Recent Prog Horm Res* **57**, 195-220.

Rockmill, B. and Roeder, G. S. (1990). Meiosis in asynaptic yeast. *Genetics* **126**, 563-574

Rodbell, M. (1971). *In vitro* assays of adenyl cyclase. *Acta Endocrinol Suppl* **153**, 337-347.

Romanienko, P. J. and Camerini-Otero, R. D. (1999). Cloning, characterization, and localization of mouse and human SPO11. *Genomics* **61**, 156-169

Romanienko, P. J. and Camerini-Otero, R. D. (2000). The mouse Spo11 gene is required for meiotic chromosome synapsis. *Mol Cell* **6**, 975-987.

Rose, K. L., Winfrey, V. P., Hoffman, L. H., Hall, D. H., Furuta, T., and Greenstein D. (1997). The POU gene *ceh-18* promotes gonadal sheath cell differentiation and function required for meiotic maturation and ovulation in *Caenorhabditis elegans*. *Dev Biol* **192,** 59-77.

Rothberg, K. G., Heuser, J. E., Donzell, W. C., Ying, Y. S., Glenney, J. R., Anderson, R. G. (1992). Caveolin, a protein component of caveolae membrane coats. *Cell* **68**, 673–682.

Sadler, S. E. and Maller, J. L. (1985). Inhibition of Xenopus oocyte adenylate cyclase by progesterone: a novel mechanism of action. Adv Cyclic Nucleotide Protein *Phosphorylation Res* **19**, 179-194.

Sagata, N., Daar, I., Oskarsson, M., Showalter, S. D., and Vande Woude, G. F. (1989). The product of the mos proto-oncogene as a candidate "initiator" for oocyte maturation. *Science* **245**, 643-646.

Sagata, N., Oskarsson, M., Copeland, T., Brumbaugh, J., Vande Woude, G. F. (1988). Function of c-mos proto-oncogene product in meiotic maturation in Xenopus oocytes. *Nature* **335**, 519-525.

Sagata N, Watanabe N, Vande Woude GF, Ikawa Y. (1989). The c-mos proto-oncogene product is a cytostatic factor responsible for meiotic arrest in vertebrate eggs. *Nature* **342**, 512-518.

Salcini, A. E., Chen, H., Iannolo, G., De Camilli, P. and Di Fiore, P. P. (1999) Epidermal growth factor pathway substrate 15, Eps15. *Int. J. Biochem. Cell Biol* **31**, 805–809

Sanderson, M. L., Hassold, T. J., and Carrell, D. T. (2008). Proteins involved in meiotic recombination: a role in male infertility? Syst Biol Reprod Med **54**, 57-74.

Santolini, E., Puri, C., Salcini, A. E., Gagliani, M. C., Pelicci, P. G., Tacchetti, C. and Di Fiore, P. P. (2000) Numb is an endocytic protein. *J. Cell Biol.* **151**, 1345–1352

Santini, F. and Keen, J. H. (2002). A glimpse of coated vesicle creation? Well almost! *Nat Cell Biol* **4**, 230-232.

Sato, K., Sato, M., Audhya, A., Oegema, K., Schweinsberg, P., and Grant, B.D. (2006). Dynamic regulation of caveolin-1 trafficking in the germ line and embryo of *Caenorhabditis elegans*. *Mol Biol Cell* **17***,* 3085-3094.

Sato, M., Sato, K., Liou, W., Pant, S., Harada, A., and Grant, B.D. (2008). Regulation of endocytic recycling by *C. elegans* Rab35 and its regulator RME-4, a coated-pit protein. *EMBO J* **27**, 1183-1196

Schade, M. A., Reynolds, N. K., Dollins, C. M., and Miller, K. G. (2005). Mutations that rescue the paralysis of *Caenorhabditis elegans ric-8* (synembryn) mutants activate the Ga_s pathway and define a third major branch of the synaptic signaling network. *Genetics* **169**, 631-649.

Scherthan, H., Weich, S., Schwegler, H., Heyting, C., Härle, M., and Cremer, T. (1996). Centromere and telomere movements during early meiotic prophase of mouse and man are associated with the onset of chromosome pairing. *J Cell Biol* **134**, 1109-1125.

Schlessinger, J. (2000). Cell signaling by receptor tyrosine kinases. *Cell.* **103**, 211-25.

Schmitt, A.M, Shi, J., Wolf, A. M., Lu, C. C., King, L. A., and Zou, Y. (2006). Wnt-Ryk signalling mediates medial-lateral retinotectal topographic mapping. *Nature* **439**, 31-37

Schwab, M. S., Roberts, B. T., Gross, S. D., Tunquist, B. J., Taieb, F. E., Lewellyn, A. L., and Maller, J. L. (2001). Bub1 is activated by the protein kinase p90(Rsk) during Xenopus oocyte maturation. *Curr Biol* **11**, 141-150.

Schwacha A, Kleckner N. (1997). Interhomolog bias during meiotic recombination: meiotic functions promote a highly differentiated interhomolog-only pathway. *Cell* **90**, 1123-1135

Schedl, T. and Kimble, J. (1988). fog-2, a germ-line-specific sex determination gene required for hermaphrodite spermatogenesis in Caenorhabditis elegans. *Genetics* **119**, 43-61.

Schedl, T., Graham, P. L., Barton, M. K., and Kimble, J. (1989). Analysis of the role of tra-1 in germline sex determination in the nematode Caenorhabditis elegans. *Genetics* **123**, 755-769.

Schmid, S. L. (1997) Clathrin-coated vesicle formation and protein sorting: an integrated process. *Annu Rev Biochem* **66**, 511–548

Ségalat, L., Elkes, D. A., and Kaplan, J. M. (1995). Modulation of serotonin-controlled behaviors by Go in *Caenorhabditis elegans*. *Science* **267**, 1648-1651

Segalat, L., Elkes, D. A., and Kaplan, J. M. (1995). Modulation of serotonin-controlled behaviors by G_o in *Caenorhabditis elegans*. *Science* **267**, 1648-1651.

Seugnet, L., Simpson, P., and Haenlin, M. (1997). Requirement for dynamin during Notch signaling in *Drosophila* neurogenesis. *Dev Biol* **192***,* 585-598.

Sever, S., Muhlberg, A. B. and Schmid, S. L. (1999) Impairment of dynamin's GAP domain stimulates receptor-mediated endocytosis. *Nature* **398**, 481–486

Shatz, M. and Liscovitch, M. (2008). Caveolin-1: a tumor-promoting role in human cancer. *Int J Radiat Biol* **84**, 177-189.

Sheetz, M. P. and Singer, S. J. (1974). Biological membranes as bilayer couples. A molecular mechanism of drug-erythrocyte interactions. *Proc Natl Acad Sci* **71**, 4457-4461.

Smardon, A., Spoerke, J. M., Stacey, S. C., Klein, M. E., Mackin, N., and Maine, E. M. (2000). EGO-1 is related to RNA-directed RNA polymerase and functions in germ-line development and RNA interference in *C. elegans*. *Curr Biol* **10**, 169-178.

Simonsen, A., Wurmser, A. E., Emr, S. D., and Stenmark, H. (2001). The role of phosphoinositides in membrane transport. *Curr Opin Cell Biol* **13**, 485-492.

Smith, F. M., Vearing, C., Lackmann, M., Treutlein, H., Himanen, J., Chen, K., Saul, A., Nikolov, D., Boyd, A. W. (2004). Dissecting the EphA3/Ephrin-A5 interactions using a novel functional mutagenesis screen. *J Biol Chem* **279**, 9522-9531.

Smith, P. A. and King, R. C. (1968). Genetic control of synaptonemal complexes in Drosophila melanogaster. *Genetics* **60**, 335-351.

Smith, A. V. and Roeder, G. S. (1997). The yeast Red1 protein localizes to the cores of meiotic chromosomes. *J Cell Biol* **136**, 957-967

Sijen, T., Fleenor, J., Simmer, F., Thijssen, K. L., Parrish, S., Timmons, L., Plasterk, R. H., and Fire, A. (2001). On the role of RNA amplification in dsRNA-triggered gene silencing. *Cell* **107**, 465-476.

Somekawa, S., Fukuhara, S., Nakaoka, Y., Fujita, H., Saito, Y., and Mochizuki, N. (2005). Enhanced functional gap junction neoformation by protein kinase A-dependent and Epac-dependent signals downstream of cAMP in cardiac myocytes. *Circ Res* **97**, 655-662.

Song, K. S., Scherer, P. E., Tang, Z., Okamoto, T., Li, S., Chafel, M., Chu, C., Kohtz, D. S., and Lisanti, M. P. (1996). Expression of caveolin-3 in skeletal, cardiac, and smooth muscle cells. Caveolin-3 is a component of the sarcolemma and co-fractionates with dystrophin and dystrophin-associated glycoproteins. *J Biol Chem* **271**, 15160–15165.

Sprang, S. R., Chen, Z., and Du, X. (2007). Structural basis of effector regulation and signal termination in heterotrimeric Galpha proteins. *Adv Protein Chem* **74**, 1-65.

Starich, T. A., Miller, A., Nguyen, R. L., Hall, D. H., and Shaw, J. E. (2003). The *Caenorhabditis elegans* innexin INX-3 is localized to gap junctions and is essential for embryonic development. *Dev Biol* **256**, 403-417.

Stephenson, S. A., Slomka, S., Douglas, E. L., Hewett, P. J., Hardingham, J. E. (2001). Receptor protein tyrosine kinase EphB4 is up-regulated in colon cancer.

BMC Mol Biol **2***,* 1471-2199

Stitzel, M.L., Pellettieri, J., and Seydoux, G. (2006). The *C. elegans* DYRK kinase MBK-2 marks oocyte proteins for degradation in response to meiotic maturation. *Curr Biol* **16***,* 56-62.

Stitzel, M.L., Cheng, K.C., and Seydoux, G. (2007). Regulation of MBK-2/Dyrk kinase by dynamic cortical anchoring during the oocyte-to-zygote transition. *Curr Biol* **17***,* 1545-1554.

Sweitzer, S. M. and Hinshaw, J. E. (1998) Dynamin undergoes a GTP-dependent conformational change causing vesiculation. *Cell* **93**, 1021–1029

Sym, M. and Roeder, G. S. (1994). Crossover interference is abolished in the absence of a synaptonemal complex protein. *Cell* **79**, 283-292

Takasu, M. A., Dalva, M. B., Zigmond, R. E., and Greenberg, M. E. (2002). Modulation of NMDA receptor-dependent calcium influx and gene expression through EphB receptors. *Science*. **295**, 491-495

Takei, K., McPherson, P. S., Schmid, S. L. and De Camilli, P. (1995) Tubular membrane invaginations coated by dynamin rings are induced by GTP-gamma S in nerve terminals. *Nature*. **374**, 186–190

Takei, K., Slepnev, V. I., Haucke, V., and De Camilli, P. (1999). Functional partnership between amphiphysin and dynamin in clathrin-mediated endocytosis. *Nat Cell Biol.* **1**, 33-39.

Tang, Z., Scherer, P. E., Okamoto, T., Song, K., Chu, C., Kohtz, D. S., Nishimoto, I., Lodish, H. F., and Lisanti, M. P. (1996). Molecular cloning of caveolin-3, a novel member of the caveolin gene family expressed predominantly in muscle. *J Biol Chem.* **271**, 2255–2261.

Tebar, F., Bohlander, S. K. and Sorkin, A. (1999) Clathrin assembly lymphoid myeloid leukemia (CALM) protein: localization in endocytic-coated pits, interactions

with clathrin, and the impact of overexpression on clathrin-mediated traffic. *Mol. Biol. Cell* **10**, 2687–2702

ter Haar, E., Harrison, S. C. and Kirchhausen, T. (2000) Peptide-in-groove interactions link target proteins to the beta-propeller of clathrin. *Proc. Natl. Acad. Sci. U.S.A.* **97**, 1096–1100

Tessé, S., Storlazzi, A., Kleckner, N., Gargano, S., and Zickler, D. (2003). Localization and roles of Ski8p protein in Sordaria meiosis and delineation of three mechanistically distinct steps of meiotic homolog juxtaposition. *Proc Natl Acad Sci* **100**, 12865-12870.

Theurkauf, W.E. and Hawley, R. S. (1992). Meiotic spindle assembly in Drosophila females: behavior of nonexchange chromosomes and the effects of mutations in the nod kinesin-like protein. *J Cell Biol* **116**, 1167-1180.

Toth, J., Cutforth, T., Gelinas, A. D., Bethoney, K. A., Bard, J., Harrison, C. J. (2001). Crystal structure of an ephrin ectodomain. *Dev Cell* **1**, 83-92.

Tsuda, H., Han, S.M., Yang, Y., Tong, C., Lin, Y.Q., Mohan, K., Haueter, C., Zoghbi, A., Harati, Y., Kwan, J., et al. (2008). The amyotrophic lateral sclerosis 8 protein VAPB is cleaved, secreted, and acts as a ligand for Eph receptors. Cell. 133, 949-951.

Tsukazaki, T., Chiang, T. A., Davison, A. F., Attisano, L., Wrana, J. L. (1998). SARA, a FYVE domain protein that recruits Smad2 to the TGF β receptor. *Cell* **95**:779–791

Tunquist, B. J. and Maller, J. L. (2003). Under arrest: cytostatic factor (CSF)-mediated metaphase arrest in vertebrate eggs. *Genes Dev* **17**, 683-710.

Tunquist, B. J., Schwab, M. S., Chen, L. G., and Maller, J. L. (2002). The spindle checkpoint kinase bub1 and cyclin e/cdk2 both contribute to the establishment of meiotic metaphase arrest by cytostatic factor. *Curr Biol* **12**, 1027-1033.

Ungewickell, E. J., and Hinrichsen, L. (2007). Endocytosis: clathrin-mediated membrane budding. *Curr Opin Cell Biol* 19, 417-425.

Vassilieva EV, Nusrat A. (2008). Vesicular trafficking: molecular tools and targets.

Methods Mol Biol **440**, 3-14.

Vazquez, J., Belmont, A. S., and Sedat, J. W. (2002). The dynamics of homologous chromosome pairing during male Drosophila meiosis. *Curr Biol* **12**, 1473-1483.

Vieira, A.V., Lamaze, C., and Schmid, S.L. (1996). Control of EGF receptor signaling by clathrin-mediated endocytosis. *Science* **274***,* 2086-2089.

Vigers, G. P., Crowther, R. A. and Pearse, B. M. (1986) Three-dimensional structure of clathrin cages in ice. *EMBO J* **5**, 529–534

Vihanto, M. M., Vindis, C., Djonov, V., Cerretti, D. P., and Huynh-Do, U. (2006). Caveolin-1 is required for signaling and membrane targeting of EphB1 receptor tyrosine kinase. *J Cell Sci* **119**, 2299-2309.

von Zastrow, M., and Sorkin, A. (2007). Signaling on the endocytic pathway. *Curr. Opin. Cell Biol* **19***,* 436-445.

Voronina, E., and Wessel, G. M. (2003). The regulation of oocyte maturation. *Curr Top Dev Biol* **58**, 53–110.

Wan, L., de los Santos, T., Zhang, C., Shokat, K., and Hollingsworth, N. M. (2004). Mek1 kinase activity functions downstream of RED1 in the regulation of meiotic double strand break repair in budding yeast. *Mol Biol Cell* **15,** 11-23.

Wang, W. and Struhl, G. (2004). *Drosophila* epsin mediates a select endocytic pathway that DSL ligands must enter to activate Notch. *Development* **131**:5367–5380

Wang, X., Roy, P. J., Holland, S. J., Zhang, L. W., Culotti, J. G., and Pawson, T. (1999). Multiple ephrins control cell organization in C. elegans using kinase-dependent and -independent functions of the VAB-1 Eph receptor. *Mol Cell* **4**, 903-913

Waterman, H. and Yarden, Y. (2001) Molecular mechanisms underlying endocytosis and sorting of ErbB receptor tyrosine kinases. *FEBS Lett* **490**, 142–152

Waters, J. C. and Salmon, E. D. (1995). Chromosomes take an active role in spindle assembly. *Bioessays* **17**, 911-914.

Weissman, A. M. (2001) Themes and variations on ubiquitylation. *Nat Rev Mol Cell Biol* **2**, 169–178

Whitten, S.J. and Miller, M.A. (2007). The role of gap junctions in *Caenorhabditis elegans* oocyte maturation and fertilization. *Dev. Biol.* **301***,* 432-446.

Wickner, W. and Schekman, R. (2008). Membrane fusion. *Nat Struct Mol Biol*. **15**, 658-664.

Wolfe, B. L. and Trejo, J. (2007). Clathrin-dependent mechanisms of G protein-coupled receptor endocytosis. *Traffic* **8**, 462-470.

Wolke, U., Jezuit, E. A., and Priess, J. R. (2007). Actin-dependent cytoplasmic streaming in C. elegans oogenesis. *Development* **134**, 2227-2236

Wolstenholme, J., Angell, R. R. (2000). Maternal age and trisomy--a unifying mechanism of formation. *Chromosoma* **109**, 435-438.

Woltering, D., Baumgartner, B., Bagchi, S., Larkin, B., Loidl, J., de los Santos, T., and Hollingsworth, N. M. (2000). Meiotic segregation, synapsis, and recombination checkpoint functions require physical interaction between the chromosomal proteins Red1p and Hop1p. *Mol Cell Biol* **20**, 6646-6658.

Wood, K. W., Sakowicz, R., Goldstein, L. S., and Cleveland, D. W. (1997). CENP-E is a plus end-directed kinetochore motor required for metaphase chromosome alignment. *Cell* **91**, 357-366.

Wu, Q., Lind, G. E., Aasheim, H. C., Micci, F., Silins, I., Tropé, C. G., Nesland, J. M., Lothe, R. A., and Suo, Z. (2007). The EPH receptor Bs (EPHBs) promoters are unmethylated in colon and ovarian cancers. *Epigenetics* 2, 237-243.

Wu, Q., Suo, Z., Risberg, B., Karlsson, M. G., Villman, K., Nesland, J. M. (2004).

Expression of Ephb2 and Ephb4 in breast carcinoma. *Pathol Oncol Res***10**, 26-33.

Wu, T. C. and Lichten, M. (1994). Meiosis-induced double-strand break sites determined by yeast chromatin structure. *Science* **263**, 515-518

Wunderlich, W., Fialka, I., Teis, D., Alpi, A., Pfeifer, A., Parton, R.G., Lottspeich, F., and Huber, L.A. (2001). A novel 14-kilodalton protein interacts with the mitogen-activated protein kinase scaffold mp1 on a late endosomal/lysosomal compartment. *J. Cell Biol*. **152***,* 765-776.

Wybenga-Groot, L. E., Baskin, B., Ong, S. H., Tong, J., Pawson, T., and Sicheri, F. (2001). Structural basis for autoinhibition of the Ephb2 receptor tyrosine kinase by the unphosphorylated juxtamembrane region. *Cell* **106**, 745-757

Xu, L. (2006). Regulation of Smad activities. *Biochim Biophys Acta* **1759**, 503-513.

Yamamoto, I., Kosinski, M. E., and Greenstein, D. (2006). Start me up: cell signaling and the journey from oocyte to embryo in *C. elegans*. *Dev Dyn* **235**, 571-585.

Ybe, J. A., Greene, B., Liu, S. H., Pley, U., Parham, P. and Brodsky, F. M. (1998) Clathrin self-assembly is regulated by three light-chain residues controlling the formation of critical salt bridges. *EMBO J.* **17**, 1297–1303

Ye, W. and Lafer, E. M. (1995) Clathrin binding and assembly activities of expressed domains of the synapse-specific clathrin assembly protein AP-3. *J Biol Chem* **270**, 10933–10939

Yin, Y., Yamashita, Y., Noda, H., Okafuji, T., Go, M. J., Tanaka, H. (2004). EphA receptor tyrosine kinases interact with co-expressed ephrin-A ligands in cis. *Neurosci Res* **48,** 285-296

Yu, H. G. and Koshland, D. E. (2003). Meiotic condensin is required for proper chromosome compaction, SC assembly, and resolution of recombination-dependent chromosome linkages. *J Cell Biol* **163**, 937-947.

Yuan, L., Liu, J. G., Hoja, M. R., Wilbertz, J., Nordqvist, K., and Höög, C. (2002). Female germ cell aneuploidy and embryo death in mice lacking the meiosis-specific protein SCP3. *Science* **296**, 1115-1118.

Yuan, L., Liu, J. G., Zhao, J., Brundell, E., Daneholt, B., and Höög, C. (2000). The murine SCP3 gene is required for synaptonemal complex assembly, chromosome synapsis, and male fertility. *Mol Cell* **5**, 73-83.

Zaremba, S. and Keen, J. H. (1983) Assembly polypeptides from coated vesicles mediate reassembly of unique clathrin coats. *J Cell Biol* **97**, 1339–1347

Zerial, M. and McBride, H. (2001). Rab proteins as membrane organizers. *Nat Rev Mol Cell Biol* **2**, 107-117.

Zhang, H., Squirrell, J. M, and White, J.G. (2008). RAB-11 permissively regulates spindle alignment by modulating metaphase microtubule dynamics in *C. elegans* early embryos. *Mol. Biol. Cell.* 19, 2553-2565.

Zhu, A. J., Zheng, L., Suyama, K., Scott, and M. P. (2003). Altered localization of *Drosophila* Smoothened protein activates Hedgehog signal transduction. *Genes Dev.* **17:**1240–1252

Zierhut, C., Berlinger, M., Rupp, C., Shinohara, A., and Klein, F. (2004). Mnd1 is required for meiotic interhomolog repair. *Curr Biol* **14**, 752-762

Zimmer, M., Palmer, A., Köhler, J., and Klein, R. (2003). EphB-ephrinB bi-directional endocytosis terminates adhesion allowing contact mediated repulsion. *Nat Cell Biol* **5***,* 869-878.